

Exhibit 233

Karen Kingston uncovers patents revealing “cognitive action” spike protein structures in vaccines

Video

<https://rumble.com/v1pg4gf-karen-kingston-uncovers-patents-revealing-cognitive-action-spike-protein-st.html>

Karen Kingston uncovers patents revealing "cognitive action" spike protein structures in vaccines

Health Ranger Report Published October 23, 2022

<https://rumble.com/v1pg4gf-karen-kingston-uncovers-patents-revealing-cognitive-action-spike-protein-st.html>

Highlight notes from the video:

Karen: If you go to the Moderna website, they have about 8 major patents that are for the mRNA vaccines.

This is what I call the master patent for the lipid nanotechnology.
US 10,703.789 B2

This actually has the sequences in it for the body to product the spike protein. It's bio-synthetic.

The master patent in Section 219 it says "the polymer-based self-assembled nanoparticles suchas, but not limited to, micro-sponges, may be fully programmable nanoparticles."

US 2012/0228565 A1 Patent

In the Moderna patent, 80 or 90 other patents listed. This one was filed for water-dispersible nanoparticles.

Section 003 Semiconductor nanocrystals (also known as quantum dot particles).

Qdot Label Conjugates for Cell & Tissue Staining

<https://www.thermofisher.com/us/en/home/life-science/cell-analysis/cellular-imaging/fluorescence-microscopy-and-immunofluorescence-if/qdot-nanocrystal-conjugates-for-cell-and-tissue-staining.html>

15 year deal with Moderna. Thermo Fisher had already partnered with Moderna last year to help scale up production of its COVID vaccine branded as Spikevax.

18:17

FOIA to get ingredients because they have FDA approval

Medical device technology

WO2012148684

CELL-FRIENDLY INVERSE OPAL HYDROGELS FOR CELL ENCAPSULATION, DRUG AND PROTEIN DELIVERY, AND FUNCTIONAL NANOPARTICLE ENCAPSULATION

<https://patentscope.wipo.int/search/en/detail.jsf?docId=WO2012148684>

Fluorescent Inorganic-Organic Hybrid Nanoparticles

<https://onlinelibrary.wiley.com/doi/10.1002/cnma.201800310>

Method for making semiconducting single wall carbon nanotubes

<https://patents.google.com/patent/US20130251618A1/en>

Graphene structure that encapsulates the quantum dot and delivered in the body. This patent owned by the Chinese military.

Carbon Nanotubes & Quantum Dots: Army Thinks VERY Small – January 2020

<https://breakingdefense.com/2020/01/carbon-nanotubes-quantum-dots-army-thinks-very-small/>

Three New Projects for DOD's Innovate Beyond 5G Program

Aug. 2, 2022 |

<https://www.defense.gov/News/Releases/Release/Article/3114220/three-new-projects-for-dods-innovate-beyond-5g-program/>

Activation is contingent on 5G

Quantum dots activated by LED

LED, 5G and Fiber Optics

Acidic pH-responsive nanogels as smart cargo systems for the simultaneous loading and release of short oligonucleotides and magnetic nanoparticles

<https://pubmed.ncbi.nlm.nih.gov/20355740/>

Multi-functional magnetic hydrogel: Design strategies and applications

<https://onlinelibrary.wiley.com/doi/full/10.1002/nano.202100139>

Lipid Nanoparticles—From Liposomes to mRNA Vaccine Delivery, a Landscape of Research Diversity and Advancement

<https://pubs.acs.org/doi/10.1021/acsnano.1c04996>

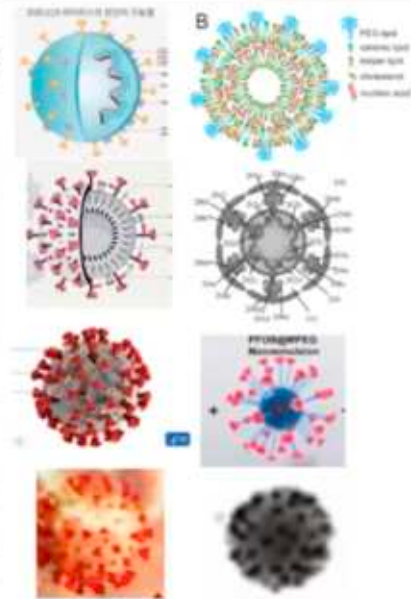
Further capable of autonomous and/or cognitive action

Intelligent sensor platforms

<https://patents.google.com/patent/US20160178652A1/en>

[0020] In one embodiment, the instant invention teaches one or more elements that in whole or in part execute one or more types of actions for creating, spawning, comprising, modifying, repairing, regenerating, reassembling, and or control and regulation of one or more cells, cellular elements, cell organelles, including like actions and behaviors involving cellular processes such as endocytosis, exocytosis, mitosis, trafficking and signaling, communication between cells, receptor upregulation and downregulation, other behaviors, and the like. Failures and defects in any of these cellular elements and processes can lead to diseases, for example, cancer. This type of efficacious behavior is not taught in prior art, including in protein cage art.

[0021] In one invention embodiment, one or more elements, with or without additional elements, and in some embodiments with minimal functionalization, enter the central nervous system, including passing the blood brain barrier (BBB) for efficacious effect. Although different protein cage



Methods and systems of prioritizing treatments, vaccination, testing and/or activities while protecting the privacy of individuals

<https://patents.google.com/patent/US20210082583A1/en>

They plan to put it in everything.

[0523] One or more elements and or platforms of one or more types may be encapsulated, packaged, stored, incorporated, and or utilize one or more methods known in the art, including for example, but not limited to: catheters; injections, including intramuscular injections; syringes; droppers and bulbs; pills; intravenous means; oral means; anal means; capsules; nanocapsules; nanoparticles; nano-devices; prescriptions; hospital and medical supplies; dental supplies; non-prescriptions; medications; over the counter products and remedies; alternative medicine supplies, systems, products and devices; hair care products; splints, casts, walkers, crutches, canes, wheelchairs, and other ambulatory aids; natural foods; vitamin and mineral supplements; first aid products; emergency health care procedures, systems, devices, and products, including combat medicine; health care products; grafts; skin patches; bandages; adhesives; wraps; masks; markers; powders; granules; geriatric care products; pediatric care products; diagnostic devices, systems, and products; medical imaging devices, systems, and products; telemedicine devices, systems, and products; in vivo monitoring systems, products, systems, and devices; in vitro monitoring systems, products, systems, and devices; laundry products; chemical, nuclear and biological sensors;





US010703789B2

(12) **United States Patent**
De Fougères et al.

(10) **Patent No.:** **US 10,703,789 B2**
(45) **Date of Patent:** ***Jul. 7, 2020**

(54) **MODIFIED POLYNUCLEOTIDES FOR THE PRODUCTION OF SECRETED PROTEINS**

(71) Applicant: **ModernaTX, Inc.**, Cambridge, MA (US)

(72) Inventors: **Antoine De Fougères**, Waterloo (BE); **Justin Guild**, Framingham, MA (US)

(73) Assignee: **ModernaTX, Inc.**, Cambridge, MA (US)

(*) Notice: Subject to any disclaimer, the term of this patent is extended or adjusted under 35 U.S.C. 154(b) by 0 days.
This patent is subject to a terminal disclaimer.

(21) Appl. No.: **16438,978**

(22) Filed: **Jan. 12, 2019**

(65) **Prior Publication Data**
US 2020/0017565 A1 Jan. 16, 2020

Related U.S. Application Data
(63) Continuation of application No. 14/987,328, filed on Jan. 4, 2016, now Pat. No. 10,385,106, which is a (Continued)

(51) **Int. Cl.**
A61K 48/00 (2006.01)
A61K 38/17 (2006.01)
A61K 47/54 (2017.01)
A61K 9/127 (2006.01)
C07K 14/535 (2006.01)
C12N 15/88 (2006.01)
A61K 9/50 (2006.01)
C07K 14/47 (2006.01)
A61K 31/7088 (2006.01)
C07K 19/00 (2006.01)
C12N 15/85 (2006.01)
A61K 38/18 (2006.01)
A61K 38/19 (2006.01)
A61K 38/48 (2006.01)
A61K 9/14 (2006.01)
A61K 47/10 (2017.01)
A61K 38/21 (2006.01)
A61K 38/36 (2006.01)
A61K 38/44 (2006.01)
A61K 39/395 (2006.01)

(52) **U.S. Cl.**
CPC *C07K 14/535* (2013.01); *A61K 9/127* (2013.01); *A61K 9/1272* (2013.01); *A61K 9/2272* (2013.01); *A61K 9/2277* (2013.01); *A61K 9/14* (2013.01); *A61K 9/5031* (2013.01); *A61K 31/7088* (2013.01); *A61K 38/2767* (2013.01); *A61K 38/2816* (2013.01); *A61K 38/2866* (2013.01); *A61K 38/291* (2013.01); *A61K 38/293* (2013.01); *A61K 38/212* (2013.01); *A61K 38/215*

(2013.01); *A61K 38/36* (2013.01); *A61K 38/363* (2013.01); *A61K 38/44* (2013.01); *A61K 38/4833* (2013.01); *A61K 38/4846* (2013.01); *A61K 39/3955* (2013.01); *A61K 47/10* (2013.01); *A61K 47/54* (2017.08); *A61K 47/542* (2017.08); *A61K 48/0083* (2013.01); *A61K 48/0066* (2013.01); *A61K 48/0075* (2013.01); *C07K 14/47* (2013.01); *C07K 14/475* (2013.01); *C07K 14/505* (2013.01); *C07K 14/525* (2013.01); *C07K 14/56* (2013.01); *C07K 14/565* (2013.01); *C07K 14/745* (2013.01); *C07K 14/75* (2013.01); *C07K 16/2887* (2013.01); *C07K 16/52* (2013.01); *C07K 19/00* (2013.01); *C12N 9/0009* (2013.01); *C12N 9/644* (2013.01); *C12N 15/85* (2013.01); *C12N 15/88* (2013.01); *C12Y 11/312007* (2013.01); *C12Y 30/421005* (2013.01); *C12Y 30/421022* (2013.01); *A61K 9/0019* (2013.01); *A61K 48/00* (2013.01); *C12N 25/4900* (2013.01)

(58) **Field of Classification Search**
CPC *C07H 21/02*; *C12N 15/87*; *C12N 15/11*
See application file for complete search history.

(56) **References Cited**
U.S. PATENT DOCUMENTS

5,489,677 A 2/1996 Sanghi et al.
5,591,722 A 1/1997 Montgomery et al.
(Continued)

FOREIGN PATENT DOCUMENTS

CA 2028849 A1 9/1991
CA 2473135 A1 6/2003
(Continued)

OTHER PUBLICATIONS

Andersen et al., "Incorporation of pseudouridine into mRNA enhances translation by diminishing PKR activation," *Nucleic Acids Res.* 38(17):5884-92 (2010).

(Continued)

Primary Examiner — Antonio Gálvez Gonzalez
(74) *Attorney, Agent, or Firm* — Clark & Elbing LLP

(57) **ABSTRACT**

A pharmaceutical composition which has a plurality of lipid nanoparticles that has a mean particle size of between 80 nm and 160 nm and contains a modified mRNA encoding a polypeptide. The lipid nanoparticles include a cationic lipid, a neutral lipid, a cholesterol, and a PEG lipid. The mRNA contains a 5'-cap, 5'-UTR, N1-methyl-pseudouridine, a 3'-UTR, and a poly-A region with at least 100 nucleotides.

14 Claims, 14 Drawing Sheets
Specification includes a Sequence Listing.



US 2012/0228565 A1

United States

Patent Application Publication

Adams et al.

Pub. No.: U.S. 2012/0228565 A1

Pub. Date:

Sep. 13, 2012

200 METHOD FOR PREPARING
NONALUMINUM DOPED SEMI-CONDUCTIVE
AND METALLIC NANOPARTICLES HAVING
ENHANCED DISPERSIBILITY IN AQUEOUS
MEDIA

210 Inventor: Edward William Adams, San
Francisco, CA, USA; Navid Pour
Bandari, CA, USA; Liang Cao, US

220 Assignee: LIFE FLUORINE CORP.
CORPORATION, San Francisco, CA,
US

230 Application No.: 12/625,825

240 Filing Date: Mar. 14, 2012

Related U.S. Application Data

250 Continuation-in-part of U.S. Appl. No. 12/593,533, filed on
Nov. 14, 2009, now U.S. Pat. No. 8,181,767, which is a
continuation of U.S. Appl. No. 12/207,541 filed on
Jan. 11, 2008, which is a continuation-in-part of
U.S. Appl. No. 12/171,284, filed on 09/19/2007,
which is a continuation-in-part of U.S. Appl. No. 11/808,345,
filed on 06/28/2007, which is a continuation-in-part of U.S. Appl. No. 11/666,555,
filed on 02/21/2007.

260 International Publication No.: 2010/25, filed on Oct.
28, 2010

Publication Classification

270 Int. Cl. A
B82Y 20/00 (2011.01)
G03F 7/20 (2011.01)

280 U.S. Cl. 2012.03 282502.07, 2012.03 282502.07, 2012.03 282502.07

290 Classification Code

Water-dispersible nanoparticles are prepared by reacting a
precursor of multiple functional groups with a solution of
an amphoteric amine as a means for dispersing the
nanoparticles. The multiple functional groups can be
functional groups or reactive groups and functional hydro-
philic groups are typically selected. Various hydro-
philic ligands are coupled with multiple functional
hydrophilic groups on the surface of the particles.
The hydrophilic ligands are selected based on the
functional groups on the particles. Methods for pre-
paring nanoparticles comprising multiple functional
groups are provided. The methods can be implemented in a
distributed manner using multiple systems and/or devices.

**METHOD FOR PREPARING
SURFACE-MODIFIED SPHERICALLY-
ASYMMETRIC NANOPARTICLES HAVING
ENHANCED DISPERSIBILITY IN AQUEOUS
MEDIA**

NO. 2011-017322, filed in the name of
DAEJUNG CHEMICALS

[0001] This application is a continuation of U.S. Pat. No. 12,141,818, filed on Oct. 27, 2012, which is a continuation of U.S. Pat. No. 12,094,572, filed on Jul. 23, 2011, which is a continuation of U.S. Pat. No. 12,047,573, filed on Mar. 17, 2010. The disclosures of these prior applications are hereby incorporated by reference into this application.

TECHNICAL FIELD

[0002] This invention relates to a method for surface-modifying spherical nanoparticles to improve their dispersibility in aqueous media. The surface-modified nanoparticles exhibit a reduced dependency on aqueous media and are more dispersible in a wide range of pH values. In the present invention, various surface-modifying agents are used to modify the surface of the nanoparticles, thereby making them dispersible in a wide range of pH values.

BACKGROUND

[0003] Spherical nanoparticles of various shapes and sizes are used in a wide range of applications. These nanoparticles are used in various fields such as medicine, biology, chemistry, and physics. However, these nanoparticles are often difficult to disperse in aqueous media. This is because the surface of these nanoparticles is often hydrophobic, which makes them difficult to disperse in water. Therefore, it is necessary to modify the surface of these nanoparticles to improve their dispersibility in aqueous media.

[0004] Spherical nanoparticles are often used in a wide range of applications. These nanoparticles are used in various fields such as medicine, biology, chemistry, and physics. However, these nanoparticles are often difficult to disperse in aqueous media. This is because the surface of these nanoparticles is often hydrophobic, which makes them difficult to disperse in water. Therefore, it is necessary to modify the surface of these nanoparticles to improve their dispersibility in aqueous media. In the present invention, various surface-modifying agents are used to modify the surface of the nanoparticles, thereby making them dispersible in a wide range of pH values. The surface-modified nanoparticles exhibit a reduced dependency on aqueous media and are more dispersible in a wide range of pH values. In the present invention, various surface-modifying agents are used to modify the surface of the nanoparticles, thereby making them dispersible in a wide range of pH values. The surface-modified nanoparticles exhibit a reduced dependency on aqueous media and are more dispersible in a wide range of pH values.

that, the nanoparticles are dispersed in aqueous media and are more dispersible in a wide range of pH values.

[0005] In the present invention, various surface-modifying agents are used to modify the surface of the nanoparticles, thereby making them dispersible in a wide range of pH values. The surface-modified nanoparticles exhibit a reduced dependency on aqueous media and are more dispersible in a wide range of pH values. In the present invention, various surface-modifying agents are used to modify the surface of the nanoparticles, thereby making them dispersible in a wide range of pH values. The surface-modified nanoparticles exhibit a reduced dependency on aqueous media and are more dispersible in a wide range of pH values.

[0006] The present invention provides a method for surface-modifying spherical nanoparticles to improve their dispersibility in aqueous media. The surface-modified nanoparticles exhibit a reduced dependency on aqueous media and are more dispersible in a wide range of pH values. In the present invention, various surface-modifying agents are used to modify the surface of the nanoparticles, thereby making them dispersible in a wide range of pH values. The surface-modified nanoparticles exhibit a reduced dependency on aqueous media and are more dispersible in a wide range of pH values.

[0007] The present invention provides a method for surface-modifying spherical nanoparticles to improve their dispersibility in aqueous media. The surface-modified nanoparticles exhibit a reduced dependency on aqueous media and are more dispersible in a wide range of pH values. In the present invention, various surface-modifying agents are used to modify the surface of the nanoparticles, thereby making them dispersible in a wide range of pH values. The surface-modified nanoparticles exhibit a reduced dependency on aqueous media and are more dispersible in a wide range of pH values.

[0008] The present invention provides a method for surface-modifying spherical nanoparticles to improve their dispersibility in aqueous media. The surface-modified nanoparticles exhibit a reduced dependency on aqueous media and are more dispersible in a wide range of pH values. In the present invention, various surface-modifying agents are used to modify the surface of the nanoparticles, thereby making them dispersible in a wide range of pH values. The surface-modified nanoparticles exhibit a reduced dependency on aqueous media and are more dispersible in a wide range of pH values.

chloride is partially soluble. A suspension of 5 g of the compound in 100 ml of water shows a turbidity.

[1005] X-ray diffraction (XRD) ($\lambda = 1.5418 \text{ \AA}$) shows a sharp peak at $2\theta = 23.8^\circ$ (corresponding to the (010) reflection) and a broad peak at $2\theta = 20.2^\circ$ (corresponding to the (001) reflection). The interlayer distance (d) is calculated as $d = 3.74 \text{ nm}$. The XRD pattern is similar to that of the compound described in Example 1 (see Example 1, Example 10, and International Patent Publication No. 2009/112279), but the (010) reflection is shifted to a lower angle ($2\theta = 23.8^\circ$) and the (001) reflection is shifted to a higher angle ($2\theta = 20.2^\circ$) compared to the compound described in Example 1 (see Example 1, Example 10, and International Patent Publication No. 2009/112279). The XRD pattern is similar to that of the compound described in Example 1 (see Example 1, Example 10, and International Patent Publication No. 2009/112279). The XRD pattern is similar to that of the compound described in Example 1 (see Example 1, Example 10, and International Patent Publication No. 2009/112279).

[1006] The compound is soluble in water and in many organic solvents such as methanol, ethanol, acetone, and acetonitrile. The compound is insoluble in hexane, heptane, and octane. The compound is soluble in water and in many organic solvents such as methanol, ethanol, acetone, and acetonitrile. The compound is insoluble in hexane, heptane, and octane. The compound is soluble in water and in many organic solvents such as methanol, ethanol, acetone, and acetonitrile. The compound is insoluble in hexane, heptane, and octane.

EXAMPLES OF THE INVENTION

[1011] The compound is soluble in water and in many organic solvents such as methanol, ethanol, acetone, and acetonitrile. The compound is insoluble in hexane, heptane, and octane. The compound is soluble in water and in many organic solvents such as methanol, ethanol, acetone, and acetonitrile. The compound is insoluble in hexane, heptane, and octane.

[1012] The compound is soluble in water and in many organic solvents such as methanol, ethanol, acetone, and acetonitrile. The compound is insoluble in hexane, heptane, and octane. The compound is soluble in water and in many organic solvents such as methanol, ethanol, acetone, and acetonitrile. The compound is insoluble in hexane, heptane, and octane.

[1013] The compound is soluble in water and in many organic solvents such as methanol, ethanol, acetone, and acetonitrile. The compound is insoluble in hexane, heptane, and octane. The compound is soluble in water and in many organic solvents such as methanol, ethanol, acetone, and acetonitrile. The compound is insoluble in hexane, heptane, and octane.

[1014] The compound is soluble in water and in many organic solvents such as methanol, ethanol, acetone, and acetonitrile. The compound is insoluble in hexane, heptane, and octane. The compound is soluble in water and in many organic solvents such as methanol, ethanol, acetone, and acetonitrile. The compound is insoluble in hexane, heptane, and octane.

[1015] The compound is soluble in water and in many organic solvents such as methanol, ethanol, acetone, and acetonitrile. The compound is insoluble in hexane, heptane, and octane. The compound is soluble in water and in many organic solvents such as methanol, ethanol, acetone, and acetonitrile. The compound is insoluble in hexane, heptane, and octane.

[1016] The compound is soluble in water and in many organic solvents such as methanol, ethanol, acetone, and acetonitrile. The compound is insoluble in hexane, heptane, and octane. The compound is soluble in water and in many organic solvents such as methanol, ethanol, acetone, and acetonitrile. The compound is insoluble in hexane, heptane, and octane.

[1017] The compound is soluble in water and in many organic solvents such as methanol, ethanol, acetone, and acetonitrile. The compound is insoluble in hexane, heptane, and octane. The compound is soluble in water and in many organic solvents such as methanol, ethanol, acetone, and acetonitrile. The compound is insoluble in hexane, heptane, and octane.

[1018] The compound is soluble in water and in many organic solvents such as methanol, ethanol, acetone, and acetonitrile. The compound is insoluble in hexane, heptane, and octane. The compound is soluble in water and in many organic solvents such as methanol, ethanol, acetone, and acetonitrile. The compound is insoluble in hexane, heptane, and octane.

[1019] The compound is soluble in water and in many organic solvents such as methanol, ethanol, acetone, and acetonitrile. The compound is insoluble in hexane, heptane, and octane. The compound is soluble in water and in many organic solvents such as methanol, ethanol, acetone, and acetonitrile. The compound is insoluble in hexane, heptane, and octane.

[1020] The compound is soluble in water and in many organic solvents such as methanol, ethanol, acetone, and acetonitrile. The compound is insoluble in hexane, heptane, and octane. The compound is soluble in water and in many organic solvents such as methanol, ethanol, acetone, and acetonitrile. The compound is insoluble in hexane, heptane, and octane.

[1021] The compound is soluble in water and in many organic solvents such as methanol, ethanol, acetone, and acetonitrile. The compound is insoluble in hexane, heptane, and octane. The compound is soluble in water and in many organic solvents such as methanol, ethanol, acetone, and acetonitrile. The compound is insoluble in hexane, heptane, and octane.

[1022] The compound is soluble in water and in many organic solvents such as methanol, ethanol, acetone, and acetonitrile. The compound is insoluble in hexane, heptane, and octane. The compound is soluble in water and in many organic solvents such as methanol, ethanol, acetone, and acetonitrile. The compound is insoluble in hexane, heptane, and octane.

[1023] The compound is soluble in water and in many organic solvents such as methanol, ethanol, acetone, and acetonitrile. The compound is insoluble in hexane, heptane, and octane. The compound is soluble in water and in many organic solvents such as methanol, ethanol, acetone, and acetonitrile. The compound is insoluble in hexane, heptane, and octane.

including, but not limited to, statistical properties of the signals and physical or chemical properties of the signals, such as frequency, amplitude and phase. The signals are also characterized as being either periodic or aperiodic, either continuous or discrete in time, and either deterministic or random. It is to be understood that the above-mentioned terms are used herein for descriptive purposes only and are not intended to limit the scope of the invention. Typically, an invention disclosed in this application is described as being a "method" or "system" without explicitly stating that it is a method or system, but it is intended that such terms refer to a method or system unless otherwise specified.

[1025] A "method" in this context refers to a procedure, process or technique for performing an action or for achieving a result. The steps in a method may be performed in any order or simultaneously and may be performed by a person or by a computer or by a combination of a person and a computer. The steps in a method may be performed by a person or by a computer or by a combination of a person and a computer. The steps in a method may be performed by a person or by a computer or by a combination of a person and a computer.

[1026] A "system" in this context refers to a combination of hardware and/or software components that are configured to perform a function. The components of a system may be interconnected in any manner and may be distributed over any medium. The components of a system may be implemented in any manner and may be implemented in any medium.

[1027] A "user" in this context refers to a person or a computer or a combination of a person and a computer that is configured to use a system. The user may be configured to use a system in any manner and may be configured to use a system in any medium. The user may be configured to use a system in any manner and may be configured to use a system in any medium.

[1028] A "method" in this context refers to a procedure, process or technique for performing an action or for achieving a result. The steps in a method may be performed in any order or simultaneously and may be performed by a person or by a computer or by a combination of a person and a computer. The steps in a method may be performed by a person or by a computer or by a combination of a person and a computer. The steps in a method may be performed by a person or by a computer or by a combination of a person and a computer.

[1029] A "method" in this context refers to a procedure, process or technique for performing an action or for achieving a result. The steps in a method may be performed in any order or simultaneously and may be performed by a person or by a computer or by a combination of a person and a computer. The steps in a method may be performed by a person or by a computer or by a combination of a person and a computer.

[1030] A "method" in this context refers to a procedure, process or technique for performing an action or for achieving a result. The steps in a method may be performed in any order or simultaneously and may be performed by a person or by a computer or by a combination of a person and a computer. The steps in a method may be performed by a person or by a computer or by a combination of a person and a computer.

[1031] A "method" in this context refers to a procedure, process or technique for performing an action or for achieving a result. The steps in a method may be performed in any order or simultaneously and may be performed by a person or by a computer or by a combination of a person and a computer. The steps in a method may be performed by a person or by a computer or by a combination of a person and a computer.

[1032] A "method" in this context refers to a procedure, process or technique for performing an action or for achieving a result. The steps in a method may be performed in any order or simultaneously and may be performed by a person or by a computer or by a combination of a person and a computer. The steps in a method may be performed by a person or by a computer or by a combination of a person and a computer.

[1033] A "method" in this context refers to a procedure, process or technique for performing an action or for achieving a result. The steps in a method may be performed in any order or simultaneously and may be performed by a person or by a computer or by a combination of a person and a computer. The steps in a method may be performed by a person or by a computer or by a combination of a person and a computer.

[1034] A "method" in this context refers to a procedure, process or technique for performing an action or for achieving a result. The steps in a method may be performed in any order or simultaneously and may be performed by a person or by a computer or by a combination of a person and a computer. The steps in a method may be performed by a person or by a computer or by a combination of a person and a computer.

[1035] A "method" in this context refers to a procedure, process or technique for performing an action or for achieving a result. The steps in a method may be performed in any order or simultaneously and may be performed by a person or by a computer or by a combination of a person and a computer. The steps in a method may be performed by a person or by a computer or by a combination of a person and a computer.

[1036] A "method" in this context refers to a procedure, process or technique for performing an action or for achieving a result. The steps in a method may be performed in any order or simultaneously and may be performed by a person or by a computer or by a combination of a person and a computer. The steps in a method may be performed by a person or by a computer or by a combination of a person and a computer.

[1037] A "method" in this context refers to a procedure, process or technique for performing an action or for achieving a result. The steps in a method may be performed in any order or simultaneously and may be performed by a person or by a computer or by a combination of a person and a computer. The steps in a method may be performed by a person or by a computer or by a combination of a person and a computer.

[1038] A "method" in this context refers to a procedure, process or technique for performing an action or for achieving a result. The steps in a method may be performed in any order or simultaneously and may be performed by a person or by a computer or by a combination of a person and a computer. The steps in a method may be performed by a person or by a computer or by a combination of a person and a computer.

[1039] A "method" in this context refers to a procedure, process or technique for performing an action or for achieving a result. The steps in a method may be performed in any order or simultaneously and may be performed by a person or by a computer or by a combination of a person and a computer. The steps in a method may be performed by a person or by a computer or by a combination of a person and a computer.

1210 a. and 1215 a. are polygons, depicted as a hexagon and a pentagon, respectively, of the die.

[1055] A "die" is a polyhedron with a finite number of flat faces. The faces of the die are typically square or rectangular, but they can be other shapes. The faces of the die are typically numbered from 1 to 6. The faces of the die are typically numbered from 1 to 6. The faces of the die are typically numbered from 1 to 6. The faces of the die are typically numbered from 1 to 6.

[1056] All the faces of the die are typically numbered from 1 to 6.

E Die 2000, FIG. 2

[1057] FIG. 2 shows a die 2000 with a flat top face 2010 and a flat bottom face 2020. The die 2000 has six faces: a top face 2010, a bottom face 2020, and four side faces 2030, 2040, 2050, and 2060. The die 2000 is shown in a perspective view. The die 2000 is shown in a perspective view. The die 2000 is shown in a perspective view. The die 2000 is shown in a perspective view.

[1058] Die 2000 is a polyhedron with a finite number of flat faces. The faces of the die are typically square or rectangular, but they can be other shapes. The faces of the die are typically numbered from 1 to 6. The faces of the die are typically numbered from 1 to 6. The faces of the die are typically numbered from 1 to 6. The faces of the die are typically numbered from 1 to 6.

1210 b. FIG. 2 shows a die 2000 with a flat top face 2010 and a flat bottom face 2020. The die 2000 has six faces: a top face 2010, a bottom face 2020, and four side faces 2030, 2040, 2050, and 2060. The die 2000 is shown in a perspective view. The die 2000 is shown in a perspective view. The die 2000 is shown in a perspective view. The die 2000 is shown in a perspective view.

[1059] Die 2000 is a polyhedron with a finite number of flat faces. The faces of the die are typically square or rectangular, but they can be other shapes. The faces of the die are typically numbered from 1 to 6. The faces of the die are typically numbered from 1 to 6. The faces of the die are typically numbered from 1 to 6. The faces of the die are typically numbered from 1 to 6.

[1060] Die 2000 is a polyhedron with a finite number of flat faces. The faces of the die are typically square or rectangular, but they can be other shapes. The faces of the die are typically numbered from 1 to 6. The faces of the die are typically numbered from 1 to 6. The faces of the die are typically numbered from 1 to 6. The faces of the die are typically numbered from 1 to 6.

[1061] Die 2000 is a polyhedron with a finite number of flat faces. The faces of the die are typically square or rectangular, but they can be other shapes. The faces of the die are typically numbered from 1 to 6. The faces of the die are typically numbered from 1 to 6. The faces of the die are typically numbered from 1 to 6. The faces of the die are typically numbered from 1 to 6.

[1062] Die 2000 is a polyhedron with a finite number of flat faces. The faces of the die are typically square or rectangular, but they can be other shapes. The faces of the die are typically numbered from 1 to 6. The faces of the die are typically numbered from 1 to 6. The faces of the die are typically numbered from 1 to 6. The faces of the die are typically numbered from 1 to 6.

Fig. 10. The initial population of the *g* and *h* alleles of the *h* locus of the *P. chalybeata* group. The *g* allele is the most abundant allele in each population. The frequency of the *g* allele is shown by the vertical bars. The frequency of the *h* allele is shown by the horizontal bars. The *g* and *h* alleles are shown in the legend. The *g* allele is shown in black and the *h* allele is shown in white.

10. Population genetic structure and divergence

[100] The genetic structure of the populations was analyzed using the Bayesian method of the STRUCTURE software. The results of the analysis are shown in Fig. 11. The populations are grouped into two main clusters: the *g* and *h* alleles. The *g* allele is the most abundant allele in each population. The *h* allele is the least abundant allele in each population.

[101] The genetic structure of the populations was analyzed using the Bayesian method of the STRUCTURE software. The results of the analysis are shown in Fig. 11. The populations are grouped into two main clusters: the *g* and *h* alleles. The *g* allele is the most abundant allele in each population. The *h* allele is the least abundant allele in each population. The genetic structure of the populations was analyzed using the Bayesian method of the STRUCTURE software. The results of the analysis are shown in Fig. 11. The populations are grouped into two main clusters: the *g* and *h* alleles. The *g* allele is the most abundant allele in each population. The *h* allele is the least abundant allele in each population.

[102] The genetic structure of the populations was analyzed using the Bayesian method of the STRUCTURE software. The results of the analysis are shown in Fig. 11. The populations are grouped into two main clusters: the *g* and *h* alleles. The *g* allele is the most abundant allele in each population. The *h* allele is the least abundant allele in each population.

[103] The genetic structure of the populations was analyzed using the Bayesian method of the STRUCTURE software. The results of the analysis are shown in Fig. 11. The populations are grouped into two main clusters: the *g* and *h* alleles. The *g* allele is the most abundant allele in each population. The *h* allele is the least abundant allele in each population. The genetic structure of the populations was analyzed using the Bayesian method of the STRUCTURE software. The results of the analysis are shown in Fig. 11. The populations are grouped into two main clusters: the *g* and *h* alleles. The *g* allele is the most abundant allele in each population. The *h* allele is the least abundant allele in each population.

population genetic structure and divergence. The genetic structure of the populations was analyzed using the Bayesian method of the STRUCTURE software. The results of the analysis are shown in Fig. 11. The populations are grouped into two main clusters: the *g* and *h* alleles. The *g* allele is the most abundant allele in each population. The *h* allele is the least abundant allele in each population.

[104] The genetic structure of the populations was analyzed using the Bayesian method of the STRUCTURE software. The results of the analysis are shown in Fig. 11. The populations are grouped into two main clusters: the *g* and *h* alleles. The *g* allele is the most abundant allele in each population. The *h* allele is the least abundant allele in each population.

11. Population genetic structure and divergence

[105] The genetic structure of the populations was analyzed using the Bayesian method of the STRUCTURE software. The results of the analysis are shown in Fig. 11. The populations are grouped into two main clusters: the *g* and *h* alleles. The *g* allele is the most abundant allele in each population. The *h* allele is the least abundant allele in each population.

[106] The genetic structure of the populations was analyzed using the Bayesian method of the STRUCTURE software. The results of the analysis are shown in Fig. 11. The populations are grouped into two main clusters: the *g* and *h* alleles. The *g* allele is the most abundant allele in each population. The *h* allele is the least abundant allele in each population.

[107] The genetic structure of the populations was analyzed using the Bayesian method of the STRUCTURE software. The results of the analysis are shown in Fig. 11. The populations are grouped into two main clusters: the *g* and *h* alleles. The *g* allele is the most abundant allele in each population. The *h* allele is the least abundant allele in each population.

being described herein, because a number of other possible configurations could be used to implement the system.

As suggested by the reference to computer-readable storage medium, the computer-readable storage medium may be a non-transitory storage medium.

It is to be understood that the above description is intended to be illustrative, not restrictive. It will be apparent to those skilled in the art that various modifications can be made without departing from the scope of the invention.

♦ ♦ ♦ ♦ ♦

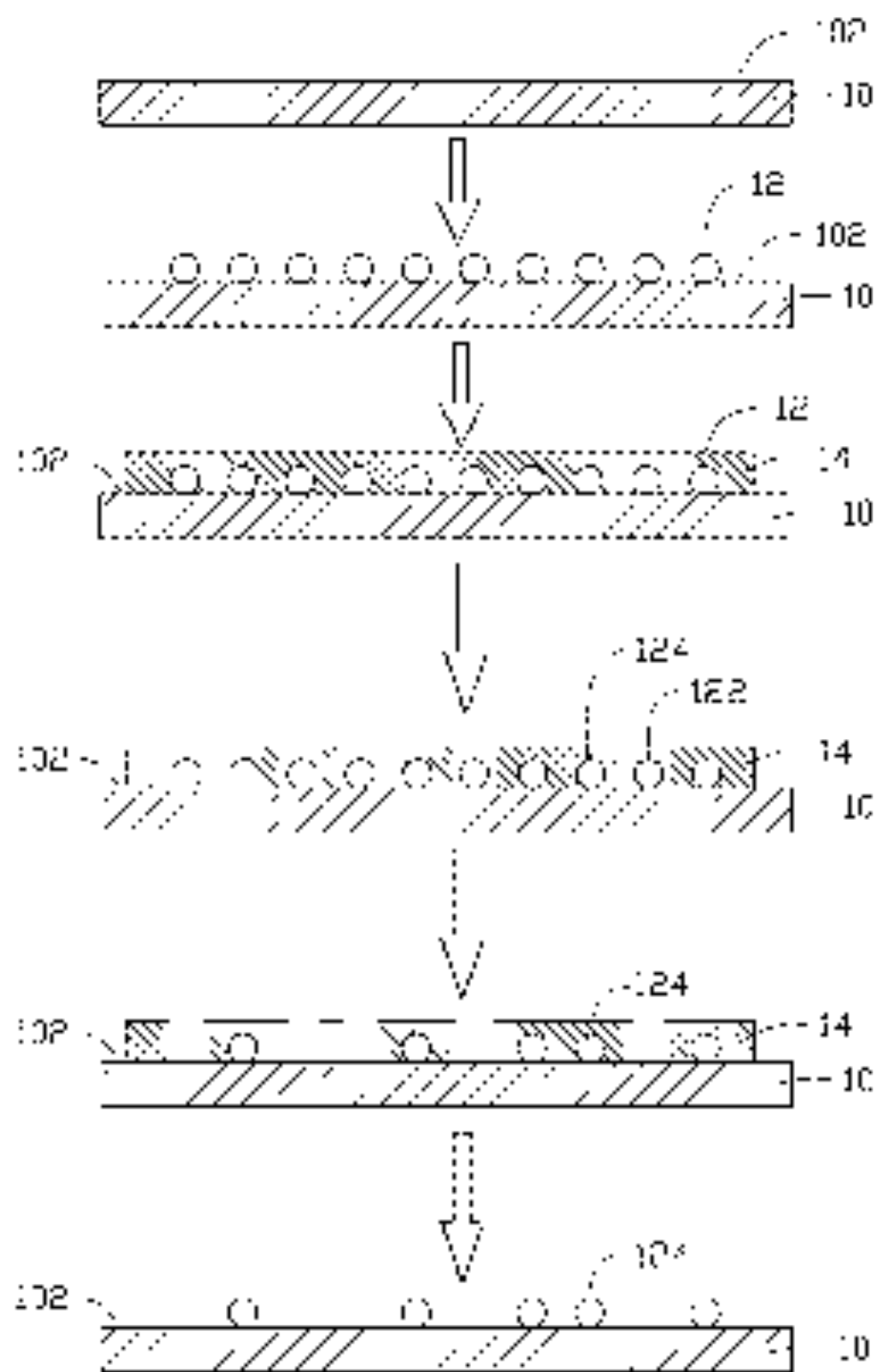


FIG. 1

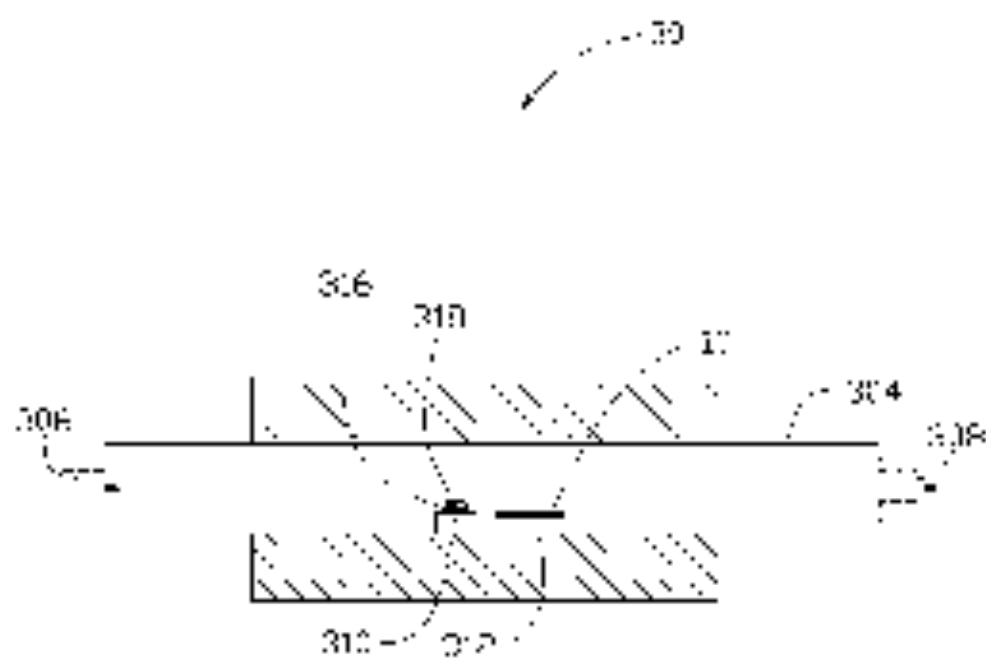


FIG. 2

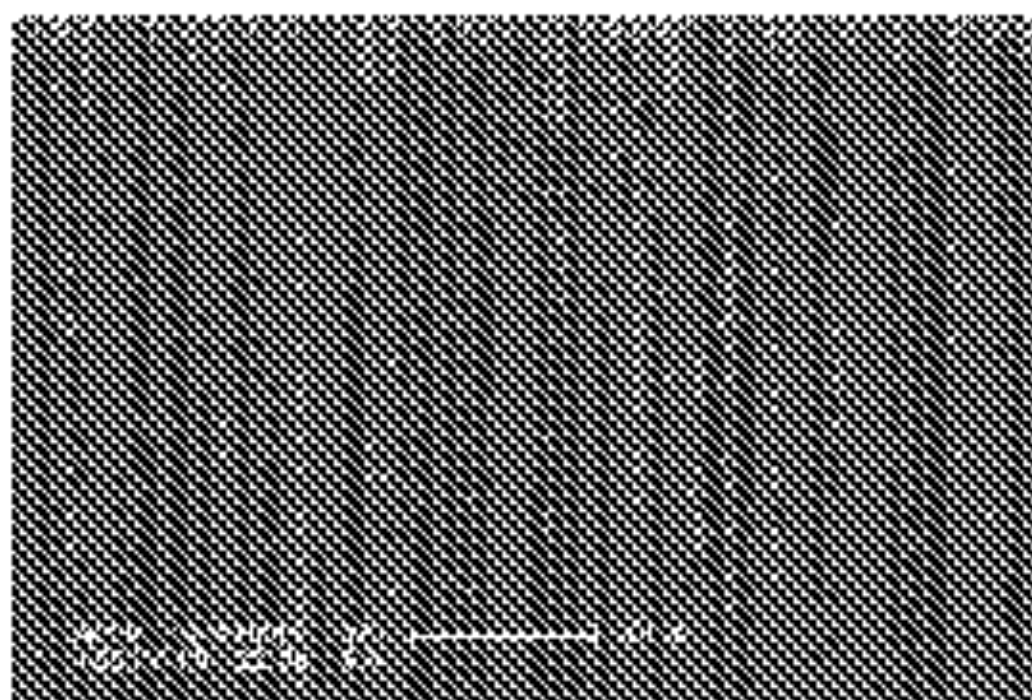


FIG. 3



FIG. 4

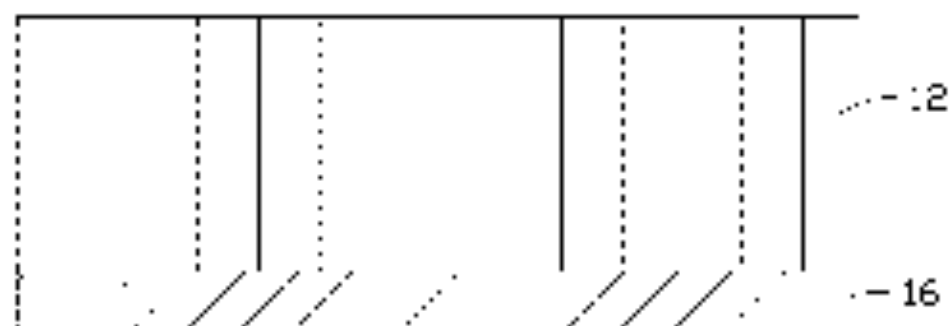


FIG. 5

17. The analysis using SWCNT, making reference to the analysis of C_{60} showing the amount of C_{60} needed to give rise to a single layer of carbon nanotubes of length L and diameter d .

18. A similar analysis of the volume of the nanotubes (SWCNT) showing the relationship:

showing a single unit of carbon nanotubes of length L and diameter d is formed when the length of the carbon nanotube has a volume of V_{CNT} and the volume of the C_{60} molecule is V_{C60} and, consequently, SWCNTs are characterized by a V_{CNT}/V_{C60} ratio of n molecules.

19. Applying a mass balance to a single layer of the single C_{60} molecule and the tube to find the actual SWCNTs in the analysis using SWCNTs.

20. Using C_{60} molecule SWCNTs making reference to the V_{CNT}/V_{C60} ratio of n molecules of C_{60} molecules showing the need of SWCNTs to give rise to a single layer of C_{60} molecules.

21. Using the length of the C_{60} molecule and reference to the molecules that are used.

22. The analysis using SWCNTs making reference to the SWCNTs and the C_{60} molecules showing the need of SWCNTs to give rise to a single layer of C_{60} molecules.

23. The analysis using SWCNTs making reference to the SWCNTs and the C_{60} molecules showing the need of SWCNTs to give rise to a single layer of C_{60} molecules.

Acidic pH-Responsive Nanogels as Smart Cargo Systems for the Simultaneous Loading and Release of Short Oligonucleotides and Magnetic Nanoparticles

Smriti R. Deka,[†] Alessandra Quarta,[†] Riccardo Di Corato,[‡] Andrea Falqui,[†] Liberato Manna,[†] Roberto Cingolani,[†] and Teresa Pellegrino^{*,†,‡}

[†]*Istituto Italiano di Tecnologia, via Morego 30, 16163, Genova, Italy, and* [‡]*National Nanotechnology Laboratory of CNR-INFM and IIT Research Unit, via per Arnesano km 5, 73100, Lecce, Italy*

Received February 1, 2010. Revised Manuscript Received March 1, 2010

Smart materials able to sense environmental stimuli can be exploited as intelligent carrier systems. Acidic pH-responsive polymers, for instance, exhibit a variation in the ionization state upon lowering the pH, which leads to their swelling. The different permeability of these polymers as a function of the pH could be exploited for the incorporation and subsequent release of previously trapped payload molecules/nanoparticles. We provide here a proof of concept of a novel use of pH-responsive polymer nanostructures based on 2-vinylpyridine and divinylbenzene, having an overall size below 200 nm, as cargo system for magnetic nanoparticles, for oligonucleotide sequences, as well as for their simultaneous loading and controlled release mediated by the pH.

1. Introduction

Research on nanocomposites aims at developing and miniaturizing structures made of different functional entities, each of them able to carry out specific tasks. In order to design multifunctional nanostructures that might serve as new medical devices, it is crucial to identify “smart materials” that are capable of responding to defined stimuli. Hydrogels are an interesting class of functional materials that have been exploited as intelligent cargo systems for the encapsulation and the delivery of different active molecules, such as oligonucleotides or anticancer drugs,^{1–4} and that can be useful for the capture and for the controlled release of inorganic nanoparticles. These polymers, whose structure is composed of a three-dimensional network of cross-linked units, can undergo substantial modifications of some of their properties (such as their total charge or their hydrophobicity/hydrophilicity balance) as a consequence of small variations in the local environment, like a change in pH or in the temperature.^{5,6}

Hydrogels in their bulk form have been applied so far in implants, contact lenses, dental materials, and vascular grafts.^{1,7} In past years, there has been increasing research activity focused on the miniaturization of hydrogel particles (henceforward referred to as “nanogels”) and on the study of their potential as drug delivery agents.¹ Research in this area has shown that in order for nanogels to have reliable structure–properties relationships one needs to finely control both their size and their purity.⁶ Size control is particularly critical because a nanogel designed for in vivo delivery of drugs, genes, or nanoparticles should be smaller

than 200 nm.^{8–13} Once injected intravenously, a nanogel smaller than this size will remain colloidally stable, it will not be sequestered immediately by the reticulo-endothelial system,¹¹ and hence, it will stay in circulation for a sufficiently long time to reach the tumor regions and pass through the pore vessels at these regions.^{1,9,14}

While nanogels based on temperature-responsive polymers are generally designed to be altered by external stimuli, those based on pH-responsive polymers can respond to variations in the intracellular or tissue environment.¹ It is known, for example, that certain cancer tissues, due to hypoxia environment, exhibit an extracellular pH around 6.5,¹⁵ while the pH of some intracellular compartments, like lysosomes, is around 4.5.¹⁶ The pH-dependent swelling behavior of a nanogel can be useful not only for the release of the cargo, but also for its loading. Indeed, when the nanogel swells, its permeability increases, allowing either for the incorporation of molecules/nanoparticles or alternatively for the release of previously trapped payloads. So far, several pH-responsive polymers have been widely used as a controlled drug delivery system.^{17–21} In some studies, pH-responsive polymers have been exploited as templates for the in situ synthesis of nanoparticles, and the resulting hybrid systems were tested mainly in catalytic applications.^{22,23} Only in a few works were pH-responsive

*Corresponding author. teresa.pellegrino@unile.it; tel. +39 0832 298 214; fax +39 0832 298 230.

- (1) Schmaljohann, D. *Adv. Drug Delivery Rev.* **2006**, *58*, 1655.
- (2) Nayak, S.; Lyon, L. A. *Angew. Chem.-Int. Ed.* **2005**, *44*, 7686.
- (3) Gupta, P.; Vermani, K.; Garg, S. *Drug Discovery Today* **2002**, *7*, 569.
- (4) Vinogradov, S. V.; Bronich, T. K.; Kabanov, A. V. *Adv. Drug Delivery Rev.* **2002**, *54*, 135.
- (5) Ganta, S.; Devalapally, H.; Shahiwala, A.; Amiji, M. *J. Controlled Release* **2008**, *126*, 187.
- (6) Raemdonck, K.; Demeester, J.; De Smedt, S. *Soft Matter* **2009**, *5*, 707.
- (7) Liu, S.; Maheshwari, R.; Kiick, K. L. *Macromolecules* **2009**, *42*, 3.
- (8) Takakura, Y.; Mahato, R. I.; Hashida, M. *Adv. Drug Delivery Rev.* **1998**, *34*, 93.

- (9) Mitrugotri, S.; Lahann, J. *Nat. Mater.* **2009**, *8*, 15.
- (10) Decuzzi, P.; Pasqualini, R.; Arap, W.; Ferrari, M. *Pharm. Res.* **2009**, *26*, 235.
- (11) Cairns, R.; Papandreou, I.; Denko, N. *Mol. Cancer Res.* **2006**, *4*, 61.
- (12) Torchilin, V. P. *Adv. Drug Delivery Rev.* **2006**, *58*, 1532.
- (13) Torchilin, V. P. *J. Controlled Release* **2001**, *73*, 137.
- (14) Prokop, A.; Davidson, J. M. *J. Pharm. Sci.* **2008**, *97*, 3518.
- (15) Gerweck, L. E.; Seetharaman, K. *Cancer Res.* **1996**, *56*, 1194.
- (16) Grabe, M.; Oster, G. *J. Gen. Physiol.* **2001**, *117*, 329.
- (17) Dai, S.; Ravi, P.; Tam, K. C. *Soft Matter* **2008**, *4*, 435.
- (18) Wu, D. Q.; Sun, Y. X.; Xu, X. D.; Cheng, S. X.; Zhang, X. Z.; Zhuo, R. X. *Biomacromolecules* **2008**, *9*, 1155.
- (19) Zhao, C.; Zhuang, X.; He, P.; Xiao, C.; He, C.; Sun, J.; Chen, X.; Jing, X. *Polymer* **2009**, *50*, 4308.
- (20) Qu, T.; Wang, A.; Yuan, J.; Gao, Q. *J. Colloid Interface Sci.* **2009**, *336*, 865.
- (21) Peppas, N. A.; Hilt, J. Z.; Khademhosseini, A.; Langer, R. *Adv. Mater.* **2006**, *18*, 1345.
- (22) Zhang, J. G.; Xu, S. Q.; Kumacheva, E. *J. Am. Chem. Soc.* **2004**, *126*, 7908.
- (23) Palioura, D.; Armes, S. P.; Anastasiadis, S. H.; Vamvakaki, M. *Langmuir* **2007**, *23*, 5761.

polymers combined with magnetic nanoparticles,^{24,25} and in such cases, the magnetic nanoparticles were always covalently linked to the nanogel networks. In most of those works, the magnetic nanoparticles were actually used as templates on which the polymer was grown around,^{25,26} or vice versa, the polymer was used as template on which the magnetic nanoparticles were nucleated (and remained bound to it). To our knowledge, there has been no report so far on the use of nanogels as carrier systems for the controlled release of magnetic nanoparticles.

Among the vast class of nanoparticles, iron oxide nanoparticles (IONPs, both maghemite and magnetite) are superparamagnetic nanocrystals that have been widely investigated as drug delivery, diagnosis, and therapeutic agents.²⁷ Due to their intrinsic magnetic properties, IONPs are ideal candidates as delivery agents: when exposed to an external magnetic field of moderate intensity, they are able to accumulate to the site where the magnet is positioned, while upon removal of the magnet, they do not undergo aggregation, as they do not exhibit any residual magnetization. Furthermore, IONPs are valuable contrast agents in magnetic resonance imaging (MRI) because their magnetic moments can affect the relaxivity of the water molecule protons present in the tissues, resulting in a negative contrast in the area where the nanoparticles are localized.²⁸ IONPs can also serve as colloidal mediators for generating heat for hyperthermia treatment in cancer therapy, under the application of appropriate alternating magnetic fields.²⁹ The inclusion of IONPs in the nanogel confers to it all the additional advantages of IONPs as described above.

In the present work, we employ acidic pH-responsive nanogels as delivery systems for different types of payloads, namely, IONPs and short oligonucleotide sequences, and combinations of them. We have modified a previously reported synthetic procedure for preparing pH-responsive nanogels³⁰ in order to obtain nanogels with sizes tunable from 40 to 200 nm, and we have tested those materials as carrier systems. A full characterization based on transmission electron microscopy (TEM), photoluminescence spectroscopy, confocal microscopy, and dynamic light scattering (DLS) was carried out in order to elucidate the loading and the release processes of short DNA sequences, of IONPs, and the combined loading and release of both payloads at the same time. Our pH and of salt concentration results show that full control over the loading and the release of IONPs and DNA is clearly achieved.

2. Experimental Section

2.1. Chemicals. All chemicals were of the highest purity available and were used as received. 2-Vinyl pyridine (2-VP, 97%), sodium tetraborate decahydrate, boric acid, as well as all the disposable materials were purchased from Sigma-Aldrich. Divinylbenzene (DVB), 2,2'-azobis(2-methylpropanamide)-dihydrochloride (AIBA), and Diamine-PEG (MW 897) were purchased from Fluka. The HPLC purified oligonucleotide sequence modified at the 5' end with Cy3 (5'-CAC CAC ACG GTC GGC AGC CAC GGT A-3', henceforth referred to as Cy3-DNA) was purchased from Thermo Electron Corporation. Doubly distilled deionized water (pH ~6) was used for the polymerization

and for all experiments. Poly(maleic anhydride-*alt*-1-tetradecene) (PC 14) was purchased from Sigma-Aldrich, although at present, this polymer is no longer commercially available. The reader can refer to a new polymer coating procedure implemented by us which employs a similar polymer, which is still commercially available.³¹

2.2. Synthesis of Nanogels via Emulsion Polymerization.

A series of polyvinyl pyridine nanogels were synthesized with a control over the size diameter of the nanogel below 200 nm, following a procedure published by Dupin et al.³⁰ and modified by us. As an example, we describe here the experimental conditions for the synthesis of nanogels of about 110 nm in diameter (as determined by transmission electron microscopy, TEM). A mixture of 2-vinyl pyridine (2-VP, 0.25 g) and divinylbenzene (DVB, 0.013 g) was dissolved in 60 mL of water in a round-bottom flask. The pH of the resulting solution was 8.3 immediately after mixing. The flask was sealed with a rubber septum, and the aqueous solution was degassed at ambient temperature by five vacuum/nitrogen cycles. The degassed solution was constantly stirred with a magnetic stirrer and heated at 60 ± 1 °C. After 20 min, the solution of the AIBA initiator (0.022 g in 1 mL water) was added to the flask, and after 15 min, the solution in the flask turned milky white, indicating the nucleation of the nanogels. This solution was left to polymerize for a further 2 h under stirring conditions at 60 °C, after which the flask was opened to air in order to expel the nitrogen atmosphere and to stop the reaction. In order to remove the residual monomers in solution, the 2-VP nanogel particles were washed at least 10 times with a Millipore Dialysis System (MWCO 100.000) on centricon tubes, and the reaction mixture was centrifuged at 4000 rpm for 30 min. Fresh water was added each time before any centrifugation. All dispersions were diluted using Milli-Q water (18.2 M Ω) that had been ultrafiltered (0.20 μ m filter) prior to use. The solution pH was adjusted by using a solution of HCl (0.1 M) or NaOH (0.1 M) and the pH was checked with a pH-meter equipped with a microelectrode (Crison pH-Meter Basic 20+). In order to tune the size of the nanogels below 200 nm in diameter, we have varied the molar ratio of 2-VP/DVB by changing the amount of 2-VP added, while keeping constant all the other reaction conditions, as described above (Table 1).

2.3. Preparation of Diamino-PEG Conjugated Iron Oxide Nanocrystals.

Iron oxide nanocrystals (diameter of 7 nm) were synthesized according to the Sun method.³² The "as synthesized" nanoparticles had a capping of oleic acid and oleylamine and were soluble in organic solvents. They were transferred into water by using a polymer coating procedure developed by us.³³ Briefly, the nanoparticles were wrapped in an amphiphilic polymer shell made of poly(maleic anhydride *alt*-1-tetradecene), and such shell was then cross-linked using a triamine. The nanocrystals were therefore soluble in water and were negatively charged, as determined by zeta potential measurements (Table 1, Supporting Information), due to the outstretched carboxylate moieties of the polymer molecules. In order to remove the excess free polymer, an ultracentrifugation step was performed at 150 000 rcf on a continuous sucrose gradient.³¹ Then, diamino-PEG molecules (molecular weight 897 Da) were bound to the carboxy groups at the nanoparticle surface via EDC chemistry. The amino-PEG molecules were introduced in order to make the nanoparticles more stable at different conditions of pH and ionic strength.³⁴ In detail, to 500 μ L of a nanocrystal solution 6 μ M, 500 μ L of a solution containing a molar ratio of diamino-PEG/NP equal to 500 were added, and after mixing, 500 μ L of a solution containing an excess molar ratio of EDC/NP (equal to 75 000) was also

(24) Bhattacharya, S.; Eckert, F.; Boyko, V.; Pich, A. *Small* **2007**, *3*, 650.

(25) Zhou, L. L.; Yuan, J. Y.; Yuan, W. Z.; Sui, X. F.; Wu, S. Z.; Li, Z. L.; Shen, D. Z. *J. Magn. Magn. Mater.* **2009**, *321*, 2799.

(26) Zhou, L. L.; Yuan, J. Y.; Yuan, W. Z.; Zhou, M.; Wu, S. Z.; Li, Z. L.; Xing, X. H.; Shen, D. Z. *Mater. Lett.* **2009**, *63*, 1567.

(27) Laurent, S.; Forge, D.; Port, M.; Roch, A.; Robic, C.; Elst, L. V.; Muller, R. N. *Chem. Rev.* **2008**, *108*, 2064.

(28) Na, H. B.; Song, I. C.; Hyeon, T. *Adv. Mater.* **2009**, *21*, 2133.

(29) Gazeau, F.; Levy, M.; Wilhelm, C. *Nanomedicine* **2008**, *3*, 831.

(30) Dupin, D.; Fujii, S.; Armes, S. P.; Reeve, P.; Baxter, S. M. *Langmuir* **2006**, *22*, 3381.

(31) Di Corato, R.; Quarta, A.; Piacenza, P.; Ragusa, A.; Figuerola, A.; Buonsanti, R.; Cingolani, R.; Manna, L.; Pellegrino, T. *J. Mater. Chem.* **2008**, *18*, 1991.

(32) Sun, S. H.; Zeng, H. *J. Am. Chem. Soc.* **2002**, *124*, 8204.

(33) Pellegrino, T.; Manna, L.; Kudera, S.; Liedl, T.; Koktysh, D.; Rogach, A. L.; Keller, S.; Radler, J.; Natile, G.; Parak, W. J. *Nano Lett.* **2004**, *4*, 703.

(34) Sperling, R. A.; Pellegrino, T.; Li, J. K.; Chang, W. H.; Parak, W. J. *Adv. Funct. Mater.* **2006**, *16*, 943.

Table 1. Experimental Conditions for the Synthesis of Nanogels of Different Diameters^a

sample name	2-VP (g)	DVB (g)	[2-VP]/[DVB] Molar ratio	TEM diameter (nm)	DLS diameter (nm)	polydispersity index
NG197	0.754	0.013	71.6	197 ± 10	223 ± 60	0.073
NG142	0.505	0.013	48.3	142 ± 7	185 ± 51	0.035
NG110	0.250	0.013	23.7	110 ± 8	137 ± 29	0.028
NG75	0.101	0.013	9.5	75 ± 7	92 ± 20	0.022

^a By varying the molar ratio between the 2-VP and the DVB (column 4), while keeping all the other reaction condition constant, it was possible to tune the sizes of the nanogels from 41 nm to 197, as determined by statistical TEM measurements (column 5) on an average of 100 nanogel particles. The hydrodynamic diameters of the same samples, as measured by dynamic light scattering, (column 6) were clearly bigger. The low polydispersity index indicates uniform size distribution (column 7) (all measurements were conducted at pH 7.5).

added. After a reaction time of 3 h at room temperature under vigorous stirring, the unbound diamino-PEG molecules were removed by performing several washing steps on centrifuge tubes having a MWCO of 30 000.

2.4. Loading and Release Experiments of Diamino-PEG Conjugated Iron Oxide Nanocrystals in the Nanogel. The loading of IONPs in the nanogels was performed as follows: 3 mL of a solution of nanogel in water (0.053 w/v (g/mL) %) were mixed with 9 μ L of a solution of PEG-coated γ -Fe₂O₃ (the concentration of nanoparticles in this solution was equal to 14.5 μ M) and the resulting mixture was stirred for 24 h at pH 3.5 at room temperature. Under these conditions, the swollen nanogels started incorporating the IONPs. The pH of the solution was then increased slowly to 7 by dropwise addition of a solution of NaOH 0.1 M (a slight turbidity appeared as soon as the pH reached 5.25, indicating shrinkage of the nanogels). Soon after, the nanogels loaded with IONPs were separated from free excess of IONPs using a magnet: the solution was placed close to the magnet, and within 1 h, the nanogels loaded with nanoparticles were attracted toward it. The nanogels were characterized by TEM and by DLS measurements. For the release experiments, the pH of the nanogel solution was decreased again to 3.5 by dropwise addition of a solution of HCl (0.1 M), in order for the nanogels to swell again. For the quantification of the average number of IONPs loaded within the nanogel, the determination of iron concentration was carried out via elemental analysis on the loaded IONPs-nanogels (as explained more in detail in the paragraph of the 2.11).

2.5. Loading Experiment of Cy3-DNA in Nanogel and Subsequent Release. For the loading experiments of oligonucleotide sequences of 25 bases, 3 mL of nanogel solution (0.053 w/v (g/mL) %) were mixed with 9 μ L (100 pmol/ μ L) of Cy3-DNA solution and the pH was adjusted to 3.5 by addition of HCl 0.1 M. The sample was left to stir for 24 h at room temperature, and soon after, the pH was increased again to 7 by dropwise addition of a solution of NaOH 0.1 M, after which it was left to stir for additional 3 h. To remove the excess of free Cy3-DNA, the final solution was centrifuged on 100 000 MWCO amicon tubes at 3000 rpm. The process was repeated until all the free Cy3-DNA was washed away, as monitored by PL spectra on the filtered solution (5 to 7 washing steps on centrifuge tube of 4 mL were usually required). The free Cy3-DNA solution was collected on the lower part of the centrifuge tube, while the Cy3-DNA/nanogels were recovered on the upper side of the filter and were redispersed in 1 mL of water.

For the quantification of Cy3-DNA loaded within the nanogel, we have recorded the PL of loaded nanogel samples (both Cy3-DNA/nanogel and Cy3-DNA-IONP/nanogel). We have then extrapolated the Cy3-DNA concentration of those samples on calibration curves of photoluminescence vs Cy3-DNA concentration (PL/Cy3-DNA concentration). These were obtained by preparing standard solutions at known Cy3-DNA concentrations, in which we have simulated the matrix. In more detail, for building the calibration curve for the Cy3-DNA/nanogel sample, to each of the standards at different DNA concentrations we have added the same amount of nanogel that we had in our sample. Likewise, in order to build the calibration curve for the Cy3-DNA-IONP/nanogel sample, to each of the standards we have added an amount of nanogel and IONP at the same concentration that we had in our sample (Figure 8S, Supporting Information).

For the release experiment of the Cy3-DNA, 50 μ L of a solution of NaCl (5 M) were added to 1 mL of the above nanogel solution loaded with Cy3-DNA, and the pH was adjusted to 3.5. The sample was left under stirring for 72 h, and soon after the solution was centrifuged on an amicon tube of MWCO 100 000. PL spectra were recorded on fractions collected both on the upper part and on the lower part of the membrane.

2.6. Simultaneous Loading in Nanogel of Both Cy3-DNA and IONPs and Subsequent Release Experiments. To load IONPs and Cy3-DNA simultaneously within the nanogels, the same procedure as described above (to load IONPs and Cy3-DNA separately) was applied. The only difference in the present case was that 3 mL of nanogel in water (0.053 w/v (g/mL) %) was mixed together with 9 μ L of the Cy3-DNA solution (100 picomol/ μ L) and with 9 μ L of the IONPs solution (14.5 μ M), after which the pH was adjusted to 3.5 using HCl 0.1 M. Also, in this case the loading and the release were monitored by TEM and by PL.

2.7. Dynamic Light Scattering. Zeta potential and dynamic light scattering measurements (DLS) were performed on a Zetasizer Nano ZS90 (Malvern, USA) equipped with a 4.0 mW He-Ne laser operating at 633 nm and with an avalanche photodiode detector. Measurements were made at 25 °C in water. All the samples were filtered before analysis. 0.2 μ m filters were used for the nanogel alone, while for nanogel samples loaded with nanoparticles and Cy3-DNA solution, 0.5 μ m filters were preferred.

2.8. UV-vis Absorption, Photoluminescence (PL) Spectroscopy. UV-visible absorption spectra were measured using a Varian Cary 300 UV-vis spectrophotometer. Photoluminescence (PL) spectra were recorded on a Cary Eclipse spectrophotometer. To record the PL spectra of Cy3-DNA alone and in nanogel, the samples were excited at 500 nm.

2.9. Transmission Electron Microscopy. TEM images were recorded on a JEOL jem 1011 microscope operated at an accelerating voltage of 100 kV. TEM samples were prepared by dropping a dilute solution of nanogel in water on carbon-coated copper grids and letting the solvent evaporate. The reported TEM diameters were measured on an average of 100 particles.

2.10. Confocal Microscopy Imaging. Confocal microscopy images were acquired with an Olympus FV-1000 microscope, equipped with an argon laser source (488 nm excitation line) and a DM488/405 type dichroic filter. The fluorescence reading channel was set at 565 ± 25 nm.

2.11. Elemental Analysis. An inductively coupled plasma atomic emission spectrometer (ICP-AES) Varian Vista AX was used to measure the concentration of Fe and thus the concentration of IONPs. The samples were digested in the following way: they were dissolved in a concentrated acid solution (HCl/HNO₃ (3/1 v/v) and were left for 24 h, before performing elemental analysis. The Fe concentration was converted into nanoparticle concentration using a procedure described by us in a previously published paper.³⁵ In detail, the average diameter of the nanoparticles was assessed via statistical analysis on TEM images. The average number of Fe atoms per nanoparticle was determined by

(35) Deka, S.; Quarta, A.; Lupo, M. G.; Falqui, A.; Boninelli, S.; Giannini, C.; Morello, G.; De Giorgi, M.; Lanzani, G.; Spinella, C.; Cingolani, R.; Pellegrino, T.; Manna, L. *J. Am. Chem. Soc.* **2009**, *131*, 2948.

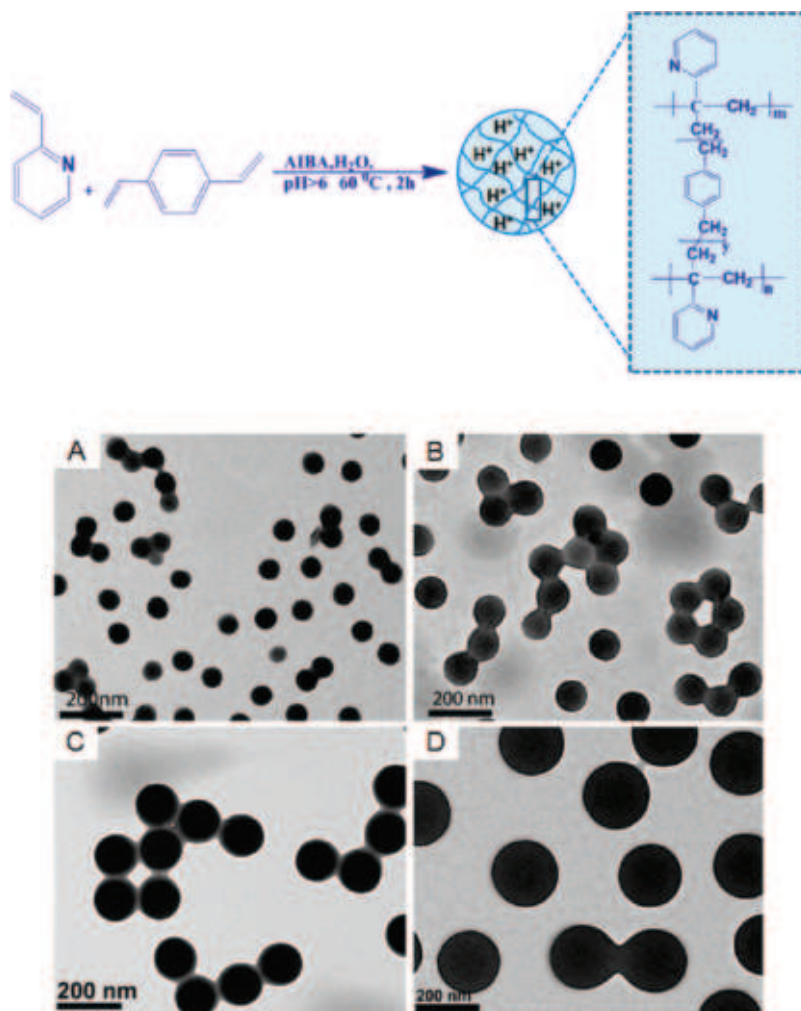


Figure 1. Sketch of the structure of the vinyl pyridine (VP) and divinylbenzene (DVB) units, which were employed for the synthesis of pH-responsive nanogels. TEM images of four different nanogel samples, with average diameters corresponding to (a) 75, (b) 110, (c) 142, and (d) 197 nm (the TEM diameters reported were estimated on an average of 100 nanogel particles; see Table 1, column 5).

building a structural model of the nanoparticle, with the same geometrical parameters of the nanoparticles as determined by TEM. Then, by knowing the average number of Fe atoms per nanoparticle and the total concentration of this species in solution, it is possible to determine the concentration of nanoparticles. In order to elucidate Fe^{3+} leakage in the condition of the loading experiment, we kept the IONPs at pH 3.5 overnight and we collected the supernatant solution, i.e., the solution separated from the IONPs by filtration on centricon filter. Finally, we measured the Fe concentration in both fractions.

3. Results and Discussion

3.1. Preparation of pH-Responsive Nanogels and Characterization of Their Swelling Behavior. The pH-responsive nanogels employed in this study are based on copolymers of divinylbenzene (DVB) and vinyl pyridine (VP) (sketch of Figure 1). They were synthesized following earlier reported procedures, with minor modifications.^{30,36} This type of surfactant-free emulsion polymerization procedure was first described by Loxley and Vincent,³⁶ who synthesized monodisperse cationic nanogels of 2-vinylpyridine by varying the amount of styrene (the hydrophobic monomer) and that of DVB (the cross-linker agent). The authors demonstrated a tight control over the particle size in the

range between 160 and 200 nm. According to a modified version of the Loxley and Vincent procedure, Dupin et al.³⁰ have reported the synthesis of sterically stabilized PVP latexes at much higher solid density, and with control over the diameter from 300 to 1000 nm. They used suitable stabilizer molecules, namely, monomethoxy-capped poly(ethylene glycol) methacrylate (PEGMA), and surfactant molecules named “336”.

Our interest in the present study was to control the size of the nanogels below 200 nm, which is a more suitable size range for the potential use of such nanogels as cargo system, as highlighted above. We were able to synthesize a series of nanogels in the size range between 40 and 200 nm, by reducing the monomer concentration of 2-VP, while keeping all the other parameters constant (Table 1 and Figure 1). Reducing the concentration of 2-VP corresponds to a decrease in the 2-VP/DVB molar ratio, or the same to an increase in the amount of DVB (the cross-linker monomer) per nanogel. The formation of smaller nanogels can be ascribed therefore to a higher degree of reticulation of the nanogel network. The smallest nanogels that we could prepare had a TEM diameter of about 40 nm (Figure 1S, Supporting Information).

For a given nanogel sample, the average diameter, as measured by DLS (Table 1, column 5), was slightly higher than that measured by TEM. This was expected, since the DLS measurements were carried out on hydrated nanogels. Moreover, the DLS

(36) Loxley, A.; Vincent, B. *Colloid Polym. Sci.* **1997**, *275*, 1108.

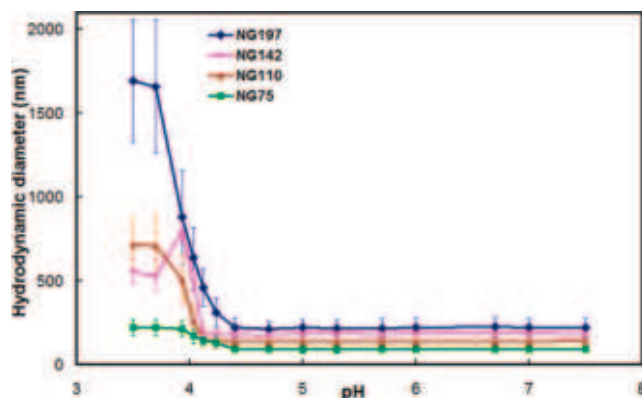


Figure 2. Swelling behavior of the nanogels. The DLS diameter is reported as a function of the pH (each measurement was carried out three times.) All nanogel samples exhibited a sharp swelling behavior below pH 4.3.

polydispersity indexes were low, confirming the uniformity in size distribution of the nanogels (Table 1, column 7).

It is also worth highlighting that in our preparation we ran the reaction for 2 h, while in previously reported methods the reaction time was 24 h.³⁰ We additionally observed that by increasing the reaction time from 2 to 24 h the size of the nanogel increased, but the final nanogel was mostly aggregated (Figure 2S, Supporting Information).

To investigate the swelling behavior of the various nanogel samples in water, the pH of each nanogel solution was lowered from an initial value of 7.5 by dropwise additions of an HCl solution. After an equilibration time of about 10 min, the nanogel diameters increased sharply at pH below 4.3, due to progressive protonation of the nitrogen of the 2-vinylpyridine residues³⁷ (Figure 2). Regardless of the starting size of the nanogels, the swelling occurred always at pH below 4.3. The various samples exhibited critical swelling transition at pH values between 4.3 and 3.9, depending on the ratio between 2-VP and DVB employed in the preparation of the nanogels (i.e., the degree of cross-linking of DVB).

The majority of the pyridine groups became protonated below pH 3.8, and the average diameters of the nanogels reached a maximum due to the electrostatic repulsions between the strongly cationic chains.

Above pH 4.5, the particles were in the swollen state, because of the absence of inner charges, and they behaved like conventional polymer latex particles.³⁷ The swelling of the nanogel particles was also confirmed by visual inspection, as the solution turned from turbid, milky-white to clear when the pH was decreased from 7 to 3.5 (Figure 3S, Supporting Information). Zeta potential measurements indicated a strong cationic character of the nanogels at pH 3.5, which is the pH at which the payload was usually loaded. However, even at pH 7 the nanogels retained a slightly positive charge (Table 2, Supporting Information).

3.2. Loading and Release Experiments of Iron Oxide Nanoparticles. For the loading and release experiments, a nanogel sample having average “TEM” diameter equal to 110 nm at pH 7 was employed (henceforward referred to as “NG110”), and the loading and release process of IONPs was monitored by TEM (Figure 3). After mixing the nanogels with IONPs (PEG-coated nanoparticles, 7 nm in diameter)^{32–34} and upon switching the pH from 7 to 3.5, the nanogel was turned into a swollen state (under

TEM, the edge of the nanogel was not sharply defined anymore; see Figure 3B). A gentle overnight shaking at room temperature was then followed by restoration of the solution pH back to 7 (by addition of NaOH), which induced the shrinkage of the nanogels, inside which the IONPs remained entrapped (Figure 3C).

By application of a magnet, the nanogels loaded with IONPs could be recovered and they were separated by the excess of free IONPs (Figure 3D), as the former were attracted faster than the latter to the magnet (Figure 3D). In order to achieve a complete cleaning of the loaded nanogel from the free IONPs, a second purification step on Sephadex column was performed. The incorporation of the IONPs in the nanogel induced an appreciable increase of the average nanogel diameter, as determined by TEM (in one sample, for instance, it varied from 110 ± 8 nm to 117 ± 12 nm).

DLS was additionally exploited to examine the behavior of the nanogels at each step of the procedure. Immediately after mixing the IONPs with the nanogel, at pH 3.5 the DLS diameter of the nanogel was around 480 ± 94 nm (Table 1, Supporting Information), which was lower than that of the nanogels when they were swollen at the same pH but in the absence of IONPs (713 ± 158 nm). This reduced swelling of the nanogels might be due to the ionic interactions in solution between the IONPs and the nanogels. After switching the pH of the same solution back to 7, the DLS diameters of the nanogels in the presence of the IONPs was 191 ± 8 nm, as opposed to the DLS diameter equal to 137 ± 29 nm for the empty nanogels (Table 1, Supporting Information). TEM characterization confirmed the presence of IONPs within the nanogel structure (Figure 3C). The nanogels loaded with IONPs could release their payload by switching the pH again from 7 to 3.5. Indeed, after 3 h at pH 3.5, most of the particles were released from nanogels, as confirmed by TEM (Figure 4).

In order to rationalize and understand the driving force for the loading, we have characterized the system in more detail by analyzing the surface charge of the individual units, namely, the nanogels and the IONPs, and that of the nanogels loaded with IONPs at various pH values. At pH 3.5, the surface charges of the swollen nanogels and those of the IONPs were both positive (zeta potentials were +56 mV and +8 mV, respectively), and at the same time, the nanogels were in the swollen state, which promoted the entrapment of the nanoparticles at their interior. We have also attempted to load the nanogels at pH 7 instead of pH 3.5. At this pH, the surface charge of the nanogels was still moderately positive, while that of the IONPs was negative. The negative charge is likely due to the charge balance at the surface of IONPs given by the sum of amino-PEG moieties and carboxyl-terminated groups of the polymer (zeta potentials are +28 and –42 mV, respectively; see Table 2, Supporting Information). Therefore, even if at this pH value the nanogels were swollen, one should expect a higher electrostatic interaction between the nanogels and the IONPs. We observed indeed that also after incubation under these conditions we could load IONPs within the nanogels (Figure 4S, Supporting Information). A loading experiment was attempted even at pH 10, at which the surface charge of the nanogel was only slightly positive (zeta potentials for the nanogels and for the IONPs were +15 and –42 mV); hence, the electrostatic interactions between the nanogels and the IONPs were weaker than at pH 7. In this case, we could still observe (by TEM) the adsorption of a few nanoparticles on the surface of the nanogels, but most nanogels had not been able to incorporate the IONPs (Figure 4S, Supporting Information).

For the quantification of IONPs loaded within the nanogel at the different pH values, the various samples were digested in HCl/HNO₃, and their iron content was estimated by means of elemental analysis, which allowed us to estimate quantitatively

(37) Fernandez-Nieves, A.; Fernandez-Barbero, A.; Vincent, B.; de las Nieves, F. J. *Macromolecules* **2000**, *33*, 2114.

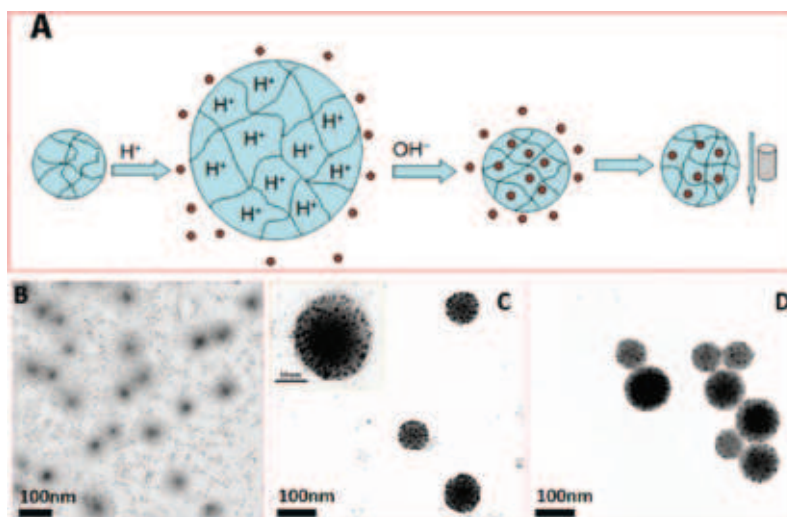


Figure 3. (A) Scheme of the loading of magnetic nanoparticles within the pH-responsive nanogels. Corresponding TEM characterization of the different steps: (B) at acidic pH the nanogels were mixed with the IONPs; (C) after 12 h, the pH was switched back to pH 7, such that the IONPs were entrapped within the nanogel network. (D) The application of a small magnet helped to remove most of the free IONPs in solution. A complete cleaning was achieved by performing an additional purification step on a Sephadex column.

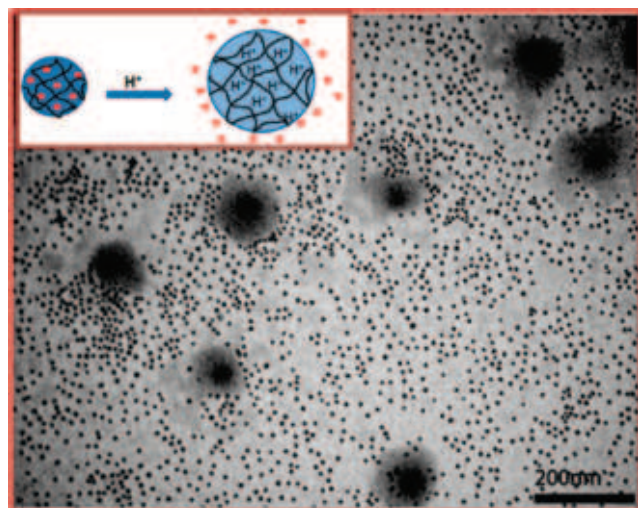


Figure 4. Release experiment of the IONPs. Switching the pH of the IONP-loaded nanogel solution from 7 to 3.5 induced the swelling of the nanogels and consequently the release of the IONPs entrapped within the polymer network.

the number of IONPs entrapped within the nanogels.³⁵ The highest concentration of IONPs was found in the beads loaded at pH 3.5, followed by those loaded at pH 7 and then by those at pH 10 (see Table 2S, Supporting Information). Those results were reproducible and provided a clear indication of the average loading efficiency of the nanogels. These data nicely correlate with the trend in IONP-loaded nanogel diameter (as estimated by the DLS), which is bigger for the gels loaded at pH 3.5, followed again by those loaded at pH 7 and at pH 10, respectively. This correlation suggests that the swelling behavior is the main driver for the encapsulation of IONPs, although a contribution due to electrostatic interactions between the nanogels and the IONP surface cannot be excluded.

Once the nanogels were loaded with IONPs, their surface charge became negative at pH 7. However, the trend in absolute values of surface charges was reversed in this case: it was higher for the nanogels loaded at pH 10, followed by those loaded at pH 7 and pH 3.5, respectively. This might likely be attributed to a

much lower fraction of nanoparticles adsorbed at the nanogel surface with respect to those trapped deeper in the network structure of the nanogel at pH 3.5 (the nanoparticles contributed with negatively charges).^{31,33}

3.3. TEM Characterization of the Entrapment of the IONPs within the Nanogels.

In order to confirm the entrapment of the IONPs, we carried out additional TEM characterization. Several bright field electron microscopy (BF-EM) images of a nanogel sample loaded with IONPs were taken at different tilts on a large angular range (from -55° to 0° , to 60°). Two BF-EM images of the same IONP loaded nanogel are shown in Figure 5A, B. Figure 5A corresponds to the specimen tilted at 0° (i.e., the plane of the sample is basically normal to the electron beam direction) and Figure 5B corresponds to the same sample tilted by 60° . From the high-tilt image, two main considerations can be made: first, the projection of the light gray zone (observed circular at 0° tilt) is elliptical at high tilt, indicating that the polymer behaves as a sphere pressed on the plane of the carbon grid in a direction perpendicular to it. Second, at high tilt the spherical nanoparticles are located inside the contours of the light-gray zone that corresponds to the polymer. This suggests that the IONPs were embedded within the first few polymer layers. If, on the other hand, the IONPs were simply attached on the surface of the polymeric crushed sphere, they should have appeared also on the external side of the light-gray zone's contour.

In order to localize the radial distribution of IONPs within the nanogels, we have performed TEM on the cross sections of the IONP-loaded nanogels, which had been embedded within a paraffin resin. The sections analyzed had thickness of 70 nm (Figure 5C) and 50 nm (inset of Figure 5C), respectively. As observed in Figure 5C, most of the IONPs were densely packed at the edge of the beads, within the first layers of the polymer, and only few of them were found deep inside in the nanogels. It is interesting to compare these results with the cross-sectional images of the same type of nanogel used as template for the gold synthesis reported by Nakamura.³⁸ In that case, as the gold nucleation occurred only at the surface on the TEM cross sections, no nanoparticles were found within the nanogel.

(38) Kensuke Akamatsu, Takaaki Tsuruoka, Hidemi Nawafune, Syuji Fujii Yoshinobu Nakamura *Langmuir* **2009**, [Online early access].

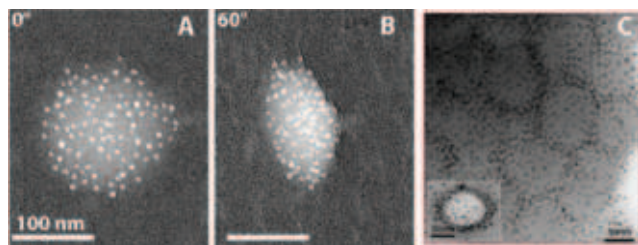


Figure 5. (A,B) Inverted bright field electron microscopy images of a sample of nanogel loaded with IONPs. (A) corresponds to the specimen tilted by 0° and (B) corresponds to the same sample tilted by 60° under the electron beam. On the tilted sample, the light gray edge, corresponding to the polymer, covers the bright spots, which are the magnetic nanoparticles. (C) Cross-sectional TEM image of nanogel loaded with IONPs recorded on a section having a thickness of 70 nm (while for the inset the section thickness is of 50 nm).

It is also worth noting that our IONP-loaded nanogels can be kept for months at pH 7 and at room temperature without observing leakage of IONPs. This is likely an indication of the entrapment of the particles within the polymer networks. Taken all together, these results point to the entrapment and localization of the IONPs within the first layers of the polymer network in the nanogel. This configuration rationalizes the loading and thus the consequent release of the IONPs that we observe. Our results are in agreement with those reported by Jang et al. who used hydrogel spheres based on a thermoresponsive polymer PNIPAM and pH-responsive units 4-vinylpyridine to entrap CdTe nanoparticles. In that case, however, the authors provided other indirect proofs that pointed to the nanoparticle entrapment.³⁹

Additionally, it is also worth noticing that, if the IONPs are left at pH 3.5 overnight, no change in the composition or shape of the nanoparticles was observed, and no leakage of Fe^{3+} was detected in the acidic medium.

On the basis of the above results, we decided in all the subsequent experiments to load the IONPs at pH 3.5, as in these conditions we achieved the highest efficiency of nanoparticle loading.

3.4. Loading and Release Experiments of Oligonucleotides.

We have applied the procedure described above to load and release short oligonucleotide sequences of about 25 bases. In order to detect the loading and release process, we have employed a sequence bearing at the 5' end the fluorophore molecule Cy3, which allowed us to track the presence of the Cy3-DNA within the nanogel by photoluminescence (PL) spectroscopy (Figure 6) and UV-visible absorption spectroscopy (Figure 5S, Supporting Information). Figure 6 shows the PL spectra of free Cy3-DNA (red line) and of the nanogels loaded with Cy3-DNA (black line), after the solution was purified from the excess Cy3-DNA (see section 1.5 of the Supporting Information). When loaded in the gels, the Cy3-DNA exhibited a PL spectrum that was red-shifted by about 3 nm with respect to that of free Cy3-DNA.

The signal recorded was due only to the Cy3-DNA loaded into the nanogel and not to free Cy3-DNA. As proof, we have recorded the PL spectra after each washing step (the solution recovered from the lower part of the centrifuge filter used for the purification). The signal of free Cy3-DNA in this solution was progressively reduced, and after 6 washing steps there was no PL signal from free Cy3-DNA. These data clearly confirmed the loading of the Cy3-DNA within the nanogel. The Cy3-DNA loading was further corroborated by DLS measurements, since an increase in the

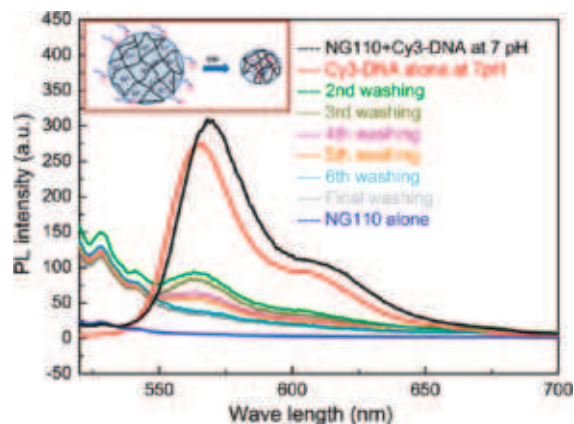


Figure 6. PL spectrum of Cy3-DNA loaded within the nanogel after the cleaning procedure had been applied (black curve); PL spectrum of the free Cy3-DNA (red curve) and starting nanogel solution (blue curve). The plot reports in addition the PL spectra of aliquots collected at the different washing steps, as well as those of the loaded nanogel solution, Cy3-DNA and nanogel only. After 6 washing steps, the free Cy3-DNA was removed completely from the solution containing the loaded nanogels. The inset shows a scheme of the loading of Cy3-DNA within the nanogel.

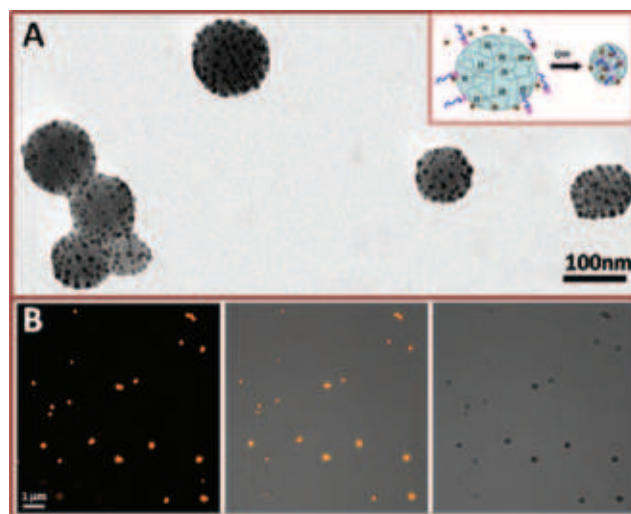


Figure 7. (A) TEM characterization of nanogels loaded simultaneously with IONPs and Cy3-DNA. (B) Confocal microscopy characterization of the sample shown in A. The fluorescent signal of the DNA bearing the Cy3 marker (left panel) is colocalized with the spots seen in the phase contrast image of the nanogel (right panel). The central panel is a merged image of both panels.

average nanogel hydrodynamic diameter was observed after loading (i.e., from 137 ± 29 nm to 165 ± 63 nm for a nanogel sample loaded at pH 3.5 and measured at pH 7 (the dye signal is quenched at pH 3.5); see Table 1S, Supporting Information).

3.5. Simultaneous Loading and Release of Oligonucleotides and IONPs. In a third series of experiments, we have loaded simultaneously IONPs and the oligonucleotide sequences in the nanogels, by mixing together solutions of IONPs, Cy3-DNA, and nanogels, according to the protocols described above. The simultaneous loading of IONPs and Cy3-DNA was confirmed by a combination of TEM measurements, by which we could locate the IONPs in the nanogels, and by confocal microscopy, by which we could identify the PL signal from the Cy3-DNA within the nanogel (Figure 7).

(39) Kuang, M.; Wang, D. Y.; Bao, H. B.; Gao, M. Y.; Mohwald, H.; Jiang, M. *Adv. Mater.* **2005**, *17*, 267.

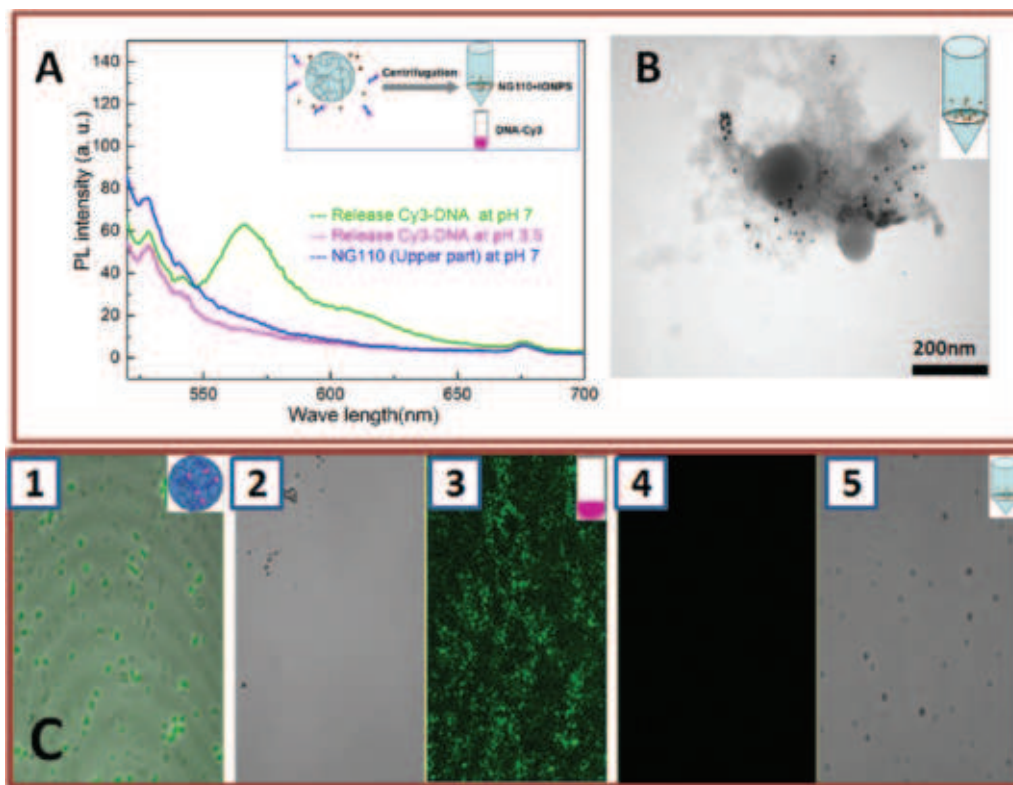


Figure 8. (A) PL characterization of the release process. The inset is a sketch showing the separation on the centrifuge filter between the IONPs and nanogels from the small Cy3-DNA molecules. The green curve corresponds to the Cy3-DNA signal recorded on the lower side of the centrifuge filter after 72 h at pH 7, while the blue curve corresponds to the PL signal recorded on the upper side of the filter. The violet curve corresponds to the PL of Cy3-DNA recovered on the lower side of the centrifuge filter (at pH 3.5, the dye signal is quenched). (B) Corresponding TEM characterization of the sample recovered on the upper side of the membrane. The IONPs released by the nanogels are retained on the upper side of the filter. In addition, the nanogel structure appears damaged after the simultaneous release of both cargo elements. (C) Confocal characterization of the release process: the image shown in C1 is obtained by merging the fluorescent and the phase contrast images of the same area of the nanogels loaded with IONPs and Cy3-DNA, before the release. C2 and C3 correspond, respectively, to the phase contrast and fluorescent signal of Cy3-DNA released by the nanogel and collected at the bottom side of the filter. C4 and C5 correspond, respectively, to the fluorescent and phase contrast images of the same areas of the sample collected on the upper side of the filter at pH 7. After the release, while the nanogels were still visible (C5), no signal was recorded in the corresponding fluorescent channel (C4), indicating the completed release of DNA by the nanogels.

Despite the confocal images were taken by working at the resolution limit of the confocal setup (hence the nanogel particles could not be focalized), on dilute solutions these fluorescent spots were colocalized with spots in the corresponding phase contrast images, and which could be ascribed to the nanogels (Figure 7B).

Additionally, under the same experimental conditions the TEM and DLS diameters of the nanogels simultaneously loaded with IONPs and Cy3-DNA were bigger than those of the corresponding nanogels loaded either with Cy3-DNA or with IONPs alone (Supporting Information Table 1S). As an example, the diameter of the loaded nanogel increased to 250 ± 50 nm (by DLS) and the zeta potential became negative (-10.5 ± 1.5 mV). Additional PL characterization of the nanogels loaded with Cy3-DNA and IONPs was performed and confirmed the presence of DNA (Supporting Information Figure 6S).

In order to release the multicargo, the nanogels were first equilibrated at pH 3.5 in a solution containing 140 mM NaCl. To achieve complete release of the DNA from the nanogel, it was necessary to keep the nanogel at pH 3.5 for 72 h. After this time, we first separated the Cy3-DNA from the nanogel and IONP portions by using centrifuge filters. By choosing an appropriate pore size for the membrane, we could retain the IONPs and the nanogel on the upper side of the membrane, while molecules like Cy3-DNA (see inset Figure 8A) were able to pass through the

membrane. By recording the PL spectra on the fraction collected at the bottom side of the membrane, we could verify the release of the oligonucleotides (Figure 8A). It is worth noting that after 24 h we could still record the fluorescent signal, not only on the lower part of the centrifuge tube, but also on the upper part of the membrane (data not shown). Only after 72 h was a complete release of the DNA achieved, since at this time no further PL signal was detected on the upper side of the membrane.

These data were also supported by confocal microscopy observations on the various aliquots that had been recovered from each side of the filter (Figure 8C). When both Cy3-DNA and the IONPs were packed within the nanogels, in the confocal fluorescence image the spots appeared point-like. In addition, they were colocalized with spots in the phase contrast image (Figure 8C1). After the complete release, on the upper side of the filter it was still possible to capture the phase contrast image of the nanogel, while no fluorescence could be recorded in the corresponding channel (Figure 8C4 and C5). The portion recovered from the lower part of the membrane still showed a fluorescent signal. This signal, however, was not clumped any more in point-like regions, but was rather distributed homogeneously in the whole field of view. This could be interpreted as arising from the Cy3-DNA that had been released from the nanogels (Figure 8C3). In the corresponding phase contrast image, the nanogels could not be seen. TEM analysis of the part retained on the upper side of

the filter indicated the presence of both released IONPs and nanogels, but the nanogels appeared disrupted in this case (Figure 8B). These findings are somehow unique, since in all previous experiments involving either DNA or IONPs, unloading the nanogels had retained their original shape. Apparently, the simultaneous release of both DNA and IONPs was responsible for this effect.

Such irreversible swelling during unloading of both DNA and IONPs deserved a deeper analysis. We tested therefore the effect of the pH on the swelling of nanogels (both with and without the cargo) by switching the pH of the medium from 8 to 3 and back. Swelling of the empty nanogels was reversible, since the curve describing their size dependence on the pH, when this was cycled from 3.5 to 8 and back, did not show any hysteresis (Figure 7S A, Supporting Information). These results are in agreement with previously published data.³⁶ A similar behavior was also observed in the case of nanogels loaded with IONPs (Figure 7S C, Supporting Information), while an appreciable hysteresis was recorded on the nanogels loaded with Cy3-DNA (Figure 7S B, Supporting Information).

The situation was drastically different when the nanogels were filled with both IONPs and Cy3-DNA (Figure 7S D, Supporting Information). This time the curve describing the size dependence on the pH, when this was increased from 3.5 to 8 (the “forward curve”), did not overlap with the corresponding curve when the pH was decreased from 8 back to 3.5 (the “backward curve”). Starting from pH 6, the nanogel size from the backward curve was always higher than that from the forward curve, pointing to a modification in the structure of the nanogel after it was used as cargo. These data, together with the TEM characterization, are indicative of the structural degradation of the nanogel after the simultaneous release of Cy3-DNA and IONPs (Figure 8).

For the quantification of DNA loaded within the nanogel, calibration curves of PL/[DNA] (photoluminescence/DNA concentration) were used (Figure 8S, Supporting Information). Using those curves, we found that, when only DNA was loaded within the nanogel, the amount of DNA that could be actually loaded corresponded to about 16% of the initial DNA added (which corresponded to an amount of DNA equal to 0.048 pmol/ μ L for 0.053 g weight of nanogels). On the other hand, the amount of DNA loaded in the case of simultaneously loading of DNA and IONPs was slightly higher and corresponded to about 20% of the initial DNA added (0.0623 pmol/ μ L of DNA for 0.053 g weight of nanogels).

3.6. Salt Effect on the Swelling of the Loaded Nanogels.

The swelling behavior of the nanogel was affected by the presence of salt in solution (Figure 9). We report here only the data related to nanogels loaded with IONPs. At pH 8, for instance, the size of the loaded nanogels was not altered significantly by the presence of salt. At pH 7.4, on the other hand, the loaded nanogels in 100 mM and 200 mM NaCl solutions were bigger than those loaded in plain water, by about 50 and 70 nm, respectively. At pH 6.5, the loaded nanogels in 100 mM and 200 mM NaCl solutions were affected significantly by the presence of salt in solution, since an increase in size of 130 and 150 nm, respectively, as compared to the sample of nanogel in water was recorded.

At pH 3.9, the differences in size were even more remarkable: the nanogels loaded with IONP in 200 mM NaCl were again the biggest (their diameter was around 850 nm, which corresponded

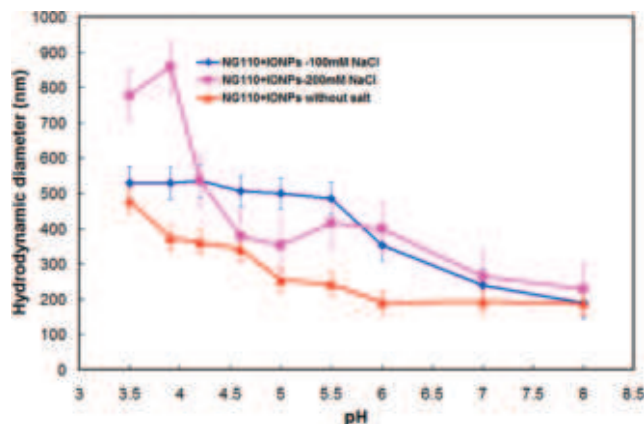


Figure 9. Salt effect on the swelling behavior of nanogels loaded with IONPs in plain water (red curve), 100 mM NaCl (blue curve), and 200 mM NaCl (violet curve).

almost to their swelling limit), followed by those loaded at 100 mM (529 nm), and was still 373 nm for the nanogel in water.

It has been reported by others⁴⁰ that on the vinyl pyridine–divinyl benzene-based nanogels, the addition of salts reduces the screening effect of the charges, resulting in a reduced swelling of the nanogels. The higher the amount of salt added, the stronger the screening effect is, and thus the lower the extent of swelling of the nanogel. Also, in our case, when the nanogels were loaded with IONPs, the swelling behavior in the presence of salt had a trend in the pH range from 7 to 4.2 that was similar to that of previous reports. Namely, the addition of 200 mM NaCl resulted in a reduced swelling with respect to 100 mM. The difference occurred for the swelling of the IONP-loaded nanogel below 4.2 in 200 mM, which is bigger than that in 100 mM. The IONPs have charged groups at their surface, and those groups can coordinate counterions in their surroundings. This results in a high local ionic strength that can break the nanogel structure and consequently increase the DLS diameter of the polymer. This behavior has been confirmed by TEM images of the nanogel under these conditions (data not shown).

The different diameters of the nanogels in a solution 100 mM NaCl indicate that the leaking of the IONPs occurred already at pH close to 6.5 (which is actually the pH of the extracellular tumor environment), while no appreciable leakage was observed at pH 7.4 (which is the pH of the blood) (Figure 9).

4. Conclusions

In this work, we have reported the fabrication of a multivalent nanosystem based on a class of functional molecules known as stimuli responsive polymers, which can work as cargo system for gene (or drug) delivery, and which can entrap at the same time inorganic magnetic nanoparticles. Differently from previously reported studies, the magnetic nanoparticles in this work are not covalently linked to the gel networks, and thus they can be loaded and released by tuning the pH. The full characterization provided when only DNA or IONPs or a combination of them were employed has allowed us to understand both the mechanism by which the different payloads are retained within the gel and the release process as a function of the pH and of the salt concentration.

The system developed in this work, especially in the case when both DNA and IONPs have been loaded, has interesting features and might find application as a therapeutic agent. It can act as a heat mediator for performing hyperthermia, as gene delivery system (for instance in si-RNA treatment), and at the same time

(40) Fujii, S.; Dupin, D.; Araki, T.; Armes, S. P.; Ade, H. *Langmuir* **2009**, *25*, 2588.

as an imaging contrast agent in MRI. The magnetic nanocarriers developed appear to have the right geometry for performing those tasks. Preliminary studies by other groups^{41–43} have shown indeed that clustering of IONPs (like in our case when they are loaded in the nanogels) improves the relaxivity signals recorded with respect to individual magnetic nanoparticles. On the other hand, hyperthermia seems more efficient when the magnetic nanoparticles are not encapsulated within a matrix, but they are freely delivered to a certain target site.²⁹ Our system appears to have the right features for such purposes. When circulating in a medium with pH below 7.4, like blood, the nanogels will be in a packed configuration, allowing for a better enhancement of the MRI signal from the IONPs. On the other hand, once the nanogels will be delivered to a compartment with a pH below 6.5, like the extracellular tumor environment, they would begin to swell, and thus they would release the IONPs. The hyperthermia treatment could be therefore performed on the IONPs, once they will be delivered into the extracellular tumor environment, where the pH is around 6.5. The further uptake by tumor cells would allow the system to experience the different pH of the intracellular compartments. For such a purpose, cellular studies are now under investigation in our laboratory.

(41) Nasongkla, N.; Bey, E.; Ren, J. M.; Ai, H.; Khemtong, C.; Guthi, J. S.; Chin, S. F.; Sherry, A. D.; Boothman, D. A.; Gao, J. M. *Nano Lett.* **2006**, *6*, 2427.

(42) Taboada, E.; Solanas, R.; Rodriguez, E.; Weissleder, R.; Roig, A. *Adv. Funct. Mater.* **2009**, *19*, 2319.

(43) Fresnais, J.; Berret, J. F.; Petesic, B. F.; Sandre, O.; Perzynski, R. *Adv. Mater.* **2008**, *20*, 1.

Additionally, it is worth noting that the nanogels developed by us could also work as a targeting tool to deliver the payload with a spatial and temporal control. The presence of magnetic nanoparticles allows spatially controlled delivery, since the nanogels feel an externally applied magnetic field and thus might be attracted to specific locations of the body, where the magnetic field will be placed. Temporally controlled delivery will be ensured by the variations in pH that the nanogels will sequentially experience during their journey (hence by the response of the nanogels to these variations) in the various body/cellular compartments. The synergy between both effects might allow a more efficient delivery of the nanogel cargos.

Acknowledgment. This work was supported in part by the European project Magnifyco (Contract NMP4-SL-2009-228622). We thank Mario Malerba for TEM sample preparation and Sergio Marras for helpful discussion.

Supporting Information Available: Experimental details; two tables summarizing the DLS and TEM diameters and the zeta potential measurements; additional TEM characterization images of the nanogels, additional PL and absorption measurements of the nanocarriers and swelling behavior of different loaded nanogel solution in the decreasing and increasing pH profiles; PL/[Cy3-DNA] calibration curves. This material is available free of charge via the Internet at <http://pubs.acs.org>.

Multi-functional magnetic hydrogel: Design strategies and applications

Fangli Gang , Le Jiang, Yi Xiao, Jiwen Zhang, Xiaodan Sun 

First published: 06 May 2021

<https://doi.org/10.1002/nano.202100139>

Abstract

Hydrogel is one of the hottest biomaterials in recent years. Especially, magnetic hydrogels (MHs) prepared by combining unique magnetic nanoparticles (MNPs) with hydrogels have attracted wide attention due to their excellent biocompatibility, mechanical properties, absorbability and rich magnetic properties (magnetocaloric, magnetic resonance imaging and intelligent response, etc.). However, the current literature mainly focuses on the application of MHs, without fully understanding the relationship between the design strategies and applications of each function in MHs. This review highlights six major functional properties of MHs, including mechanical properties, adsorption, magnetocaloric effect, magnetic resonance (MR) imaging, intelligent response and biocompatibility. Principles and design strategies of each performance are thoroughly analyzed. Furthermore, the latest applications of MHs in biomedicine, soft actuators, environmental protection, chemistry and engineering in recent 5 years are introduced from the perspective of each function. In the carefully selected representative cases, the design strategies and application principle of multi-functional MHs are detailed, respectively. The classical fabrication processing of MHs is summarized. At last, we discuss the unmet needs and potential future challenges in MHs development and highlight its emerging strategies.

1 INTRODUCTION

Hydrogels are a highly swollen three-dimensional (3D) polymer networks synthesized by hydrophilic monomers, which can be considered as polymer-reinforced water. Hydrogels with unique physicochemical properties, such as excellent softness, water content, biocompatibility, bioactivity, etc., provide a strong candidate material for many fields including biomedical and environmental engineering.^[1] Various biomimetic hydrogels have been developed to mimic natural hydration microenvironments and successfully applied in tissue engineering and cancer treatment.^[2] Hydrogels with specific microstructures (anisotropic, tubular, etc.) have also been developed to deliver drugs/cells and provide three-dimensional biochemical

microenvironments for supporting cell growth.^[3] Despite great progress has been made, conventional hydrogel systems still have some limitation. In particular, insufficient functionality severely limits its practical application potential in many fields. Therefore, it is a hot research topic to endow hydrogels with functionality.

With the rapid development of permanent magnet materials and electromagnetic technology, magnetic field as an important physical field is widely used in scientific research. The magnetic field can provide a feasible and flexible strategy for inducing the functionality of hydrogels. Thus, MHs composed of magnetic particles (γ -Fe₂O₃, Fe₃O₄, etc.) and hydrogel matrix have attracted more and more attention for their biocompatibility, controllable structure, high adsorption and rich magnetic properties (magnetocaloric, MR imaging and intelligent response, etc.).^[4] For example, MNPs endow hydrogels with remotely controllable characteristics, which can be used in drug delivery,^[5] local hyperthermia,^[6] magnetic/thermal drive,^[7] tissue image enhancement,^[8] adsorption, separation and purification,^[9] and so on. In addition, stimulus-responsive MHs have broad application prospects in soft robot.^[10]

As everyone knows, the versatility of materials will enrich their potential in practical applications. In turn, different applications can also dictate the material desired properties. Therefore, in this paper, from the design concepts and application strategies of multi-functional MHs (Figure 1), we review the latest research progress on MHs. Six main functional properties of MHs are highlighted: mechanical properties, adsorption, magnetocaloric effects, MR imaging, intelligent response and biocompatibility. Focusing on its specific functions, the potential applications of MHs in biomedicine, environmental protection, soft actuators, chemical catalysis and engineering are further analyzed. Finally, the common preparation methods of multi-functional MHs are systematically reviewed.

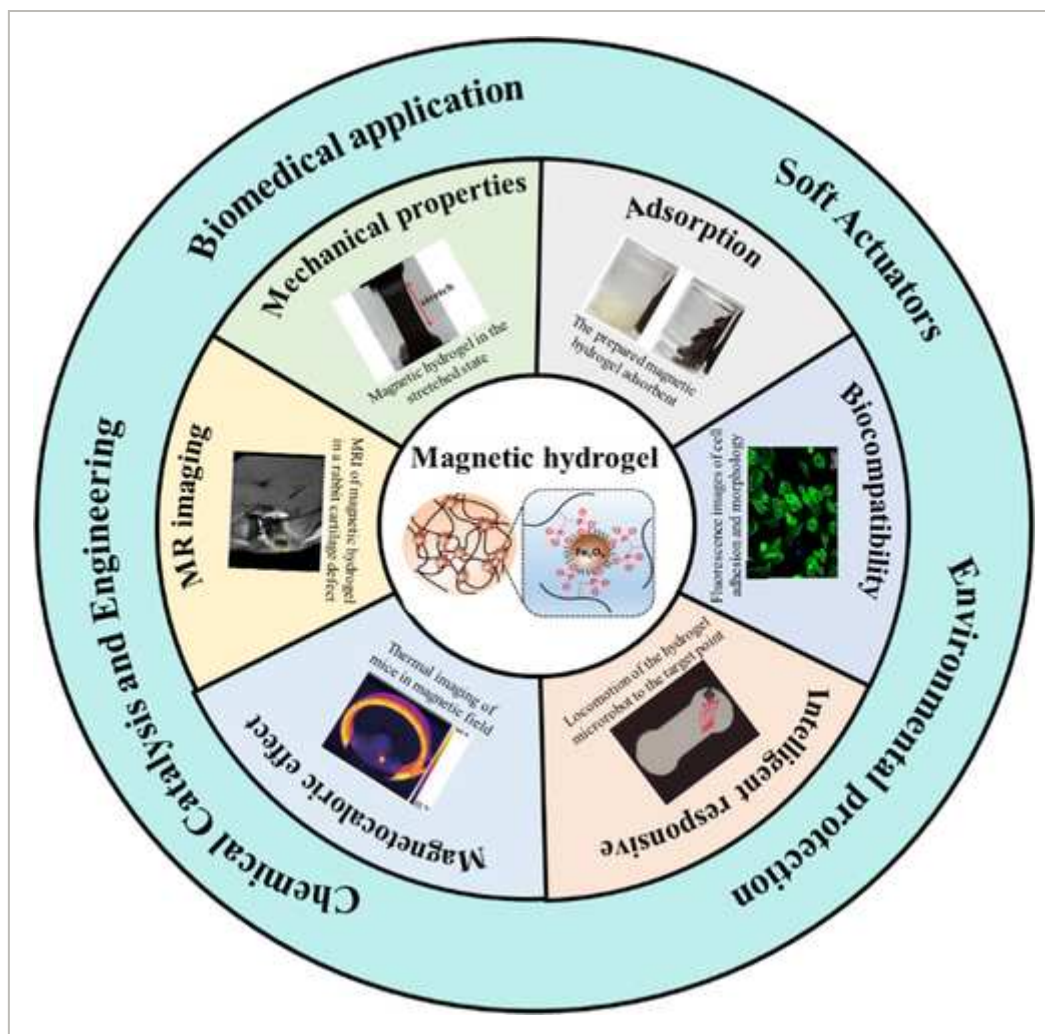


FIGURE 1

[Open in figure viewer](#) | [PowerPoint](#)

Schematic illustration of multifunctional MHs and their applications

2 DESIGN STRATEGIES AND APPLICATIONS FOR MULTIPLE FUNCTIONALITIES OF MAGNETIC HYDROGELS

MHs are generally formed by the interaction between magnetic components ($\gamma\text{-Fe}_2\text{O}_3$, Fe_3O_4 , etc.) and hydrogel matrix through non-covalent or covalent bonds. This combination simultaneously absorbs the advantages of hydrogel (high water content, flexibility, etc.) and magnetic particles (smart response, etc.). There are differences in raw material selection, design strategies and application fields of MHs with specific performance. For example, in most literatures, the composite MNPs in MHs are generally spherical nanoparticles with a diameter of 1~20 nm, and some MNPs with significant magnetocaloric effect have a ring shape.^[11] Biomedical MHs focuses on biocompatible hydrogel matrix, while engineering application MHs uses cheap and readily available materials. Therefore, it is of great significance to study MHs

from the six functions of mechanical properties, adsorption, magnetocaloric effect, magnetic resonance imaging, intelligent response and biocompatibility.

In general, the good dispersity of MNPs in the matrix is the fundamental factor in preparing high-performance composite gels. However, most MNPs have a high specific surface area and can easily agglomerate (Figure 2A). The MHs obtained by simply compounding MNPs and hydrogel matrix often exhibits uneven network structure and unstable properties. Notably, the introduction of functionalized MNPs or special hydrogels components can effectively solve these problems. Both of these aims to increase the dispersity and crosslinking degree of the MNPs in the hydrogels (Figure 2B,C). The difference is that the former focuses on the modification of MNPs (Fe_3O_4 , MnFe_2O_4 , etc.), mainly including increasing functional groups (e.g., carboxylic groups),^[12] chemical loading,^[13] coating (e.g., tannic acid),^[14] etc. While the latter usually selects specific hydrogel components with a large number of active functional groups (carboxyl, hydroxyl, etc.), which can coordinate with Fe ions and easily gelled. Polyacrylamide,^[15] polyvinyl alcohol,^[16] hyaluronic acid,^[17] fibrin,^[18] and nano-cellulose are commonly used MHs with high coordination activity. The MHs obtained by these two methods have uniform structure, stable performance and enhanced mechanical properties. Under the action of long-range magnetic field, functional MNPs exhibit remarkable intelligent response (mobility), magnetocaloric effect and MR imageability. The hydrogel matrix, as a structural and mechanical support, is also affected by MNPs to produce corresponding behaviors, including deformation, movement, thermogenesis and MR imaging. By regulating the types or proportions of MNPs and hydrogel matrix to control multiple functions of MHs, so as to promote its fascinating application prospects in different fields.

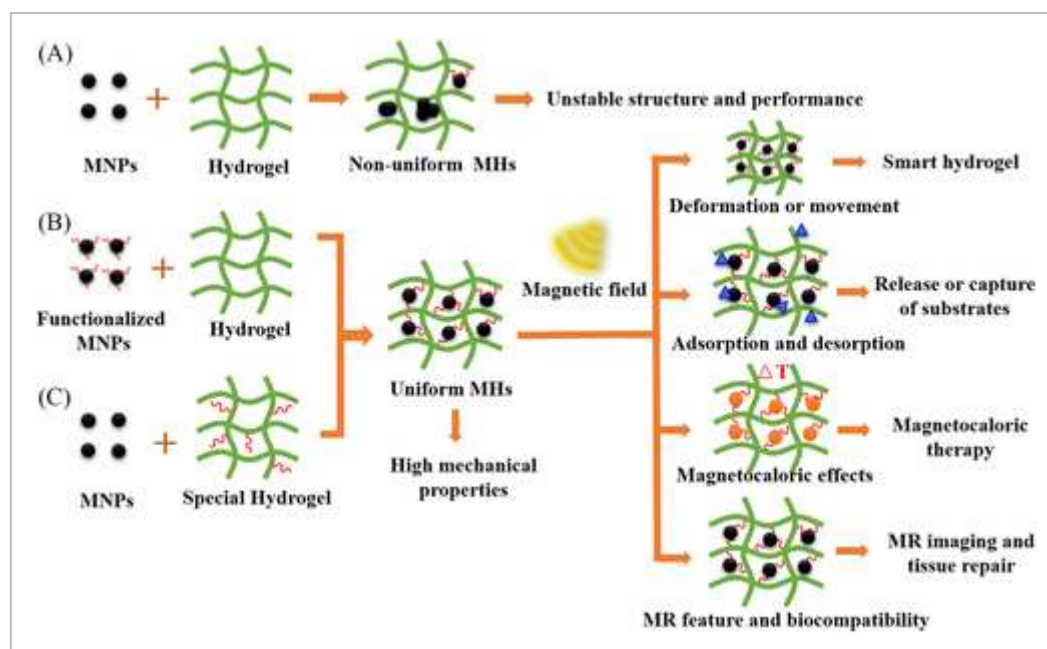


FIGURE 2

Design strategies of MHs. Structure and properties of MHs prepared by A, MNPs + hydrogel, B, functionalized MNPs + hydrogel and C, MNPs + special hydrogel

2.1 Mechanical properties

Mechanical property is a set of commonly used indexes, which is the resistance to failure of materials under load (such as tension, compression, torsion, impact, cyclic load, etc.). Generally, the mechanical properties of hydrogels mainly include strength, stiffness, toughness and fatigue strength. For hydrogels, their mechanical properties determine their usage and service life.

At present, there are mainly four ways to improve the mechanical properties of hydrogels: (1) the “sacrifice bond” is introduced to dissipate energy effectively, thereby enhancing the mechanical properties of hydrogels. A variety of non-covalent interactions such as hydrogen bonding, complexation, supramolecular recognition and hydrophobic association have been applied to prepare high-strength hydrogel.^[19] The most representative example is double network hydrogels. (2) The “pulley effect” is used to reduce the internal stress in the crosslinking network and greatly enhance the mechanical properties of the hydrogels. Topological hydrogel is a kind of material with high strength by using O-shaped crosslinking ring which can slide freely on the polymer chain as a controllable crosslinking point.^[20] (3) the fracture and reconstruction of some reversible non-covalent bonds will also give hydrogels high-strength,^[21] while providing certain recoverability and self-healing properties. (4) The introduction of nanoparticles has been shown to significantly alter hydrogel mechanical properties.^[22] This paper focuses on MNPs composite hydrogel materials. On the one hand, the rigid MNPs can not only improve the compression modulus, storage modulus and thermal stability of the composite hydrogel, but also adjust the water absorption, retention, saturation magnetization and pore size of the MHs by changing its content. On the other hand, the reversible interaction between MNPs and hydrogel components can endow MHs with good self-healing, thermal stability, shear-thinning, and mechanical properties (rigidity and viscoelasticity). Therefore, the design and application of high-performance MHs with intrinsic magnetism have received much attention from scientists.

High-strength MHs, as an important branch of nanocomposite hydrogels, have important applications in biomedical and soft actuators.^[23] Biomaterials are a promising strategy for repairing damaged or diseased tissue. In general, in order to ensure the clinical safety of biomaterials, rigorous in vitro biological evaluation must be carried out in advance. In vitro simulation, hydrogels can be used as mechanical support for cell growth and differentiation. Unlike most in vitro cell culture 2D substrates (petri dishes, porous plates), hydrogels provide a 3D microenvironmental cell experience,^[24] better mimicking the in vivo biological environment.

Up to now, a variety of MHs have been used as multi-functional in vitro culture platform to explore the effects of different conditions (e.g., magnetic field and hyperthermia) on cell function and morphology.^[25] Gu et al. reported a magnetic polyacrylamide hydrogel with cell adhesion microarray interface,^[25] which can effectively promote the formation of multicellular spheroids. It is considered as a prevailing tool to study the microenvironmental regulation of therapeutic problems and tumor cell physiology. In addition, as a polymer material most similar to biological tissue, hydrogels can be used as scaffolds for tissue engineering to repair or replace damaged tissues. As one of the three key elements of tissue engineering, it is very important for scaffolds to have excellent mechanical properties. In particular, for osteochondral repair materials, excellent compressive and anti-fatigue properties ensure that they can withstand repeated mechanical stress without being damaged, so as to steadily continue to exercise their biological functions. However, it is still a great challenge to develop MHs that match the mechanical properties of normal tissues for repairing osteochondral defects in situ.

2.2 Adsorption

As a highly absorbent and high water-retaining material, 3D network hydrogels have been widely applied in many fields, such as food preservation, drought resistance in arid areas. Moreover, hydrogels have a broad application prospect in wastewater treatment by virtue of their high adsorption capacity.^[26] Heavy metals (Pb, Cu, Cs, etc.), organic compounds (pesticides, etc.) and dyes are all water pollutants causing worldwide environmental problems. These pollutants are non-biodegradable, carcinogenic and highly toxic and should be removed from wastewater prior to disposal. Compared with traditional hydrogels, MHs, as an environment-friendly 3D nanomaterial with high physical strength, high adsorption rate and renewability, has attracted increasing attention in wastewater treatment.^[27] As shown in Table 1, the combination of magnetic additives (such as magnetite) and hydrogel matrix can simultaneously adsorb contaminants such as heavy metal ions and dyes. Some MHs have a removal rate of more than 99.5%. Moreover, the optimized MHs has high-sensitivity, high-selectivity, fast-adsorption and reusability.

TABLE 1. Typical examples of magnetic hydrogels successfully applied in the removal of heavy metals, organic compounds, inorganic salts and dyes

Magnetic additive	Hydrogel matrix	Contaminant	Remarks ^a	Ref.

Magnetic additive	Hydrogel matrix	Contaminant	Remarks ^a	Ref.
		and congo red)	g ⁻¹ congo red	
Iron oxide nanoparticles	Prussian blue/polyvinyl alcohol	¹³⁷ Cs	Excellent selectivity, high removal efficiency (>99.5%)	[29]
γ -Fe ₂ O ₃	(3-acrylamiddopropyl) trimethylammonium chloride/lanthanum nitrate	Fluoride	q _{max} = 136.78 ± 2.19 mg g ⁻¹ , the adsorption capacity reaches 93% in 10 minutes, better fluoride adsorption at low pH (2.8-4.0)	[30]
Graphene oxide/magnetite	Ascorbic acid	Au(CN) ₂ ⁻	q _{max} = 309 mg g ⁻¹ , the spent hydrogel could be easily collected using a magnetic separator	[31]
Fe ₃ O ₄	Xylan/poly(acrylic	Methylene	q _{max} = 438.60 mg g ⁻¹ , porous structure,	[32]

^a (n cycle refers to the adsorption/desorption cycle n times, and q_{max} refers to the maximum adsorption capacity).

The adsorption principle of MHs is shown in Figure 3A. Porous hydrogels containing active functional groups such as carboxyl, hydroxyl and amino groups can act as adsorbents to remove contaminants through electrostatic, ionic exchange or complexation with contaminants such as heavy metal ions. More importantly, the incorporation of MNPs can promote the separation, collection and reuse of hydrogel adsorbents,^[42] and also have a positive effect on the adsorption of MHs (Figure 3B-D).^[43] The main results are as follows: (1) MNPs embedded in MHs can increase the cross-linking degree and porosity of the system, providing a channel for the entry, exit and adsorption of some substances. (2) When the amount of MNPs is in a certain range, the adsorption amount of MHs is positively correlated with the amount of MNPs. The reason is that with the increase of MNPs addition, the surface of the hydrogel becomes rougher, which can increase the surface area and adsorption capacity of MHs. However, once the amount of MNPs exceeds a certain value, the saturation absorptivity of MHs will decrease unexpectedly. This may be attributed to the excessive coordination of the active groups in the hydrogel system with MNPs, resulting in a decrease in the number of free active groups and insufficient binding to pollutants.^[44]

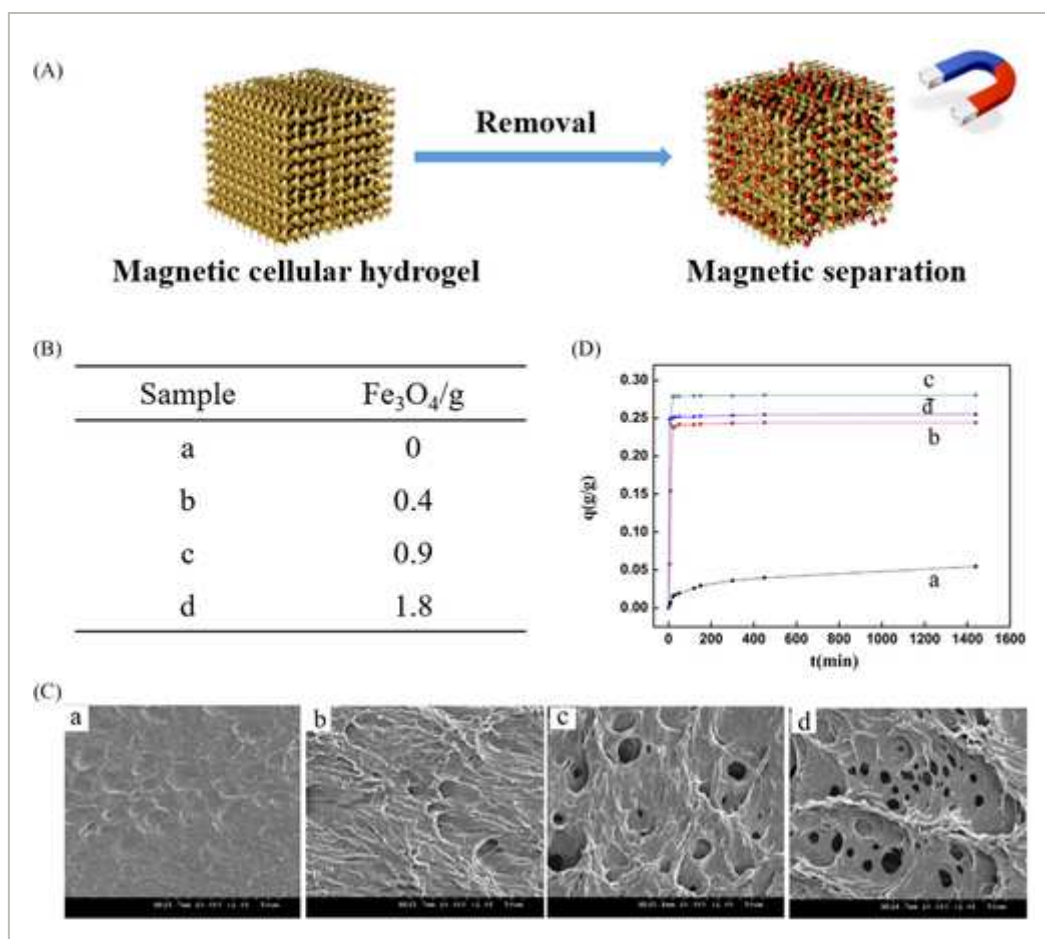


FIGURE 3

[Open in figure viewer](#) | [PowerPoint](#)

A, Schematic diagram of removing contaminants from wastewater using MHs. B, MHs with different Fe₃O₄ contents. C, SEM images of different MHs. D, Adsorption kinetics of Cr^{VI} on the MHs adsorbent. Reprinted with permission.^[44] Copyright 2018, Elsevier

The complete adsorption process of MHs is described in Figure 4. First, the prepared MHs were added to the treated wastewater, and the complete adsorption was guaranteed by shaken in an end-over-end manner. Then, under the assistance of magnets, magnetic separation is carried out on contaminants-loaded hydrogel. In this way, treated water and renewable hydrogels are obtained. The reutilization of MHs requires regeneration solution to desorb the contaminants on the hydrogel, and then magnetic separation to obtain reusable adsorption materials. The realization of this process is attributed to the large surface area, multiple adsorption (hydrogen bond, hydrophobic interaction, etc.), suitable pore size distribution and paramagnetism of MHs. Therefore, MHs can be considered as a low-cost, efficient and recyclable adsorbent, and have great attraction and broadly applicable in wastewater treatment.

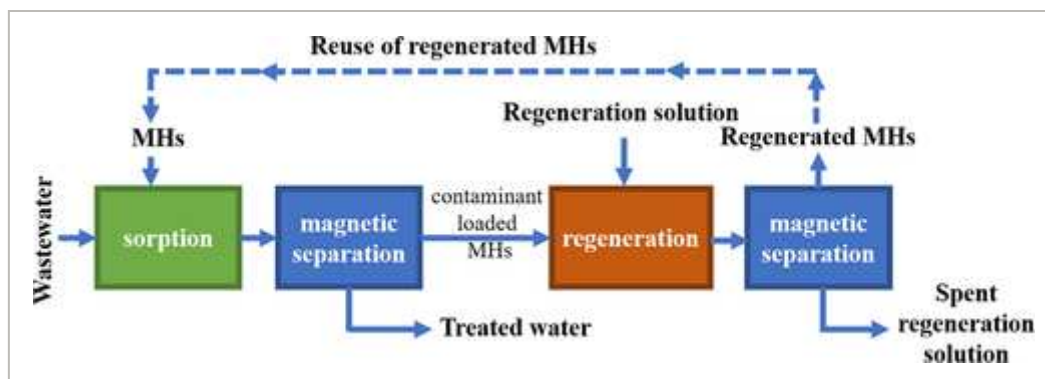


FIGURE 4

[Open in figure viewer](#) | [PowerPoint](#)

The process flow chart of removing contaminants from wastewater using MHs

Because magnetic separation methods can selectively recover the desired proteins from biological fluids, MHs materials have been extensively studied in protein separation.^[45] For biomedical applications, especially tissue engineering, the tendency of hydrogel to adsorb protein in biological media should be considered as an important characteristic. It has been demonstrated that magnetic apatite nanoparticles introduced into poly(vinyl alcohol) (PVA)/sodium alginate hydrogel could generate magnetic response and enhance hydrogels.^[46] When pH = 4.5, the maximum adsorption capacity of nano-beads for bovine serum albumin was the highest, reaching $127.3 \text{ mg}\cdot\text{g}^{-1}$. In addition to the above applications, the absorbability of MHs could also be used for enzyme immobilization,^[47] dehydrators,^[48] data storage,^[49] moisture transport,^[50] and so on.

2.3 Magnetocaloric effects

Magnetocaloric effect refers to the phenomenon that the magnetic energy is transferred to the particles in the form of heat when the ferromagnet or paramagnetism is placed in the alternating magnetic field (AMF) and the magnetic direction is randomly transformed between parallel and anti-parallel. This phenomenon can be used to destroy morbid cells in organisms and control drug release. As a common magnetocaloric agent, superparamagnetic iron oxide (SPIOs) nanoparticles have obtained considerable development in tumor ablation. However, SPIOs have shortcomings such as short residence time in vivo, limited timeliness, and many injections. Notably, the magnetic particles were incorporated into hydrogels will greatly prolong the residence time in vivo. Not only that, hydrogel matrix with a 3D internal network microstructure, high water content and biocompatibility, which are analogous with those of the natural tissue, plays a key role in the application of MHs. On the one hand, hydrogel matrix provides a microenvironment for magnetocaloric therapy,^[51] effectively avoiding heat damage to normal tissues, and provides adjustable 3D scaffolds for cell adhesion, migration and differentiation.^[52] On the other hand, injectable hydrogels with pores or microchannels are one

of the best candidates for local drug delivery.^[53] The magnetocaloric effect of MHs can be designed to sustain and control the release of one or more combined therapeutic drugs. Studies demonstrated that the anisotropic magnetic coupling inside the gel is the main reason for the thermogenesis of MHs. Moreover, compared with the disordered MHs, the self-assembled oriented MHs has stronger thermogenesis.^[54]

The practical application of MHs magnetocaloric effect is mainly reflected in biomedicine, including tumor treatment and tissue repair. Surgery is currently one of the most common methods for solid tumor treatment. However, wound infection and postoperative recurrence are major challenges facing the surgical treatment of solid tumors. Neoadjuvant and postoperative adjuvant therapies play an important role in improving the prognosis of patients. MHs have been applied to target tumors by remote heating with an external magnetic field and controlled release of anticancer drugs from hydrogels for cancer therapy.^[55] Compared with photothermal therapy, magnetocaloric therapy has unlimited tissue penetration depth and is effective for deep-seated tumors such as liver cancer and glioma. Moreover, an AMF-triggered delivery system enables on-demand drug delivery with more effective anticancer chemotherapy effects. However, increasing the efficacy of 42°C therapeutic temperature without resistance to induced thermal stress has been a challenge. Therefore, Zhang et al. designed an injectable magnetic hydrogel nano-enzyme (MHZ) utilizing the inclusion interaction between α -cyclodextrin and PEGylated nanoparticles.^[56] Employing this hydrogel could improve the tumor oxidative stress level by generating reactive oxygen species via nanozyme catalyzed reaction based on hyperthermia (Figure 5). Magnetic Fe_3O_4 nanoparticles play a dual role of nanozymes and magnetic heating simultaneously in the hydrogel system. On the one hand, the magneto-heat generated after MHZ injection into tumor tissue promoted Fe_3O_4 nanozymes to produce more $\cdot\text{OH}$. On the other hand, $\cdot\text{OH}$ further damages the highly expressed protective heat shock protein 70 in hyperthermia, thereby improving the efficacy of hyperthermia. As such, this MHs exerts dual functions of catalytic therapy and hyperthermia to synergistically treat tumors and overcome the resistance of tumor cells to induced thermal stress. This developed system offers a universal platform for safer and precise synergistic therapy of solid tumors.

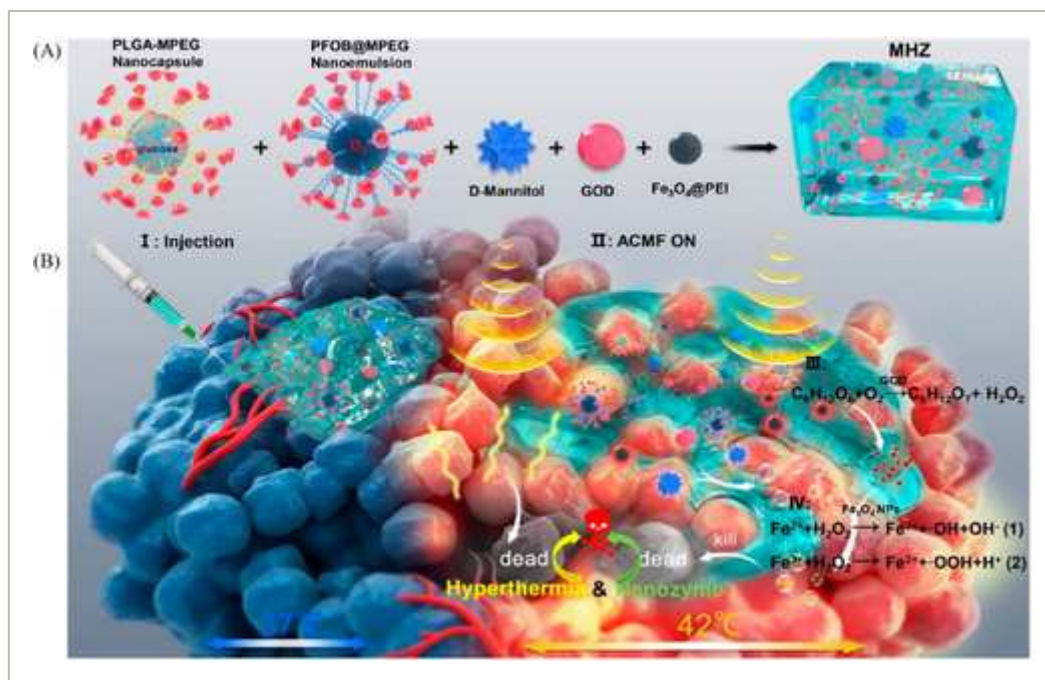


FIGURE 5

[Open in figure viewer](#) | [PowerPoint](#)

Schematic diagram of enhanced tumor synergistic therapy by injectable MHZ.^[42] A, Synthetic procedure for MHZ. B, The synergistic mechanism of MHZ on the generation of hyperthermia and ROS for cancer therapy. Reprinted with permission.

^[42] Copyright 2019, American Chemical Society

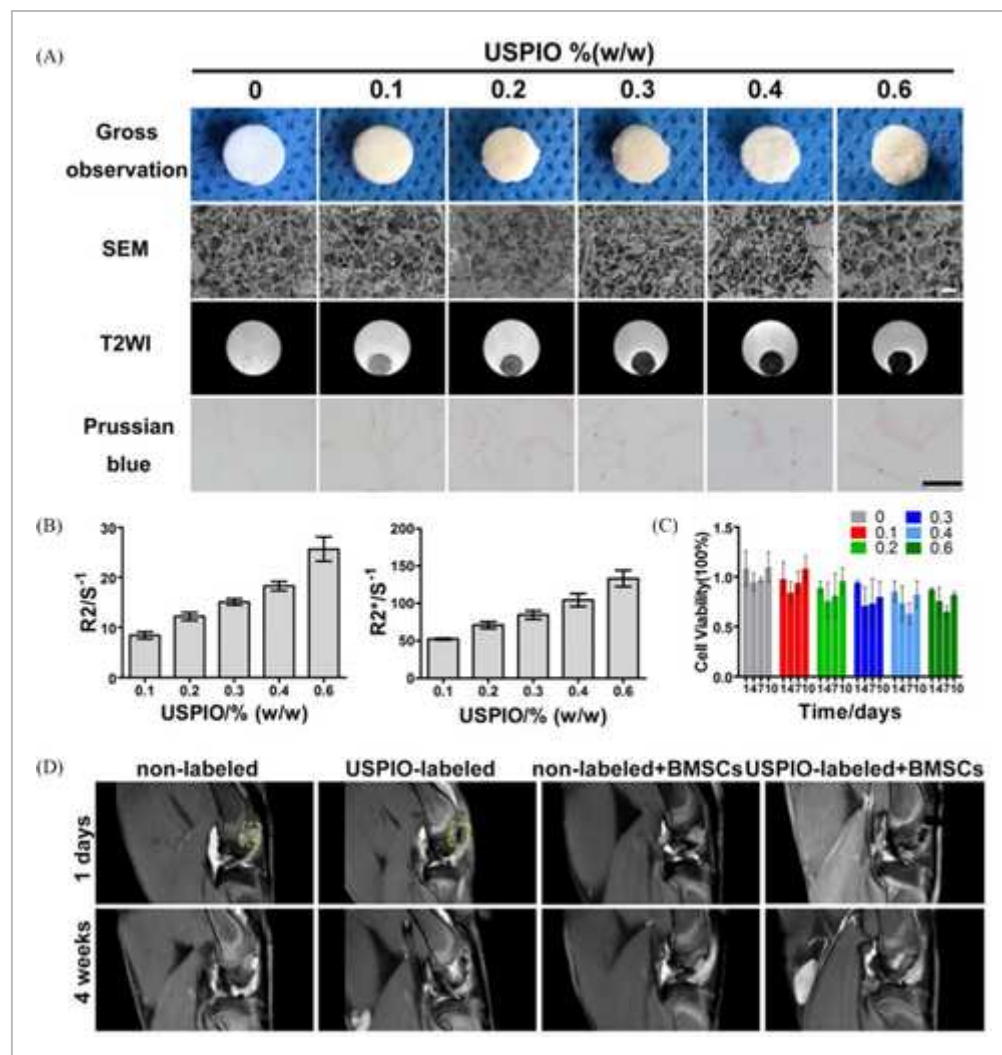
In the past decade, the combination of hyperthermia-based physical therapy and biomaterials has exhibited significant potential in tissue repair. In vitro cell experiments have proved that mild thermal stimulation could effectively promote osteochondral repair.^[57] Further in vivo experiments are yet to be studied. In addition, hyperthermia plays an important role in inhibiting local inflammatory response, relieving pain and protecting joint function.^[58] Therefore, hydrogels with magnetothermal effect can be expected to have great application prospects in the treatment of rheumatoid arthritis and osteoarthritis.

It is worth mentioning that the superior magnetocaloric effect of MHs is conducive to develop discoloration hydrogel,^[59] which may provide a new platform for color display. This remarkable magnetochromatic property is attributed to the superior magnetocaloric effect of 1D magnetic chain immobilized in a thermosensitive hydrogel. Under an AMF, the magnetocaloric effect of aggregated magnetic chains leads to hydrophilic–hydrophobic transition of the hydrogel, which reduces the inter-particle distance of the 1D magnetic chains and results in a blueshift of the diffraction wavelength. Thus, the MHs also shows the potential to monitor magnetic hyperthermia with significant changes in its color and appearance.

2.4 MR imaging

Non-invasive imaging is a powerful tool that can provide effective feedback for clinical diagnosis. MR imaging has become one of the most powerful detection methods in contemporary clinical diagnosis due to its characteristics such as safety, functional sequence diversity, good soft tissue contrast and penetration depth. However, in practical application, the relaxation time of different tissues or tumors overlaps with each other, which leads to the diagnosis difficult. Therefore, the contrast agent began to be studied in order to enhance the signal contrast and improve the image resolution. Due to its biocompatibility and superparamagnetism, Fe_3O_4 -based superparamagnetic contrast agents are widely used in cancer detection, drug delivery monitoring and stent implantation labeling. Significantly, the incorporation of magnetic particles with MR imaging into the hydrogel system will endow the gels a good imaging capability.^[60] This non-invasive imaging of materials could provide effective feedback for the real-time degradation of biomaterials and the remodeling of new tissues in vivo.^[61] Moreover, non-invasive monitoring methods help to reduce the number of experimental subjects. The reason is that the experimental data can be obtained repeatedly to avoid unnecessary sacrifice in histological analysis at different time points. In addition, non-invasive continuous observation will provide more effective information, reduce individual differences, and contribute to the clinical transformation of tissue engineering.

For the first time, Chen developed a functional, visualizable superparamagnetic iron oxide (USPIO)-labeled natural hydrogel system for semi-quantitative monitoring the cartilage degradation process and elucidated the regeneration of hyaline cartilage by multiparametric MRI.^[62] USPIO particles with diameter of $\sim 15.7 \pm 2.0$ nm and a concentration less than 25 $\mu\text{g Fe/mL}$ had no effect on chondrogenesis and cell proliferation of human bone marrow mesenchymal stem cells (hBMSCs).^[63] In this experiment, cellulose nanocrystal (CNC)/silk fibroin (SF) blend hydrogel was selected as scaffold for tissue engineering to promote cartilage regeneration. It has a moderate degradation rate to coincide with cartilage regeneration, which is essential to maintain the structural integrity and mechanical properties of the joint. As shown in Figure 6A, the USPIO-labeled CNC/SF hydrogel has an interconnected network structure and uniform porosity. Prussian blue staining exhibited that USPIO was evenly distributed in the hydrogel matrix, and the material showed no obvious cytotoxicity. This biocompatible hydrogel with pore sizes ranging from 70 to 250 μm , are effective in promoting cartilage formation.^[64] Next, MRI characterization of the composite hydrogel was performed with T2-weighted imaging (T2WI) sequence, indicating that the signal contrast of the prepared hydrogel increased with USPIO content. In vivo MR imaging further demonstrated that the USPIO-labeled hydrogel had sufficient MR contrast to monitor the degradation process (Figure 6D). Therefore, this system may provide meaningful insights for non-invasive monitoring and therapeutic efficacy of implanted hydrogels in tissue engineering.

**FIGURE 6**

[Open in figure viewer](#) | [PowerPoint](#)

Non-invasive monitoring of hydrogel degradation by multiparametric MR imaging.^[62] A, In vitro SEM observation, MRI characterization and Prussian blue staining of CNC/SF hydrogels incorporated USPIO. B, R_2 and R_2^* relaxometry rates and (C) cytotoxicity of USPIO-labeled hydrogel. D, MRI analysis of the in vivo degradation of non-labeled and USPIO-labeled CNC/SF hydrogels in a rabbit cartilage defect model. Reproduced with permission.^[62] Copyright 2018, Ivyspring International Publisher

2.5 Intelligent response

Smart hydrogel is a kind of material that can perceive small physical/chemical stimuli (such as temperature, light, magnetism, pH) and make significant response behaviors.^[65] Because of this intelligence, hydrogel has a fascinating application prospect in tissue engineering, drug-controlled release and soft actuators. Especially, as an external stimulus of stimulus-responsive materials, magnetic field has the advantages of instant action, contactless control and easy

integration into electronic devices. Therefore, the research and development of smart MHs has been very active in recent years.^[66]

Over the past few decades, tissue engineering has been successfully applied to the repair of various tissues (retinas, ligaments, fats, blood vessels, etc.). With the potential of hydrogel to construct microenvironment, the scaffolds based on multi-functional MHs have attracted much attention due to their intelligence. On the one hand, under the guidance of magnetic field, MHs can move directionally or be induced into specific tissue-like microstructure,^[67] providing a suitable growth environment for tissue reconstruction. Schmidt proposed a novel magnetic templating technology which can induce highly aligned 3D tubular microstructures in naturally derived hydrogel scaffolds.^[68] The scaffold was constructed by adding soluble magnetic alginate particles (MAM) containing nano-iron oxide to the hydrogel precursor solution. The diameter of MAM is 100 nm–20 μm , and a concentration of 5 mg mL⁻¹ of MAM is the upper-limit allowing for optimal chain length on the millimeter scale. Under an external magnetic field, the gel forms an aligned columnar structure (Figure 7A). The removal of MAM results in scaffolds with aligned tubular microarchitectures that can facilitate cell remodeling in various applications. Moreover, the hydrogels with electromagnetic effects can realize the above functions, while constructing electric microenvironment under external electrical stimulation to simulate directional tissue, guide cell proliferation and tissue regeneration.^[69] On the other hand, magnetic scaffolds can control the biological behavior of cells through the magnetic response between MNPs and magnetic field^[70]; thus, promoting revascularization, cartilage/bone regeneration,^[71] neuroregulation,^[72] and wound repair.^[67] Carlo et al. described a 3D magnetic hyaluronic hydrogel that provides non-invasive neuromodulation by magneto-mechanically stimulating primary dorsal root ganglion (DRG) neurons (Figure 7B).^[73] Mechanosensitive PIEZO2 channel is activated by magnetic particles embedded in the system through membrane stretching. Mechanosensitive TRPV4 channel is activated by magnetically induced deformation of HA hydrogel. Under acute magneto-mechanical stimulation, calcium influx in DRG neurons is induced through TRPV4 and piezo2 channels, avoiding the step of exogenous ion channel transfection.^[74] Under chronic magneto-mechanical stimulation, is able to reduce piezo2 channel expression, playing a role in chronic pain modulation. This general strategy offers a way to achieve remote magnetic modulation of different types of excitable cells through 3D magnetic biomaterials.

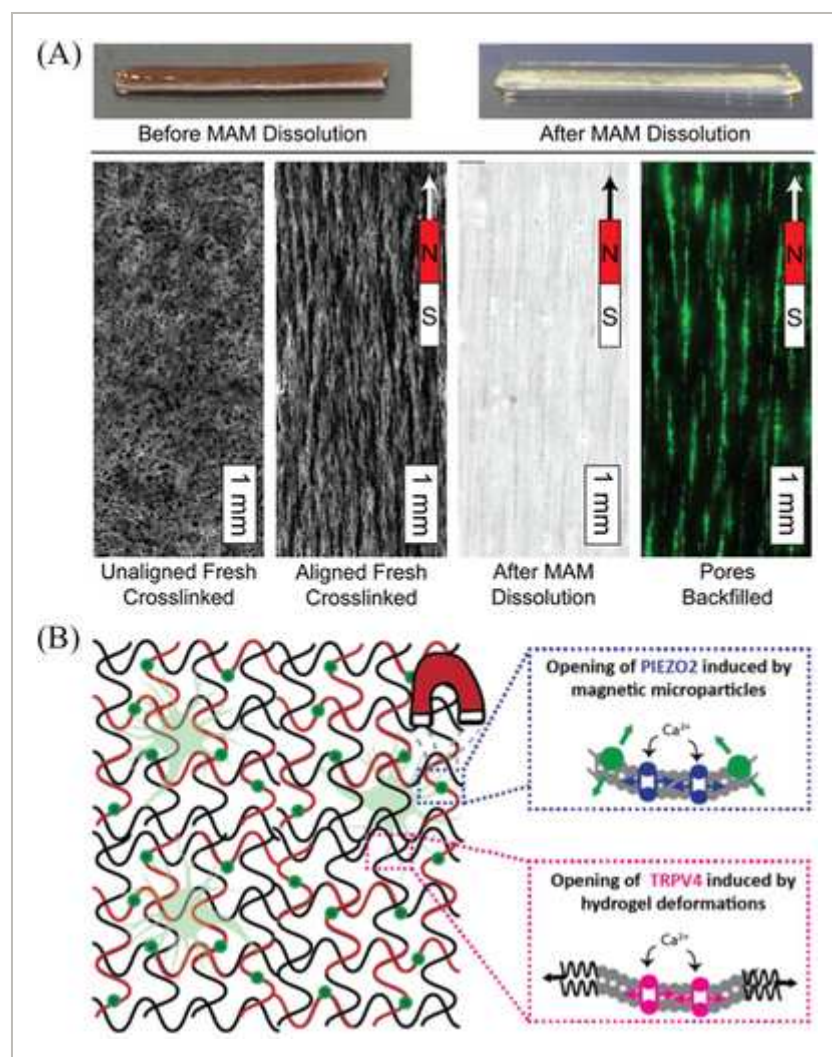


FIGURE 7

[Open in figure viewer](#) | [↓ PowerPoint](#)

A, Macroscopic view of crosslinked hydrogel, and porous microarchitecture after removal of MAM.^[68] Copyright 2020, IOP Publishing Ltd. B, Mechanism of magneto-mechanical stimulation of dorsal root ganglion neurons by magnetic hyaluronic acid (HA) hydrogels.^[73] Copyright 2018, WILEY-VCH Verlag GmbH & Co. KGaA, Weinheim.

Another important application of smart soft material is soft robot. The advent of soft robots has made great strides in robotics, wearable devices and other areas by using complete software systems that can safely interact with any random surface while provide excellent mechanical flexibility. The latest development in soft robotics have benefited from advances in soft actuators and sensors that enable robots to work mechanically unimpeded; thus, expanding the range of robotic applications.^[75] Soft actuator generally refers to a soft body that can reliably adapt to any surface and cause various motions of the robot. Up to now, many attempts have been made to fabricate soft actuators sensitive to external stimuli.^[76] Especially, MHs with flexibility and sensitivity to external magnetic fields are expected to form a new research focus in the coming era of soft robots.^[77] What is more, taking advantage of the

minimal invasions and the drive ability to use magnetic fields of magnetic microrobots, therapeutic drugs can be delivered to target areas.^[78] This controlled release method can significantly reduce the dosage and minimize the side effects on normal cells. Sukho park presented a novel hydrogel actuator (Figure 8),^[79] which can deliver anticancer drugs to cancer targets through a customized near-infrared (NIR) and electromagnetic actuation (EMA) integrated system, then retrieve problematic MNPs. First, the microrobot reaches the predetermined lesion target through the magnetic field of EMA. Next, after the NIR irradiation, the hydrogel matrix was decomposed, drug particles and MNPs were left in the target tissue. Finally, with the assistance of EMA magnetic field, the disassembled MNPs were recovered from the target region, and the remaining anticancer drugs are continuously released to generate therapeutic effects. This hydrogel actuator can compensate for the inherent disadvantages of MNPs (toxicity) by retrieval of MNPs, thereby maintaining the advantages of electromagnetic drive (target characteristics and drug delivery). In the future, developing a practical drug delivery hydrogel robot is an attractive topic.

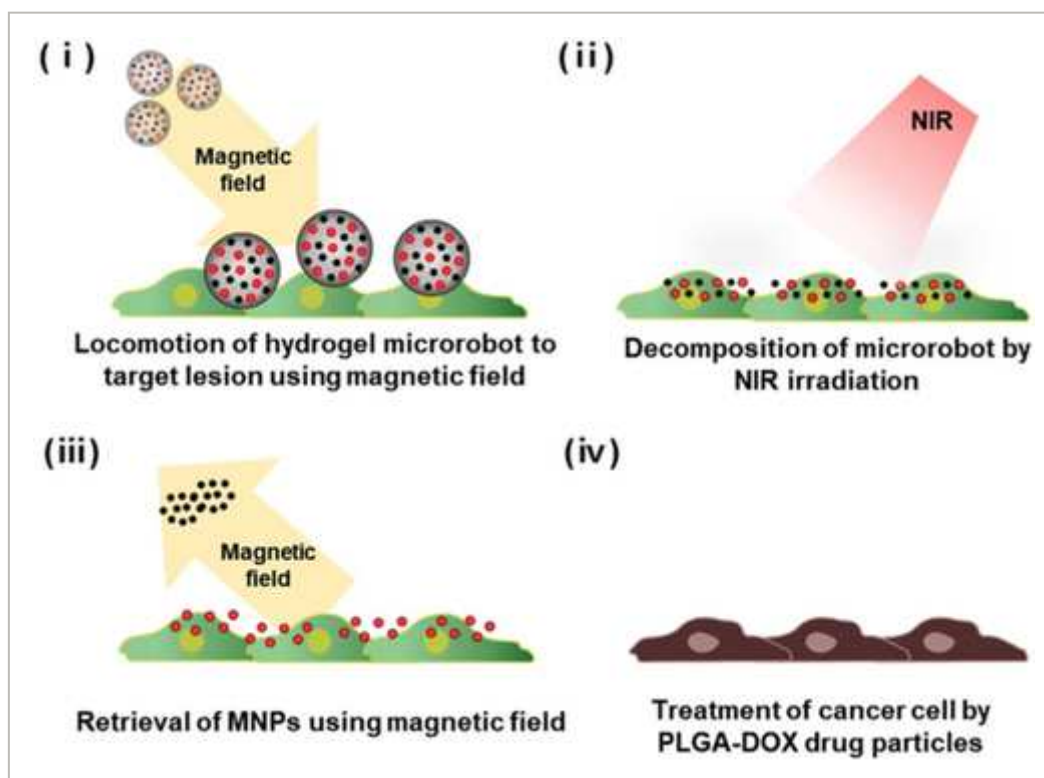


FIGURE 8

[Open in figure viewer](#) | [PowerPoint](#)

Schematic diagram of the treatment process using retrievable biodegradable hydrogel microrobot for drug delivery.

Reproduced with permission.^[79] Copyright 2019, Elsevier

2.6 Biocompatibility

Biocompatibility refers to the degree of compatibility of materials with human body after implantation, that is, whether they will cause toxic effects on human tissues. It mainly includes blood compatibility and histocompatibility. Blood compatibility refers to the ability of materials to interact with blood directly without causing coagulation, thrombosis, damaging blood composition and function. Hydrogel directly contacting blood requires good blood compatibility, such as hemostatic dressing.^[80] Histocompatibility is the affinity between materials and tissues without being eroded by tissues when they come into contact with organs. Tissue engineering and regenerative medicine research put more emphasis on the histocompatibility and cytocompatibility of hydrogels.^[81] Generally, strict biocompatibility evaluation is required first to ensure the clinical safety of biomaterials. At present, the biocompatibility evaluation of hydrogels is mainly from the following aspects: cytotoxicity, hemolysis test, acute systemic toxicity, subacute toxicity test, implant test evaluation and so on.

In recent years, MHs find widespread applications in biomedical fields due to their similar structure to native extracellular matrix, hydrated environment, tunable properties (mechanical, biocompatibility) and unique active response characteristics. Fibrin, chitosan, hyaluronic acid, collagen and other natural biomaterials are the preferred raw materials for preparing medical MHs hydrogel matrix.^[82] The reason is that they have excellent biocompatibility, low toxicity, enzyme degradation and degradation products are not easy to trigger immune response. Some compounds are decomposed into small molecules (water, carbon dioxide, etc.) that can be metabolized by human body, such as polyglycolic acid. Therefore, these compounds can also be widely used in the synthesis of biocompatible MHs. In addition, the concentration of MNPs in most MHs is generally less than 1 wt.%, but it has a positive effect on cells. Huang has proposed that the existence of magnetic Fe_3O_4 nanoparticles can promote the growth of stem cells and accelerate the cell cycle process.^[83] When MNPs are incorporated into the scaffold, their magnetic field effect may affect ion channels on cell membrane and initiate changes in cytoskeleton structure.^[84] However, the biosafety issues related to MNPs is the impact of MNPs released from the degradation of implanted MHs. In general, MNPs (1–20 nm in diameter) selected for preparing MHs can be absorbed by the interaction with proteins and cells. They can then distribute to different organs, where they may stay in the same nanostructure or be metabolized.^[85]

Liu and his colleagues created a magnetic hydrogel (MagGel) containing type II collagen, hyaluronic acid and polyethylene glycol to provide a biomimetic, bioactive and biodegradable platform for cartilage tissue engineering.^[86] In cell experiments, MagGel has the highest average cell adhesion density, indicating its excellent cytocompatibility. This is attributed to the synergistic effect of hydrogel matrix and magnetic nanoparticles to improve cytocompatibility,^[87] including adhesion and growth. First, hydrogel mimics the extracellular matrix, providing a favorable environment for cells. Second, the interaction between magnetic nanoparticles and

BMSCs might promote cell adhesion and growth. In addition, BMSCs were observed to phagocytize magnetic nanoparticles in cell culture without any effect on cell adhesion or morphology (Figure 9).^[88] The authors suggest that the ingested nanoparticles may eventually be decomposed by lysosomes and excreted by exocytosis.

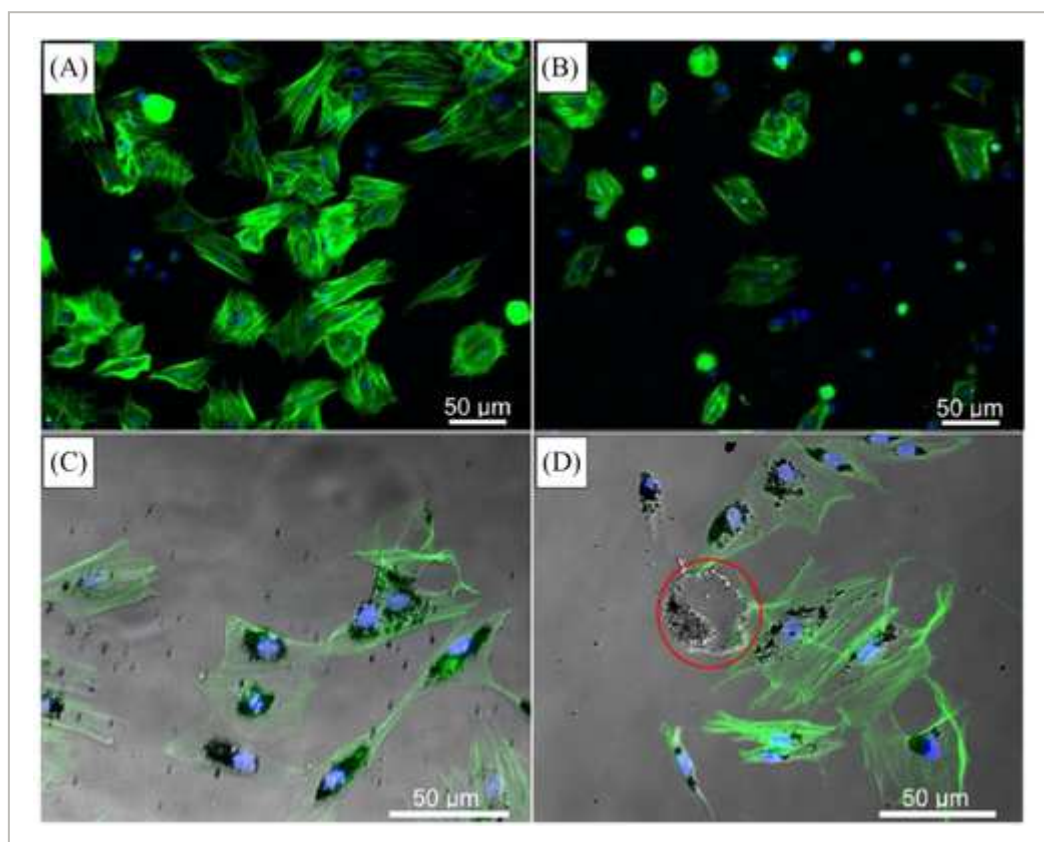


FIGURE 9

[Open in figure viewer](#) | [Download PowerPoint](#)

Cytocompatibility of magnetic nanocomposite hydrogels (MagGel).^[86] Fluorescence images of BMSCs adhesion and morphology cultured on (a) MagGel and (b) gel. c-d, The endocytosis of magnetic nanoparticles by BMSCs. Black: magnetic nanoparticles; Blue: nucleus; Green: F-actin; Red circle: magnetic nanoparticles outside of the BMSCs. Reproduced with permission.^[86] Copyright 2015, American Chemical Society

3 FABRICATION PROCESSING OF MHs

MHs are generally composed of polymer matrix and magnetic components embedded in the matrix (such as $\gamma\text{-Fe}_2\text{O}_3$, Fe_3O_4). Up to now, various methods have been developed to prepare MHs, including blending method, in-situ precipitation method and grafting-onto method.

The blending method refers to simply mixing the pre-prepared MNPs with hydrogel precursor solution, so that MNPs is covered in hydrogels (Figure 10A).^[89] This is the simplest and most commonly method for fabricating MHs. However, the hydrogel obtained by simple blending

method usually has the defects of uneven distribution of magnetic particles in colloids. This may result in unstable properties (mechanical, magnetocaloric, MR imaging) of the prepared MHs.

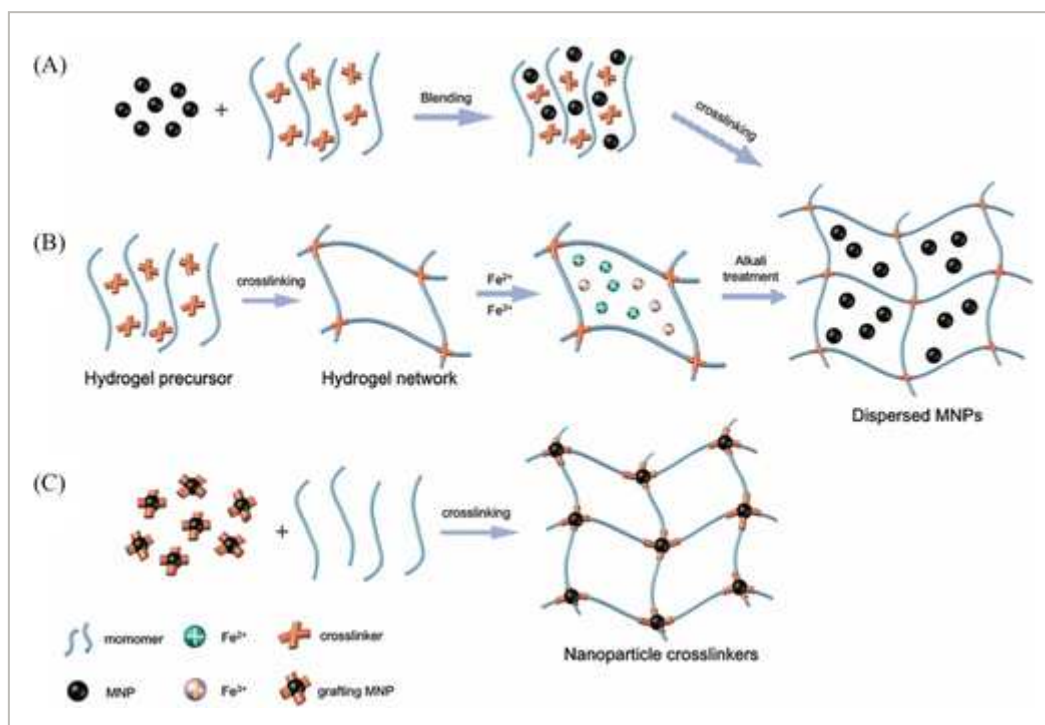


FIGURE 10

[Open in figure viewer](#) | [PowerPoint](#)

Preparation technology of MHs. a, The blending method:^[89] the prepared MNPs was mixed with a hydrogel precursor solution and crosslink hydrogels to embed the MNPs. b, In-situ precipitation method:^[91] MNPs was prepared by in-situ precipitation reaction in polymer hydrogel network after cross-linking reaction. c, The grafting-onto method:^[93] MNPs and hydrogel systems are connected by covalent or coordination bonds. Reprinted with permission.^[94] Copyright 2012, WILEY-VCH Verlag GmbH & Co. KGaA, Weinheim

In the in-situ precipitation method,^[90] the hydrogel network work as a chemical reactor, within which metal ions react with precipitating agents (NaOH, $\text{NH}_3 \cdot \text{H}_2\text{O}$, etc.) to generate MNPs (Figure 10B). For example, Ye and Shen prepared a novel magnetic chitosan/polyvinyl alcohol hydrogel beads (MCPHBs) by freeze-thaw method combined with in-situ precipitation method.^[91] First, the prepared PVA solution was mixed with CS solution, and then Fe^{3+} and Fe^{2+} solutions were added. Then, the mixed solution was added to the beaker containing ammonium hydroxide to form MNPs. Finally, MHs beads were obtained by repeated freezing and thawing. However, the preparation of MHs by in-situ precipitation is often limited by alkali-resistant hydrogel matrix.

Apparently, for both blending method and in-situ precipitation, there are no bonding interactions between MNPs and hydrogel networks. Therefore, the stability of MNPs dispersed in hydrogels cannot be guaranteed. The generalized grafting-onto method,^[92] including modifying or changing the structure and properties of MNPs, can connect MNPs and hydrogel systems through covalent or coordination bonds (Figure 10C). This direct coupling allows MNPs to be stably and uniformly embedded in the hydrogel. Recently, our group fabricated a magnetic nano-Fe₃O₄ composite polyolefin-chitosan (AAD-CS-Fe) double network hydrogel by grafting-onto method.^[93] A large amount of Fe ions is exposed on the surface of nano-Fe₃O₄ pre-etched by HCl, which can be cross-linked with the active groups (carboxyl and hydroxyl) in the hydrogel system. In this way, magnetic AAD-CS-Fe hydrogel with uniform structure and stable properties can be obtained.

4 CONCLUSION REMARKS

MHs are composed of magnetic components (such as γ -Fe₂O₃) and hydrogel matrix. The incorporation of MNPs can enhance the initial performances (mechanical properties, adsorption, etc.) of the hydrogel, while providing further magnetic properties (magnetocaloric, MR imaging and intelligent response, etc.). In recent years, MHs have attracted worldwide attention as a potential multi-functional intelligent soft platform. This paper focuses on six major functions of MHs, including mechanical properties, adsorption, magnetocaloric effects, MR imaging, intelligent response and biocompatibility. The design strategies of various functions, as well as its application prospects in biomedicine, soft actuators, environmental protection, chemical catalysis and engineering in recent 5 years are reviewed. In addition, the classical fabrication processing of MHs was introduced.

To further promote the development and practical application of MHs, its future research focuses include the following aspects:

1. At present, the magnetic component in MHs is mainly confined to iron-containing nanoparticles. Further exploration of other MNPs to enhance thermotherapy, MRI contrast and intelligent response is of great significance for promoting the practical application of multi-functional MHs.
2. MHs have important application prospects in biomedical fields, mainly including tissue engineering, because of their unparalleled advantages such as in situ magnetocaloric therapy, magnetocaloric drive and MR imaging. However, a lot of work remains to be done on the long-term fate of implanting MHs to truly achieve clinical application, such as metabolism and biodegradability evaluation.^[95]
3. The development of MHs in the future depends largely on the synthesis of novel multi-functional hydrogels. Combining magnetic stimulation with other stimuli, such as light,^[96]

electricity,^[97] temperature,^[98] pH,^[99] and redox,^[100] MHs will become more intelligent and versatile.

ACKNOWLEDGMENTS

This work was supported by the Natural Sciences Foundation of China (21977083); Natural Sciences Foundation of China (No. 52072210); Tsinghua University-Peking Union Medical College Hospital Initiative Scientific Research Program (grant number 20191080871); Tsinghua University Initiative Scientific Research Program [grant number 2017THZWYX07].

CONFLICT OF INTEREST

The authors declare no conflict of interest.

Biographies



Fangli Gang received her PhD degree in chemical biology from Northwest A&F University in 2020. Currently, she joined the Biology department of Xinzhou Teachers University. Her research interests are mainly focused on functional hydrogel materials and their biomedical applications.



Xiaodan Sun received her PhD degree in engineering from Tsinghua University under the supervision of Prof. Hengde Li. At present, she is an associate researcher in the School of Materials of Tsinghua University. Her current research is on the nano biomaterials, osteochondral tissue engineering, nerve tissue engineering, tumor diagnosis and treatment.



REFERENCES

1 a) Y. S. Zhang, A. Khademhosseini, *Science* 2017, **356**, eaaf3627;

[Google Scholar](#)

b) T. Nonoyama, J. P. Gong, *Proc. Inst. Mech. Eng. H* 2015, **229**, 853;

[Google Scholar](#)

c) N. A. Jalili, M. Muscarello, A. K. Gaharwar, *Bioeng. Transl. Med.* 2016, **1**, 2975.

[Google Scholar](#)

2 a) Z. Gu, K. Huang, Y. Luo, L. Zhang, T. Kuang, Z. Chen, G. Liao, *WIREs Nanomed Nanobiotechnol.* 2018, **10**, e1520;

[Google Scholar](#)

b) Y. Wu, H. Wang, F. Gao, Z. Xu, F. Dai, W. Liu, *Adv. Funct. Mater.* 2018, **28**, 1801000.

[Google Scholar](#)

3 a) N. Rodkate, M. Rutnakornpituk, *Carbohydr. Polym.* 2016, **151**, 251;

[Google Scholar](#)

b) M. Karzar Jeddi, M. Mahkam, *Int. J. Biol. Macromol.* 2019, **135**, 829.

[Google Scholar](#)

4 a) N. S. Satarkar, D. Biswal, J. Z. Hilt, *Soft Matter* 2010, **6**, 2364;

[Google Scholar](#)

b) J. Zhang, Q. Huang, J. Du, *Polym. Int.* 2016, **65**, 1365.

[Google Scholar](#)

5 a) X. Chen, M. Fan, H. Tan, B. Ren, G. Yuan, Y. Jia, J. Li, D. Xiong, X. Xing, X. Niu, X. Hu, *Mater. Sci. Eng. C Mater. Biol. Appl.* 2019, **101**, 619;

[Google Scholar](#)

b) X. Hu, Y. Wang, L. Zhang, M. Xu, J. Zhang, W. Dong, *Int. J. Biol. Macromol.* 2018, **107**, 1811.

[Google Scholar](#)

6 Y. P. Jia, K. Shi, F. Yang, J. F. Liao, R. X. Han, L. P. Yuan, Y. Hao, M. Pan, Y. Xiao, Z. Y. Qian, X. W. Wei, *Adv. Funct. Mater.* 2020, **30**, 2001059.

[Google Scholar](#)

7 R. Patwa, N. Saha, P. Saha, *AIP Conference Proceedings* 2020, **2205**, 020027.

[Google Scholar](#)

8 a) T. Jin, F. J. Nicholls, W. R. Crum, H. Ghuman, S. F. Badylak, M. Modo, *Biomaterials* 2017, **113**, 176;

[Google Scholar](#)

b) X. Yang, Y. Sun, S. Kootala, J. Hilborn, A. Heerschap, D. Ossipov, *Carbohydr. Polym.* 2014, **110**, 95.

[Google Scholar](#)

9 Y. Guo, J. Bae, Z. Fang, P. Li, F. Zhao, G. Yu, *Chem. Rev.* 2020, **120**, 7642.

[Google Scholar](#)

10 a) J. Yeom, A. Choe, S. Lim, Y. Lee, S. Na, H. Ko, *Sci. Adv.* 2020, **6**, eaba5785;

[Google Scholar](#)

b) Y. Ye, Y. Zhang, Y. Chen, X. Han, F. Jiang, *Adv. Funct. Mater.* 2020, **30**, 2003430;

[Google Scholar](#)

c) K. Liu, Y. Zhang, H. Cao, H. Liu, Y. Geng, W. Yuan, J. Zhou, Z. L. Wu, G. Shan, Y. Bao, Q. Zhao, T. Xie, P. Pan, *Adv. Mater.* 2020, **32**, e2001693.

[Google Scholar](#)

11 F. Gao, W. Xie, Y. Miao, D. Wang, Z. Guo, A. Ghosal, Y. Li, Y. Wei, S. Feng, L. Zhao, H. Fan, *Adv. Healthcare Mater.* 2019, **8**, e1900203.

[Google Scholar](#)

12 H. Liu, J. Yang, Y. Yin, H. Qi, *Chin. J. Chem.* 2020, **38**, 1263.

[Google Scholar](#)

13 K. Liu, X. Pan, L. Chen, L. Huang, Y. Ni, J. Liu, S. Cao, H. Wang, *ACS Sustain. Chem. Eng.* 2018, **6**, 6395.

[Google Scholar](#)

14 X. Hu, Y. Wang, M. Xu, L. Zhang, J. Zhang, W. Dong, *Polymer Testing* 2018, **71**, 344.

[Google Scholar](#)

15 Y. Wang, J. Zhang, C. Qiu, J. Li, Z. Cao, C. Ma, J. Zheng, G. Huang, *Carbohydr. Polym.* 2018, **196**, 82.

[Google Scholar](#)

16 M. Chen, G. Gong, L. Zhou, F. Zhang, *RSC Adv.* 2017, **7**, 21476.

[Google Scholar](#)

17 L. Shi, Y. Zeng, Y. Zhao, B. Yang, D. Ossipov, C.W. Tai, J. Dai, C. Xu, *ACS Appl. Mater. Interfaces* 2019, **11**, 46233.

[Google Scholar](#)

18 A. B. Bonhome-Espinosa, F. Campos, I. A. Rodriguez, V. Carriel, J. A. Marins, A. Zubarev, J. D. G. Duran, M. T. Lopez-Lopez, *Soft Matter* 2017, **13**, 2928.

[Google Scholar](#)

19 a) S. Liu, A. K. Bastola, L. Li, *ACS Appl. Mater. Interfaces* 2017, **9**, 41473;

[Google Scholar](#)

b) F. Chen, Q. Chen, L. Zhu, Z. Tang, Q. Li, G. Qin, J. Yang, Y. Zhang, B. Ren, J. Zheng, *Chem. Mat.* 2018, **30**, 1743;

[Google Scholar](#)

c) S. Azevedo, A. M. S. Costa, A. Andersen, I. S. Choi, H. Birkedal, J. F. Mano, *Adv. Mater.* 2017, **29**, 1700759.

[Google Scholar](#)

20 A. Bin Imran, K. Esaki, H. Gotoh, T. Seki, K. Ito, Y. Sakai, Y. Takeoka, *Nat. Commun.* 2014, **5**, 5124.

[Google Scholar](#)

21 a) X. H. Wang, F. Song, D. Qian, Y. D. He, W. C. Nie, X. L. Wang, Y. Z. Wang, *Chem. Eng. J.* 2018, **349**, 588;

[Google Scholar](#)

b) H. Wang, H. Zhu, W. Fu, Y. Zhang, B. Xu, F. Gao, Z. Cao, W. Liu, *Macromol. Rapid Commun.* 2017, **38**, 1600695.

[Google Scholar](#)

22 a) P. Zhu, M. Hu, Y. Deng, C. Wang, *Adv. Eng. Mater.* 2016, **18**, 1799;

[Google Scholar](#)

b) Y. Zhai, H. Duan, X. Meng, K. Cai, Y. Liu, L. Lucia, *Macromol. Mater. Eng.* 2015, **300**, 1290.

[Google Scholar](#)

23 a) Z. Liu, J. Liu, X. Cui, X. Wang, L. Zhang, P. Tang, *Pharmaceutics* 2018, **10**, 145;

[Google Scholar](#)

b) S. Veloso, P. Ferreira, J. Martins, P. Coutinho, E. Castanheira, *Smart Mater. Struct.* 2016, **25**, 027001;

[Google Scholar](#)

c) H. Li, G. Go, S.Y. Ko, J. O. Park, S. Park, *Smart Mater. Struct.* 2016, **25**, 027001;

[Google Scholar](#)

d) D. I. Kim, S. Song, S. Jang, G. Kim, J. Lee, Y. Lee, S. Park, *Smart Mater. Struct.* 2020, **29**, 085024.

[Google Scholar](#)

24 a) Q. Liu, H. Li, K.Y. Lam, *Bioelectrochemistry* 2019, **129**, 90;

[Google Scholar](#)

b) R. Singh, A. Wieser, S. Reakasame, R. Detsch, B. Dietel, C. Alexiou, A. R. Boccaccini, I. Cicha, *J. Biomed. Mater. Res. A* 2017, **105**, 2948;

[Google Scholar](#)

c) M. Santhosh, J. H. Choi, J. W. Choi, *Nanomaterials (Basel)* 2019, **9**, 1293.

[Google Scholar](#)

25 a) J. Huang, P. Zhang, M. Li, P. Zhang, L. Ding, *Biochem. Eng. J.* 2016, **114**, 262;

[Google Scholar](#)

b) S. Tang, K. Hu, J. Sun, Y. Li, Z. Guo, M. Liu, Q. Liu, F. Zhang, N. Gu, *ACS Appl. Mater. Interfaces* 2017, **9**, 10446;

[CAS](#) | [PubMed](#) | [Web of Science®](#) | [Google Scholar](#)

c) X. Shi, Z. Shi, D. Wang, M. W. Ullah, G. Yang, *Macromol. Biosci.* 2016, **16**, 1506.

[Google Scholar](#)

26 a) J. Li, S. Dong, Y. Wang, X. Dou, H. Hao, *J. Environ. Sci. (China)* 2020, **91**, 177;

[Google Scholar](#)

b) G.M. Ispas, S. Porav, D. Gligor, R. Turcu, I. Crăciunescu, *Water Environ. J.* 2020, **34**, 916.

[Google Scholar](#)

27 a) N. Malatji, E. Makhado, K. E. Ramohlola, K. D. Modibane, T. C. Maponya, G. R. Monama, M. J. Hato, *Environ. Sci. Pollut. Res.* 2020, **27**, 44089;

[Google Scholar](#)

b) N. Sarkar, G. Sahoo, S. K. Swain, *Journal of Molecular Liquids* 2020, **302**, 112591.

[Google Scholar](#)

28 R. Sahraei, Z. Sekhavat Pour, M. Ghaemy, *J. Clean. Prod.* 2017, **142**, 2973.

[Google Scholar](#)

29 H. M. Yang, J. R. Hwang, D. Y. Lee, K. B. Kim, C. W. Park, H. R. Kim, K. W. Lee, *Sci. Rep.* 2018, **8**, 11476.

[Crossref](#) | [PubMed](#) | [Web of Science®](#) | [Google Scholar](#)

30 S. Dong, Y. Wang, *Water. Res.* 2016, **88**, 852.

[Google Scholar](#)

31 K. Sun, W. Peng, H. Li, S. Song, *Hydrometallurgy* 2018, **176**, 208.

[Google Scholar](#)

32 X. F. Sun, B. Liu, Z. Jing, H. Wang, *Carbohydr. Polym.* 2015, **118**, 16.

[Google Scholar](#)

33 J. Li, Y. Wang, X. Dou, H. Hao, S. Dong, X. Shao, Y. Deng, *J. Environ. Sci. (China)* 2020, **89**, 264.

[Google Scholar](#)

34 Y. Meng, C. Li, X. Liu, J. Lu, Y. Cheng, L. P. Xiao, H. Wang, *Sci. Total Environ.* 2019, **685**, 847.

[Google Scholar](#)

35 S. C. Tan, H. K. Lee, *Microchim. Acta* 2019, **186**, 545.

[Google Scholar](#)

36 S. Wang, X. Li, M. Li, X. Li, X. Li, S. Li, Q. Zhang, H. Li, *Appl. Sci.* 2020, **10**, 5665.

[Google Scholar](#)

37 M. Khan, I. M. C. Lo, *J. Hazard. Mater.* 2017, **322**, 195.

[Google Scholar](#)

38 S. Dong, Y. Wang, Y. Zhao, X. Zhou, H. Zheng, *Water Res.* 2017, **126**, 433.

[Google Scholar](#)

39 A. A. Edathil, E. Alhseinat, F. Banat, *International Journal of Greenhouse Gas Control* 2019, **83**, 117.

[Google Scholar](#)

40 S. Pirsā, F. Asadzadeh, I. Karimi Sani, *J. Inorg. Organomet. Polym. Mater.* 2020, **30**, 3188.

[Google Scholar](#)

41 P. Pal, A. A. Edathil, L. Chaurasia, K. Rambabu, F. Banat, *J. Inorg. Organomet. Polym. Mater.* 2020, **30**, 3188.

[Google Scholar](#)

42 D. P. Facch, A. L. Cazetta, E. A. Canesin, V. C. Almeida, E. G. Bonafé, M. J. Kipper, A. F. Martins, *Chem. Eng. J.* 2018, **337**, 595.

[Google Scholar](#)

43 G. Yao, W. Bi, H. Liu, *Colloids and Surfaces A* 2020, **588**, 124393.

[Google Scholar](#)

44 E. Yan, M. Cao, X. Ren, J. Jiang, Q. An, Z. Zhang, J. Gao, X. Yang, D. Zhang, *J. Phys. Chem. Solids* 2018, **121**, 102.

[Google Scholar](#)

45 a) K. Rajar, E. Alveroglu, *Journal of Molecular Structure* 2017, **1146**, 592;

[Google Scholar](#)

b) M. Soleymani, A. Akbari, G. R. Mahdavinia, *Polymer Bulletin* 2018, **76**, 2321;

[Google Scholar](#)

c) G. R. Mahdavinia, M. Soleymani, H. Etemadi, M. Sabzi, Z. Atlasi, *Int. J. Biol. Macromol.* 2018, **107**, 719.

[Google Scholar](#)

46 G. R. Mahdavinia, S. Mousanezhad, H. Hosseinzadeh, F. Darvishi, M. Sabzi, *Carbohydr. Polym.* 2016, **147**, 379.

[Google Scholar](#)

47 J. Song, W. He, H. Shen, Z. Zhou, M. Li, P. Su, Y. Yang, *Chem. Commun. (Camb)* 2019, **55**, 2449.

[Google Scholar](#)

48 S. Li, Z. Zhu, Z. Hu, H. Sun, P. Mu, C. Xiao, W. Liang, L. Chen, A. Li, *J. Appl. Polym. Sci.* 2018, **135**, 46869.

[Google Scholar](#)

49 Q. Gui, Y. Zhou, S. Liao, Y. He, Y. Tang, Y. Wang, *Soft Matter* 2019, **15**, 393.

[Google Scholar](#)

50 M. K. Lima-Tenório, E. T. Tenório-Neto, M. R. Guilherme, F. P. Garcia, C. V. Nakamura, E. A. G. Pineda, A. F. Rubira, *Chem. Eng. J.* 2015, **259**, 620.

[Google Scholar](#)

51 X. Zhou, L. Wang, Y. Xu, W. Du, X. Cai, F. Wang, Y. Ling, H. Chen, Z. Wang, B. Hu, Y. Zheng, *RSC Adv.* 2018, **8**, 9812.

[Google Scholar](#)

52 Y. Zhang, Y. Cheng, C. Chen, Q. Liu, X. Bi, L. Duan, J. Liu, M. Wan, L. Huang, K. Hu, *J. Biomed. Nanotechnol.* 2018, **14**, 594.

[Google Scholar](#)

53 B. Chen, J. Xing, M. Li, Y. Liu, M. Ji, *Colloids Surf. B Biointerfaces* 2020, **190**, 110896.

[Google Scholar](#)

54 K. Hu, J. Sun, Z. Guo, P. Wang, Q. Chen, M. Ma, N. Gu, *Adv. Mater.* 2015, **27**, 2507.

[Google Scholar](#)

55 a) H. Wu, L. Song, L. Chen, Y. Huang, Y. Wu, F. Zang, Y. An, H. Lyu, M. Ma, J. Chen, N. Gu, Y. Zhang, *Nanoscale* 2017, **9**, 16175;

[Google Scholar](#)

b) H. Wu, L. Song, L. Chen, W. Zhang, Y. Chen, F. Zang, H. Chen, M. Ma, N. Gu, Y. Zhang, *Acta Biomater.* 2018, **74**, 302;

[Google Scholar](#)

c) R. Jahanban-Esfahlan, H. Derakhshankhah, B. Haghshenas, B. Massoumi, M. Abbasian, M. Jaymand, *Int. J. Biol. Macromol.* 2020, **156**, 438.

[Google Scholar](#)

56 H. Wu, L. Liu, L. Song, M. Ma, N. Gu, Y. Zhang, *ACS Nano* 2019, **13**, 14013.

[Google Scholar](#)

57 a) J. Huang, Z. Jia, Y. Liang, Z. Huang, Z. Rong, J. Xiong, D. Wang, *RSC Adv.* 2020, **10**, 541;

[Google Scholar](#)

b) A. B. Bonhome-Espinosa, F. Campos, D. Durand-Herrera, J. D. Sanchez-Lopez, S. Schaub, J. D. G. Duran, M. T. Lopez-Lopez, V. Carriel, *J. Mech. Behav. Biomed. Mater.* 2020, **104**, 103619.

[Google Scholar](#)

58 a) S. Zhang, L. Wu, J. Cao, K. Wang, Y. Ge, W. Ma, X. Qi, S. Shen, *Colloids Surf. B Biointerfaces* 2018, **170**, 224;

[Google Scholar](#)

b) S. M. Lee, H. J. Kim, Y. J. Ha, Y. N. Park, S. K. Lee, Y. B. Park, K. H. Yoo, *ACS Nano* 2013, **7**, 50;

[Google Scholar](#)

c) S. Wang, J. Lv, S. Meng, J. Tang, L. Nie, *Adv. Healthcare Mater.* 2020, **9**, e1901541.

[Google Scholar](#)

59 W. Wang, X. Fan, F. Li, J. Qiu, M.M. Umair, W. Ren, B. Ju, S. Zhang, B. Tang, *Adv. Optical Mater.* 2018, **6**, 1701093.

[Google Scholar](#)

60 a) T. Cheng, M. Mishkovsky, M. J. Junk, K. Munnemann, A. Comment, *Macromol. Rapid Commun.* 2016, **37**, 1074;

[Google Scholar](#)

b) R. Bakalova, B. Nikolova, S. Murayama, S. Atanasova, Z. Zhelev, I. Aoki, M. Kato, I. Tsoneva, T. Saga, *Anal. Bioanal. Chem.* 2016, **408**, 905.

[Google Scholar](#)

61 a) Q. Li, Z. Feng, H. Song, J. Zhang, A. Dong, D. Kong, W. Wang, P. Huang, *Biomater. Sci.* 2020, **8**, 3301;

[Google Scholar](#)

b) V. Nandwana, S.-R. Ryoo, T. Zheng, M. M. You, V. P. Dravid, *ACS Biomater. Sci. Eng.* 2019, **5**, 3049.

[Google Scholar](#)

62 Z. Chen, C. Yan, S. Yan, Q. Liu, M. Hou, Y. Xu, R. Guo, *Theranostics* 2018, **8**, 1146.

[Google Scholar](#)

63 E. Roeder, C. Henrionnet, J. C. Goebel, N. Gambier, O. Beuf, D. Grenier, B. Chen, P. Vuissoz, P. Gillet, A. Pinzano, *PLoS One* 2014, **9**, e98451.

[Google Scholar](#)

64 Q. Zhang, H. Lu, N. Kawazoe, G. Chen, *Acta Biomater.* 2014, **10**, 2005.

[Google Scholar](#)

65 Q. Liu, M. Liu, H. Li, K. Y. Lam, *International Journal of Solids and Structures* 2020, **190**, 76.

[Google Scholar](#)

66 a) B. Rashidzadeh, E. Shokri, G. R. Mahdavinia, R. Moradi, S. Mohamadi-Aghdam, S. Abdi, *Int. J. Biol. Macromol.* 2020, **154**, 134;

[Google Scholar](#)

b) W. Shi, J. Huang, R. Fang, M. Liu, *ACS Appl. Mater. Interfaces* 2020, **12**, 5177;

[Google Scholar](#)

c) O. Goncharuk, Y. Samchenko, D. Sternik, L. Kernosenko, T. Poltorats'ka, N. Pasmurtseva, M. Abramov, E. Pakhlov, A. Derylo-Marczewska, *Applied Nanoscience* 2020, **10**, 4559;

[Google Scholar](#)

d) M. R. Nematollahi, M. Montazer, *J. Appl. Polym. Sci.* 2020, **137**, 48961.

[Google Scholar](#)

67 M. Noh, Y. H. Choi, Y.-H. An, D. Tahk, S. Cho, J. W. Yoon, N. L. Jeon, T. H. Park, J. Kim, N. S. Hwang, *ACS Biomater. Sci. Eng.* 2019, **5**, 3909.

[Google Scholar](#)

68 C. S. Lacko, I. Singh, M. A. Wall, A. R. Garcia, S. L. Porvasnik, C. Rinaldi, C. E. Schmidt, *J. Neural. Eng.* 2020, **17**, 016057.

[Google Scholar](#)

69 K. Liu, L. Han, P. Tang, K. Yang, D. Gang, X. Wang, K. Wang, F. Ren, L. Fang, Y. Xu, Z. Lu, X. Lu, *Nano Lett.* 2019, **19**, 8343.

[Google Scholar](#)

70 M. Namdari, A. Eatemadi, *Artif. Cells Nanomed. Biotechnol.* 2017, **45**, 731.

[Google Scholar](#)

71 H. Y. Lin, H. Y. Huang, S. J. Shiue, J. K. Cheng, *J. Magn. Magn. Mater.* 2020, **504**, 166680.

[Google Scholar](#)

72 J. J. Pavon, J. P. Allain, D. Verma, M. Echeverry-Rendon, C. L. Cooper, L. M. Reece, A. R. Shetty, V. Tomar, *Macromol. Biosci.* 2019, **19**, e1800225.

[Google Scholar](#)

73 A. Tay, A. Sohrabi, K. Poole, S. Seidlits, D. Di Carlo, *Adv. Mater.* 2018, **30**, 1800927.

[Google Scholar](#)

74 A. Tay, F. E. Schweizer, D. Di Carlo, *Lab. Chip.* 2016, **16**, 1962.

[Google Scholar](#)

75 a) Y. Lin, Y. Sun, Y. Dai, W. Sun, X. Zhu, H. Liu, R. Han, D. Gao, C. Luo, X. Wang, *Talanta* 2020, **207**, 120300;

[Google Scholar](#)

b) J. Y. Wang, Q. Y. Guo, Z. Y. Yao, N. Yin, S. Y. Ren, Y. Li, S. Li, Y. Peng, J. L. Bai, B. A. Ning, J. Liang, Z. X. Gao, *Mikrochim. Acta* 2020, **187**, 333.

[Google Scholar](#)

76 L. Vikingsson, A. Vinals-Guitart, A. Valera-Martínez, J. Riera, A. Vidaurre, G. Gallego Ferrer, J. L. Gómez Ribelles, *J. Mater. Sci.* 2016, **51**, 9979.

[Google Scholar](#)

77 a) X. Ma, Z. Yang, Y. Wang, G. Zhang, Y. Shao, H. Jia, T. Cao, R. Wang, D. Liu, *ACS Appl. Mater. Interfaces* 2017, **9**, 1995;

[Google Scholar](#)

b) J. Li, F. Ji, D. H. L. Ng, J. Liu, X. Bing, P. Wang, *Chemical Engineering Journal* 2019, **369**, 611.

[Google Scholar](#)

78 a) G. Babaladimath, V. Badalamoole, *Polymer International* 2018, **67**, 983;

[Google Scholar](#)

b) J. Supramaniam, R. Adnan, N. H. Mohd Kaus, R. Bushra, *Int. J. Biol. Macromol.* 2018, **118**, 640;

[Google Scholar](#)

c) M. P. Kesavan, S. Ayyanaar, N. Lenin, M. Sankarganesh, J. Dhiveethu Raja, J. Rajesh, *J. Biomed. Mater. Res. A* 2018, **106**, 543.

[Google Scholar](#)

79 a) D. I. Kim, H. Lee, S. H. Kwon, Y. J. Sung, W. K. Song, S. Park, *Adv. Healthcare Mater.* 2020, **9**, e2000118;

[Google Scholar](#)

b) D. I. Kim, H. Lee, S. H. Kwon, H. Choi, S. Park, *Sensors and Actuators B: Chemical* 2019, **289**, 65.

[Google Scholar](#)

80 a) Y. Hong, F. Zhou, Y. Hua, X. Zhang, C. Ni, D. Pan, Y. Zhang, D. Jiang, L. Yang, Q. Lin, Y. Zou, D. Yu, D. N. Arnot, X. Zou, L. Zhu, S. Zhang, H. Ouyang, *Nat. Commun.* 2019, **10**, 2060;

[Google Scholar](#)

b) Y. Huang, X. Zhao, Z. Zhang, Y. Liang, Z. Yin, B. Chen, Y. Han, B. Guo, *Chem. Mat.* 2020, **32**, 6595.

[Google Scholar](#)

81 S. Khorshidi, A. Karkhaneh, *J. Tissue Eng. Regen. Med.* 2018, **12**, 1974.

[Google Scholar](#)

82 a) M. S. Amini-Fazl, R. Mohammadi, K. Kheiri, *International Journal of Biological Macromolecules* 2019, **132**, 506;

[Google Scholar](#)

b) W. Xie, Q. Gao, Z. Guo, D. Wang, F. Gao, X. Wang, Y. Wei, L. Zhao, *ACS Appl. Mater. Interfaces* 2017, **9**, 33660.

[Google Scholar](#)

83 D. Huang, J. Hsiao, Y. Chen, L. Chien, M. Yao, Y. Chen, B. Ko, S. Hsu, L. Tai, H. Cheng, S. Wang, C. Yang, Y. Chen, *Biomaterials* 2009, **30**, 3645.

[Google Scholar](#)

84 S. Hughes, A. El Haj, J. Dobson, *Med. Eng. Phys.* 2005, **27**, 754.

[Google Scholar](#)

85 G. Liu, J. Gao, H. Ai, X. Chen, *small* 2013, **9**, 1533.

[Google Scholar](#)

86 N. Zhang, J. Lock, A. Sallee, H. Liu, *ACS Appl. Mater. Interfaces* 2015, **7**, 20987.

[Google Scholar](#)

87 a) S. Hughes, A. J. El Haj, J. Dobson, *Med. Eng. Phys.* 2005, **27**, 754;

[Google Scholar](#)

b) J. F. Shen, Y. L. Chao, L. Du, *Neurosci. Lett.* 2007, **415**, 164.

[Google Scholar](#)

88 S. Park, H. S. Kim, W. J. Kim, H. S. Yoo, *Int. J. Pharm.* 2012, **424**, 107.

[Google Scholar](#)

89 a) J. Liang, B. He, P. Li, J. Yu, X. Zhao, H. Wu, J. Li, Y. Sun, Q. Fan, *Chem. Eng. J.* 2019, **358**, 552;

[Google Scholar](#)

b) F. Fan, J. Sun, B. Chen, Y. Li, K. Hu, P. Wang, M. Ma, N. Gu, *Science China Materials* 2018, **61**, 1112.

[Google Scholar](#)

90 A. A. Mohamed, G. A. Mahmoud, M. R. E. Eldin, E. A. Saad, *Polymer-Plastics Technology and Materials* 2019, **59**, 357.

[Google Scholar](#)

91 W. Wang, H. Zhang, J. Shen, M. Ye, *Colloids and Surfaces A: Physicochemical and Engineering Aspects* 2018, **553**, 672.

[Google Scholar](#)

92 M. Hayati, G. R. Bardajee, M. Ramezani, S. S. Hosseini, F. Mizani, *Polym. Int.* 2020, **69**, 156.

[Google Scholar](#)

93 F. Gang, H. Yan, C. Ma, L. Jiang, Y. Gu, Z. Liu, L. Zhao, X. Wang, J. Zhang, X. Sun, *Chem. Commun.* 2019, **55**, 9801.

[Google Scholar](#)

94 Y. Li, G. Huang, X. Zhang, B. Li, Y. Chen, T. Lu, T. J. Lu, F. Xu, *Adv. Funct. Mater.* 2013, **23**, 660.

[Google Scholar](#)

95 Z. Liu, J. Liu, X. Cui, X. Wang, L. Zhang, P. Tang, *Front. Chem.* 2020, **8**, 124.

[Google Scholar](#)

96 S. Cho, A. Kim, W. Shin, M. B. Heo, H. J. Noh, K. S. Hong, J. Cho, Y. T. Lim, *Int. J. Nanomedicine* 2017, **12**, 2607.

[Google Scholar](#)

97 K. H. Didehban, L. Mohammadi, J. Azimvand, *Materials Chemistry and Physics* 2017, **195**, 162.

[Google Scholar](#)

98 H. Qiao, J. Jia, W. Chen, B. Di, O. A. Scherman, C. Hu, *Adv. Healthcare Mater.* 2019, **8**, e1801458.

[Google Scholar](#)

99 S. Rittikulsittichai, A. G. Kolhatkar, S. Sarangi, M. A. Vorontsova, P. G. Vekilov, A. Brazdeikis, T. R. Lee, *Nanoscale* 2016, **8**, 11851.

[Google Scholar](#)

100 J. T. Auletta, G. J. LeDonne, K. C. Gronborg, C. D. Ladd, H. T. Liu, W. W. Clark, T. Y. Meyer, *Macromolecules* 2015, **48**, 1736.

[Google Scholar](#)

[Download PDF](#)

About Wiley Online Library

[Privacy Policy](#)

[Terms of Use](#)

[About Cookies](#)

[Manage Cookies](#)

[Accessibility](#)

[Wiley Research DE&I Statement and Publishing Policies](#)

[Developing World Access](#)

[Help & Support](#)

[Contact Us](#)

[Training and Support](#)

[DMCA & Reporting Piracy](#)

[Opportunities](#)

[Subscription Agents](#)

[Advertisers & Corporate Partners](#)

[Connect with Wiley](#)

[The Wiley Network](#)

[Wiley Press Room](#)

Copyright © 1999-2022 John Wiley & Sons, Inc. All rights reserved

WILEY

Lipid Nanoparticles—From Liposomes to mRNA Vaccine Delivery, a Landscape of Research Diversity and Advancement

Rumiana Tenchov, Robert Bird, Allison E. Curtze, and Qiongqiong Zhou*



Cite This: *ACS Nano* 2021, 15, 16982–17015



Read Online

ACCESS |



Metrics & More



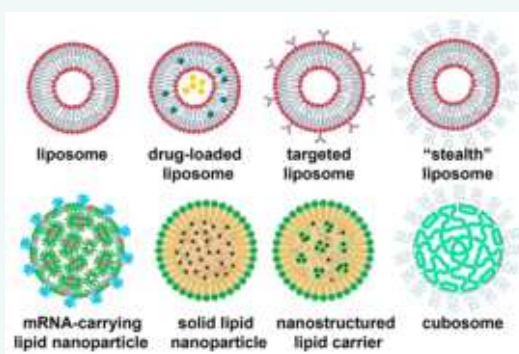
Article Recommendations



Supporting Information

ABSTRACT: Lipid nanoparticles (LNPs) have emerged across the pharmaceutical industry as promising vehicles to deliver a variety of therapeutics. Currently in the spotlight as vital components of the COVID-19 mRNA vaccines, LNPs play a key role in effectively protecting and transporting mRNA to cells. Liposomes, an early version of LNPs, are a versatile nanomedicine delivery platform. A number of liposomal drugs have been approved and applied to medical practice. Subsequent generations of lipid nanocarriers, such as solid lipid nanoparticles, nanostructured lipid carriers, and cationic lipid–nucleic acid complexes, exhibit more complex architectures and enhanced physical stabilities. With their ability to encapsulate and deliver therapeutics to specific locations within the body and to release their contents at a desired time, LNPs provide a valuable platform for treatment of a variety of diseases. Here, we present a landscape of LNP-related scientific publications, including patents and journal articles, based on analysis of the CAS Content Collection, the largest human-curated collection of published scientific knowledge. Rising trends are identified, such as nanostructured lipid carriers and solid lipid nanoparticles becoming the preferred platforms for numerous formulations. Recent advancements in LNP formulations as drug delivery platforms, such as antitumor and nucleic acid therapeutics and vaccine delivery systems, are discussed. Challenges and growth opportunities are also evaluated in other areas, such as medical imaging, cosmetics, nutrition, and agrochemicals. This report is intended to serve as a useful resource for those interested in LNP nanotechnologies, their applications, and the global research effort for their development.

KEYWORDS: lipid nanoparticle, liposome, cationic lipid, solid lipid nanoparticle, nanostructured lipid carrier, immunoliposome, “stealth” liposome, drug delivery



Lipid nanoparticles (LNPs) have emerged across the pharmaceutical industry as promising vehicles to deliver a variety of therapeutic agents. The application of LNPs has also been extended to other fields, such as medical imaging, cosmetics, nutrition, agriculture, and other innovative areas such as nanoreactors. Currently in the spotlight as a vital component of the COVID-19 mRNA vaccines, LNPs play a key role in effectively protecting and transporting mRNA to cells.

Liposomes, an early version of LNPs, are an extremely versatile nanocarrier platform because they can transport hydrophobic or hydrophilic molecules, including small molecules, proteins, and nucleic acids. In fact, liposomes are the earliest nanomedicine delivery platform to successfully proceed from concept to clinical application. A number of liposomal drug formulations have been approved and successfully applied to medical practice.

The next generations of LNPs, including solid lipid nanoparticles, nanostructured lipid carriers, and cationic lipid–nucleic acid complexes, exhibit more complex internal architectures and enhanced physical stabilities. With their ability to control the location and timing of drug delivery in the body, LNPs can be used to deliver treatments for a variety of diseases. Increasingly, scientists are moving beyond traditional biopharmaceuticals to more complex and specialized therapies that can fight disease at the genetic level.

Received: June 11, 2021

Accepted: June 21, 2021

Published: June 28, 2021



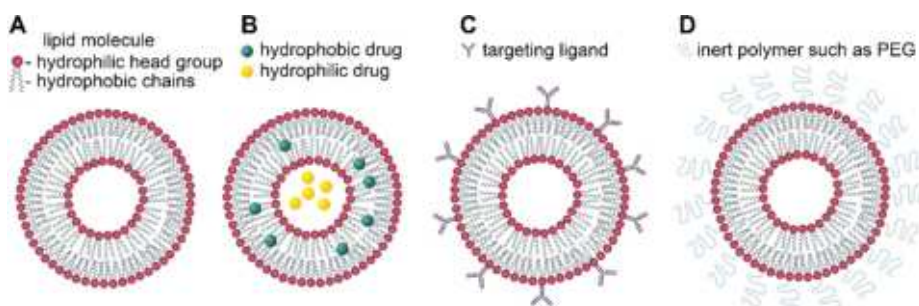


Figure 1. Schematic representation of (A) liposome, (B) liposome encapsulating hydrophobic and hydrophilic drugs, (C) immunoliposome functionalized with targeting ligands, and (D) sterically stabilized (“stealth”) liposome functionalized with inert polymers such as PEG.

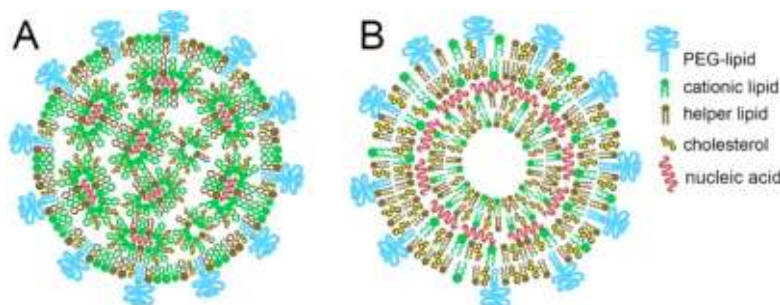


Figure 2. Suggested structures of lipid nanoparticle nucleic acid carriers: nucleic acids organized in inverse lipid micelles inside the nanoparticle (A); nucleic acids intercalated between the lipid bilayers (B).^{26–29}

In this review, we provide an overview of the current knowledge regarding LNP structures and properties, primarily from the viewpoint of their pharmaceutical applications. We then discuss the multiple applications of LNPs, including drug delivery, medical imaging, cosmetics, and others. Furthermore, we present a landscape of LNP-related research based on a thorough analysis of the CAS Content Collection.^{1,2} The CAS Content Collection is the largest human-curated collection of published scientific knowledge, proven useful for quantitative analysis of global scientific publications against variables such as time, research area, formulation, application, and chemical composition. The growth and diversity of LNP-related publications and their distribution among research areas and applications, as well as countries and organizations, are examined. Lists of the most widely used chemical substances involved in LNP formulations are provided, including phospholipids, PEG-lipids, and cationic lipids. We hope this report can serve as a useful resource for those interested in LNP nanotechnologies and the global research effort for their development.

LIPID NANOPARTICLE BASICS

Liposomes—The Earliest Generation of Lipid Nanoparticles. The term “liposome” was coined in the 1960s, shortly after it was found that closed lipid bilayer vesicles (Figure 1A) form spontaneously in water.^{3–5} The term “lipid nanoparticle” came into use much later, in the early 1990s, with the beginning of the era of nanoscience and nanotechnology. Since liposomes are made of lipids and in most cases are nanosized, they are rightfully considered as the earliest generation of lipid nanoparticles.

The potential of liposomes as drug delivery systems was recognized almost immediately after their discovery. For example, it is known that over 40% of small-molecule drugs

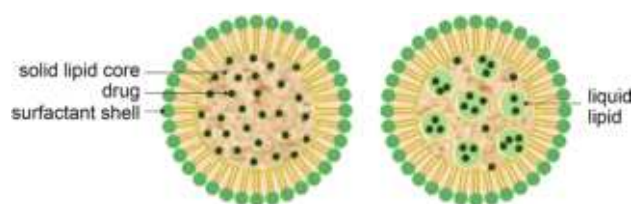


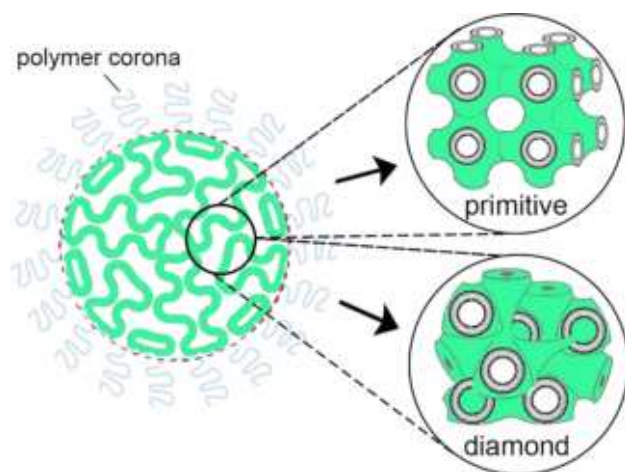
Figure 3. Schematic presentation of a solid lipid nanoparticle (left) and a nanostructured lipid carrier (right).

for cancer treatment exhibit low solubility in water, so the benefits of drug delivery systems capable of encapsulating these drugs and enhancing their aqueous solubilities was immediately appreciated. Liposomes were the earliest nanomedicine delivery platform to successfully proceed from concept to clinical application, with a number of approved pharmaceutical preparations. For example, the earliest approved liposomal drug was Doxil, a lipid nanoparticle formulation of the antitumor agent doxorubicin, which is used to treat ovarian cancer.⁶ Another liposomal drug, Epaxal, is a lipid nanoparticle formulation of a protein antigen used as a hepatitis vaccine.⁷ Many other liposomal formulations have been approved for use as drugs and vaccines, as shown in Table S1 in the Supporting Information. Liposomes have been used in numerous clinical trials to deliver anticancer, anti-inflammatory, antibiotic, antifungal, anesthetic, and other drugs and gene therapies.

Phospholipids such as phosphatidylcholines, phosphatidylethanolamines, phosphatidylserines, and phosphatidylglycerols, along with stabilizers such as cholesterol, are common liposome substituents. Liposomes consist of one or several lipid bilayers, ranging in size between 20 and ~1000 nm. Hydrophilic drugs can be enclosed in the aqueous interior of liposomes, while hydrophobic drugs can be entrapped in the hydrocarbon chain

Table 1. Common Ingredients Used for the Preparation of SLN and NLC^{36,40–43}

Lipids	Emulsifiers/coemulsifiers
Triglycerides	Lecithin
Trimyristin (Dynasan 114)	Poloxamer 188
Tripalmitin (Dynasan 116)	Poloxamer 407
Tristearin (Dynasan 118)	Tyloxapol
Mono-, di-, and triglyceride mixtures	Polysorbate 20
Witeposol bases	Polysorbate 60
Glyceryl stearates (Imwitor 900)	Polysorbate 80
Glyceryl behenates (Compritol 888 ATO)	Sodium cholate
Glyceryl palmitostearates (Precirol ATO S)	Sodium glycocholate
Waxes	Taurodeoxycholic acid sodium
Beeswax	Butanol and Butyric acid
Cetyl palmitate	Cetylpyridinium chloride
Hard fats	Sodium dodecyl sulfate
Stearic acid	Sodium oleate
Palmitic acid	Polyvinyl alcohol
Behenic acid	Cremophor EL
Other lipids	
Miglyol 812	
Paraffin	

**Figure 4.** Cubosomes are nanoparticles comprising lipid in a bicontinuous bilayer cubic phase (either primitive or diamond type).

region of the lipid bilayer (Figure 1B), making liposomes a versatile drug delivery platform. The structures of liposomes depend strongly on how they are prepared. Liposomes may be either unilamellar (small unilamellar vesicles (SUV) with diameters of 20–100 nm, large unilamellar vesicles (LUV) with diameters of 100–1000 nm, or giant unilamellar vesicles (GUV) with diameters >1000 nm) or multilamellar vesicles (MLV), with diameters of >500 nm, in which concentric bilayers form an onion-like multilayer structure (Figure S1) in the Supporting Information.⁸ Drug delivery systems primarily use SUV and smaller MLV, while GUV are used mainly as models for cells.

Size is a critical parameter in determining liposome drug encapsulation and half-life in circulation, with smaller liposomes having more chances of escaping phagocyte uptake.⁹ It has been generally accepted that particles used for pharmaceutical purposes, and especially those for parenteral administration,

need to be ≤ 100 nm.^{10–12} The size of nanoparticles can be measured using a variety of techniques such as dynamic light scattering, size exclusion chromatography, nuclear magnetic resonance spectroscopy, and microscopy. The particle size distribution of LNPs can be controlled using manufacturing methods such as extrusion, sonication, and homogenization; more recently, microfluidic methods have been successfully used for LNP manufacture and size control.

The surface charges of LNPs are generally determined by the lipid head groups, which may be either positively or negatively charged or zwitterionic. The surface potential, which depends on the surface charge density, controls the interactions between particles and the adsorption of counterions and hence the stability of the nanoparticles. Uncharged particles or particles with low charge densities tend to aggregate over time, while more highly charged particles repel each other, preventing aggregation. The surface charge of nanoparticles is most often expressed by their zeta potentials, the electrical potential of a particle measured from a plane just outside the layer of fluid bound to the particle; it is commonly calculated from its electrophoretic mobility. Zeta potentials vary linearly with the fraction of ionic lipids incorporated into the liposomes; zeta potentials < -30 mV or > 30 mV are generally sufficient to maintain interparticle repulsion and stable particle suspensions.^{13–15}

Cationic Lipid Nanoparticles, Complexes with Nucleic Acids. Progress in understanding of the genetics of cellular pathogenesis has made possible therapeutic targeting of numerous genes involved in human diseases.¹⁶ Nucleic acids have a variety of roles in medicine, including gene therapy agents and RNA therapeutics.¹⁷ However, the development of nucleic acid therapeutics is hindered by difficulties in their cellular delivery. The negative charges and hydrophilicity of nucleic acids impedes their passive diffusion across plasma membranes. In addition, the association of nucleic acids with serum proteins, their uptake by phagocytes, and their degradation by endogenous nucleases interferes with their efficient delivery. As a result, nucleic acids require delivery vectors to protect them from degradation and to deliver them to the target cells for efficient uptake. Viral and nonviral vectors are used to deliver nucleic acids to cells. Cationic LNPs, comprising stable complexes between synthetic cationic lipids and anionic nucleic acids, are the most widely used nonviral delivery system for nucleic acid drugs.^{18,19}

A large number of cationic lipid amphiphiles have been synthesized and tested for use as nucleic acid carriers. The molecular architecture of the cationic lipids is similar to that of natural lipids, except for the presence of an ionizable (cationic) head group instead of the zwitterionic or anionic head group of the natural lipids. They comprise a hydrophobic part with two alkyl chains or a cholesterol moiety, a positively charged polar head group, and a linker connecting the polar group with the hydrophobic moiety. Ionizable lipids which are positively charged only inside the cell and uncharged in the bloodstream due to a change in pH value are preferred because they are less toxic than nonionizable cationic lipids.²⁰ The structures of the most frequently used cationic lipids in LNP formulations according to the CAS Content Collection are presented further in this review (Table 12).

Complexation with positively charged lipids (Figure 2) stabilizes nucleic acids and increases their resistance to nuclease degradation, allowing them to be delivered to their desired target cells. Nucleic acids enter cells by adsorption of the LNPs to the

Table 2. Example Ligands and Receptors Tested as LNP-Targeting Agents in Cancer Therapies^{88–92}

Targeting ligand	Target receptor	Targeted cancer
Folate ^{93,94}	Folate receptor	Cancers overexpressing folate receptor
Transferrin ^{95,96}	Transferrin receptor	Cancers overexpressing transferrin receptor
Granulocyte-macrophage colony-stimulating factor (GM-CSF) ⁹⁷	GM-CSF receptor	Leukemic blasts
RGD (Arg-Gly-Asp tripeptide) ⁹⁸	Cellular adhesion molecules, such as integrins	Vasculature endothelial cells in solid tumors
NGR (Asn-Gly-Arg tripeptide) ⁹⁹	Aminopeptidase N (CD13)	Vasculature endothelial cells in solid tumors
Anti-VEGFR antibody ¹⁰⁰	Vasculature endothelial growth-factor receptor VEGFR (FLK1)	Vasculature endothelial cells in solid tumors
Anti-ERBB2 antibody (Trastuzumab) ¹⁰¹	ERBB2 (erythroblastic oncogene B2) receptor	Cancers overexpressing ERBB2 receptor, such as in breast and ovarian cancers
Anti-CD20 antibody (Rituximab, Ibritumomab tiuxetan) ¹⁰²	CD20, B-cell surface antigen	Non-Hodgkin's lymphoma, B-cell lymphoproliferative diseases
Anti-CD22 antibody (Epratuzumab) ^{103,104}	CD22, B-cell surface antigen	Non-Hodgkin's lymphoma, B-cell lymphoproliferative diseases
Anti-CD33 antibody (Gemtuzumab) ^{105,106}	CD33, a sialo-adhesion molecule, leukocyte differentiation antigen	Acute myeloid leukemia
Anti-CD25 antibody (Denileukin difitox) ^{107,108}	Interleukin-2 receptor	Cutaneous T-cell lymphoma
Antitenascin antibody ¹⁰⁹	Extracellular-matrix protein overexpressed in many tumors	Glial tumors, breast cancer
Anti-MUC1 antibody ^{110,111}	MUC1, an aberrantly glycosylated epithelial mucin	Breast and bladder cancer
Anti-TAG72 antibody ^{59,61}	TAG72, oncofetal antigen tumor-associated glycoprotein-72	Colorectal, ovarian and breast cancer
Anti-CEA antibody ^{110,112}	Carcinoembryonic antigen (CEA)	Colorectal, small-cell lung and ovarian cancers

Table 3. Examples of Stimuli-Responsive Liposomes for Enhanced Anticancer Drug Delivery

Stimuli	Anticancer Drug	Liposome Composition	Tumor
Temperature	Doxorubicin	DPPC:MSPC:DSPE-PEG2000 (86.5:9.7:3.8, mol %) ¹²⁶	Ovarian cancer
		DPPC:MSPC:DSPEmPEG2000 (21.6:2.6:1.0, molar ratio) ¹²⁷	Breast tumor
pH	Doxorubicin	DOPE, DSPE-PEG-H ₂ K(R ₂) ₂ (lipid-peptide conjugate with the pH-sensitive peptide H ₂ K(R ₂) ₂) ¹²⁸	Glioma, Glioblastoma
Magnetic field	5-Fluorouracil	Phosphatidylcholine ¹²⁹	Colon carcinoma
Laser irradiation	AMD3100	Soybean phosphatidylcholine ¹³⁰	Osteosarcoma, Breast cancer

cell surface followed by their endocytosis and release of the nucleic acids into the cell. Adsorption of LNPs to and fusion with the cell membrane are electrostatically promoted because cell membranes commonly bear negative charges and the nanoparticle lipids for nucleic acid delivery bear positive charges; their attraction thus drives membrane fusion and endocytosis. Once the nucleic acids have entered the cell, release from their complexes with cationic lipids is necessary for nucleic acid delivery. The cell's anionic lipids likely help to release nucleic acids from LNPs by neutralizing the charge of their cationic lipid carriers, disrupting the electrostatic interactions between the lipid carriers and the nucleic acids. Binding of anionic lipids to the cationic lipids also disrupts the nanoparticle architecture, leading to formation of nonlamellar structures.^{21,22} The efficacy of cationic lipid vectors in delivering nucleic acids has been proposed to correlate to their ability to promote the formation of nonlamellar lipid phases.^{19,23} Short-lived nonlamellar structures are believed to mediate the processes of membrane fusion; the intermediates that form in membrane fusion are similar to those that form during lamellar–nonlamellar phase transformations.^{24,25}

Solid Lipid Nanoparticles and Nanostructured Lipid Carriers. While liposomes are useful as drug carriers, they require complex production methods using organic solvents, exhibit low efficiency at entrapping drugs, and are difficult to perform on large scales. Solid lipid nanoparticles (SLN) and nanostructured lipid carriers (NLC) were developed to address some of these shortcomings (Figure 3). While conventional liposomes comprise liquid-crystalline lipid bilayers, SLN

comprise solid lipids,^{30,31} and NLC comprise mixtures of solid and liquid-crystalline lipids.^{32,33} The particle sizes of SLN and NLC vary between 40 and ~1000 nm. SLN and NLC exhibit enhanced physical stabilities, addressing one of the main limitations of liposome-based formulations. SLN and NLC also have higher loading capacities and higher bioavailabilities of their cargoes, are produced easily on large scale without the use of organic solvents, and are more stable to sterilization than other LNPs. In addition, the reduced mobility of molecules in the solid state allows SLN and NLC to control the release of their drug payloads more precisely. However, on long-term storage, crystallization of SLN can expel the incorporated drugs into the surrounding media.³⁴ NLC were then designed by introducing small amounts of lipids liquid at room temperature into SLN, reducing the degree of crystallinity of the lipid core. The reduced crystallinity of NLC suppresses expulsion of the drug from the matrix and enhances the drug-loading capacities and physical and chemical long-term stabilities of the nanoparticles.^{35,36}

SLN and NLC are composed of lipids and stabilizing agents such as surfactants and other coating materials (Figure 3). Typical lipid constituents are shown in Table 1, including fatty acids, fatty alcohols, glycerides, and waxes. Surfactants, located at the lipid–water interface, reduce the interfacial tension between the lipid and the aqueous phases and improve the stabilities of the resultant formulations. A list of commonly used surfactants/emulsifiers in LNP preparation is also included in Table 1. SLN and NLC are usually produced using various organic solvent-free methods, such as high-pressure homoge-

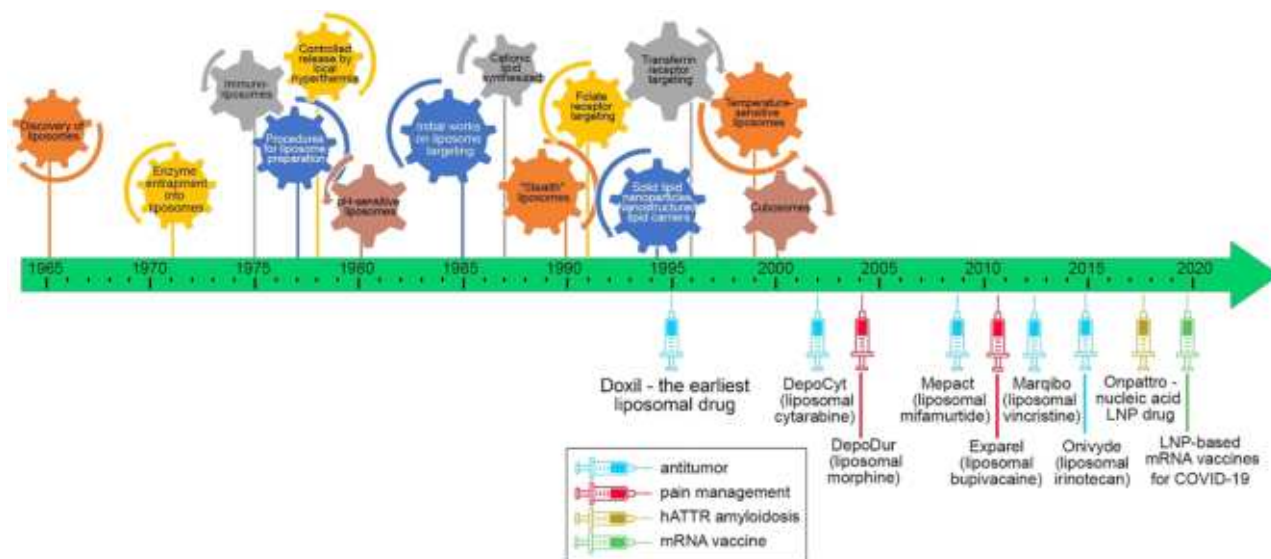


Figure 5. Timeline of liposome/LNP advancement. (Upper part) Technological advancement. Publications on LNPs, correlated to the timeline of LNP advancement: The discovery of liposomes;³ Enzyme entrapment into liposomes;¹³⁶ Immunoliposomes;^{80,137,138} Procedures for liposome formation;^{139,140} Thermoresponsive liposomes to local hyperthermia;^{124,141,142} pH-sensitive liposomes;¹²¹ Liposome targeting;^{77,143,144} Cationic lipids for gene delivery;^{18,145,146} Long-circulating (“Stealth”) liposomes;^{115,116,147} Folate receptor targeting;^{81,84,144,148,149} Solid lipid nanoparticles and nanostructures lipid carriers;^{31,35,150,151} HER2 receptor targeting;^{152–154} Transferrin receptor targeting;^{155–158} Temperature-sensitive liposomes;^{122,142,159,160} Stimuli-responsive liposomes;^{123,149,161} Cubosomes.^{46,47,50,162} (Lower part) Examples of FDA-approved LNP drugs. The earliest approved liposomal drug Doxil;⁶ The earliest FDA-approved LNP-based nucleic acid (siRNA) drug Onpatro;¹⁶³ LNP-based mRNA vaccines for COVID-19 approved;^{164,165} Useful general reviews.^{166–173} For a full list of approved LNP-based drugs, see Table S1 in the Supporting Information.

nization, high-speed stirring, ultrasonication, emulsion/solvent evaporation, double emulsion, phase inversion, and solvent injection.^{31,37–39}

Nonlamellar Lipid Nanoparticles. Other types of LNP structures have also been investigated for use in drug delivery. Technologies relating to the use of nonlamellar lipid phases in drug delivery and the use of inverted cubic and hexagonal liquid-crystalline phases in controlled release formulations for delivery of inhaled drugs were published in the 1980s.^{44,45}

More recently, cubosomes, highly stable nanoparticles formed from lipid cubic phases (Figure 4) and stabilized by polymer-based outer coronas, were developed as lipid pharmaceutical nanocarriers.^{46–50} Liquid-crystalline lipid cubic phases consist of single lipid bilayers that form a bicontinuous periodic lattice structure with pores formed by two interwoven water channels. Cubosomes are highly stable under physiological conditions. The composition of a cubosome can be tuned to customize its pore sizes and to include bioactive lipids; the polymeric outer corona can be used to control where the cubosome payload is released. Cubosomes provide a significantly higher membrane surface area for loading of membrane proteins and small-molecule drugs than do liposomes. This combination of properties allows cubosomes to be used in a variety of applications, such as drug delivery systems, membrane bioreactors, artificial cells, and biosensors.

Cubosomes are composed of amphiphilic lipids and a stabilizer. The amphiphilic lipid is the major component; upon hydration, the lipid spontaneously forms a cubic liquid-crystalline phase. The stabilizer is typically a polymer that prevents the reconstitution of the cubosome into a bulk cubic phase. The most frequent compositions of cubosomes use monoolein (glyceryl monooleate) as the lipid component with poloxamer 407 as a stabilizing surfactant; the monoglyceride/

surfactant mixture makes up between 2.5% and 10% of the total weight of the dispersion. Polyvinyl alcohol is also used in addition to poloxamer 407 as a stabilizer for the dispersion.⁵¹

Hexosomes are another type of LNP, in which lipids form a nonlamellar phase—the inverted hexagonal phase H_{II} . Their compositions are similar to those of cubosomes, containing amphiphilic lipids, a polymeric stabilizer, and water.^{52,53} Micelles are nonlamellar lipid nanosized particles with a hydrophobic core and hydrophilic shell; they have been used successfully to solubilize poorly water-soluble pharmaceuticals.^{54,55} Reverse micelles, with a hydrophilic core and hydrophobic shell, have been used to encapsulate hydrophilic molecules such as nucleic acids in complex lipid carriers.^{26,27,56,57}

Ethosomes. Ethosomes are phospholipid nanoparticles containing a high proportion (20–45%) of ethanol. The added ethanol increases the permeabilities and elasticities of the ethosomes, allowing them to perform transdermal delivery of drugs and cosmetics by squeezing through the pores of stratum corneum, the outermost layer of skin. This delivery route offers an alternative method to deliver liposomal formulations, avoiding the complications caused by the gastrointestinal tract in oral drug delivery.⁵⁸ Commercial products using ethosomal formulations include anticellulite (Cellutight EF, Noicellex, Skin Genuity, Osmotics Lipoduction) and antiaging (Decorin) agents, hair growth stimulants including Minoxidil (Nanominox) and Acyclovir (Supravir), and topical creams for the treatment of herpes virus infections.⁵⁹

Echogenic Liposomes. Echogenic liposomes are acoustically active liposomes utilized as ultrasound contrast agents.⁶⁰ They have been developed following the discovery that microscopic bubbles of gas reflect diagnostic ultrasound waves. Gas–liquid interfaces provide a large discontinuity in

density and reflect sound very efficiently. Encapsulated into liposomes, gas microbubbles provide improvements in medical acoustic imaging.⁶¹ Echogenic liposomes also offer additional therapeutic applications, such as ultrasound-controlled drug delivery^{60,62,63} and ultrasound-enhanced thrombolysis (sonothrombolysis).^{64,65}

Procedures for LNP Formation. A wide variety of techniques are used to control the properties of LNPs, including their sizes, numbers of concentric bilayers (lamellarity), and their ability to encapsulate various compounds.^{66–69}

The film hydration method represents the simplest and oldest method used for liposome preparation. Lipids are initially dissolved in an organic solvent and then dried down to yield a thin film at the bottom of a vial. The lipid film is hydrated to produce a liposomal dispersion. The hydration conditions affect the structure of the formed vesicles—giant unilamellar vesicles (GUV) are formed by gentle hydration, while multilamellar vesicles (MLV) with poor size homogeneity are formed upon intense agitation. Probe or bath sonication can be used to produce small unilamellar vesicles (SUV). Consecutive extrusion through polycarbonate filters of defined pore sizes can also be used to control liposome diameter; the number of extrusion cycles is important in determining the homogeneity of the liposomes formed.⁷⁰

Another traditional liposome preparation technique is reverse phase evaporation, involving formation of a water-in-oil emulsion between an aqueous phase and an organic phase containing lipids. The mixture is briefly sonicated to homogenize it; removal of the organic phase under reduced pressure yields a gel and then a liposomal suspension.⁷¹ The solvent injection technique for liposome formation involves the rapid injection of a lipid solution (in ethanol or diethyl ether) into an aqueous medium.⁷² The detergent removal liposome preparation technique involves dissolution of phospholipids in an aqueous solution containing detergents at their critical micelle concentrations (CMC) followed by removal of the detergents by dialysis or other means. Dilution of the resultant suspension with water or aqueous solutions reconstitutes the formed micelles; over time, the micelles convert to liposomes.⁷⁰ In the heating method for liposome preparation, lipids are hydrated and then heated above the transition temperature of the phospholipids in the presence of a hydrating agent such as glycerin or propylene glycol. This method is attractive because it does not involve an organic solvent.^{8,73}

A successful recent liposome production technique is microfluidic hydrodynamic focusing, in which a stream of lipid in alcohol solution is forced to flow in the central channel of a device, intersected, and sheathed by coaxial stream(s) of an aqueous phase. Reciprocal diffusion of alcohol and water across the focused alcohol/water interface causes the lipid to precipitate and self-assemble into liposomes.^{69,72,74} Other recently developed techniques for producing liposomes include cross-flow injection⁶⁹ and methods using supercritical fluids.^{68,72}

Similarly, preparation of other types of LNP, such as SLN, NLC, and cubosomes, includes various methods for homogenization (high-shear homogenization, hot or cold homogenization, high-speed homogenization), ultrasonication, and microfluidization.^{75,76} Ultrasonication, extrusion, and microfluidic methods have been most often used to control LNP size, according to the CAS Content Collection.

Functional Modifications of LNPs. Despite their advantages, unmodified LNP drug delivery systems have significant

limitations such as lack of targeting selectivity, short blood circulation time, and instability *in vivo*. Improved LNP formulations were designed to overcome each of these shortcomings.

Targeted Liposomes. Targeted liposomes were designed with surface-attached ligands (Figure 1C) to recognize and bind to specific receptors on cells.⁷⁷ Generally, targeted liposomes are prepared by conjugating small-molecule ligands, peptides or monoclonal antibodies to the surface of LNPs.^{78,79} Antibodies were initially used to construct actively targeted liposomes (immunoliposomes). For example, the efficiency of liposomes modified with an IgM ligand was 100 times higher than that of unmodified liposomes.⁸⁰ Certain receptors, such as the folate receptor and the transferrin receptor, are overexpressed on many cancer cells, and their corresponding ligands have been used to direct liposomes to these types of cells or tissues.^{81–84} Folate receptors bind strongly to their ligand, folic acid, allowing for specificity for tumor cells over noncancerous cells. The lack of immunogenicity of folic acid and the ability of its conjugates to be taken into cells nondestructively by endocytosis make folates preferable to protein-based targeting ligands. Folate receptors are also overexpressed on macrophages, which are present in inflammatory diseases such as psoriasis, Crohn's disease, atherosclerosis, and rheumatoid arthritis; thus, folate-mediated targeting can also be used to deliver antiinflammatory drugs.⁸⁵ Transferrin receptors are overexpressed in rapidly proliferating cancer cells to meet the increased iron demands of tumor cells, making possible the development of transferrin receptor-targeted anticancer therapies.⁸⁶ The epidermal growth factor receptor (EGFR), a tyrosine kinase receptor, is overexpressed in many solid tumors, including colorectal, nonsmall-cell lung cancer, squamous cell carcinoma, and breast cancer, making it an attractive target for therapeutic drug delivery.⁸⁷ Examples of ligands used in LNP targeting are shown in Table 2.

"Stealth" Liposomes. While immunoliposomes were highly selective for specific cell types, they were rapidly removed from the blood flow by phagocytes. To remedy this, liposomes were coated with biocompatible inert polymers, typically poly(ethylene glycol) (PEG), making them invisible to phagocytes ("stealth" liposomes) (Figure 1D). PEGylation (covalently attaching PEG to a compound) was initially invented to help protein drugs to avoid the body's immune response^{113,114} but was later found to be also very effective at improving the surface properties of the liposomes by preventing access to their surface through steric hindrance.^{115–117} The circulatory half-life of liposomes depends on the length and density of the polymer chains on the liposome surface, allowing stable, sterically stabilized liposomes to be prepared.¹¹⁸ The increased circulation half-lives of sterically stabilized liposomes also increase their passive accumulation in cancer tissues by the enhanced permeation and retention (EPR) effect, further increasing their effectiveness.¹¹⁹

Stimuli-Responsive Liposomes. Another useful liposome modification includes formulations designed to release encapsulated drugs controllably when exposed to physicochemical or biochemical stimuli (stimuli-responsive liposomes). These drug delivery systems respond to specific triggers to release their cargo where needed, increasing drug efficacy and reducing adverse effects. Liposomes responsive to temperature, changes in pH, enzymes, light, magnetic and electrical fields, and ultrasound have been studied.¹²⁰ Among these stimuli, pH change is the most promising due to the existence of multiple pH gradients in the body.¹²¹ When triggered by a stimulus, LNPs



Figure 6. Approved LNP drugs and the diseases they target (more details in Table S1).



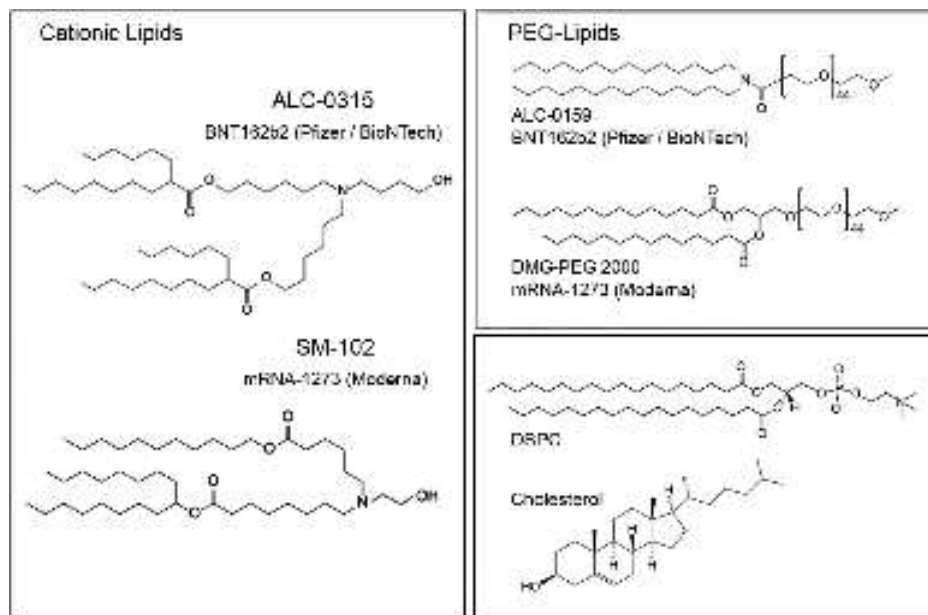
Figure 7. Key players operating in the global LNP drug delivery market according to a recent market analysis¹⁸⁰ and the summary of the LNP-based marketed drugs (Table S1).

undergo a phase transition (either between the gel and liquid-crystal phases or between lamellar and nonlamellar phases), increasing their membrane permeability.¹²² Temperature-responsive systems have been studied extensively for anticancer drug delivery.^{120,123} When exposed to mild local hyperthermia, the lipids approach their liquid-crystalline phase transition temperatures, creating disorder between their solid and fluid domains and becoming more permeable to water-soluble molecules. This results in burst release of the entrapped drug within the tumor.^{124,125} Table 3 provides examples of stimuli-responsive liposomes.

Toxicity of Lipids Used in LNP Formulations. Since LNPs are mainly composed of natural lipids, they have been considered pharmacologically inactive and minimally toxic. However, in some cases, LNPs are not immunologically inert¹³¹ while LNP constituents are unnatural compounds which may be toxic to human cells.¹³² For example, while cationic lipids offer great promise as carriers for the delivery of fragile compounds such as nucleic acids, some cationic lipids cause cytotoxicity.¹³³ In some cases, cationic lipids reduce mitosis in cells, form vacuoles in the cytoplasm of cells, and cause detrimental effects on key cellular proteins such as protein kinase C.¹³⁴ The cytotoxicity of cationic lipids depends on the structures of their

Table 4. Lipid Constituents of the LNP Carriers of the COVID-19 mRNA Vaccines^{164,165,195–197}

Lipid Name	Role	Abbreviation or Lab Code	CAS Registry Number
BNT162b2 vaccine (Pfizer/BioNTech)			
(4-hydroxybutyl)azanediyil bis(hexane-6,1-diyl)bis(2-hexyldecanoate)	ionizable cationic lipid	ALC-0315	2036272-55-4
(2-hexyldecanoate), 2-[(polyethylene glycol)-2000]-N,N-ditetradecylacetamide	PEG-lipid	ALC-0159	1849616-42-7
1,2-distearoyl- <i>sn</i> -glycero-3-phosphocholine	helper lipid	DSPC	816-94-4
cholesterol	helper lipid	Chol	57-88-5
mRNA-1273 vaccine (Moderna)			
heptadecan-9-yl 8-((2-hydroxyethyl)(6-oxo-6-(undecyloxy)hexyl)amino)octanoate	ionizable cationic lipid	SM-102	2089251-47-6
1,2-dimyristoyl- <i>rac</i> -glycero-3-methoxypolyethylene glycol-2000	PEG-lipid	PEG2000-DMG	160743-62-4
1,2-distearoyl- <i>sn</i> -glycero-3-phosphocholine	helper lipid	DSPC	816-94-4
cholesterol	helper lipid	Chol	57-88-5

**Figure 8. Structures of the lipid constituents of the LNPs of the COVID-19 mRNA vaccines**^{164,165,195–197}

hydrophilic head groups; amphiphiles with quaternary ammonium head groups are more toxic than those with tertiary amine head groups.¹³⁴ The effect of the hydrophobic chains on the toxicity of lipids is not well studied, hindering the design of less toxic lipids. The hydrophobic portions of lipid molecules strongly modulate their phase behavior and their usefulness for LNP, but the presence of certain lipid phases also correlates to membrane damage and cytotoxicity.²⁵ PEG–lipid conjugates may also cause undesired toxicity, while LNPs containing PEG–lipid conjugates are known to interact with immune cells to generate undesired antibodies against some PEGylated lipids.¹³⁵

Timeline of Liposome/LNP Advancement. A timeline of liposome/LNP advancement is shown in Figure 5.

APPLICATIONS OF LIPID NANOPARTICLES

Drug and Vaccine Delivery. *Clinically Approved LNP-Based Pharmaceuticals.* Liposomes have been recognized as a powerful tool in medicine for over 50 years. Their ability to encapsulate and deliver therapeutics controllably to specific locations within the body makes them useful for treating a variety of diseases. A number of LNP drug formulations have been approved and used in medical practice (Figure 6).^{88,174–179} More information on these formulations is included in Table S1 in the Supporting Information. A selection of key players operating in the global liposome drug delivery market according

to a recent market analysis,¹⁸⁰ as well as from the summary of the LNP-based marketed drugs (Table S1), is shown in Figure 7.

The largest single application of LNPs in drug delivery is in cancer treatment (Figure 6), because of the improved bioavailability and selectivity of LNP-encapsulated anticancer agents over the free drugs. Lipid-based nanocarriers reduce the toxicity of anticancer drugs to normal tissues, increase the water solubilities of hydrophobic drugs, extend the drug residence time, and improve control over drug release.^{92,181,182}

LNPs also improve the efficacy of cancer therapies through the enhanced permeability and retention (EPR) effect.¹⁸³ Rapid but defective angiogenesis in tumors leads to blood vessels that possess large fenestrations (>100 nm in size) through which LNP can readily pass. The tumor blood vessels are thus much more permeable to LNPs, allowing their selective accumulation in tumors when administered intravenously. In addition, dysfunctional lymphatic drainage in tumors reduces the rate at which LNPs leave tumors and thus improves their retention. The accumulation of LNPs in tumors as a result of the EPR effect allows the nanoparticles to release the anticancer agents selectively in the vicinity of tumor cells.

Doxil was the earliest approved anticancer nanoformulation and the earliest approved liposomal drug. The formulation was designed to improve the pharmacokinetics and biodistribution of the anthracycline drug doxorubicin, which is a potent

Table 5. Clinical Trials of LNP-Formulated mRNA Drugs and Vaccines^{208,210}

Disease	mRNA/encoding sequence	NCT Number/Phase
Infectious disease vaccines		
Rabies	mRNA/Rabies virus glycoprotein (RABV-G)	NCT03713086/Phase I
Zika Virus	mRNA-1893/Structural proteins of Zika virus	NCT04064905/Phase I
	mRNA-1325/Zika virus antigen	NCT03014089/Phase I
Cytomegalovirus (CMV)	mRNA-1647 and mRNA-1443/Pentamer complex and full-length membrane-bound glycoprotein B and pp65 T cell antigen of CMV	NCT03382405/Phase I
hMPV and PIV3	mRNA-1653: Fusion proteins of hMPV and PIV3	NCT03392389/Phase I
Tuberculosis	GSK 692,342/Immunogenic fusion protein (M72) derived from <i>Mycobacterium tuberculosis</i>	NCT01669096/Phase II
Influenza	VAL-506440/H10N8 antigen	NCT03076385/Phase I
	VAL-339851/H7N9 antigen	NCT03345043/Phase I
COVID-19	ChulaCov19 mRNA/SARS-Cov2-spike protein-binding IgG antibody	NCT04566276/Phase I/II
	self-amplifying mRNA (SAM) platform/anti-Spike IgG antibodies GMCs	NCT04758962/Phase I
	Chimpanzee Adenovirus serotype 68 (ChAd) and self-amplifying mRNA (SAM) vectors/Spike (ChAdV68-S)	NCT04776317/Phase I
Cancer immunotherapy		
Melanoma	mRNA-4157/personalized cancer vaccine targeting 20 tumor-associated antigens	NCT03897881/Phase II
	RBL001.1; RBL002.2; RBL003.1; RBL004.1/malignant melanoma-associated antigens	NCT02410733/Phase I
Ovarian Cancer	W_ova1 vaccine: Three ovarian cancer tumor associated antigens mRNAs	NCT04163094/Phase I
Triple-negative breast cancer	IVAC_WAREHOUSE_bre1_uID; IVAC_MUTANOME_uID/personalized cancer vaccine targeting tumor-associated antigens	NCT02316457/Phase I
Solid tumors	mRNA-4157/personalized cancer vaccine targeting 20 tumor-associated antigens	NCT03313778/Phase I
Melanoma, Colon cancer, Gastrointestinal cancer, Genitourinary cancer, hepatocellular cancer	NCI-4650/mRNA-based, Personalized Cancer Vaccine	NCT03480152/Phase I/II
Melanoma, NSCLC, Bladder Cancer, Colorectal Cancer, Triple Negative Breast Cancer, Renal Cancer, Head	RO7198457/personalized cancer vaccine targeting tumor-associated antigens	NCT03289962/Phase I
Relapsed/Refractory Solid Tumor Malignancies or Lymphoma, Ovarian Cancer	mRNA-2416/OX40L	NCT03323398/Phase I and II
Solid Tumor Malignancies, Lymphoma, Triple Negative Breast Cancer, Head and Neck Squamous Cell Carcinoma, Non-Hodgkin Lymphoma, Urothelial Cancer	mRNA-2752/Human OX40L, IL-23, and IL-36 γ	NCT03739931/Phase I
Adult Glioblastoma	Autologous total tumor mRNA and pp65 full length lysosomal associated membrane protein (LAMP) mRNA loaded DOTAP liposome vaccine	NCT04573140/Phase I
Protein-replacement therapies		
Propionic Acidemia	mRNA-3927/ α and β subunits of the mitochondrial enzyme propionyl-CoA carboxylase	NCT04159103/Phase I and II
Isolated Methylmalonic Acidemia	mRNA-3704/methylmalonyl-coenzyme A mutase (MUT)	NCT03810690/Phase I and II
Ornithine Transcarbamylase Deficiency	MRT5201/Ornithine transcarbamylase	NCT03767270/Phase I and II
Cystic Fibrosis	MRT5005/Human Cystic Fibrosis Transmembrane Regulator protein (CFTR)	NCT03375047/Phase I and II
Carnitine Palmitoyl Transferase 2 Deficiency	CPT2 mRNA/Carnitine Palmitoyl Transferase 2	NCT00336167/Phase I
Hereditary Transthyretin Amyloidosis with Polyneuropathy	Cas9 mRNA/NTLA-2001 (CRISPR/Cas9 technology)	NCT04601051/Phase I

anticancer agent but is cardiotoxic.¹⁸⁴ Doxil takes advantage of EPR, using sterically stabilized nanoparticles (~100 nm) to extend the circulation time in human plasma while reducing doxorubicin's cardiotoxicity. It was developed as an intravenous injection for the management of advanced ovarian cancer, multiple myeloma, and HIV-associated Kaposi's sarcoma.⁶ The LNPs used for Doxil are composed of hydrogenated soy phosphatidylcholine, cholesterol, and DSPE-PEG2000.¹⁸⁵

The second largest group of liposomal drugs comprises fungicides (Figure 6). Amphotericin B, a broad-spectrum polyene antibiotic, has been in medical use for decades and is considered the gold standard for treating invasive fungal

infections. It targets cell membranes, exhibiting higher affinity for ergosterol-containing membranes typical of fungal cells than for cholesterol-containing mammalian cell membranes.¹⁸⁶ While it has high antifungal activity, amphotericin B also has severe side effects, particularly nephrotoxicity. It is amphipathic and characterized by complicated self-association behavior, with different types of aggregates displaying different solubilities and toxicities; the aggregation state also correlates to drug efficacy.¹⁸⁷ Thus, controlling the aggregation state of the drug may enhance its therapeutic effect and lower its toxicity. Such aggregation control has been achieved via lipid nanoformulations.^{188,189} Several lipid-based nanoparticle preparations of

Table 6. Notable Patents from the CAS Content Collection Related to the Use of LNP in Theranostic Formulations

Patent #	Title	Key Feature
WO2016024281	Theranostic compositions and methods for therapeutics prescreening	A theranostic composition and method for determining the cell-specific potency of drugs is provided. Lipid nanoparticles are fabricated using a microfluidic apparatus.
WO2013012891	Intraperitoneally administered nanocarriers that release their therapeutic load based on the inflammatory environment of cancers	Nanocarrier compositions that release their therapeutic load specifically at the site of intraperitoneal cancers. These nanocarriers comprise a plurality of porous nanoparticles loaded with pharmaceutically active agents in combination with imaging agents, thus providing a theranostic value, and are encapsulated by a lipid bilayer.
WO2019083365	Delivery vectors	Liposome compositions that selectively deliver a cargo such as an active pharmaceutical ingredient or an imaging agent to the blood brain barrier (BBB) of a subject. The liposomes may be used for therapeutic, diagnostic, or theranostic purposes.
WO2018218052	Nanoparticle-lipid composite carriers as theranostic agents	Nanoparticle-lipid composite carriers comprising a lipid core and an outer shell of functionalized nanoparticles for use as theranostic agents, particularly for diagnosis and/or treatment of cancers and related diseases.
WO2018185290	Use of a liposome encapsulating a sugar compound in theranostic CEST imaging	Agents comprising a liposome encapsulating a suitable sugar compound, for use in Chem. Exchange Saturation Transfer (CEST) imaging for diagnostic and theranostic purposes. The liposomes can be shielded and/or targeted to a sugar uptake site such as a tumor. The invention has particular utility in modulating the glycemic response in the subject.
WO2018146700	A biodegradable nano-theranostic composite and process of preparation thereof	A biodegradable nanotheranostic composite in which graphene oxide is coated as a film on the inner side and outer side of the liposome. The composite can perform targeted combined chemo- and photothermal therapy. The nanotheranostic nanocomposite is designed to collapse and biodegrade after use.
US20180178043	Focused ultrasound hyperthermia	Focused ultrasound hyperthermia method is applied repeatedly using image guidance. Hyperthermia is applied after a drug or biopharmaceutical and/or their labeled equivalents (theranostics) have been administered to cause the enhanced tissue distribution and/or controlled release of the drug encapsulated in thermosensitive lipid nanoparticles. The drug and/or the drug delivery system are labeled for imaging to allow real time monitoring and modulation.
WO2017173089	Systems and methods for enhancing delivery of diagnostic and/or therapeutic compositions <i>in vivo</i> using electric pulses	Systems and methods for manipulation of tumors with pulsed elec. fields. These systems and methods can be used for theranostic applications in oncological diagnosis and treatment, especially when combined with liposome-delivered drugs.
WO2016198859	Precision therapeutics	Pharmaceutical composition comprising a combination of imaging lipid nanoparticles and therapeutic agent(s). Imaging LNPs may have receptor-targeting ligands. Image-guided hyperthermia applied to target sites enables the imaging LNPs and therapeutic agent(s) to partition from the blood into target tissues for therapy by means of hyperpermeability and retention (HPR). Therapeutic outcomes can be followed by clinically relevant imaging modalities such as MRI.
WO2012040710	Stabilized nanobubbles comprising lipid membranes for diagnostic and therapeutic applications	Stabilized echogenic nanobubbles for diagnostic, therapeutic, and theranostic applications. The stabilized nanobubble includes a membrane-defining internal void, containing gas. The membrane comprises a lipid and nonionic triblock copolymer effective to control the size of the nanobubble. The gas has a low solubility in water and includes a perfluorocarbon.

Table 7. Notable Patents from the CAS Content Collection Related to the Use of LNPs in Food and Nutrition Formulations

Patent #	Title	Key Feature
EP3417846	Food and/or nutraceutical composition, in the form of liposomes, comprising endocannabinoid	A food and/or nutraceutical composition, for example in the form of liposomes, which comprises an endocannabinoid, an active ingredient and an excipient.
WO2014140268	Solid lipid nanoparticles	Food-grade SLN comprise a solid lipid phase core comprising lipophilic and/or amphiphilic active ingredient and an emulsifier comprising mono- and diglyceride citric acid ester.
WO2017095138	Curcumin-containing lipid nanoparticle complex comprising ginsenosides	Curcumin-containing lipid nanoparticles containing ginsenosides exhibit improved stabilities, dispersibilities, and bioavailabilities. They can be used in curcumin-containing products such as antioxidant food compositions.
WO2004064805	Lipid-based cochleate preparations of fragile nutrients for the food, cosmetic and pharmaceutical industries	Cochleate-containing nanoparticles including one or more cochleates of fragile nutrients such as β -carotene are disclosed.
US20100196543	Microencapsulated citrus phytochemicals and application to beverages	A beverage includes citrus juice, microencapsulated citrus phytochem, ≤ 90 mg unencapsulated hesperidin, ≤ 150 mg unencapsulated naringin, and ≤ 0.9 mg unencapsulated limonin. Phytochemicals (such as limonoids and flavonoids) are microencapsulated to conceal their bitter taste.
EP1894477	Food protein and charged emulsifier interaction	A coated denatured supramolecular protein core with food applications comprises an electrostatically bound lipid monolayer. Thus, heat-denatured whey protein aggregates may be coated with sulfated Bu oleate to form liposome-like structures.
WO2013008261	Food product of the type to be stored and consumed refrigerated or frozen	A food product of the type to be stored and consumed refrigerated or frozen comprises an active ingredient encapsulated in liposomes, thus increasing its stability and its antioxidant capacity. Liposomes containing vitamin A are formulated with α -tocopherol, rosmarinic acid, and lecithin.
WO2011119953	Orally bioavailable lipid-based constructs for delivery of biotin derivatives	Lipid-based compositions facilitate efficient oral absorption of biotin compounds for inducing weight loss. An orally bioavailable composition comprises gelatin, liposomes, and lipid particles and a biotin-derived targeting agent.
US20170127712	Dietary supplement compositions with enhanced delivery matrix, gummies, chocolates, atomizers and powders containing same, and methods of making same	A dietary supplement composition includes liposomal vesicles, an active ingredient, a phospholipid contained in the liposomal vesicles, and a coating material. The liposomal vesicles have a barrier coating made of a biopolymer, polyethylene glycol, and/or chitosan. The dietary supplement composition may be incorporated in gummies, chocolates, atomizers, or powders.
WO9922601	Enhanced infant formula containing liposome encapsulated nutrients and agents	Liposomes are used in an infant formula to improve the delivery and stability of nutrients, and they enhance their bioavailability. The formula more closely resembles the ultrastructure and infrastructure of natural human milk due to the presence of liposomes. The phospholipid concentration is the same as that in human milk.

Table 8. Notable Patents from the CAS Content Collection Related to Use of LNPs in Agrochemical Formulations

Patent #	Title	Key Feature
US20190104734	Cure and prevent diseases in plants, bushes and trees using rhamnolipid liposomes	A fertilizer using rhamnolipid-containing liposomes eliminates disease in plants, bushes, and trees by breaking down the cell walls of disease-causing bacteria.
US20150150245	Liposome formulations	Liposomal formulations comprise pesticides, nematocides, or herbicides for control of pests and weeds. The formulations can be applied to pre- or postemergent crops and to soil, plant media, plants, plant tissues, and seeds.
WO9817110	Formulations for enhancing the efficacy of pesticides, especially herbicides	Formulations comprise the active ingredient and a liposome-forming excipient such as a diacylphosphatidylcholine or diacylphosphatidylethanolamine having a cationic hydrophilic moiety and a hydrophobic moiety comprising two hydrocarbon acyl chains. The formulations also comprise an amphiphilic quaternary ammonium ingredient.
WO9821945	Lecithin-microencapsulated boron pesticides	Liposomal microencapsulated boron-containing products are disclosed to be used in agricultural formulations. Boron-containing materials formulated according to the invention may be applied to agricultural field crops and fruits.
WO2002052939	Controlled-release formulations of anionic herbicides	An herbicidal formulation comprising an herbicide incorporated in a micelle using a quaternary amine cation or a lipid vesicle, adsorbed on a clay mineral. Suitable in particular for negatively charged herbicides at pH above 6. The formulation provides slow release and reduced leaching of the herbicide to deep soil layers, thus reducing contamination of underground water and soil. Furthermore, because the herbicide stays near the target, efficiency is enhanced and smaller dosage may be used.
US20100233224	Photolytic release of biocides for high efficiency decontamination through phospholipid nanoparticles	Biocide-filled liposome vesicles contain photosensitizers. Irradiation of the liposome vesicles with light causes the vesicle membranes to break, releasing the biocidal agents. Preferred biocidal agents include hydrogen peroxide, benzalkonium chloride, and photooxidizing nanoparticles such as titanium dioxide, iron oxide, and biocides such as Ucaricide 25 and Ucaricide 50 (Dow Chem. Co).

amphotericin B have been developed (Figure 6; Table S1), which exhibit favorable pharmacokinetic profiles and significantly reduce the side effects of this drug.¹⁸⁸

Nucleic acid therapeutics are an emerging class of drugs showing potential for treating various diseases. However, since nucleic acids are polyvalent anionic and highly hydrophilic molecules, they are hardly taken up into cells. They are also easily degraded by nucleases in the blood. Therefore, they require a delivery vector in order to enter cells and to be effective. LNP carriers are one of the successful methods for delivering nucleic acid drugs.^{190,191} The nucleic acid drug Patisiran (ONPATTRO), an siRNA formulated in LNPs to reduce transthyretin protein formation in the liver, recently received FDA approval for the treatment of hereditary transthyretin-mediated amyloidosis. It is the earliest approved siRNA drug and the earliest LNP-formulated nucleic acid drug, marking an important milestone in nucleic acid therapeutics development.^{163,192}

LNPs in the COVID-19 mRNA Vaccines. The latest successful use of LNPs is as the delivery vehicle in the two recently approved COVID-19 messenger RNA (mRNA) vaccines by Pfizer/BioNTech and Moderna, which have been developed with unparalleled speed and have shown notable effectiveness in disease prevention.^{29,164,165,193,194} The vaccines deliver mRNA encoding for the SARS-CoV-2 spike protein into the cytoplasm of host cells; the mRNA is translated into the spike protein, which acts as an antigen and leads to development of an immune response to the virus. The mechanism of action of the mRNA mediated vaccines is depicted in Figure S2 in the Supporting Information.

The compositions of the lipid nanoparticles of the two mRNA vaccines are very similar. Both contain an ionizable lipid which is positively charged at low pH (enabling RNA complexation) and neutral at physiological pH (reducing the potential toxic effects and facilitating payload release). They also contain a PEGylated lipid to reduce antibody association (opsonization) by serum proteins and clearance by phagocytes thus conferring longer systemic circulation. The phospholipid distearoylphosphatidylcholine (DSPC) and cholesterol help to pack the cargo into the LNPs (Table 4).^{164,165,195–198} The molar ratios of the cationic lipid:PEG-lipid:cholesterol:DSPC are (46.3:1.6:42.7:9.4) for the Pfizer and (50:1.5:38.5:10) for the Moderna vaccine.¹⁹⁹ Those nanoparticles are 80–100 nm in diameter²⁰⁰ and contain approximately 100 mRNA molecules per lipid nanoparticle.²⁰¹

Proprietary cationic lipids—ALC-0315 (Pfizer) and SM-102 (Moderna) (Figure 8)—are used in the COVID-19 vaccine nanoparticles; both lipids are tertiary amines which are protonated (and thus positively charged) at low pH. Their hydrocarbon chains are connected through biodegradable ester groups, enabling safe clearance after mRNA delivery. The cationic lipids used in the mRNA vaccines contain branched hydrocarbon chains (Figure 8), which optimize the formation of nonlamellar phases and the mRNA delivery efficiency. The PEG-lipids are both PEG-2000 conjugates. The LNPs are prepared at low pH (pH 4.0), at which the ionizable lipid is positively charged, so that it can easily form complexes with mRNA.²⁰² A microfluidic device is used to mix a stream containing mRNA in water with a stream containing a lipid mixture in ethanol. When rapidly mixed, the constituents of these two streams form nanoparticles which entrap the negatively charged mRNA.^{203–205}

LNP-Based mRNA Vaccines and Therapeutics in Clinical Trials. mRNA vaccines and therapeutics hold great promise in

prevention and treatment of diseases. LNP-enabled intracellular delivery of mRNA allows the expression of virtually any desired protein inside the host cells.²⁰⁶ An important feature of mRNA-based therapeutics is the low risk of insertional mutagenesis.²⁰⁷ Unlike DNA therapies, mRNA does not need the machinery of the nucleus to perform its task. Because mRNA does not integrate into the host genome, the risk of carcinogenesis and mutagenesis from mRNA-based therapeutics is reduced, improving their safety. Lastly, the manufacture of mRNA is more readily standardized than the production of DNA and affords much better reproducibility.²⁰⁸

mRNA vaccines have revolutionized vaccine development because of their high efficacies, accelerated development cycles, and potential for low-cost manufacture.²⁰⁹ The rapid development of mRNA vaccines would not have been possible without advances in LNP technologies to deliver nucleic acids. LNP-based mRNA vaccines have entered clinical trials against a variety of infectious diseases, such as nucleoside-modified mRNA vaccines for Zika virus, cytomegalovirus, tuberculosis, and influenza (Table 5).²¹⁰ mRNA therapeutic vaccines have great potential in cancer immunotherapy against melanoma, ovarian cancer, breast cancer, and other solid tumors (Table 5).^{208,209} LNP vectors are crucial for the successful intracellular delivery of mRNA to the cytosol of immune cells, particularly antigen-presenting immune cells, which are responsible for triggering the desired immune responses.

The use of mRNA for the expression of therapeutic proteins bears promise in treating a wide range of diseases. Protein replacement therapy is a medical therapy that replaces or supplements a protein which is deficient or missing in a patient.²¹¹ It is achieved by engineering mRNA to code for the protein of interest.²¹² LNPs are the preferred vehicle to deliver mRNA to cells, but LNP-based mRNA drugs typically require repetitive dosing through prolonged time-periods and thus need careful safety analyses and tests. The earliest study using LNP-formulated mRNA for protein replacement therapy was published only in 2016, using LNP-entrapped mRNA encoding human frataxin as a potential therapeutic agent against Friedreich's ataxia.²¹³

Medical Imaging. Medical imaging plays an essential role in modern precision medicine. Medical imaging is used to improve disease diagnosis, monitor drug delivery, verify response to therapy, and guide minimally invasive procedures. Traditional imaging methods such as magnetic resonance imaging (MRI), computed tomography (CT), positron emission tomography (PET), and single photon emission computed tomography (SPECT) have limited resolution and specificity. Nanoparticle delivery systems such as LNPs and their versatile surface functionalization provide opportunities to enhance the resolution and specificity of those imaging methods.²¹⁴

Due to the EPR effect, liposomes are more likely to accumulate in tumor tissue than normal tissues. Radiolabeled liposomes have been applied for imaging of various cancers. A recent application of the radiolabeled liposomes is in early detection of cancer metastases, by localizing the sentinel lymph node, the initial lymph node receiving metastatic tumor cells.²¹⁵ Various PET and SPECT radioisotopes have been conjugated to liposomes for use as imaging agents.²¹⁶ The most common radionuclides for radiolabeling liposomes are technetium-99m (^{99m}Tc), indium-111 (¹¹¹In), and gallium-67 (⁶⁷Ga).^{217–223} These radionuclides have different half-lives and photon energies, so they may be applied to meet the requirements of a particular application. For example, ^{99m}Tc has a half-life of 6 h

and allows imaging up to 24 h after injection, while ¹¹¹In has a longer half-life of 68 h and is useful when delayed imaging of a slow physiological process is needed. There are various methods for liposome radiolabeling. Radiolabels may be encapsulated in the aqueous core of the liposome during the manufacturing process or nonspecifically attached to the liposome surface. A chelator with high affinity for the radionuclide may be covalently attached to the head group of a lipid and the lipid–chelator conjugate added to the liposome formulation during production, this way enhancing its stability.²¹⁶

Liposomes can also provide a suitable biocompatible nanocarrier platform for developing MRI diagnostics.²²⁴ For example, liposomes comprising a gadolinium-chelating lipid, such as 1,2-distearoyl-*sn*-glycero-3-phosphoethanolamine-*N*-diethylenetriamine pentaacetic acid (PE-DTPA (Gd)) have been administered intravenously to visualize thrombi or obstructions in blood vessels.²²⁵ One of the important advantages of entrapment of MRI contrast agents into liposomes is the reduced toxicity of the formulations.²²⁶

The term theranostics was recently coined as a portmanteau of therapeutics and diagnostics. Theranostics combine pharmaceutical and diagnostic techniques to simultaneously or sequentially diagnose and treat diseases at their earliest stages.²²⁷ LNPs incorporating diagnostic and pharmaceutical agents are called hybrid LNPs. Diagnostic probes such as fluorescent dyes or quantum dots can be encapsulated into liposomes;²²⁸ at the same time, pharmaceutical agents such as doxorubicin, docetaxel, cisplatin, asanginex, or endostatin can be entrapped in LNPs.^{229,230} For example, liposome–quantum dot hybrids loaded with the cytotoxic drug doxorubicin have been developed as theranostics. Encapsulation of quantum dots into the lipid bilayers of LNPs makes the quantum dots soluble under physiological conditions while liposomes loaded with doxorubicin are retained by tumors and more selective for cancer cells than the free drug, resulting in LNPs capable of both labeling and killing cancer cells.²²⁹ Notable examples of patents from the CAS Content Collection related to the use of LNPs in theranostic formulations are listed in Table 6.

Cosmetics. The cosmetics industry was among the earliest to recognize and employ nanotechnology advances in various product development. Anticipated advantages of liposomal cosmetic formulations include enhanced stability and efficacy of these formulations, as well as successful penetration of the ingredients into the skin. A variety of marketed liposomal cosmetics are currently in use. The earliest product incorporating liposomes, Capture, was introduced by C. Dior in 1986. It contains thymus extract, collagen and elastin peptides, and hyaluronic acid in soya lecithin liposomes.²³¹ Another product containing hyaluronic acid in a liposomal delivery preparation is the Advanced Night Repair Protective Recovery Complex introduced by Estée Lauder. The formulation neutralizes and repairs the damage caused by UV-generated free radicals and moisturizes as well. L'Oréal has introduced an antiwrinkle liposomal product, Revitalift Double Lifting, containing pro retinol A.²³² Royal Jelly Lift Concentrate of Jafra Cosmetics International includes liposomes with a complex mixture of amino acids, vitamins, and minerals, to stimulate cell renewal and prevent skin wrinkles.²³² Liposomes are also formulated in commercial products with various extracts, moisturizers, antibiotics, and proteins, for uses such as wound healing, sunburn relief, hair conditioners, antiaging products, and long-lasting perfumes. A summary of marketed LNP cosmetic products is included as Table S2 in the Supporting Information.

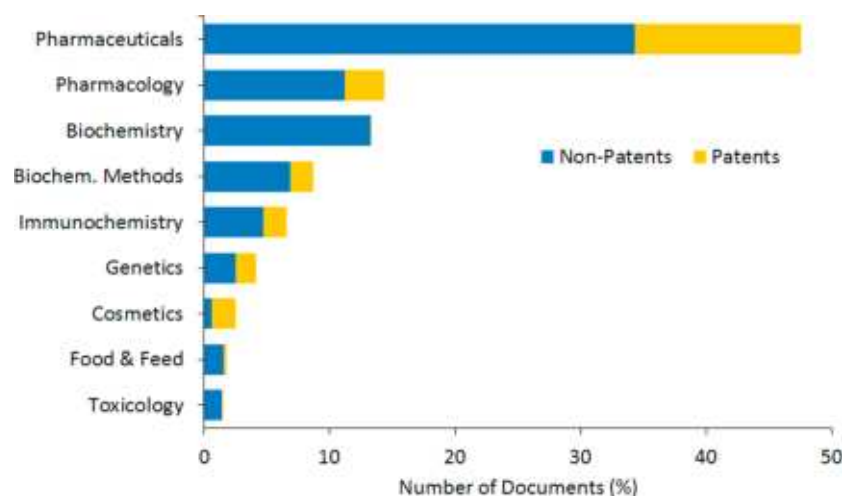


Figure 9. Distribution of LNP-related documents among top research areas in the CAS Content Collection in the years 2000–2021, presented as percentage of all LNP documents.

Nutrition. LNPs are increasingly prominent in the food industry and in nutrition.^{233–235} LNPs have been used to control the delivery of functional components such as proteins, enzymes, vitamins, and flavors in various food and nutritional applications. The term “nutraceutical” is used to describe formulations potentially providing both pharmaceutical and nutritional benefits.^{236–238} These formulations may involve nutrients, dietary supplements, herbal preparations, and genetically engineered and processed foods. Recently, the use of solid lipid nanoparticles (SLN) and nanostructured lipid carriers (NLC) in food and dietary supplements has markedly increased due to their advantages in higher loading capacities, higher bioavailabilities of their cargoes, and easier large-scale production. For example, SLN are used to incorporate food-related bioactive compounds including essential oils such as peppermint oil, vitamins such as vitamins A, B₂, B₁₂, D₂, and E, palm oil, coconut oil, copaiba oil, rosmarinic acid, resveratrol, and hesperidine.²³⁹ NLC have been used to encapsulate food-related ingredients such as rutin, curcumin, quercetin, astaxanthin, vitamin C, vitamin A palmitate, α -lipoic acid, and green tea extract.²³⁹ Notable examples of patents from the CAS Content Collection related to LNP formulations for use in nutrient and nutraceutical encapsulation and delivery are presented in Table 7.

Agriculture. LNPs have been studied in agriculture as delivery systems for agrochemicals and as model membrane systems. A list of notable patents from the CAS Content Collection related to LNPs in agrochemical formulations is presented in Table 8.

Nanoreactors. A recent application of LNPs is as nanoreactors, nanoscale chemical reactors applied to nanotechnology and nanobiotechnology. For example, LNPs have been used as nanoreactors for the size-controlled synthesis of metal nanoparticles.^{240–242} Metal nanoparticles are used in electronics, biosensors, and catalysis and are also used in biomedical applications such as imaging, drug delivery, and photothermal therapy. The sizes of nanoparticles determine many of their properties; thus, control over metal nanoparticle size is important in controlling their properties and in determining their suitability for use. For instance, nanosized liposomes encapsulating tetrachloroauric acid were used to prepare 2–5 nm gold nanoparticles.²⁴⁰ The controlled diffusion of the

reducing agent—sodium borohydride—through the liposomal membrane regulated the particle formation kinetics and resulted in ultrasmall nanoparticles with a narrow size distribution. In another example, stable palladium nanoparticles with sizes between 1–3 nm were prepared by reduction of a palladium precursor within liposomal nanoreactors using glycerol as both the reducing agent and stabilizer.²⁴² Palladium nanoparticles ~5 nm in diameter were prepared in the aqueous mesophase channels of lipidic cubic phases by reduction of Pd²⁺ salts and used as supported catalysts for Suzuki–Miyaura cross-coupling reactions.²⁴³ Similar methods using nanoreactors have been used for the synthesis of nonmetallic nanoparticles. For example, monodisperse nanocrystals of CdS, ZnCdS, and HgCdS have been synthesized in the cores of liposomes, using them as nanoreactors for precipitation or crystallization.²⁴⁴

Nanoreactors have also been proposed as tools for treatment of disease and eliminating harmful substances by allowing the production of therapeutic agents *in situ*. For example, the antioxidant enzyme catalase has been encapsulated inside liposomes comprising a cisplatin prodrug-conjugated phospholipid, for enhanced chemo-radiotherapy of cancer.²⁴⁵ The liposomes protect the enzyme from proteolysis and enhance its stability. The enzyme has been able to trigger decomposition of hydrogen peroxide produced by tumor cells thus producing oxygen in order to overcome hypoxia-induced treatment resistance of the tumor. At the same time, the entrapped cisplatin prodrug is oxidized, releasing cisplatin, and subsequent radiation therapy results in successful tumor growth inhibition.^{246,247} Polymeric dots (Pdots) loaded in liposomes have been used to reduce inflammation through *in situ* photocatalytic hydrogen generation.²⁴⁸ Pdots containing π -conjugated polymers generate hydrogen when exposed to light, while liposomes hold the reagents and Pdots together. As hydrogen is formed in the liposomes, it diffuses across the lipid bilayer to reduce reactive oxygen species (ROS) abundant in diseased and damaged tissue.²⁴⁸ In addition, liposome-based nanoreactors may also be useful for delivering enzymes for eliminating harmful substances. For example, the ability of the exogenous cholinesterase enzymes to act as scavengers of organophosphate toxins has been explored. Butyrylcholinesterase has been encapsulated in liposomes, which protect the enzyme from proteolysis. The organophosphate toxins can diffuse through the

liposomal membrane and be neutralized by the encapsulated enzyme.^{249,250}

Membrane Models in Basic Science. Lipid models have been used for decades to investigate membrane-related processes and characteristics. While biomembranes are heterogeneous multicomponent structures with sophisticated molecular organization, model LNP systems are much simpler and more stable, and therefore amenable to study of the structure and function of biological membranes. Virtually all of our current understanding of membrane lipid phase behavior results from the use of lipid membranes as model systems.^{251–260}

INSIGHTS ON LIPID NANOPARTICLES FROM THE CAS CONTENT COLLECTION

In what follows, we used the CAS Content Collection to get an overview of the current LNP research landscape, classifying and

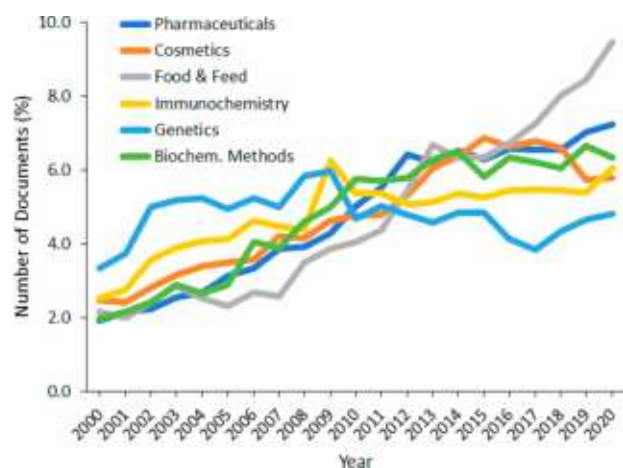


Figure 10. LNP-related patents (%) in the top research areas over time in the years 2000–2020. The percentages are calculated within the given research area.

quantifying all documents related to LNPs from the years 2000–2020. As the largest human-curated collection of published scientific knowledge, this data collection curated by CAS

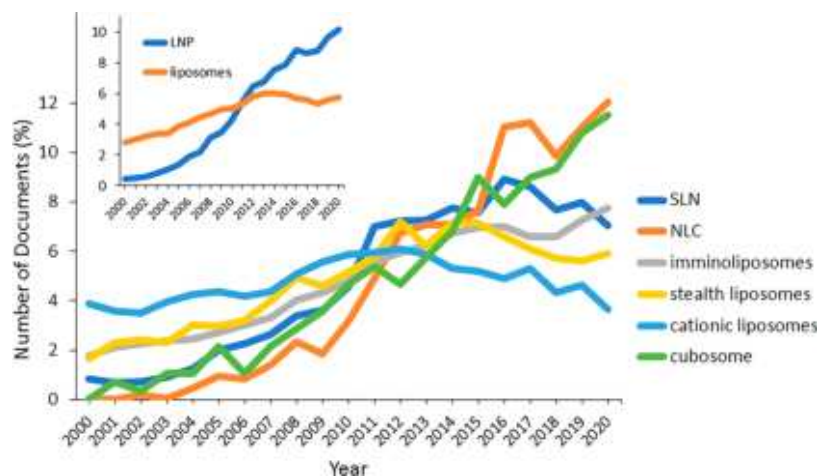


Figure 11. Number of LNP-related documents per year (%) in the CAS Content Collection in the years 2000–2020, with respect to different types of LNPs. The percentages are calculated within the given type. The inset shows the LNP vs liposome documents (%) per year.

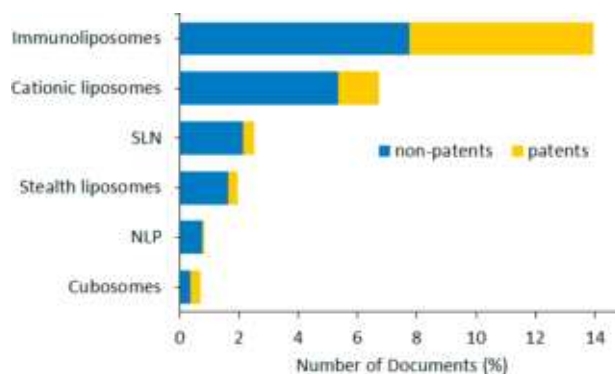


Figure 12. Number of LNP-related documents (patents and nonpatents) in the CAS Content Collection in the years 2000–2020, with respect to different types of LNPs.

scientists is particularly useful for quantitative analysis of publications with respect to variables such as time, research area, formulation, and application, as well as the details of chemical compositions.

Landscape of LNP Research Publications. Currently, there are over 216,000 LNP-related scientific publications in the CAS Content Collection, including patents and nonpatents (journal articles, books, dissertations, meeting abstracts, *etc.*), of which over 170,000 are from the period 2000–2020. The distribution of these documents among the top research areas is presented in Figure 9. LNP-related studies are dominated by pharmaceutical research in both patents and nonpatents. The research areas of cosmetics, genetics, and immunochemistry have the highest percentages of patent publications (Figure 9).

The evolving distribution of documents within these research areas over the past 20 years is shown in Figure 10. The research areas with the fastest growth are pharmaceuticals, food and feed, and cosmetics. The decrease in the number of documents in genetic research in the past decade may be due to the limited success of delivering DNA for gene therapy using lipid vectors (lipofection). A review of gene therapy clinical trials performed worldwide before 2017²⁶¹ reported that only 4.4% of the trials used lipid vectors in gene delivery, while most trials used viral vectors. Although LNPs have many advantages in gene delivery (low immunogenicities, facile production on a large scale, and

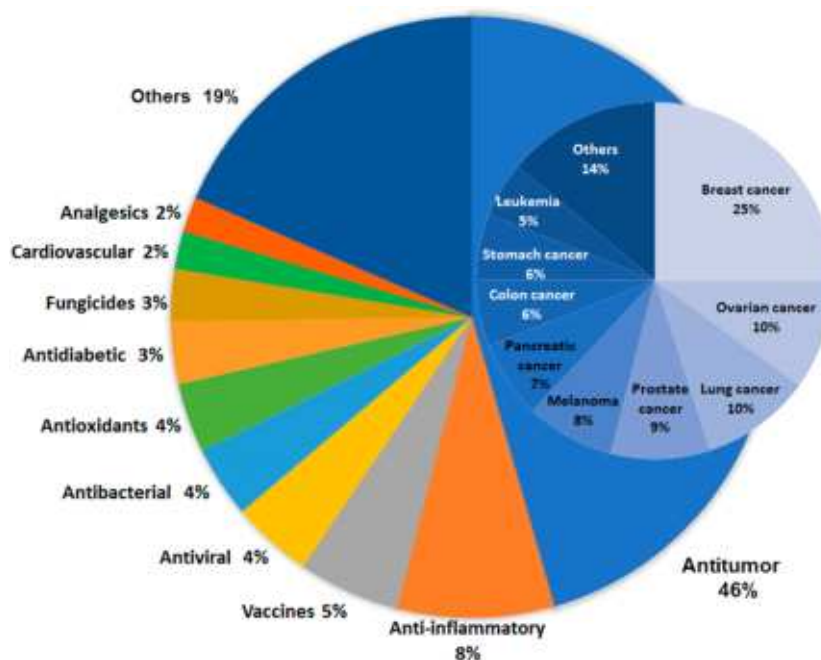


Figure 13. Distribution of documents in the CAS Content Collection related to LNP pharmaceutical formulations with respect to their target diseases.

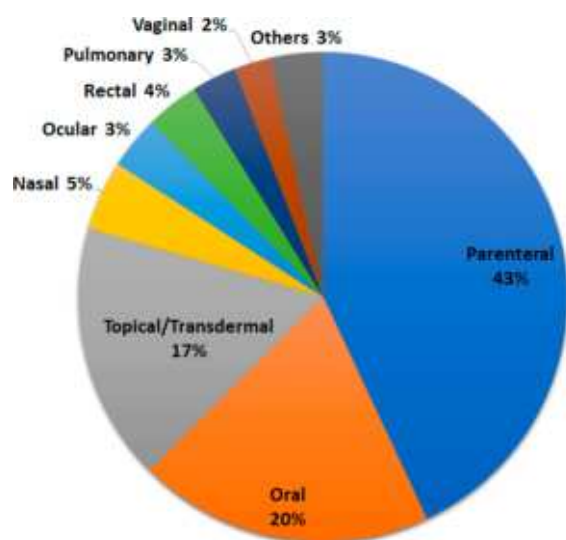


Figure 14. Distribution of documents related to LNP drug delivery with respect to their delivery route.

the ability to deliver large genes), viral vectors have been used more often because current LNPs are not as efficient as viral vectors in delivering genes.²⁶² The recent rise in interest in RNA therapeutics may hopefully change that perception. While gene therapy requires delivery of DNA into the cell nucleus through the nuclear membrane, entry into the cytoplasm is sufficient for RNA drugs and vaccines, enhancing their chances for success. The effectiveness of the recently developed mRNA vaccines using LNPs as delivery agents may reawaken interest in LNPs for nucleic acid delivery. Indeed, the number of nucleic acid delivery-related LNP patents filed during the first quarter of 2021 is more than half of the number of such patents published in all of 2020.

Table 9. Advantages and Disadvantages of the Three Major LNP Administration Routes¹⁷⁵

Administration route	Advantages	Disadvantages
Parenteral	Good bioavailability Appropriate for all LNP types No liver toxicity Good reproducibility	Painful, causing discomfort May require administration at medical facilities
Oral	Comfort of use Acceptable by patients	Low bioavailability Hepatic toxicity Inconsistent reproducibility
Topical/transdermal	Comfort of use Acceptable by patients Satisfactory reproducibility	Limited penetration Lag-time delay

Distribution of Research Documents with Regard to the LNP Type. As discussed above, there are various types of LNPs, with different properties and applications; their usage has changed over time and with improvements in the understanding of LNP properties and technologies. The distribution of the types of LNPs in related documents published between 2000 and 2020 is shown in Figure 11.

The terminology used for lipid nanoparticles has changed over time. Many more publication records in the CAS Content Collection contain the term “liposome” (~147,000 for the period 2000–2020) than “lipid nanoparticle” (~26,000 for the same period), even though “lipid nanoparticles” forms a broader class of nanoparticles than “liposomes”, including also formulations such as solid lipid nanoparticles (SLN), nanostructured lipid carriers (NLC), cubosomes, *etc.* While “lipid nanoparticle” is a more general term than “liposome”, the term “liposome” was invented earlier, when these lipid vesicles were

	parenteral/ injections	topical/ transdermal	oral	nasal	ophthalmic	inhalation
immunoliposomes / ligands	1873	682	797	353	193	260
stealth / sterically stabilized	234	15	23	1	6	7
solid lipid nanoparticles (SLN)	204	514	433	50	82	51
nanostructured lipid carriers (NLC)	78	281	147	37	58	20
cationic liposomes	293	47	34	37	21	18
lipoplexes	272	50	28	26	15	22
ethosomes	8	329	12	5	2	2
cubosomes	11	17	11	1	5	0

Figure 15. Correlation of the number of documents for the various LNP types with their delivery routes.

	antitumor	gene therapy	anti- inflammatory	antiviral	anti- bacterial	anti- infective	vaccines	anti- diabetic	fungicides	cardio- vascular	analgesics	immuno- therapy
immunoliposomes / ligands	13289	1987	1729	896	499	386	975	382	398	329	341	1861
stealth / sterically stabilized	5253	273	645	331	171	108	235	169	212	144	158	311
nanostructured lipid carriers (NLC)	181	13	92	14	35	10	3	15	29	2	13	2
solid lipid nanoparticles (SLN)	508	76	171	54	78	24	9	56	68	2	34	11
cationic liposomes / lipoplexes	1208	1916	105	116	53	22	214	11	13	11	15	145

Figure 16. Correlation of the number of documents for the various LNP types and therapies they have been applied to.

discovered in the 1960s. The term “lipid nanoparticle” was coined only in the early 1990s (the earliest document in the CAS Content Collection referring to lipid nanoparticles is from 1992), at the beginning of the era of nanoscience and nanotechnology. The more rapid increase in the number of documents using the term “lipid nanoparticles” than in documents using “liposome” (Figure 11, inset) may arise from its more recent coinage.

In the LNP subcategories, immunoliposomes and cationic liposomes are reported in the largest numbers of documents (Figure 12), while the fastest growth in publication is observed in the most recent areas—solid lipid nanoparticles (SLN), cubosomes, and especially nanostructured lipid carriers (NLC), which are steadily becoming the preferred formulation type for many applications (Figure 11) due to their advantages including higher drug-loading capacity, long-term colloidal stability, enhanced oral bioavailability of hydrophobic drugs, and improved drug release properties.²⁶³

LNP-Based Drug Delivery Systems. *Distribution of Documents in the CAS Content Collection Related to*

Pharmaceutical Formulations with Respect to Target Diseases. As seen above, LNP-related research is dominated by scientific areas related to drug delivery—pharmaceuticals, pharmacology, and also biochemistry, biochemical methods, immunochemistry, and genetics (Figure 9). Documents using LNPs in pharmaceutical formulations were classified by their target diseases to understand how different LNP types are used in practice. The distribution of treatment areas using LNP formulations in drug delivery-related documents in the CAS Content Collection is presented in Figure 13. The use of LNPs in antitumor drug formulations dominates the use of LNPs. Antitumor LNP formulations are used to treat a wide range of cancers; the largest single use (>25%) was in treating breast cancer, with more than 10% of antitumor formulations used for ovarian and lung cancers and significant proportions used for melanoma, leukemia, and prostate, pancreatic, colon, and stomach cancers (Figure 13, inset).

Distribution of Documents Related to Drug Delivery with Respect to Their Delivery Route. Most of the LNP pharmaceutical formulations are for parenteral, oral, or dermal

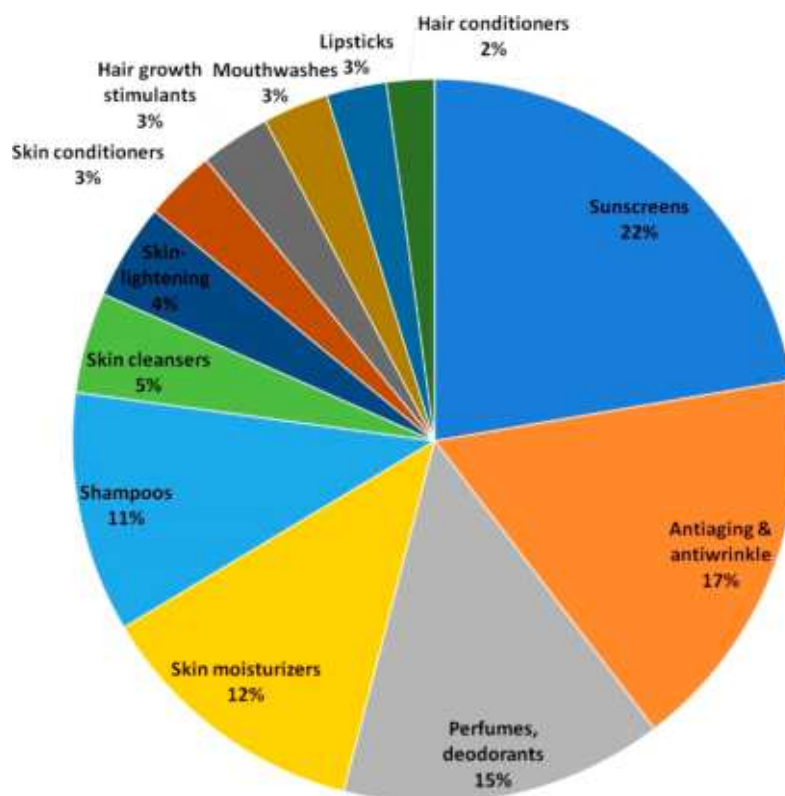


Figure 17. Distribution of LNP-related documents with respect to cosmetic product types.

Country/Region	Organization	Country/Region
34.6 USA	1.10 University of California	USA
24.9 China	0.56 Massachusetts Institute of Technology	USA
7.2 Japan	0.55 China Pharmaceutical University	China
4.6 S. Korea	0.49 Fudan University	China
4.3 Germany	0.45 Shenyang Pharmaceutical University	China
3.0 France	0.37 Zhejiang University	China
2.6 Canada	0.34 Sichuan University	China
1.7 India	0.33 Suzhou Zhiweitang Biotechnology Co., Ltd.	China
1.6 UK	0.33 Shanghai Jiao Tong University	China
1.4 Israel	0.31 Boston Scientific Scimed, Inc.	USA
1.4 Switzerland	0.31 Peking University	China
1.2 Russia	0.29 Genentech, Inc.	USA
1.2 Taiwan	0.29 University of Texas	USA
1.1 Italy	0.29 United States Dept. of Health and Human Services	USA
1.1 Denmark	0.27 Abbott Cardiovascular Systems Inc.	USA
1.0 Spain	0.26 The Johns Hopkins University	USA
0.9 Brazil	0.26 Harvard University	USA
0.8 Netherlands	0.25 Novartis AG	Switzerland
0.8 Belgium	0.23 Schering Corporation	Germany
0.5 Australia	0.23 Centre National de la Recherche Scientifique	France
0.3 Norway	0.22 Immunomedics, Inc.	USA
0.3 Hungary	0.22 Bristol-Myers Squibb Company	USA
0.2 Turkey	0.22 Massachusetts General Hospital	USA
0.2 Mexico	0.20 Yale University	USA
0.2 Poland	0.20 Duke University	USA
	0.20 Merck & Co., Inc.	USA

Figure 18. LNP-related patents classified by the top countries and organizations, presented as percent of the total number of LNP-related patents in the years 2000–2020.

administration (Figure 14). The major advantages and disadvantages of these routes are summarized in Table 9.

Correlation between Various LNP Types and Their Delivery Routes. The correlation between the various kinds of LNP preparations and their delivery routes is illustrated in Figure 15.

The strongest correlation was in the use of immunoliposomes for parenteral applications. Some formulations such as ethosomes are designed mainly for topical administration, while solid lipid nanoparticles and nanostructured lipid carriers can be applied topically, orally, and parenterally.

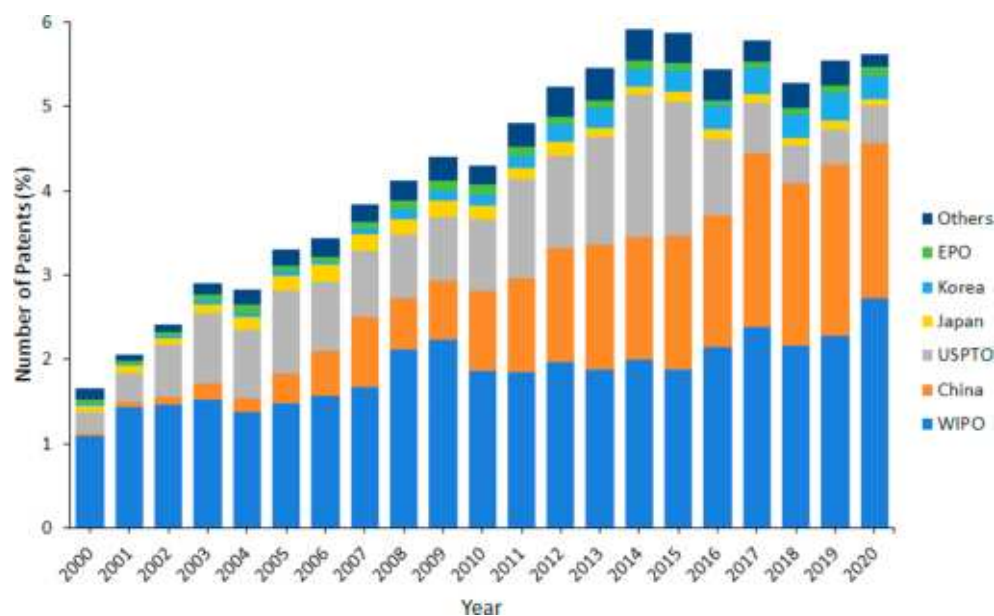


Figure 19. LNP-related patents per year for the top patent offices presented as percent of the total number of LNP-related patents in the years 2000–2020.

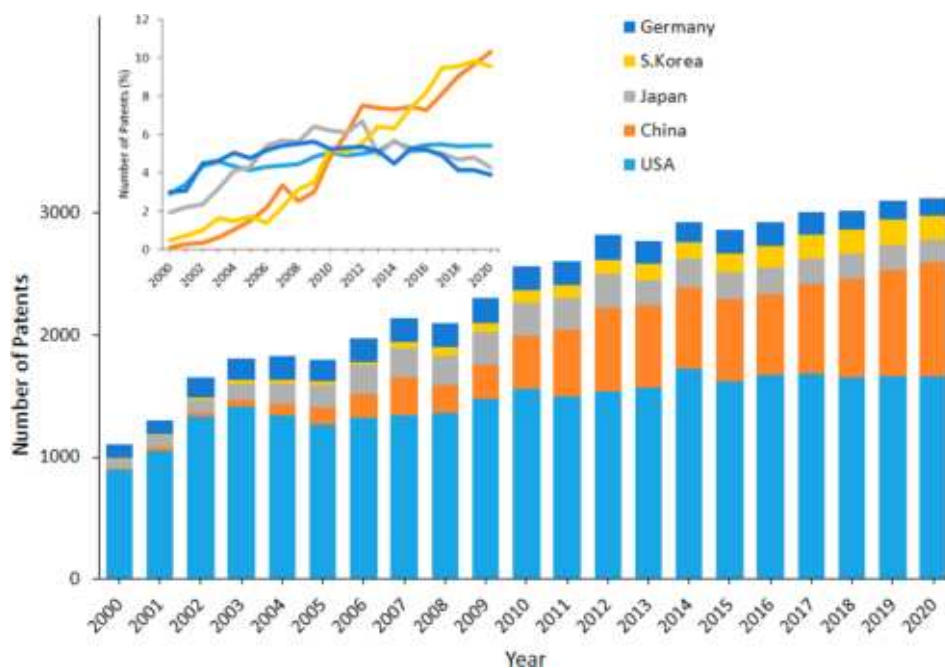


Figure 20. LNP-related patents per year in the years 2000–2020 for the top five countries presented as the total number of LNP-related patents. Inset: Percentage of the total number of LNP patents for the given country.

Correlation of the Various LNP Types and Therapies They Have Been Applied to. Different types of LNPs have different advantages and disadvantages and thus are appropriate for different therapies. Figure 16 illustrates the correlations between LNP types and the therapies to which they have been applied. Immunoliposomes, sterically stabilized liposomes, and cationic liposomes are the most commonly used LNPs for antitumor therapy. Understandably, cationic liposomes are the preferred formulation for gene therapy, and immunoliposomes are preferred as delivery vehicles for immunotherapies, including cancer immunotherapy.

LNP-Based Cosmetics. In cosmetics, LNP formulations are most prevalent in patents for sunscreens, antiaging preparations, and perfumes (Figure 17). Nanostructured lipid carriers (NLC) are the preferred carriers for sunscreens because of their ability to enhance the photostability of normally photolabile UV absorbers and to allow their sustained release over time, reducing skin irritation.²⁶⁴ Various active ingredients are used to prevent, delay, and treat skin aging, such as antioxidants, biological growth factors, herbal ingredients, and retinoids. Such preparations have been termed cosmeceuticals, because they are intended to have both cosmetic and pharmaceutical benefits.

Table 10. Number of Patents for the Four Most Widely Used Phospholipid Classes in LNP Formulations^a

R1 / R2	Phosphatidylcholines (PCs)	Phosphatidylethanolamines (PEs)	Phosphatidylglycerols (PGs)	Phosphatidylserines (PSs)
6:0 / 6:0	37	19	7	3
7:0 / 7:0	14	8		
8:0 / 8:0	30	5	5	5
11:0 / 11:0	29			
10:0 / 10:0	82	16	8	5
12:0 / 12:0	406	104	154	18
13:0 / 13:0	12		1	
14:1c9 / 14:1c9	23			
14:0 / 16:0	95			
14:0 / 14:0	1407	445	612	176
14:0 / 18:0	41			
15:0 / 15:0	41	5		
16:0 / 2:0	10			
16:0 / 14:0	88		4	2
16:0 / 16:0	2507	827	755	314
16:1c9 / 16:1c9	45	21		
16:4me3,7,11,15 / 16:4me3,7,11,15	47	116	3	
16:0 / 18:0	130			
16:0 / 18:2c9,12		11		
16:0 / 18:1c9	660	217	155	68
16:0 / 20:4c5,8,11,14		6		
17:0 / 17:0	18	3	2	
18:0 / 14:0	21	20		
18:0 / 16:0	99		15	
18:0 / 18:0	1930	841	417	134
18:0 / 18:1c9	74	65	6	7
18:0 / 18:2c9,12		10	2	
18:0 / 22:6c4,7,10,13,16,19		7		
18:1c9 / 14:0	9	4		
18:1c9 / 18:1c9	1391	1537	430	271
18:1c9 / 16:0	40		9	
18:1c9 / 18:0	11			
18:1t9 / 18:1t9	139	50	6	2
18:1y17 / 18:1y17				2
18:2c9,12 / 18:2c9,12	77	42	8	11
18:2c9,12 / 16:0			2	3
18:3c9,12,15 / 18:3c9,12,15	6	27	5	
19:0 / 19:0	12			
20:4c5,8,11,14 / 16:0			2	2
20:0 / 20:0	83	18	8	9
20:4c5,8,11,14 / 18:0			2	
20:4c5,8,11,14 / 20:4c5,8,11,14		8	13	
21:0 / 21:0	10			
22:1c13 / 22:1c13		10	2	2
22:0 / 22:0	53			
24:0 / 24:0	34			
22:6c4,7,10,13,16,19 / 16:0		5	2	2
22:6c4,7,10,13,16,19 / 18:0			2	3
22:6c4,7,10,13,16,19 / 22:6c4,7,10,13,16,19	33	28	5	2

^aThe structures of these phospholipids are shown at the top of the table. Designation nomenclature: All acyl chain residues are fully specified, using a systematic nomenclature, as follows. The two chain lengths, in units of carbon atoms (and with the first carbon of the chain defined as the one bonded through an oxygen atom to the glycerol backbone), are given, each to the left of a colon (:). The two chain descriptors are separated from each other by a backslash. In the default configuration the hydrocarbon chains are saturated. Modifications to each chain are indicated to the right of the colon and are listed according to number, kind, and location. First, to the right of the colon appears the number of modifications on that

Table 10. continued

chain. A zero (0) indicates that the chain is in the default configuration, with no modifications. Following the number of modifications, the modifications themselves are listed. Following each modification is a number indicating the carbon atom position on the chain where the modification is located. The letters “c” and “t” denote the cis and trans configuration, respectively, of the double bond, followed by a number or set of numbers identifying double bond position; “y” denotes triple bond; “me” denotes methyl isobranched.

Carriers for such cosmetic formulations include liposomes, solid lipid nanoparticles (SLN), and nanostructured lipid carriers (NLC).²⁶⁵ The use of nanoencapsulation in fragrance products improves their efficiency and allows sustained release of scents over time.²⁶⁶

INSIGHTS ON LNP-RELATED PATENTS FROM THE CAS CONTENT COLLECTION

As of June, 2021, there are over 45,000 patents related to LNPs/liposomes in the CAS Content Collection, over 41,000 of which

Table 11. Number of Patents for the Most Widely Used PEG-lipids in LNPs

R1/R2	Common/ Commercial Name	CAS RN	Number of patents
PEG-PE^a			
18:0/18:0	DSPE-PEG	145035-96-7; 170931-04-1	483
16:0/16:0	DPPE-PEG	145035-97-8; 170931-03-0	94
18:1c9/18:1c9	DOPE-PEG	145035-95-6; 262601-19-4	43
14:0/14:0	DMPE-PEG	211567-66-7; 211733-74-3	38
18:1c9/16:0		170127-34-1	5
12:0/12:0		2055341-27-8	4
18:2c9,12/18:2c9,12		736998-47-3	4
mPEG-glycerides			
14:0/14:0	DMG-PEG	160743-62-4 1397695-86-1	245
18:0/18:0	DSG-PEG; Sunbright DSG 2H; Sunbright DSG 20H	308805-39-2 850628-36-3	36
16:0/16:0	DPG-PEG	162409-28-1	17
18:1c9/18:1c9		160743-61-3	5
mPEG-PE			
18:0/18:0	DSPE-mPEG; Sunbright DSPE 020CN	156543-00-9; 247925-28-6; 474922-77-5; 459428-35-4	329
16:0/16:0	DPPE-mPEG	205494-72-0	29
14:0/14:0	DMPE-mPEG	474922-82-2; 261764-82-3	33
18:1c9/18:1c9		226940-29-0	20
amino-mPEG			
14:0/14:0	ALC-0159	1849616-42-7	6
12:0/12:0		1849616-44-9	1
12:0/14:0		1849616-45-0	1
16:0/16:0		1849616-43-8	1
18:0/18:0		741737-56-4	1
Chol-PEG			
PEG-cholesterol	PEG-cholesterol	27321-96-6	54
mPEG-cholesterol	mPEG-cholesterol	99559-58-7	11

^aFor the structures of the various PEG-lipid subclasses, see Figure 21, lower panel.

are in the years 2000–2021. The majority of LNP patents come from inventors in the US and China (Figure 18). The largest recipient of LNP patent filings is the World Intellectual Property Organization (WIPO). While the proportion of patents filed with WIPO has stayed nearly constant between 2000 and 2020, the share of patents filed with the China National Intellectual Property Administration (CNIPA) has increased significantly, from less than 1% of patents in 2000 to over 33% of all patents in 2020. Over this period, the fraction of LNP patents filed with the US Patent and Trademark Office (USPTO) decreased significantly, particularly between 2010 and 2018 (Figure 19).

Distribution of LNP-Related Patents by Country and Organization. The top five countries contributing to the growth in LNP patents are the USA, China, Japan, South Korea, and Germany. While the involvement of USA, Japan, and Germany in LNP research has remained stable after the initial growth in the years 2000–2005, the involvement of China and South Korea in LNP research has increased consistently during the same period (Figure 20).

Most Widely Used Lipids in LNP Formulations in Patents. There are many components used in LNPs, with the composition determined by the intended morphology and application. Along with the most common constituents—phospholipids and cholesterol—LNPs frequently include cationic ionizable lipids and PEG–lipid conjugates (PEG-lipids), as well as various other components. A collection of ~45,000 LNP-related patents were identified in the CAS Content Collection. The most widely used members of various lipid classes were identified in these patents.

Cholesterol (CAS RN 57-88-5) is the lipid component used in the largest number of patents—over 3,200 patents have used LNP formulations including cholesterol.

Phospholipids (Table 10) are the most prevalent class of lipids involving LNPs. Phosphatidylcholines (PCs), phosphatidylethanolamines (PEs), phosphatidylglycerols (PGs), and phosphatidylserines (PSs) are the most common phospholipid constituents. Preferred phospholipid species with respect to their hydrocarbon chains include saturated dimyristoyl (14:0/14:0), dipalmitoyl (16:0/16:0), and distearoyl (18:0/18:0) chains, as well as unsaturated dioleoyl (18:1c9/18:1c9) chains (Table 10). Phospholipids from natural sources, such as soya total phospholipids, soya phosphatidylcholines, hydrogenated soya phosphatidylcholines, and egg phosphatidylcholines, have also been commonly used in LNP formulations.

PEG–Lipid Conjugates. Since the discovery that PEG–lipid conjugates can significantly increase the circulatory half-lives in the sterically stabilized “stealth” liposomes, PEG-lipids have been widely used in pharmaceutical LNP formulations. The major classes PEG-lipids found in patents are listed in Table 11, with their structures depicted in Figure 21.

Cationic Lipids. The most often used cationic lipids in LNP formulations were identified and listed in Table 12. They typically comprise various amine derivatives, e.g., DOGS and DC-Chol, quaternary ammonium compounds, e.g., DOTMA,

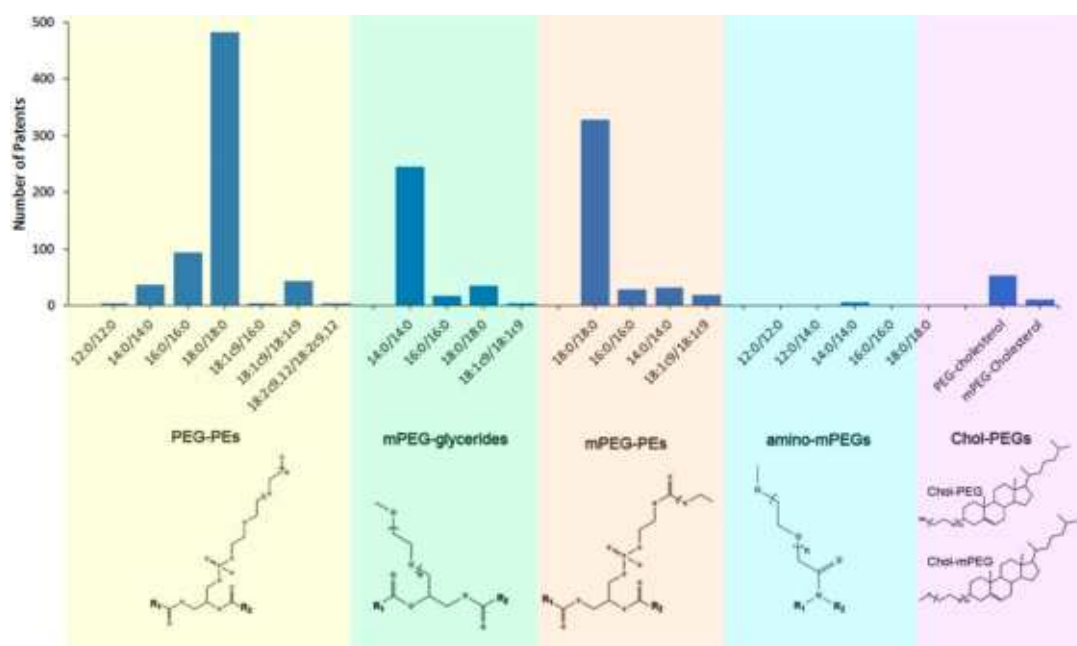


Figure 21. Number of patents for the most widely used PEG-lipids in patents on LNPs.

DOTAP, DORIE, and DMRIE, cationic phosphatidylcholines such as EDOPC and EDMPC, combinations of amines, *e.g.*, DOSPA and GAP-DLRIE, and amidinium salts, *e.g.*, Vectamidine.^{18,19,267–275} Cationic multicharged head groups such as DOSPA and DOGS have been reported to be more effective than single-charged cationic lipids such as DOTMA, DOTAP, DC-Chol, and DMRIE.^{276,277} The increased effectiveness may be related to the greater ability of highly charged cationic lipids to condense and protect nucleic acids, but the increased binding of multicharged ligands to nucleic acids may also obstruct or inhibit nucleic acid release inside the cell. In addition, the combination of quaternary ammonium salts and polyamines enhances delivery efficiency. Indeed, the earliest cationic lipid incorporating both quaternary ammonium and polyamine moieties, Lipofectamine (CAS RN 158571-62-1), comprising a 3:1 mixture of DOSPA and dioleoylphosphatidylethanolamine (DOPE), is a highly effective transfection agent.

SUMMARY AND OUTLOOK

Insights on LNP Compositions Inferred from the Research Landscape. Based on the landscape analysis of the LNP-related documents in the CAS Content Collection, the following aspects may be worth considering when selecting lipid compositions for LNP formulations.

- **Biocompatibility.** Naturally occurring lipids are preferable, because they are likely to be metabolizable in the target species. The most widely used class of lipids in LNP formulations are phospholipids, which are also the major class of biomembrane lipids.
- **Fluidity.** Cholesterol is well-known as a powerful modulator of lipid bilayer fluidity; it is able to enhance the fluidity of solid bilayers and to reduce the fluidity of liquid bilayers. It is also one of the major components of biomembranes and is highly biocompatible.
- **Phase state and phase transition temperature.** Phase state is an important characteristic of LNPs—it contributes to their stabilities and encapsulation efficiencies and controls

their interactions with biomembranes and cargo release. The phase transition temperatures of the individual lipids in the LNP as well as their miscibilities should be considered. Generally, lipids with longer alkyl chains and higher degrees of saturation have higher transition temperatures.

- **Electric charge (zeta potential).** The electric charges of LNPs affect their stability, their rate of cargo release, their circulating half-lives in the bloodstream, and their fusion with biomembranes. Naturally occurring membrane lipids are either zwitterionic (PCs, PEs) or negatively charged (PGs, PSs). In many uses, such as in nucleic acid delivery, the presence of positive-charged lipids is beneficial, leading to the development and use of synthetic cationic lipids. Since cationic lipids are not natural constituents of cells, their biocompatibilities and the toxicities of their degradation products should be considered.
- **Toxicity** is especially relevant to formulations including cationic lipids, which are synthetic and whose toxicities may not be known or have been observed in biological systems. In many cases, the effectiveness of a cationic lipid in LNP formulations correlates to increased toxicity. For example, multivalent cationic lipids have been more effective than monovalent cationic lipids in LNP formulations but are also much more toxic to cells. Identification of cationic lipids with similar structures to natural lipids known to be effective in LNPs such as cationic ethylphosphatidylcholines or cationic cholesterols may yield LNPs with reduced side effects.
- **Size** is a critical parameter in determining LNP circulation half-life and drug encapsulation. The size of LNPs strongly depends on how they are prepared. Ultrasonication, extrusion, and microfluidic methods have been most often used to control LNP size.
- **Circulation time and phagocytic uptake.** Coating LNPs with an inert polymer such as PEG considerably extends their residence in blood circulation by preventing phagocytes from reaching the surface of LNPs and

Table 12. List of the Most Widely Used Cationic Lipids in LNPs in Patents

CAS Registry Number	Chemical Structure	Common/Commercial Name	Number of References
3700-67-2		DDAB	2532
113669-21-9		DOTAP	2422
137056-72-5		Cholesterol (2-dimethylaminoethyl) carbamate; DC-Chol	904
112-99-2		Di-octadecylamine ; Armeen 2-18; Distearylamine; Genamin SH 200	821
104162-48-3		DOTMA	806
105488-80-0		CLONfectin; Vectamidine	585
153312-64-2		DMRIE	357
124050-77-7		DOGS Transfectam	323
127512-29-2		1,2-Di(oleoyloxy)-3-(dimethylamino)propane; DODAP	303
871258-12-7		DLinDMA	245
1224606-06-7		DLin-MC3-DMA; MC 3; RV 28	238
168479-03-6		DOSPA	229
183283-20-7		EDOPC	204
1190197-97-7		DLin-K-XTC2-DMA; Dlin-KC2-DMA; XTC	200
104162-47-2		DODMA; MBN 305A; N-[2,3-Di(oleoyloxy)propyl]-N,N-dimethylamine	181
16724-63-3		Armeen 2-16 Dipalmitylamine	174
17361-44-3		Alamine 205 Dimyristylamine NSC 91530	122
1169768-05-1		DLin-K-DM4	91
874291-25-5		DLenDMA	90

Table 12. continued

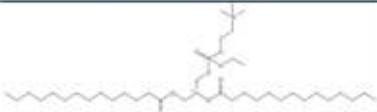
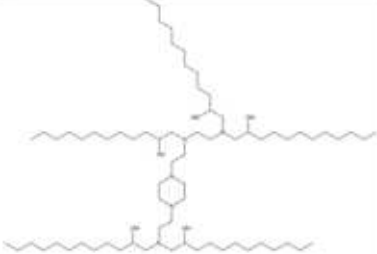

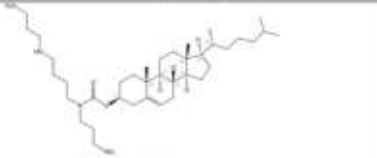
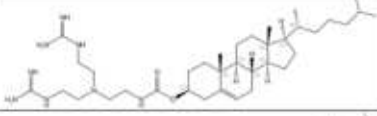

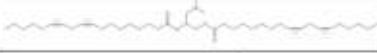
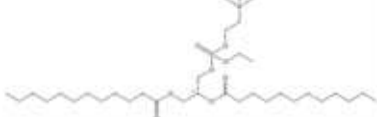


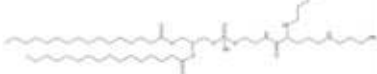



CAS Registry Number	Chemical Structure	Common/Commercial Name	Number of References
183283-19-4		EDMPC	88
1220890-25-4		C12-200 Tech G 1	87
178532-92-8		DOSPER	87
179075-30-0		GL 67 N4-Spermine cholesteryl carbamate	83
182056-06-0		BGTC; Bisguanidinium tren- cholesterol	73
908860-82-2		CLinDMA	52
1019000-51-1		DLinDAP	49
230949-32-3		EDLPC	48
153312-60-8		DORIE	44
1351586-50-9		L 319 RV 92	41
124076-29-5			39
1226778-72-8		ALN 100 ALNY 100	36
1208381-69-4		Octyl CLinDMA	36
2089251-47-6		SM-102	36

Table 12. continued



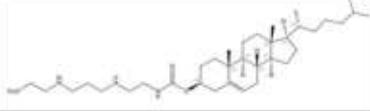

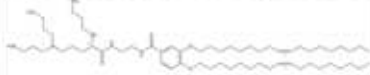

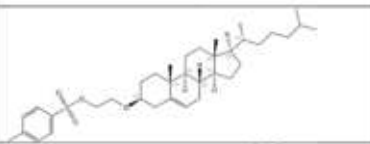

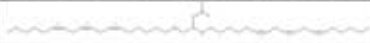
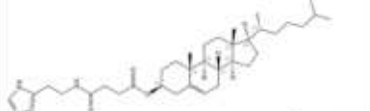
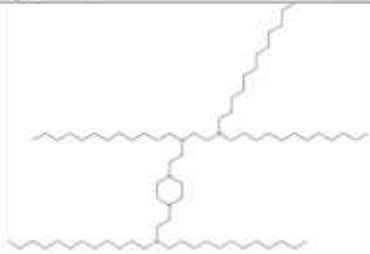
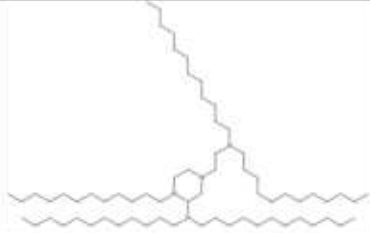










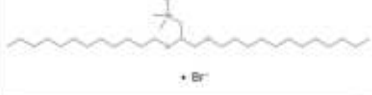


CAS Registry Number	Chemical Structure	Common/Commercial Name	Number of References
1318793-78-0		YSK 05	35
908860-85-5		DMOBA	33
200337-52-6		CDAN GL 138	31
1415795-37-7		HGT 4003	29
760939-62-6		MVL 5	29
1169768-13-1		Dlin-C-DAP	28
30656-75-8		Cholest-5-en-3β- oxyethane tosylate	28
1361106-13-9		Compound 32	28
1260141-95-4		γ-DLenDMA	28
449791-79-1		HisChol	28
1413010-97-5		KL22	27
1413010-89-5		KL10	27
396727-98-3		Dimyristyloxypropyl- amine	26
789482-14-0			26
1208381-72-9			25

Table 12. continued

CAS Registry Number	Chemical Structure	Common/Commercial Name	Number of References
1208381-70-7			25
908860-83-3		CpLinDMA PCLinDMA	24
200337-57-1		CTAP	21
1169768-15-3		DLin-5-DMA	13
1169768-10-8		DLin-2-DMAP	13
959664-11-0		Dioleylamine-A-succinyl paromomycin DOSP	13
1192257-55-8		C2-DLinDMA	11
208040-06-6		GAP-DLRIE	10
1217306-47-2		DLin-K-C4-DMA	9
1217306-46-1		DLin-K-C3-DMA	9

inhibiting their ability to uptake LNPs through steric hindrance.

- Cargo release. Effective LNPs rely on a delicate balance between stability and cargo release. LNPs need to be stable enough to safely transport their cargo to their targets yet capable of falling apart to release their cargo at the desired location. In many cases, external stimuli can be used to facilitate drug release. For example, when the pH at the desired location differs from the pH at other sites, ionizable lipids can facilitate drug release at that desired location. Cargo release from LNPs containing cationic lipids can also be triggered by lipid exchange with biomembranes, inducing the formation of nonlamellar phases.
- Encapsulation efficiency and stability. Replacing traditional liposome formulations with solid lipid nanoparticles (SLN) or especially with nanostructured lipid carriers (NLC) may enhance the stability and encapsulation efficiency of lipid nanocarriers significantly.

Perspectives. Nanotechnology has significantly widened the horizons in science and particularly in medicine. Due to their small size and high surface area, drug nanoformulations such as the LNPs have different properties than the corresponding bulk materials, and the changes in the biochemical, electronic, magnetic, and optical properties of nanoparticle drug formulations have been used to therapeutic benefit. As a result, nanomedicine has brought impressive progress in modern drug therapy against many diseases. Application of nanotechnological strategies to drug delivery has improved the effectiveness,

selectivity, residence time, and biodistribution of conventional drug carrier systems while reducing their limitations. Furthermore, nanoparticle drug formulations have reduced the toxicities and improved the solubilities and bioavailabilities of conventional medicines. The continuous efforts in synthesis and screening of functionalized lipid nanomaterials by chemically optimizing their molecular structures to enable tunable biodegradability *in vivo* would promote the development of more versatile, highly efficient, and biocompatible delivery vehicles.

As ongoing research attempts to address the needs of personalized medicine, more sophisticated and multifunctional nanocarrier designs are being developed. LNPs with complex structures are being designed to overcome biological barriers specific to individual patient or disease status as demanded by precision, or personalized, medicine. The objective of precision medicine is to utilize patient information such as genetic profile, age, lifestyle, environmental conditions, or comorbidities in order to develop an individualized treatment approach. Tailored nanocarrier designs, adapted by patient data and engineered to permeate particular barriers, can markedly improve the delivery of and response to precision medicine therapies.²⁷⁸

The use of LNPs in medicine is likely to expand significantly. The development of LNP types and varieties with enhanced drug delivery properties such as the nanostructured lipid carriers and the ionizable cationic nanoparticles brings further advantages to the LNP formulations and enlarges the prospects of their applications. LNPs hold great promise in genetic medicine where gene editing, vaccine development, immuno-

oncology, and other genetic therapies rely on the ability to efficiently deliver nucleic acids into cells. LNPs have advantages over other gene and vaccine delivery systems because they are easier to manufacture, are less immunogenic, can carry larger payloads, and can be designed for multiple dosages. Nucleic acid therapeutics are an emerging class of drugs showing potential for treating disease. LNPs have come out as successful and efficient carriers for such drugs. The successful use of LNPs as a delivery vector for the COVID-19 mRNA vaccines will likely broaden the horizons for research in mRNA vaccines.

From a materials science perspective, the success of LNPs in medicine is important, as it motivates further fundamental and applied nanoparticle research. The use of LNPs in the controlled synthesis of metal nanoparticles may also be important in expanding their use in display technologies and other uses. Expansion of the LNP technologies in other areas is also noticeable. Numerous cosmetic products are already in the market, with much more in development. Additional areas such as nutrition, nutraceuticals, agrochemistry, and nanoreactors are already exploring the benefits of lipid-based nanoencapsulation. Further, LNPs may have environmental applications, such as in metal detoxification. Based on the current progress and success, LNPs can certainly be recognized as one of the most advantageous and promising areas in modern nanotechnology.

ASSOCIATED CONTENT

Supporting Information

The Supporting Information is available free of charge at <https://pubs.acs.org/doi/10.1021/acsnano.1c04996>.

Table S1. Clinically approved LNP formulations. Table S2. Marketed LNP cosmetic preparations. Figure S1. Classification of liposomes according to their size and lamellarity. Figure S2. Mechanism of action of mRNA mediated vaccination. (PDF)

AUTHOR INFORMATION

Corresponding Author

Qiongqiong Zhou – CAS, a division of the American Chemical Society, Columbus, Ohio 43210, United States; orcid.org/0000-0001-6711-369X; Email: qzhou@cas.org

Authors

Rumiana Tenchov – CAS, a division of the American Chemical Society, Columbus, Ohio 43210, United States; orcid.org/0000-0003-4698-6832

Robert Bird – CAS, a division of the American Chemical Society, Columbus, Ohio 43210, United States

Allison E. Curtze – CAS, a division of the American Chemical Society, Columbus, Ohio 43210, United States

Complete contact information is available at: <https://pubs.acs.org/doi/10.1021/acsnano.1c04996>

Notes

The authors declare no competing financial interest.

ACKNOWLEDGMENTS

We sincerely appreciate Zachary Baum for proofreading, Laura Czuba for project coordination, and Peter Jap and Cristina Tomeo for insightful discussion. We are also grateful to Manuel Guzman, Gilles Georges, Michael Dennis, Carmin Gade, Dawn George, Cynthia Casebolt and Hong Xie for executive sponsorship.

VOCABULARY

Lipid nanoparticle (LNP), nanosized particle composed mainly of lipids, used predominantly in drug delivery but also in cosmetics, nutrition, etc.; liposome, a vesicle comprising at least one lipid bilayer; major types of liposomes are small unilamellar liposomes (SUV) having a single bilayer and multilamellar liposomes (MLV) having several lipid bilayers; solid lipid nanoparticles (SLN), LNPs comprising solid lipids; nanostructured lipid carriers (NLC), LNPs comprising a mixture of solid and liquid-crystalline lipids. Both SLN and NLC are widely used in drug delivery because of their enhanced physical stabilities, high loading capacities, high bioavailabilities of their cargoes, and facile production on a large scale; cationic lipid, synthetic lipid compound similar to the natural lipids, except for the presence of an ionizable (cationic) head group instead of the zwitterionic or anionic head group of the natural lipids; invented and applied mainly for delivery of nucleic acids; “stealth” liposome, sterically stabilized liposome coated with biocompatible inert polymers (mostly PEG), making them invisible to phagocytes, thus exhibiting long circulation half-life; immunoliposome, targeted liposome generated by coupling a ligand, typically an antibody, to the liposomal surface, allowing for active tissue targeting through binding to cell-specific receptors.

REFERENCES

- (1) CAS Content Collection. <https://www.cas.org/about/cas-content> (accessed 2021-06-09).
- (2) CAS Data. <https://www.cas.org/cas-data> (accessed 2021-06-09).
- (3) Bangham, A. D.; Standish, M. M.; Watkins, J. C. Diffusion of Univalent Ions across Lamellae of Swollen Phospholipids. *J. Mol. Biol.* **1965**, *13*, 238–252.
- (4) Gregoriadis, G. Liposomes in Drug Delivery: How It All Happened. *Pharmaceutics* **2016**, *8*, 1–5.
- (5) Weissig, V. Liposomes Came First: The Early History of Liposomology. In *Liposomes: Methods and Protocols*, 2nd ed.; D'Souza, G. G. M., Ed.; Humana Press: New York, 2017; Vol. 1522, pp 1–15.
- (6) Working, P. K.; Dayan, A. D. Pharmacological-Toxicological Expert Report. Caelyx. (Stealth Liposomal Doxorubicin Hcl). *Hum. Exp. Toxicol.* **1996**, *15*, 751–785.
- (7) Bulbake, U.; Doppalapudi, S.; Kommineni, N.; Khan, W. Liposomal Formulations in Clinical Use: An Updated Review. *Pharmaceutics* **2017**, *9*, 1–33.
- (8) Laouini, A.; Jaafar-Maalej, C.; Limayem-Blouza, I.; Sfar, S.; Charcosset, C.; Fessi, H. Preparation, Characterization and Applications of Liposomes: State of the Art. *Journal of Colloid Science and Biotechnology* **2012**, *1*, 147–168.
- (9) Harashima, H.; Sakata, K.; Funato, K.; Kiwada, H. Enhanced Hepatic Uptake of Liposomes through Complement Activation Depending on the Size of Liposomes. *Pharm. Res.* **1994**, *11*, 402–406.
- (10) Nagayasu, A.; Uchiyama, K.; Kiwada, H. The Size of Liposomes: A Factor Which Affects Their Targeting Efficiency to Tumors and Therapeutic Activity of Liposomal Antitumor Drugs. *Adv. Drug Delivery Rev.* **1999**, *40*, 75–87.
- (11) Allen, T. M.; Everest, J. M. Effect of Liposome Size and Drug Release Properties on Pharmacokinetics of Encapsulated Drug in Rats. *J. Pharmacol. Exp. Ther.* **1983**, *226*, 539–544.
- (12) Nanoscience and Nanotechnologies: Opportunities and Uncertainties. https://royalsociety.org/-/media/Royal_Society_Content/policy/publications/2004/9693.pdf (accessed 2021-04-25).
- (13) Smith, M. C.; Crist, R. M.; Clogston, J. D.; McNeil, S. E. Zeta Potential: A Case Study of Cationic, Anionic, and Neutral Liposomes. *Anal. Bioanal. Chem.* **2017**, *409*, 5779–5787.
- (14) Freitas, C.; Müller, R. H. Effect of Light and Temperature on Zeta Potential and Physical Stability in Solid Lipid Nanoparticle (SLN) Dispersions. *Int. J. Pharm.* **1998**, *168*, 221–229.

- (15) Honary, S.; Zahir, F. Effect of Zeta Potential on the Properties of Nano-Drug Delivery Systems - a Review (Part 2). *Tropical Journal of Pharmaceutical Research* **2013**, *12*, 265–273.
- (16) Venter, J. C.; Adams, M. D.; Myers, E. W.; Li, P. W.; Mural, R. J.; Sutton, G. G.; Smith, H. O.; Yandell, M.; Evans, C. A.; Holt, R. A.; Gocayne, J. D.; Amanatides, P.; Ballew, R. M.; Huson, D. H.; Wortman, J. R.; Zhang, Q.; Kodira, C. D.; Zheng, X. Q. H.; Chen, L.; Skupski, M.; et al. The Sequence of the Human Genome. *Science* **2001**, *291*, 1304–1351.
- (17) Sridharan, K.; Gogtay, N. J. Therapeutic Nucleic Acids: Current Clinical Status. *Br. J. Clin. Pharmacol.* **2016**, *82*, 659–672.
- (18) Felgner, P. L.; Gadek, T. R.; Holm, M.; Roman, R.; Chan, H. W.; Wenz, M.; Northrop, J. P.; Ringold, G. M.; Danielsen, M. Lipofection - A Highly Efficient, Lipid-Mediated DNA-Transfection Procedure. *Proc. Natl. Acad. Sci. U. S. A.* **1987**, *84*, 7413–7417.
- (19) Koynova, R.; Tenchov, B. Cationic Lipids: Molecular Structure/Transfection Activity Relationships and Interactions with Biomembranes. In *Nucleic Acid Transfection* Bielke, W., Erbacher, C., Eds.; Springer-Verlag: Berlin, Heidelberg, 2010; Vol. 296, pp 51–93.
- (20) Hajji, K. A.; Ball, R. L.; Deluty, S. B.; Singh, S. R.; Strelkova, D.; Knapp, C. M.; Whitehead, K. A. Branched-Tail Lipid Nanoparticles Potently Deliver mRNA *In Vivo* Due to Enhanced Ionization at Endosomal Ph. *Small* **2019**, *15*, 1805097.
- (21) Tarahovsky, Y. S.; Arsenault, A. L.; MacDonald, R. C.; McIntosh, T. J.; Epan, R. M. Electrostatic Control of Phospholipid Polymorphism. *Biophys. J.* **2000**, *79*, 3193–3200.
- (22) Tarahovsky, Y. S.; Koynova, R.; MacDonald, R. C. DNA Release from Lipoplexes by Anionic Lipids: Correlation with Lipid Mesomorphism, Interfacial Curvature, and Membrane Fusion. *Biophys. J.* **2004**, *87*, 1054–1064.
- (23) Koynova, R.; Wang, L.; MacDonald, R. C. An Intracellular Lamellar - Nonlamellar Phase Transition Rationalizes the Superior Performance of Some Cationic Lipid Transfection Agents. *Proc. Natl. Acad. Sci. U. S. A.* **2006**, *103*, 14373–14378.
- (24) Siegel, D. P. The Relationship between Bicontinuous Inverted Cubic Phases and Membrane Fusion. In *Bicontinuous Liquid Crystals*; Lynch, M. L., Spicer, P. T., Eds.; Taylor & Francis Group, CRC Press: Boca Raton, 2005; pp 59–98.
- (25) Koynova, R.; Tenchov, B. Phase Transitions of Lipids. In *Wiley Encyclopedia of Chemical Biology*; Begley, T. P., Ed.; John Wiley & Sons: Hoboken, 2009; Vol. 2, pp 601–615.
- (26) Scheideler, M.; Vidakovic, I.; Prassl, R. Lipid Nanocarriers for MicroRNA Delivery. *Chem. Phys. Lipids* **2020**, *226*, 104837.
- (27) Evers, M. J. W.; Kulkarni, J. A.; van der Meel, R.; Cullis, P. R.; Vader, P.; Schiffelers, R. M. State-of-the-Art Design and Rapid-Mixing Production Techniques of Lipid Nanoparticles for Nucleic Acid Delivery. *Small Methods* **2018**, *2*, 1700375.
- (28) Kulkarni, J. A.; Thomson, S. B.; Zaifman, J.; Leung, J.; Wagner, P. K.; Hill, A.; Tam, Y. Y. C.; Cullis, P. R.; Petkau, T. L.; Leavitt, B. R. Spontaneous, Solvent-Free Entrapment of Sirna within Lipid Nanoparticles. *Nanoscale* **2020**, *12*, 23959–23966.
- (29) Li, Y.; Tenchov, R.; Smoot, J.; Liu, C.; Watkins, S.; Zhou, Q. A Comprehensive Review of the Global Efforts on Covid-19 Vaccine Development. *ACS Cent. Sci.* **2021**, *7*, 512–533.
- (30) Paliwal, R.; Paliwal, S. R.; Kenwat, R.; Kurmi, B. D.; Sahu, M. K. Solid Lipid Nanoparticles: A Review on Recent Perspectives and Patents. *Expert Opin. Ther. Pat.* **2020**, *30*, 179–194.
- (31) Muller, R. H.; Mader, K.; Gohla, S. Solid Lipid Nanoparticles (SLN) for Controlled Drug Delivery - A Review of the State of the Art. *Eur. J. Pharm. Biopharm.* **2000**, *50*, 161–177.
- (32) Haider, M.; Abdin, S. M.; Kamal, L.; Orive, G. Nanostructured Lipid Carriers for Delivery of Chemotherapeutics: A Review. *Pharmaceutics* **2020**, *12*, 288.
- (33) Iqbal, M. A.; Md, S.; Sahni, J. K.; Baboota, S.; Dang, S.; Ali, J. Nanostructured Lipid Carriers System: Recent Advances in Drug Delivery. *J. Drug Targeting* **2012**, *20*, 813–830.
- (34) Mehnert, W.; Mader, K. Solid Lipid Nanoparticles - Production, Characterization and Applications. *Adv. Drug Delivery Rev.* **2001**, *47*, 165–196.
- (35) Muller, R. H.; Radtke, M.; Wissing, S. A. Solid Lipid Nanoparticles (SLN) and Nanostructured Lipid Carriers (NLC) in Cosmetic and Dermatological Preparations. *Adv. Drug Delivery Rev.* **2002**, *54*, S131–S155.
- (36) Montoto, S. S.; Muraca, G.; Ruiz, M. E. Solid Lipid Nanoparticles for Drug Delivery: Pharmacological and Biopharmaceutical Aspects. *Frontiers in Molecular Biosciences* **2020**, *7*, 587997.
- (37) Bondi, M. L.; Craparo, E. F. Solid Lipid Nanoparticles for Applications in Gene Therapy: A Review of the State of the Art. *Expert Opin. Drug Delivery* **2010**, *7*, 7–18.
- (38) Hörmann, K.; Zimmer, A. Drug Delivery and Drug Targeting with Parenteral Lipid Nanoemulsions - A Review. *J. Controlled Release* **2016**, *223*, 85–98.
- (39) Duong, V. A.; Nguyen, T. T.; Maeng, H. J. Preparation of Solid Lipid Nanoparticles and Nanostructured Lipid Carriers for Drug Delivery and the Effects of Preparation Parameters of Solvent Injection Method. *Molecules* **2020**, *25*, 4781.
- (40) Severino, P.; Andreani, T.; Macedo, A. S.; Fanguero, J. F.; Santana, M. H. A.; Silva, A. M.; Souto, E. B. Current State-of-Art and New Trends on Lipid Nanoparticles (SLN and NLC) for Oral Drug Delivery. *J. Drug Delivery* **2012**, *2012*, 750891.
- (41) Mishra, V.; Bansal, K. K.; Verma, A.; Yadav, N.; Thakur, S.; Sudhakar, K.; Rosenholm, J. M. Solid Lipid Nanoparticles: Emerging Colloidal Nano Drug Delivery Systems. *Pharmaceutics* **2018**, *10*, 191.
- (42) Puglia, C.; Bonina, F. Lipid Nanoparticles as Novel Delivery Systems for Cosmetics and Dermal Pharmaceuticals. *Expert Opin. Drug Delivery* **2012**, *9*, 429–441.
- (43) Borges, A.; de Freitas, V.; Mateus, N.; Fernandes, I.; Oliveira, J. Solid Lipid Nanoparticles as Carriers of Natural Phenolic Compounds. *Antioxidants* **2020**, *9*, 998.
- (44) Engstrom, S.; Larson, K.; Lindman, B.; Engstroem, S.; Larsson, K. V. Controlled-Release Composition for Biologically Active Material - Comprising L2-Phase Containing a Monoglyceride, a Triglyceride and a Polar Liquid. WO8800059-A, 1988.
- (45) Engstrom, S.; Larsson, K.; Lindman, B.; Engstroem, S. Preparation of Controlled Release Composition for Biologically Active Material - from Amphipathic Agents to Give Cubic Liquid Crystal Phase. WO8402076-A1, 1984.
- (46) Barauskas, J.; Johnson, M.; Tiberg, F. Cubic Phase Nanoparticles (Cubosome): Principles for Controlling Size, Structure, and Stability. *Langmuir* **2005**, *21*, 2569–2577.
- (47) Spicer, P. T. Progress in Liquid Crystalline Dispersions: Cubosomes. *Curr. Opin. Colloid Interface Sci.* **2005**, *10*, 274–279.
- (48) Garg, G.; Saraf, S.; Saraf, S. Cubosomes: An Overview. *Biol. Pharm. Bull.* **2007**, *30*, 350–353.
- (49) Karami, Z.; Hamidi, M. Cubosomes: Remarkable Drug Delivery Potential. *Drug Discovery Today* **2016**, *21*, 789–801.
- (50) Barriga, H. M. G.; Holme, M. N.; Stevens, M. M. Cubosomes: The Next Generation of Smart Lipid Nanoparticles? *Angew. Chem., Int. Ed.* **2019**, *58*, 2958–2978.
- (51) Rarokar, N. R.; Khedekar, P. B. Cubosomes: A Vehicle for Delivery of Various Therapeutic Agents. *MOJ. Toxicology* **2018**, *4*, 19–21.
- (52) Hirlekar, R.; Jain, S.; Patel, M.; Garse, H.; Kadam, V. Hexosomes: A Novel Drug Delivery System. *Curr. Drug Delivery* **2010**, *7*, 28–35.
- (53) Yaghmur, A.; Glatter, O. Characterization and Potential Applications of Nanostructured Aqueous Dispersions. *Adv. Colloid Interface Sci.* **2009**, *147–48*, 333–342.
- (54) Torchilin, V. P. Lipid-Core Micelles for Targeted Drug Delivery. *Curr. Drug Delivery* **2005**, *2*, 319–27.
- (55) Gill, K. K.; Kaddoumi, A.; Nazzal, S. Peg-Lipid Micelles as Drug Carriers: Physicochemical Attributes, Formulation Principles and Biological Implication. *J. Drug Targeting* **2015**, *23*, 222–231.
- (56) Groo, A.-C.; Matougui, N.; Umerska, A.; Saulnier, P. Reverse Micelle-Lipid Nanocapsules: A Novel Strategy for Drug Delivery of the Plectasin Derivate Ap138 Antimicrobial Peptide. *Int. J. Nanomed.* **2018**, *13*, 7565–7574.

- (57) Zatsepin, T. S.; Kotelevtsev, Y. V.; Koteliansky, V. Lipid Nanoparticles for Targeted siRNA Delivery - Going from Bench to Bedside. *Int. J. Nanomed.* **2016**, *11*, 3077–3086.
- (58) Touitou, E.; Dayan, N.; Bergelson, L.; Godin, B.; Eliaz, M. Ethosomes - Novel Vesicular Carriers for Enhanced Delivery: Characterization and Skin Penetration Properties. *J. Controlled Release* **2000**, *65*, 403–418.
- (59) Sudhakar, C. K.; Upadhyay, N.; Jain, S.; Charyulu, R. N. Ethosomes as Non-Invasive Loom for Transdermal Drug Delivery System. In *Nanomedicine and Drug Delivery*, 1st ed.; Sebastian, M., Ninan, N., Haghi, A. K., Eds.; Apple Academic Press: New York, 2012.
- (60) Huang, S. L. Liposomes in Ultrasonic Drug and Gene Delivery. *Adv. Drug Delivery Rev.* **2008**, *60*, 1167–1176.
- (61) Alkan-Onyuksel, H.; Demos, S. M.; Lanza, G. M.; Vonesh, M. J.; Klegerman, M. E.; Kane, B. J.; Kuzsak, J.; McPherson, D. D. Development of Inherently Echogenic Liposomes as an Ultrasonic Contrast Agent. *J. Pharm. Sci.* **1996**, *85*, 486–490.
- (62) Huang, S. L.; Hamilton, A. J.; Pozharski, E.; Nagaraj, A.; Klegerman, M. E.; McPherson, D. D.; MacDonald, R. C. Physical Correlates of the Ultrasonic Reflectivity of Lipid Dispersions Suitable as Diagnostic Contrast Agents. *Ultrasound Med. Biol.* **2002**, *28*, 339–348.
- (63) Buchanan, K. D.; Huang, S.; Kim, H.; MacDonald, R. C.; McPherson, D. D. Echogenic Liposome Compositions for Increased Retention of Ultrasound Reflectivity at Physiologic Temperature. *J. Pharm. Sci.* **2008**, *97*, 2242–2249.
- (64) Holland, C. K.; McPherson, D. D. Echogenic Liposomes for Targeted Drug Delivery. *Proceedings. IEEE International Symposium on Biomedical Imaging* **2009**, *2009*, 755–758.
- (65) Shekhar, H.; Kleven, R. T.; Peng, T.; Palaniappan, A.; Karani, K. B.; Huang, S.; McPherson, D. D.; Holland, C. K. *In Vitro* Characterization of Sonothrombolysis and Echocontrast Agents to Treat Ischemic Stroke. *Sci. Rep.* **2019**, *9*, 9902.
- (66) Nkanga, C. I.; Bapolisi, A. M.; Okafor, N. I.; Krause, R. W. M. General Perception of Liposomes: Formation, Manufacturing and Applications, Liposomes - Advances and Perspectives. In *Liposomes - Advances and Perspectives*; IntechOpen: London, 2019.
- (67) Has, C.; Sunthar, P. A Comprehensive Review on Recent Preparation Techniques of Liposomes. *J. Liposome Res.* **2020**, *30*, 336–365.
- (68) Patil, Y. P.; Jadhav, S. Novel Methods for Liposome Preparation. *Chem. Phys. Lipids* **2014**, *177*, 8–18.
- (69) Koynova, R.; Tenchov, B. Recent Progress in Liposome Production, Relevance to Drug Delivery and Nanomedicine. *Recent Pat. Nanotechnol.* **2015**, *9*, 86–93.
- (70) Pattni, B. S.; Chupin, V. V.; Torchilin, V. P. New Developments in Liposomal Drug Delivery. *Chem. Rev.* **2015**, *115*, 10938–10966.
- (71) Machado, A. R.; Assis, L. M. d.; Machado, M. I. R.; Souza-Soares, L. A. d. Importance of Lecithin for Encapsulation Processes. *Afr. J. Food Sci.* **2014**, *8*, 176–183.
- (72) Maherani, B.; Arab-Tehrany, E.; Mozafari, M. R.; Gaiani, C.; Linder, M. Liposomes: A Review of Manufacturing Techniques and Targeting Strategies. *Curr. Nanosci.* **2011**, *7*, 436–452.
- (73) Mozafari, M.; Liposomes, R. An Overview of Manufacturing Techniques. *Cell. Mol. Biol. Lett.* **2005**, *10*, 711–719.
- (74) Carugo, D.; Bottaro, E.; Owen, J.; Stride, E.; Nastruzzi, C. Liposome Production by Microfluidics: Potential and Limiting Factors. *Sci. Rep.* **2016**, *6*, 25876.
- (75) Mukherjee, S.; Ray, S.; Thakur, R. S. Solid Lipid Nanoparticles: A Modern Formulation Approach in Drug Delivery System. *Indian J. Pharm. Sci.* **2009**, *71*, 349–358.
- (76) Rizwan, S. B.; Boyd, B. J. Cubosomes: Structure, Preparation and Use as an Antigen Delivery System. In *Subunit Vaccine Delivery. Advances in Delivery Science and Technology*; Foged, C., Rades, T., Perrie, Y., Hook, S., Eds.; Springer: New York, NY, 2015.
- (77) Torchilin, V. P. Liposomes as Targetable Drug Carriers. *Crit. Rev. Ther. Drug Carrier Syst.* **1985**, *2*, 65–115.
- (78) Deshpande, P. P.; Biswas, S.; Torchilin, V. P. Current Trends in the Use of Liposomes for Tumor Targeting. *Nanomedicine (London, U. K.)* **2013**, *8*, 1509–1528.
- (79) Byrne, J. D.; Betancourt, T.; Brannon-Peppas, L. Active Targeting Schemes for Nanoparticle Systems in Cancer Therapeutics. *Adv. Drug Delivery Rev.* **2008**, *60*, 1615–1626.
- (80) Weissmann, G.; Bloomgarden, D.; Kaplan, R.; Cohen, C.; Hoffstein, S.; Collins, T.; Gotlieb, A.; Nagle, D. General Method for Introduction of Enzymes by Means of Immunoglobulin-Coated Liposomes, into Lysosomes of Deficient Cells. *Proc. Natl. Acad. Sci. U. S. A.* **1975**, *72*, 88–92.
- (81) Lee, R. J.; Low, P. S. Delivery of Liposomes into Cultured KB Cells via Folate Receptor-Mediated Endocytosis. *J. Biol. Chem.* **1994**, *269*, 3198–3204.
- (82) Guo, W. J.; Lee, T.; Sudimack, J.; Lee, R. J. Receptor-Specific Delivery of Liposomes via Folate-Peg-Chol. *J. Liposome Res.* **2000**, *10*, 179–195.
- (83) Leamon, C. P.; Reddy, J. A. Folate-Targeted Chemotherapy. *Adv. Drug Delivery Rev.* **2004**, *56*, 1127–1141.
- (84) Sudimack, J.; Lee, R. J. Targeted Drug Delivery via the Folate Receptor. *Adv. Drug Delivery Rev.* **2000**, *41*, 147–162.
- (85) Kularatne, S. A.; Low, P. S. Targeting of Nanoparticles: Folate Receptor. In *Cancer Nanotechnology: Methods and Protocols*; Grobmyer, S. R., Moudgil, B. M., Eds.; 2010; Vol. 624, pp 249–265.
- (86) Li, X.; Ding, L.; Xu, Y.; Wang, Y.; Ping, Q. Targeted Delivery of Doxorubicin Using Stealth Liposomes Modified with Transferrin. *Int. J. Pharm.* **2009**, *373*, 116–123.
- (87) Kim, S. K.; Huang, L. Nanoparticle Delivery of a Peptide Targeting Egfr Signaling. *J. Controlled Release* **2012**, *157*, 279–286.
- (88) Lian, T.; Ho, R. J. Y. Trends and Developments in Liposome Drug Delivery Systems. *J. Pharm. Sci.* **2001**, *90*, 667–680.
- (89) Yoo, J.; Park, C.; Yi, G.; Lee, D.; Koo, H. Active Targeting Strategies Using Biological Ligands for Nanoparticle Drug Delivery Systems. *Cancers* **2019**, *11*, 640.
- (90) Toporkiewicz, M.; Meissner, J.; Matuszewicz, L.; Czogalla, A.; Sikorski, A. F. Toward a Magic or Imaginary Bullet? Ligands for Drug Targeting to Cancer Cells: Principles, Hopes, and Challenges. *Int. J. Nanomed.* **2015**, *10*, 1399–1414.
- (91) Large, D. E.; Soucy, J. R.; Hebert, J.; Auguste, D. T. Advances in Receptor-Mediated, Tumor-Targeted Drug Delivery. *Advanced Therapeutics* **2019**, *2*, 1800091.
- (92) Allen, T. M. Ligand-Targeted Therapeutics in Anticancer Therapy. *Nat. Rev. Cancer* **2002**, *2*, 750–763.
- (93) Lee, R. J.; Low, P. S. Folate-Targeted Liposomes for Drug Delivery. *J. Liposome Res.* **1997**, *7*, 455–466.
- (94) Gabizon, A.; Horowitz, A. T.; Goren, D.; Tzemach, D.; Mandelbaum-Shavit, F.; Qazen, M. M.; Zalipsky, S. Targeting Folate Receptor with Folate Linked to Extremities of Poly(ethylene Glycol)-Grafted Liposomes: *In Vitro* Studies. *Bioconjugate Chem.* **1999**, *10*, 289–298.
- (95) Ishida, O.; Maruyama, K.; Tanahashi, H.; Iwatsuru, M.; Sasaki, K.; Eriguchi, M.; Yanagie, H. Liposomes Bearing Polyethyleneglycol-Coupled Transferrin with Intracellular Targeting Property to the Solid Tumors *In Vivo*. *Pharm. Res.* **2001**, *18*, 1042–1048.
- (96) Derycke, A. S. L.; De Witte, P. A. M. Transferrin-Mediated Targeting of Hypericin Embedded in Sterically Stabilized PEG-Liposomes. *Int. J. Oncol.* **2002**, *20*, 181–187.
- (97) Salvatore, G.; Beers, R.; Margulies, I.; Kreitman, R. J.; Pastan, I. Improved Cytotoxic Activity toward Cell Lines and Fresh Leukemia Cells of a Mutant Anti-Cd22 Immunotoxin Obtained by Antibody Phage Display. *Clin. Cancer Res.* **2002**, *8*, 995–1002.
- (98) Ruoslahti, E.; Rajotte, D. An Address System in the Vasculature of Normal Tissues and Tumors. *Annu. Rev. Immunol.* **2000**, *18*, 813–827.
- (99) Pasqualini, R.; Koivunen, E.; Kain, R.; Lahdenranta, J.; Sakamoto, M.; Stryhn, A.; Ashmun, R. A.; Shapiro, L. H.; Arap, W.; Ruoslahti, E. Aminopeptidase N Is a Receptor for Tumor-Homing Peptides and a Target for Inhibiting Angiogenesis. *Cancer Res.* **2000**, *60*, 722–727.
- (100) Brekken, R. A.; Overholser, J. P.; Stastny, V. A.; Waltenberger, J.; Minna, J. D.; Thorpe, P. E. Selective Inhibition of Vascular Endothelial Growth Factor (Vegf) Receptor 2 (Kdr/Flk-1) Activity by

a Monoclonal Anti-Vegf Antibody Blocks Tumor Growth in Mice. *Cancer Res.* **2000**, *60*, 5117–5124.

(101) Noonberg, S. B.; Benz, C. C. Tyrosine Kinase Inhibitors Targeted to the Epidermal Growth Factor Receptor Subfamily - Role as Anticancer Agents. *Drugs* **2000**, *59*, 753–767.

(102) Borisch, B.; Semac, I.; Soltermann, A.; Palomba, C.; Hoessli, D. C. Anti-Cd20 Treatments and the Lymphocyte Membrane: Pathology for Therapy. In *Verhandlungen Der Deutschen Gesellschaft Fur Pathologie 85. Tagung: Pathologie Fur Das 21. Jahrhundert*; Kirchner, T., Ed.; Urban und Fischer: 2001; Vol. 85, pp 161–166.

(103) Leonard, J. P.; Link, B. K. Immunotherapy of Non-Hodgkin's Lymphoma with HL2 (Epratuzumab, an Anti-Cd22 Monoclonal Antibody) and Hu1d10 (Apolizumab). *Semin. Oncol.* **2002**, *29*, 81–86.

(104) Messmann, R. A.; Vitetta, E. S.; Headlee, D.; Senderowicz, A. M.; Figg, W. D.; Schindler, J.; Michiel, D. F.; Creekmore, S.; Steinberg, S. M.; Kohler, D.; Jaffe, E. S.; Stetler-Stevenson, M.; Chen, H. C.; Ghetie, V.; Sausville, E. A. A Phase I Study of Combination Therapy with Immunotoxins Igg-Hd37-Deglycosylated Ricin a Chain (Dga) and Igg-Rfb4-Dga (Combotox) in Patients with Refractory Cd19(+), Cd22(+) B Cell Lymphoma. *Clin. Cancer Res.* **2000**, *6*, 1302–1313.

(105) Jurcic, J. G. Antibody Therapy for Residual Disease in Acute Myelogenous Leukemia. *Critical Reviews in Oncology Hematology* **2001**, *38*, 37–45.

(106) Stadtmauer, E. A. Trials with Gemtuzumab Ozogamicin (Mylotarg (R)) Combined with Chemotherapy Regimens in Acute Myeloid Leukemia. *Clin. Lymphoma* **2002**, *2*, S24–S28.

(107) Duvic, M.; Kuzel, T.; Olsen, E. A.; Martin, A. G.; Foss, F. M.; Kim, Y. H.; Heald, P. W.; Bacha, P.; Nichols, J.; Liepa, A. Quality-of-Life Improvements in Cutaneous T-Cell Lymphoma Patients Treated with Denileukin Diftitox (Ontak (R)). *Clin. Lymphoma* **2002**, *2*, 222–228.

(108) Olsen, E.; Duvic, M.; Frankel, A.; Kim, Y.; Martin, A.; Vonderheid, E.; Jegasothy, B.; Wood, G.; Gordon, M.; Heald, P.; Oseroff, A.; Pinter-Brown, L.; Bowen, G.; Kuzel, T.; Fivenson, D.; Foss, F.; Glode, M.; Molina, A.; Knobler, E.; Stewart, S.; et al. Pivotal Phase Iii Trial of Two Dose Levels of Denileukin Diftitox for the Treatment of Cutaneous T-Cell Lymphoma. *J. Clin. Oncol.* **2001**, *19*, 376–388.

(109) Reardon, D. A.; Akabani, G.; Coleman, R. E.; Friedman, A. H.; Friedman, H. S.; Herndon, J. E.; Cokgor, I.; McLendon, R. E.; Pegram, C. N.; Provenzale, J. M.; Quinn, J. A.; Rich, J. N.; Regalado, L. V.; Sampson, J. H.; Shafman, T. D.; Wikstrand, C. J.; Wong, T. Z.; Zhao, X. G.; Zalutsky, M. R.; Bigner, D. D. Phase Ii Trial of Murine I-131-Labeled Antitenascin Monoclonal Antibody 81c6 Administered into Surgically Created Resection Cavities of Patients with Newly Diagnosed Malignant Gliomas. *J. Clin. Oncol.* **2002**, *20*, 1389–1397.

(110) Goldenberg, D. M. Targeted Therapy of Cancer with Radiolabeled Antibodies. *J. Nucl. Med.* **2002**, *43*, 693–713.

(111) Epenetos, A. A.; Hird, V.; Lambert, H.; Mason, P.; Coulter, C. Long Term Survival of Patients with Advanced Ovarian Cancer Treated with Intraperitoneal Radioimmunotherapy. *Int. J. Gynecol. Cancer* **2000**, *10*, 44–46.

(112) Behr, T. M.; Liersch, T.; Greiner-Bechert, L.; Griesinger, F.; Behe, M.; Markus, P. M.; Gratz, S.; Angerstein, C.; Brittinger, G.; Becker, H.; Goldenberg, D. M.; Becker, W. Radioimmunotherapy of Small-Volume Disease of Metastatic Colorectal Cancer: Results of a Phase Ii Trial with the Iodine-131-Labeled Humanized Anti-Carcinoembryonic Antigen Antibody Hm-14 (Retraction of Vol 94, Pg 1373, 2002). *Cancer* **2015**, *121*, 2290–2290.

(113) Davis, F. F.; Van Es, T.; Palczuk, N. C. Non-Immunogenic Polypeptides. NL7409770-A, 1975.

(114) Davis, F. F. The Origin of Pegnology. *Adv. Drug Delivery Rev.* **2002**, *54*, 457–458.

(115) Klibanov, A. L.; Maruyama, K.; Torchilin, V. P.; Huang, L. Amphipathic Polyethyleneglycols Effectively Prolong the Circulation Time of Liposomes. *FEBS Lett.* **1990**, *268*, 235–237.

(116) Blume, G.; Cevc, G. Liposomes for the Sustained Drug Release in Vivo. *Biochim. Biophys. Acta, Biomembr.* **1990**, *1029*, 91–97.

(117) Zalipsky, S. Chemistry of Polyethylene-Glycol Conjugates with Biologically-Active Molecules. *Adv. Drug Delivery Rev.* **1995**, *16*, 157–182.

(118) Hassan, S.; Prakash, G.; Ozturk, A. B.; Saghadzadeh, S.; Sohail, M. F.; Seo, J.; Dokmeci, M. R.; Zhang, Y. S.; Khademhosseini, A. Evolution and Clinical Translation of Drug Delivery Nanomaterials. *Nano Today* **2017**, *15*, 91–106.

(119) Andresen, T. L.; Jensen, S. S.; Jorgensen, K. Advanced Strategies in Liposomal Cancer Therapy: Problems and Prospects of Active and Tumor Specific Drug Release. *Prog. Lipid Res.* **2005**, *44*, 68–97.

(120) Rahim, M. A.; Jan, N.; Khan, S.; Shah, H.; Madni, A.; Khan, A.; Jabar, A.; Khan, S.; Elhissi, A.; Hussain, Z.; Aziz, H. C.; Sohail, M.; Khan, M.; Thu, H. E. Recent Advancements in Stimuli Responsive Drug Delivery Platforms for Active and Passive Cancer Targeting. *Cancers* **2021**, *13*, 670.

(121) Yatvin, M. B.; Kreutz, W.; Horwitz, B. A.; Shinitzky, M. Ph-Sensitive Liposomes - Possible Clinical Implications. *Science* **1980**, *210*, 1253–1254.

(122) Mills, J. K.; Needham, D. The Materials Engineering of Temperature-Sensitive Liposomes. *Methods Enzymol.* **2004**, *387*, 82–113.

(123) Mura, S.; Nicolas, J.; Couvreur, P. Stimuli-Responsive Nanocarriers for Drug Delivery. *Nat. Mater.* **2013**, *12*, 991–1003.

(124) Yatvin, M. B.; Weinstein, J. N.; Dennis, W. H.; Blumenthal, R. Design of Liposomes for Enhanced Local Release of Drugs by Hyperthermia. *Science* **1978**, *202*, 1290–1293.

(125) Papahadjopoulos, D.; Jacobson, K.; Nir, S.; Isac, T. Phase-Transitions in Phospholipid Vesicles - Fluorescence Polarization and Permeability Measurements Concerning Effect of Temperature and Cholesterol. *Biochim. Biophys. Acta, Biomembr.* **1973**, *311*, 330–348.

(126) Needham, D.; Park, J. Y.; Wright, A. M.; Tong, J. H. Materials Characterization of the Low Temperature Sensitive Liposome (Ltsl): Effects of the Lipid Composition (Lysolipid and Dspe-Peg2000) on the Thermal Transition and Release of Doxorubicin. *Faraday Discuss.* **2013**, *161*, 515–534.

(127) Han, H. D.; Jeon, Y. W.; Kwon, H. J.; Jeon, H. N.; Byeon, Y.; Lee, C. O.; Cho, S. H.; Shin, B. C. Therapeutic Efficacy of Doxorubicin Delivery by a CO₂ Generating Liposomal Platform in Breast Carcinoma. *Acta Biomater.* **2015**, *24*, 279–285.

(128) Zhao, Y.; Ren, W.; Zhong, T.; Zhang, S.; Huang, D.; Guo, Y.; Yao, X.; Wang, C.; Zhang, W. Q.; Zhang, X.; Zhang, Q. Tumor-Specific Ph-Responsive Peptide-Modified Ph-Sensitive Liposomes Containing Doxorubicin for Enhancing Glioma Targeting and Anti-Tumor Activity. *J. Controlled Release* **2016**, *222*, 56–66.

(129) Clares, B.; Biedma-Ortiz, R. A.; Saez-Fernandez, E.; Prados, J. C.; Melguizo, C.; Cabeza, L.; Ortiz, R.; Arias, J. L. Nano-Engineering of 5-Fluorouracil-Loaded Magnetoliposomes for Combined Hyperthermia and Chemotherapy against Colon Cancer. *Eur. J. Pharm. Biopharm.* **2013**, *85*, 329–338.

(130) Li, H. P.; Yang, X.; Zhou, Z. W.; Wang, K. K.; Li, C. Z.; Qiao, H. Z.; Oupicky, D.; Sun, M. J. Near-Infrared Light-Triggered Drug Release from a Multiple Lipid Carrier Complex Using an All-in-One Strategy. *J. Controlled Release* **2017**, *261*, 126–137.

(131) Szebeni, J.; Barenholz, Y. Adverse Immune Effects of Liposomes: Complement Activation, Immunogenicity and Immune Suppression. In *Harnessing Biomaterials for Nanomedicine: Preparation, Toxicity and Applications*; Pan Stanford Publishing Pte Ltd.: New York, 2009; pp 1–19.

(132) Inglut, C. T.; Sorrin, A. J.; Kuruppu, T.; Vig, S.; Cicalo, J.; Ahmad, H.; Huang, H.-C. Immunological and Toxicological Considerations for the Design of Liposomes. *Nanomaterials* **2020**, *10*, 190.

(133) Dass, C. R. Lipoplex-Mediated Delivery of Nucleic Acids: Factors Affecting in Vivo Transfection. *J. Mol. Med.* **2004**, *82*, 579–591.

(134) Lv, H. T.; Zhang, S. B.; Wang, B.; Cui, S. H.; Yan, J. Toxicity of Cationic Lipids and Cationic Polymers in Gene Delivery. *J. Controlled Release* **2006**, *114*, 100–109.

(135) Yang, Q.; Lai, S. K. Anti-Peg Immunity: Emergence, Characteristics, and Unaddressed Questions. *WIREs Nanomedicine and Nanobiotechnology* **2015**, *7*, 655–677.

(136) Gregoriadis, G.; Leathwood, P. D.; Ryman, B. E. Enzyme Entrapment in Liposomes. *FEBS Lett.* **1971**, *14*, 95–99.

- (137) Manjappa, A. S.; Chaudhari, K. R.; Venkataraju, M. P.; Dantuluri, P.; Nanda, B.; Sidda, C.; Sawant, K. K.; Murthy, R. S. R. Antibody Derivatization and Conjugation Strategies: Application in Preparation of Stealth Immunoliposome to Target Chemotherapeutics to Tumor. *J. Controlled Release* **2011**, *150*, 2–22.
- (138) Park, J. W.; Benz, C. C.; Martin, F. J. Future Directions of Liposome- and Immunoliposome-Based Cancer Therapeutics. *Semin. Oncol.* **2004**, *31*, 196–205.
- (139) Szoka, F.; Papahadjopoulos, D. Procedure for Preparation of Liposomes with Large Internal Aqueous Space and High Capture by Reverse-Phase Evaporation. *Proc. Natl. Acad. Sci. U. S. A.* **1978**, *75*, 4194–4198.
- (140) Deamer, D.; Bangham, A. D. Large Volume Liposomes by an Ether Vaporization Method. *Biochim. Biophys. Acta, Nucleic Acids Protein Synth.* **1976**, *443*, 629–634.
- (141) Anyarambhatla, G. R.; Needham, D. Enhancement of the Phase Transition Permeability of Dppc Liposomes by Incorporation of Mppc: A New Temperature-Sensitive Liposome for Use with Mild Hyperthermia. *J. Liposome Res.* **1999**, *9*, 491–506.
- (142) Needham, D.; Dewhirst, M. W. The Development and Testing of a New Temperature-Sensitive Drug Delivery System for the Treatment of Solid Tumors. *Adv. Drug Delivery Rev.* **2001**, *53*, 285–305.
- (143) Lammers, T.; Kiessling, F.; Hennink, W. E.; Storm, G. Drug Targeting to Tumors: Principles, Pitfalls and (Pre-) Clinical Progress. *J. Controlled Release* **2012**, *161*, 175–187.
- (144) Low, P. S.; Henne, W. A.; Doorneweerd, D. D. Discovery and Development of Folic-Acid-Based Receptor Targeting for Imaging and Therapy of Cancer and Inflammatory Diseases. *Acc. Chem. Res.* **2008**, *41*, 120–129.
- (145) Farhood, H.; Gao, X.; Son, K.; Yang, Y. Y.; Lazo, J. S.; Huang, L.; Barsoum, J.; Bottega, R.; Epand, R. M. Cationic Liposomes for Direct Gene-Transfer in Therapy of Cancer and Other Diseases. In *Gene Therapy for Neoplastic Diseases*; Huber, B. E., Lazo, J. S., Eds.; 1994; Vol. 716, pp 23–35.
- (146) Lasic, D. D.; Strey, H.; Stuart, M. C. A.; Podgornik, R.; Frederik, P. M. The Structure of DNA-Liposome Complexes. *J. Am. Chem. Soc.* **1997**, *119*, 832–833.
- (147) Papahadjopoulos, D.; Allen, T. M.; Gabizon, A.; Mayhew, E.; Matthay, K.; Huang, S. K.; Lee, K. D.; Woodle, M. C.; Lasic, D. D.; Redemann, C.; Martin, F. J. Sterically Stabilized Liposomes - Improvements in Pharmacokinetics and Antitumor Therapeutic Efficacy. *Proc. Natl. Acad. Sci. U. S. A.* **1991**, *88*, 11460–11464.
- (148) Leamon, C. P.; Low, P. S. Delivery of Macromolecules into Living Cells - A Method That Exploits Folate Receptor Endocytosis. *Proc. Natl. Acad. Sci. U. S. A.* **1991**, *88*, 5572–5576.
- (149) Torchilin, V.; Multifunctional, P. Stimuli-Sensitive Nanoparticulate Systems for Drug Delivery. *Nat. Rev. Drug Discovery* **2014**, *13*, 813–827.
- (150) Schwarz, C.; Mehnert, W.; Lucks, J. S.; Muller, R. H. Solid Lipid Nanoparticles (Sln) for Controlled Drug-Delivery 0.1. Production, Characterization and Sterilization. *J. Controlled Release* **1994**, *30*, 83–96.
- (151) Muller, R. H.; Mehnert, W.; Lucks, J. S.; Schwarz, C.; Zurmuhlen, A.; Weyhers, H.; Freitas, C.; Ruhl, D. Solid Lipid Nanoparticles (SLN) - An Alternative Colloidal Carrier System for Controlled Drug-Delivery. *Eur. J. Pharm. Biopharm.* **1995**, *41*, 62–69.
- (152) Hayes, M. E.; Drummond, D. C.; Hong, K.; Zheng, W. W.; Khorosheva, V. A.; Cohen, J. A.; Noble, C. O.; Park, J. W.; Marks, J. D.; Benz, C. C.; Kirpotin, D. B. Increased Target Specificity of Anti-HER2 Genospheres by Modification of Surface Charge and Degree of Pegylation. *Mol. Pharmaceutics* **2006**, *3*, 726–736.
- (153) Shmeeda, H.; Tzernach, D.; Mak, L.; Gabizon, A. Her2-Targeted Pegylated Liposomal Doxorubicin: Retention of Target-Specific Binding and Cytotoxicity after *in Vivo* Passage. *J. Controlled Release* **2009**, *136*, 155–160.
- (154) Laginha, K. M.; Moase, E. H.; Yu, N.; Huang, A.; Allen, T. M. Bioavailability and Therapeutic Efficacy of Her2 Scfv-Targeted Liposomal Doxorubicin in a Murine Model of HER2-Overexpressing Breast Cancer. *J. Drug Targeting* **2008**, *16*, 605–610.
- (155) Huwylar, J.; Wu, D. F.; Partridge, W. M. Brain Drug Delivery of Small Molecules Using Immunoliposomes. *Proc. Natl. Acad. Sci. U. S. A.* **1996**, *93*, 14164–14169.
- (156) Li, H. Y.; Qian, Z. M. Transferrin/Transferrin Receptor-Mediated Drug Delivery. *Med. Res. Rev.* **2002**, *22*, 225–250.
- (157) Qian, Z. M.; Li, H. Y.; Sun, H. Z.; Ho, K. Targeted Drug Delivery via the Transferrin Receptor-Mediated Endocytosis Pathway. *Pharmacol. Rev.* **2002**, *54*, 561–587.
- (158) Singh, M. Transferrin as a Targeting Ligand for Liposomes and Anticancer Drugs. *Curr. Pharm. Des.* **1999**, *5*, 443–451.
- (159) Kong, G.; Anyarambhatla, G.; Petros, W. P.; Braun, R. D.; Colvin, O. M.; Needham, D.; Dewhirst, M. W. Efficacy of Liposomes and Hyperthermia in a Human Tumor Xenograft Model: Importance of Triggered Drug Release. *Cancer Res.* **2000**, *60*, 6950–6957.
- (160) Needham, D.; Anyarambhatla, G.; Kong, G.; Dewhirst, M. W. A New Temperature-Sensitive Liposome for Use with Mild Hyperthermia: Characterization and Testing in a Human Tumor Xenograft Model. *Cancer Res.* **2000**, *60*, 1197–1201.
- (161) Ganta, S.; Devalapally, H.; Shahiwala, A.; Amiji, M. A Review of Stimuli-Responsive Nanocarriers for Drug and Gene Delivery. *J. Controlled Release* **2008**, *126*, 187–204.
- (162) Spicer, P. T.; Hayden, K. L.; Lynch, M. L.; Ofori-Boateng, A.; Burns, J. L. Novel Process for Producing Cubic Liquid Crystalline Nanoparticles (Cubosomes). *Langmuir* **2001**, *17*, 5748–5756.
- (163) Akinc, A.; Maier, M. A.; Manoharan, M.; Fitzgerald, K.; Jayaraman, M.; Barros, S.; Ansell, S.; Du, X. Y.; Hope, M. J.; Madden, T. D.; Mui, B. L.; Semple, S. C.; Tam, Y. K.; Ciufolini, M.; Wittigmann, D.; Kulkarni, J. A.; van der Meel, R.; Cullis, P. R. The Onpatro Story and the Clinical Translation of Nanomedicines Containing Nucleic Acid-Based Drugs. *Nat. Nanotechnol.* **2019**, *14*, 1084–1087.
- (164) Emergency Use Authorization (Eua) of the Pfizer-Biontech Covid-19 Vaccine to Prevent Coronavirus Disease 2019 (COVID-19) in Individuals 16 Years of Age and Older. <https://www.fda.gov/media/144414/download> (accessed 2020-12-22).
- (165) Emergency Use Authorization (Eua) of the Moderna Covid-19 Vaccine to Prevent Coronavirus Disease 2019 (Covid-19) in Individuals 18 Years of Age and Older. <https://www.fda.gov/media/144638/download> (accessed 2020-12-22).
- (166) Allen, T. M.; Cullis, P. R. Drug Delivery Systems: Entering the Mainstream. *Science* **2004**, *303*, 1818–1822.
- (167) Allen, T. M.; Cullis, P. R. Liposomal Drug Delivery Systems: From Concept to Clinical Applications. *Adv. Drug Delivery Rev.* **2013**, *65*, 36–48.
- (168) Szoka, F.; Papahadjopoulos, D. Comparative Properties and Methods of Preparation of Lipid Vesicles (Liposomes). *Annu. Rev. Biophys. Bioeng.* **1980**, *9*, 467–508.
- (169) Torchilin, V. Tumor Delivery of Macromolecular Drugs Based on the Epr Effect. *Adv. Drug Delivery Rev.* **2011**, *63*, 131–135.
- (170) Torchilin, V. P. Recent Advances with Liposomes as Pharmaceutical Carriers. *Nat. Rev. Drug Discovery* **2005**, *4*, 145–160.
- (171) Barenholz, Y. Doxil (R) - the First FDA-Approved Nano-Drug: Lessons Learned. *J. Controlled Release* **2012**, *160*, 117–134.
- (172) Radler, J. O.; Koltover, I.; Salditt, T.; Safinya, C. R. Structure of DNA-Cationic Liposome Complexes: DNA Intercalation in Multilamellar Membranes in Distinct Interhelical Packing Regimes. *Science* **1997**, *275*, 810–814.
- (173) Chan, C.; Du, S.; Dong, Y. Z.; Cheng, X. L. Computational and Experimental Approaches to Investigate Lipid Nanoparticles as Drug and Gene Delivery Systems. *Curr. Top. Med. Chem.* **2021**, *21*, 92–114.
- (174) Manchanda, S.; Das, N.; Chandra, A.; Bandyopadhyay, S.; Chaurasia, S. Chapter 2 - Fabrication of Advanced Parenteral Drug-Delivery Systems. In *Drug Delivery Systems*; Tekade, R. K., Ed.; Academic Press: London, 2020; pp 47–84.
- (175) Chaubet, F.; Rodriguez-Ruiz, V.; Boissière, M.; Velasquez, D. Pharmacology: Drug Delivery. In *Encyclopedia of Biomedical Engineering*; Narayan, R., Ed.; Elsevier: Oxford, 2019; pp 440–453.

- (176) Bobo, D.; Robinson, K. J.; Islam, J.; Thurecht, K. J.; Corrie, S. R. Nanoparticle-Based Medicines: A Review of FDA-Approved Materials and Clinical Trials to Date. *Pharm. Res.* **2016**, *33*, 2373–2387.
- (177) Jiang, W.; von Roemeling, C. A.; Chen, Y.; Qie, Y.; Liu, X.; Chen, J.; Kim, B. Y. S. Designing Nanomedicine for Immunology. *Nature Biomedical Engineering* **2017**, *1*, 1–11.
- (178) Sainz, V.; Coniot, J.; Matos, A. L.; Peres, C.; Zupancic, E.; Moura, L.; Silva, L. C.; Florindo, H. F.; Gaspar, R. S. Regulatory Aspects on Nanomedicines. *Biochem. Biophys. Res. Commun.* **2015**, *468*, 504–510.
- (179) Weissig, V.; Pettinger, T. K.; Murdock, N. Nanopharmaceuticals (Part I): Products on the Market. *Int. J. Nanomed.* **2014**, *9*, 4357–4373.
- (180) Liposome Drug Delivery Market. <https://www.transparencymarketresearch.com/liposome-drug-delivery-market.html> (accessed 2021-01-05).
- (181) García-Pinel, B.; Porras-Alcalá, C.; Ortega-Rodríguez, A.; Sarabia, F.; Prados, J.; Melguizo, C.; López-Romero, J. M. Lipid-Based Nanoparticles: Application and Recent Advances in Cancer Treatment. *Nanomaterials* **2019**, *9*, 638.
- (182) Pucci, C.; Martinelli, C.; Ciofani, G. Innovative Approaches for Cancer Treatment: Current Perspectives and New Challenges. *Ecantermedicalscience* **2019**, *13*, 961.
- (183) Matsumura, Y.; Maeda, H. A New Concept for Macromolecular Therapeutics in Cancer-Chemotherapy - Mechanism of Tumorotropic Accumulation of Proteins and the Antitumor Agent Smancs. *Cancer Res.* **1986**, *46*, 6387–6392.
- (184) Blum, R. H.; Carter, S. K. Adriamycin - New Anticancer Drug with Significant Clinical Activity. *Ann. Intern. Med.* **1974**, *80*, 249–259.
- (185) Mamidi, R.; Weng, S.; Stellar, S.; Wang, C.; Yu, N.; Huang, T.; Tonelli, A. P.; Kelley, M. F.; Angiuoli, A.; Fung, M. C. Pharmacokinetics, Efficacy and Toxicity of Different Pegylated Liposomal Doxorubicin Formulations in Preclinical Models: Is a Conventional Bioequivalence Approach Sufficient to Ensure Therapeutic Equivalence of Pegylated Liposomal Doxorubicin Products? *Cancer Chemother. Pharmacol.* **2010**, *66*, 1173–1184.
- (186) Kamiński, D. M. Recent Progress in the Study of the Interactions of Amphotericin B with Cholesterol and Ergosterol in Lipid Environments. *Eur. Biophys. J.* **2014**, *43*, 453–467.
- (187) Starzyk, J.; Gruszecki, M.; Tutaj, K.; Luchowski, R.; Szlajak, R.; Wasko, P.; Grudzinski, W.; Czub, J.; Gruszecki, W. I. Self-Association of Amphotericin B: Spontaneous Formation of Molecular Structures Responsible for the Toxic Side Effects of the Antibiotic. *J. Phys. Chem. B* **2014**, *118*, 13821–13832.
- (188) Faustino, C.; Pinheiro, L. Lipid Systems for the Delivery of Amphotericin B in Antifungal Therapy. *Pharmaceutics* **2020**, *12*, 29.
- (189) Juliano, R. L.; Grant, C. W.; Barber, K. R.; Kalp, M. A. Mechanism of the Selective Toxicity of Amphotericin B Incorporated into Liposomes. *Mol. Pharmacol.* **1987**, *31*, 1–11.
- (190) Yonezawa, S.; Koide, H.; Asai, T. Recent Advances in SiRNA Delivery Mediated by Lipid-Based Nanoparticles. *Adv. Drug Delivery Rev.* **2020**, *154–155*, 64–78.
- (191) Dong, Y. Z.; Siegwart, D. J.; Anderson, D. G. Strategies, Design, and Chemistry in SiRNA Delivery Systems. *Adv. Drug Delivery Rev.* **2019**, *144*, 133–147.
- (192) Adams, D.; Gonzalez-Duarte, A.; O’Riordan, W. D.; Yang, C. C.; Ueda, M.; Kristen, A. V.; Tournev, I.; Schmidt, H. H.; Coelho, T.; Berk, J. L.; Lin, K. P.; Vita, G.; Attarian, S.; Planté-Bordeneuve, V.; Mezei, M. M.; Campistol, J. M.; Buades, J.; Brannagan, T. H., 3rd; Kim, B. J.; Oh, J.; et al. Patisiran, an RNAi Therapeutic, for Hereditary Transthyretin Amyloidosis. *N. Engl. J. Med.* **2018**, *379*, 11–21.
- (193) Loh, T. The Vaccine Revolution Is Coming inside Tiny Bubbles of Fat. https://www.bloomberg.com/news/articles/2021-03-04/the-vaccine-revolution-is-coming-inside-tiny-bubbles-of-fat?cmpid=socialflow-twitter-business&utm_campaign=socialflow-organic&utm_medium=social&utm_content=business&utm_source=twitter (accessed 2021-04-19).
- (194) Cross, R. Without These Lipid Shells, There Would Be No mRNA Vaccines for COVID-19. *Chem. Eng. News* **2021**, 99.
- (195) Pfizer-Biontech Covid-19 Vaccine- BNT162b2 Injection, Suspension. <https://dailymed.nlm.nih.gov/dailymed/drugInfo.cfm?setid=908ecbe7-2f1b-42dd-94bf-f917ec3c5af8> (accessed 2020-12-22).
- (196) Miller, K. What’s in the Pfizer and Moderna Covid-19 Vaccines? <https://www.prevention.com/health/a35002158/pfizer-vs-moderna-covid-19-vaccine-ingredients/> (accessed 2020-12-22).
- (197) Vaccines and Related Biological Products Advisory Committee Meeting. Moderna COVID-19 Vaccine. FDA Briefing Document. <https://www.fda.gov/media/144434/download> (accessed 2020-12-22).
- (198) Zhang, X. F.; Zhao, W. Y.; Nguyen, G. N.; Zhang, C. X.; Zeng, C. X.; Yan, J. Y.; Du, S.; Hou, X. C.; Li, W. Q.; Jiang, J.; Deng, B. B.; McComb, D. W.; Dorkin, R.; Shah, A.; Barrera, L.; Gregoire, F.; Singh, M.; Chen, D. L.; Sabatino, D. E.; Dong, Y. Z. Functionalized Lipid-Like Nanoparticles for *in Vivo* mRNA Delivery and Base Editing. *Science Advances* **2020**, *6*, No. eabc2315.
- (199) DeFrancesco, L. Whither Covid-19 Vaccines? *Nat. Biotechnol.* **2020**, *38*, 1132–1145.
- (200) Sabnis, S.; Kumarasinghe, E. S.; Salerno, T.; Mihai, C.; Ketova, T.; Senn, J. J.; Lynn, A.; Bulychiev, A.; McFadyen, I.; Chan, J.; Almarsson, Ö.; Stanton, M. G.; Benenato, K. E. A Novel Amino Lipid Series for mRNA Delivery: Improved Endosomal Escape and Sustained Pharmacology and Safety in Non-Human Primates. *Mol. Ther.* **2018**, *26*, 1509–1519.
- (201) Yanez Arteta, M.; Kjellman, T.; Bartesaghi, S.; Wallin, S.; Wu, X.; Kvist, A. J.; Dabkowska, A.; Székely, N.; Radulescu, A.; Bergenholtz, J.; Lindfors, L. Successful Reprogramming of Cellular Protein Production through mRNA Delivered by Functionalized Lipid Nanoparticles. *Proc. Natl. Acad. Sci. U. S. A.* **2018**, *115*, E3351–E3360.
- (202) Schoenmaker, L.; Witzigmann, D.; Kulkarni, J. A.; Verbeke, R.; Kersten, G.; Jiskoot, W.; Crommelin, D. J. A. mRNA-Lipid Nanoparticle Covid-19 Vaccines: Structure and Stability. *Int. J. Pharm.* **2021**, *601*, 120586.
- (203) Sealy, A. Manufacturing Moonshot: How Pfizer Makes Its Millions of Covid-19 Vaccine Doses. <https://edition.cnn.com/2021/03/31/health/pfizer-vaccine-manufacturing/index.html> (accessed 2021-04-19).
- (204) Hope, M. J.; Mui, B.; Lin, P. J. C.; Barbosa, C.; Madden, T.; Ansell, S. M.; Du, X.; Lin, J. C. P.; Barbosa, C. J.; Madden, T. D.; Lin, P. J. Lipid Nanoparticle Used for Administering Therapeutic Agent to Patient Comprises Cationic Lipid, Neutral Lipid, Steroid, Polymer Conjugated Lipid, and Therapeutic Agent or Its Salt Encapsulated within or Associated with Lipid Nanoparticle. WO2018081480-A1, 2018.
- (205) Chen, D. L.; Love, K. T.; Chen, Y.; Eltoukhy, A. A.; Kastrop, C.; Sahay, G.; Jeon, A.; Dong, Y. Z.; Whitehead, K. A.; Anderson, D. G. Rapid Discovery of Potent SiRNA-Containing Lipid Nanoparticles Enabled by Controlled Microfluidic Formulation. *J. Am. Chem. Soc.* **2012**, *134*, 6948–6951.
- (206) Kowalski, P. S.; Rudra, A.; Miao, L.; Anderson, D. G. Delivering the Messenger: Advances in Technologies for Therapeutic mRNA Delivery. *Mol. Ther.* **2019**, *27*, 710–728.
- (207) Sahin, U.; Karikó, K.; Türeci, Ö. mRNA-Based Therapeutics — Developing a New Class of Drugs. *Nat. Rev. Drug Discovery* **2014**, *13*, 759–780.
- (208) Gomez-Aguado, I.; Rodriguez-Castejon, J.; Vicente-Pascual, M.; Rodriguez-Gascon, A.; Solinis, M. A.; del Pozo-Rodriguez, A. Nanomedicines to Deliver mRNA: State of the Art and Future Perspectives. *Nanomaterials* **2020**, *10*, 364.
- (209) Pardi, N.; Hogan, M. J.; Porter, F. W.; Weissman, D. mRNA Vaccines - A New Era in Vaccinology. *Nat. Rev. Drug Discovery* **2018**, *17*, 261–279.
- (210) Clinical Trials. <https://www.clinicaltrials.gov/> (accessed 2021-03-10).
- (211) Gorzelany, J. A.; de Souza, M. P. Protein Replacement Therapies for Rare Diseases: A Breeze for Regulatory Approval? *Sci. Transl. Med.* **2013**, *5*, 178fs10–178fs10.

- (212) Vlatkovic, I. Non-Immunotherapy Application of LNP-mRNA: Maximizing Efficacy and Safety. *Biomedicines* **2021**, *9*, 530.
- (213) Nabhan, J. F.; Wood, K. M.; Rao, V. P.; Morin, J.; Bhamidipaty, S.; LaBranche, T. P.; Gooch, R. L.; Bozal, F.; Bulawa, C. E.; Guild, B. C. Intrathecal Delivery of Frataxin mRNA Encapsulated in Lipid Nanoparticles to Dorsal Root Ganglia as a Potential Therapeutic for Friedreich's Ataxia. *Sci. Rep.* **2016**, *6*, 20019.
- (214) Lamichhane, N.; Udayakumar, T. S.; D'Souza, W. D.; Simone, C. B.; Raghavan, S. R.; Polf, J.; Mahmood, J. Liposomes: Clinical Applications and Potential for Image-Guided Drug Delivery. *Molecules* **2018**, *23*, 288.
- (215) Morton, D. L.; Chan, A. D. The Concept of Sentinel Node Localization: How It Started. *Semin. Nucl. Med.* **2000**, *30*, 4–10.
- (216) Goins, B. A. Radiolabeled Lipid Nanoparticles for Diagnostic Imaging. *Expert Opin. Med. Diagn.* **2008**, *2*, 853–873.
- (217) Laverman, P.; Boerman, O. C.; Storm, G. Radiolabeling of Liposomes for Scintigraphic Imaging. In *Methods Enzymol*; Duzgunes, N., Ed.; Academic Press: Cambridge, MA, 2003; Vol. 373, pp 234–248.
- (218) Espinola, L. G.; Beaucaire, J.; Gottschalk, A.; Caride, V. J. Radiolabeled Liposomes as Metabolic and Scanning Tracers in Mice. Ii. In-111 Oxine Compared with Tc-99m Dtpa, Entrapped in Multilamellar Lipid Vesicles. *J. Nucl. Med.* **1979**, *20*, 434–40.
- (219) Ogihara, I.; Kojima, S.; Jay, M. Differential Uptake of Gallium-67-Labeled Liposomes between Tumors and Inflammatory Lesions in Rats. *J. Nucl. Med.* **1986**, *27*, 1300–1307.
- (220) Kubo, A.; Nakamura, K.; Sammiya, T.; Katayama, M.; Hashimoto, T.; Hashimoto, S.; Kobayashi, H.; Teramoto, T. Indium-111-Labelled Liposomes: Dosimetry and Tumour Detection in Patients with Cancer. *Eur. J. Nucl. Med.* **1993**, *20*, 107–113.
- (221) Oyen, W. J.; Boerman, O. C.; Storm, G.; van Bloois, L.; Koenders, E. B.; Claessens, R. A.; Perenboom, R. M.; Crommelin, D. J.; van der Meer, J. W.; Corstens, F. H. Detecting Infection and Inflammation with Technetium-99m-Labeled Stealth Liposomes. *J. Nucl. Med.* **1996**, *37*, 1392–1397.
- (222) Ogawa, M.; Umeda, I. O.; Kosugi, M.; Kawai, A.; Hamaya, Y.; Takashima, M.; Yin, H.; Kudoh, T.; Seno, M.; Magata, Y. Development of 111in-Labeled Liposomes for Vulnerable Atherosclerotic Plaque Imaging. *J. Nucl. Med.* **2014**, *55*, 115–120.
- (223) Lamichhane, N.; Dewkar, G. K.; Sundaresan, G.; Mahon, R. N.; Zweit, J. [(18F)-Fluorinated Carboplatin and [(111)in]-Liposome for Image-Guided Drug Delivery. *Int. J. Mol. Sci.* **2017**, *18*, 1079.
- (224) Nakada, T. Clinical Application of High and Ultra High-Field Mri. *Brain Dev.* **2007**, *29*, 325–335.
- (225) Šimečková, P.; Hubatka, F.; Kotouček, J.; Turánek Knötigová, P.; Mašek, J.; Slavík, J.; Kováč, O.; Neča, J.; Kulich, P.; Hřebík, D.; Stráská, J.; Pěňčíková, K.; Procházková, J.; Diviš, P.; Macaulay, S.; Mikulík, R.; Raška, M.; Machala, M.; Turánek, J. Gadolinium Labelled Nanoliposomes as the Platform for Mri Theranostics: *In Vitro* Safety Study in Liver Cells and Macrophages. *Sci. Rep.* **2020**, *10*, 4780.
- (226) Navon, G.; Panigel, R.; Valensin, G. Liposomes Containing Paramagnetic Macromolecules as Mri Contrast Agents. *Magn. Reson. Med.* **1986**, *3*, 876–880.
- (227) Wang, L. S.; Chuang, M. C.; Ho, J. A. Nanotheranostics—A Review of Recent Publications. *Int. J. Nanomed.* **2012**, *7*, 4679–4695.
- (228) Svenson, S. Theranostics: Are We There Yet? *Mol. Pharmaceutics* **2013**, *10*, 848–856.
- (229) Al-Jamal, W. T.; Kostarelos, K. Liposomes: From a Clinically Established Drug Delivery System to a Nanoparticle Platform for Theranostic Nanomedicine. *Acc. Chem. Res.* **2011**, *44*, 1094–1104.
- (230) Muthu, M. S.; Kulkarni, S. A.; Raju, A.; Feng, S. S. Theranostic Liposomes of Tpgs Coating for Targeted Co-Delivery of Docetaxel and Quantum Dots. *Biomaterials* **2012**, *33*, 3494–3501.
- (231) Gross, U.; Roding, J.; Stanzl, K.; Zastrow, L. Phospholipid- and Fluorocarbon-Containing Cosmetic. US5643601, July 1, 1997, 1997.
- (232) Wu, X.; Guy, R. H. Applications of Nanoparticles in Topical Drug Delivery and in Cosmetics. *J. Drug Delivery Sci. Technol.* **2009**, *19*, 371–384.
- (233) Gibbs, B. F.; Kermasha, S.; Alli, I.; Mulligan, C. N. Encapsulation in the Food Industry: A Review. *Int. J. Food Sci. Nutr.* **1999**, *50*, 213–224.
- (234) Mohammadi, A.; Jafari, S. M.; Mahoonak, A. S.; Ghorbani, M. Liposomal/Nanoliposomal Encapsulation of Food-Relevant Enzymes and Their Application in the Food Industry. *Food Bioprocess Technol.* **2021**, *14*, 23–38.
- (235) Reineccius, G. A. Liposomes for Controlled-Release in the Food-Industry. In *Encapsulation and Controlled Release of Food Ingredients*; Risch, S. J., Reineccius, G. A., Eds; ACS Symposium Series 590; Washington DC, 1995; Vol. 590, pp 113–131.
- (236) Acosta, E. Bioavailability of Nanoparticles in Nutrient and Nutraceutical Delivery. *Curr. Opin. Colloid Interface Sci.* **2009**, *14*, 3–15.
- (237) Espin, J. C.; Garcia-Conesa, M. T.; Tomas-Barberan, F. A. Nutraceuticals: Facts and Fiction. *Phytochemistry* **2007**, *68*, 2986–3008.
- (238) Huang, Q.; Yu, H.; Ru, Q. Bioavailability and Delivery of Nutraceuticals Using Nanotechnology. *J. Food Sci.* **2010**, *75*, R50–R57.
- (239) Katouzian, I.; Esfajani, A. F.; Jafari, S. M.; Akhavan, S. Formulation and Application of a New Generation of Lipid Nano-Carriers for the Food Bioactive Ingredients. *Trends Food Sci. Technol.* **2017**, *68*, 14–25.
- (240) Genc, R.; Ortiz, M.; O'Sullivan, C. K. Diffusion-Controlled Synthesis of Gold Nanoparticles: Nano-Liposomes as Mass Transfer Barrier. *J. Nanopart. Res.* **2014**, *16*, 1–5.
- (241) Gudlur, S.; Sanden, C.; Matouskova, P.; Fasciani, C.; Aili, D. Liposomes as Nanoreactors for the Photochemical Synthesis of Gold Nanoparticles. *J. Colloid Interface Sci.* **2015**, *456*, 206–209.
- (242) Clergeaud, G.; Geng, R.; Ortiz, M.; O'Sullivan, C. K. Liposomal Nanoreactors for the Synthesis of Monodisperse Palladium Nanoparticles Using Glycerol. *Langmuir* **2013**, *29*, 15405–15413.
- (243) Duss, M.; Vallooran, J. J.; Manni, L. S.; Kieliger, N.; Handschin, S.; Mezzenga, R.; Jessen, H. J.; Landau, E. M. Lipidic Mesophase-Embedded Palladium Nanoparticles: Synthesis and Tunable Catalysts in Suzuki-Miyaura Cross-Coupling Reactions. *Langmuir* **2019**, *35*, 120–127.
- (244) Korgel, B. A.; Monbouquette, H. G. Controlled Synthesis of Mixed Core and Layered (Zn,Cd)S and (Hg,Cd)S Nanocrystals within Phosphatidylcholine Vesicles. *Langmuir* **2000**, *16*, 3588–3594.
- (245) Zhang, R.; Song, X.; Liang, C.; Yi, X.; Song, G.; Chao, Y.; Yang, Y.; Yang, K.; Feng, L.; Liu, Z. Catalase-Loaded Cisplatin-Prodrug-Constructed Liposomes to Overcome Tumor Hypoxia for Enhanced Chemo-Radiotherapy of Cancer. *Biomaterials* **2017**, *138*, 13–21.
- (246) Mukerabigwi, J. F.; Ge, Z. S.; Kataoka, K. Therapeutic Nanoreactors as *In Vivo* Nanoplatforms for Cancer Therapy. *Chem. - Eur. J.* **2018**, *24*, 15706–15724.
- (247) Li, Y.; Zhou, Y.; Han, W.; Shi, M.; Zhao, H.; Liu, Y.; Zhang, F.; Zhang, J. Novel Lipidic and Bionzymatic Nanosomes for Efficient Delivery and Enhanced Bioactivity of Catalase. *Int. J. Pharm.* **2017**, *532*, 157–165.
- (248) Zhang, B. Y.; Wang, F.; Zhou, H.; Gao, D. Y.; Yuan, Z.; Wu, C. F.; Zhang, X. J. Polymer Dots Compartmentalized in Liposomes as a Photocatalyst for *In Situ* Hydrogen Therapy. *Angew. Chem., Int. Ed.* **2019**, *58*, 2744–2748.
- (249) Schumacher, I.; Arad, A.; Margalit, R. Butyrylcholinesterase Formulated in Liposomes. *Biotechnol. Appl. Biochem.* **1999**, *30*, 225–230.
- (250) Koyani, R.; Pérez-Robles, J.; Cadena-Nava, R. D.; Vazquez-Duhalt, R. Biomaterial-Based Nanoreactors, an Alternative for Enzyme Delivery. *Nanotechnol. Rev.* **2017**, *6*, 405–419.
- (251) Koynova, R.; Tenchov, B. Phase Transitions and Phase Behavior of Lipids. In *Encyclopedia of Biophysics*; Roberts, G. C. K., Ed.; Springer Verlag: Berlin, 2013; pp 1841–1854.
- (252) Nagle, J. F.; Tristram-Nagle, S. Structure of Lipid Bilayers. *Biochim. Biophys. Acta, Rev. Biomembr.* **2000**, *1469*, 159–195.
- (253) Simons, K.; Vaz, W. L. C. Model Systems, Lipid Rafts, and Cell Membranes. *Annu. Rev. Biophys. Biomol. Struct.* **2004**, *33*, 269–295.

- (254) van Meer, G.; Voelker, D. R.; Feigenson, G. W. Membrane Lipids: Where They Are and How They Behave. *Nat. Rev. Mol. Cell Biol.* **2008**, *9*, 112–124.
- (255) Kinnunen, P. K. J.; Laggner, P. Phospholipid Phase Transitions. *Chem. Phys. Lipids* **1991**, *57*, 109–408.
- (256) *Handbook of Biological Physics*; Lipowsky, R., Sackmann, E., Eds.; Elsevier Science: Amsterdam, 1995; Vol. 1.
- (257) Mouritsen, O. G. *Life - as a Matter of Fat. The Emerging Science of Lipidomics*; Springer: Berlin, 2005.
- (258) Cevc, G.; Marsh, D. *Phospholipid Bilayers*; John Wiley & Sons, Inc.: New York, 1987.
- (259) Marsh, D. *Handbook of Lipid Bilayers*; CRC Press: Boca Raton, London, NY, 1990.
- (260) Gruner, S. M. Intrinsic Curvature Hypothesis for Biomembrane Lipid-Composition - A Role for Nonbilayer Lipids. *Proc. Natl. Acad. Sci. U. S. A.* **1985**, *82*, 3665–3669.
- (261) Ginn, S. L.; Amaya, A. K.; Alexander, I. E.; Edelstein, M.; Abedi, M. R. Gene Therapy Clinical Trials Worldwide to 2017: An Update. *J. Gene Med.* **2018**, *20*, No. e3015.
- (262) Capone, F.; Nappi, F.; Galli, M. C. Chapter 11 - Gene Therapy Clinical Trials: Past, Present and Future. In *Second Generation Cell and Gene-Based Therapies*; Vertès, A. A., Smith, D. M., Qureshi, N., Dowden, N. J., Eds.; Academic Press: Cambridge MA, 2020; pp 285–301.
- (263) Khan, S.; Baboota, S.; Ali, J.; Khan, S.; Narang, R. S.; Narang, J. K. Nanostructured Lipid Carriers: An Emerging Platform for Improving Oral Bioavailability of Lipophilic Drugs. *International journal of pharmaceutical investigation* **2015**, *5*, 182–191.
- (264) Damiani, E.; Puglia, C. Nanocarriers and Microcarriers for Enhancing the Uv Protection of Sunscreens: An Overview. *J. Pharm. Sci.* **2019**, *108*, 3769–3780.
- (265) Souto, E. B.; Fernandes, A. R.; Martins-Gomes, C.; Coutinho, T. E.; Durazzo, A.; Lucarini, M.; Souto, S. B.; Silva, A. M.; Santini, A. Nanomaterials for Skin Delivery of Cosmeceuticals and Pharmaceuticals. *Appl. Sci.* **2020**, *10*, 1594
- (266) Vijaya, N.; Umamathi, T.; Baby, A. G.; Dorothy, R.; Rajendran, S.; Arockiaselvi, J.; Al-Hashem, A. Nanomaterials in Fragrance Products. In *Nanocosmetics*; Nanda, A., Nanda, S., Nguyen, T. A., Rajendran, S., Slimani, Y., Eds.; Elsevier: Cambridge, MA, 2020; Chapter 13, pp 247–265.
- (267) Plank, C.; Mechtler, K.; Szoka, F. C.; Wagner, E. Activation of the Complement System by Synthetic DNA Complexes: A Potential Barrier for Intravenous Gene Delivery. *Hum. Gene Ther.* **1996**, *7*, 1437–1446.
- (268) MacDonald, R. C.; Ashley, G. W.; Shida, M. M.; Rakhmanova, V. A.; Tarahovsky, Y. S.; Pantazatos, D. P.; Kennedy, M. T.; Pozharski, E. V.; Baker, K. A.; Jones, R. D.; Rosenzweig, H. S.; Choi, K. L.; Qiu, R. Z.; McIntosh, T. J. Physical and Biological Properties of Cationic Triesters of Phosphatidylcholine. *Biophys. J.* **1999**, *77*, 2612–2629.
- (269) Farhood, H.; Serbina, N.; Huang, L. The Role of Dioleoyl Phosphatidylethanolamine in Cationic Liposome-Mediated Gene-Transfer. *Biochim. Biophys. Acta, Biomembr.* **1995**, *1235*, 289–295.
- (270) Felgner, J. H.; Kumar, R.; Sridhar, C. N.; Wheeler, C. J.; Tsai, Y. J.; Border, R.; Ramsey, P.; Martin, M.; Felgner, P. L. Enhanced Gene Delivery and Mechanism Studies with a Novel Series of Cationic Lipid Formulations. *J. Biol. Chem.* **1994**, *269*, 2550–2561.
- (271) Li, S.; Huang, L. *In Vivo* Gene Transfer via Intravenous Administration of Cationic Lipid-Protamine-DNA (Lpd) Complexes. *Gene Ther.* **1997**, *4*, 891–900.
- (272) Zabner, J.; Fasbender, A. J.; Moninger, T.; Poellinger, K. A.; Welsh, M. J. Cellular and Molecular Barriers to Gene-Transfer by a Cationic Lipid. *J. Biol. Chem.* **1995**, *270*, 18997–19007.
- (273) Hofland, H. E. J.; Shephard, L.; Sullivan, S. M. Formation of Stable Cationic Lipid/DNA Complexes for Gene Transfer. *Proc. Natl. Acad. Sci. U. S. A.* **1996**, *93*, 7305–7309.
- (274) Boukhnikachvili, T.; Aguerre-Chariol, O.; Airiau, M.; Lesieur, S.; Ollivon, M.; Vacus, J. Structure of in-Serum Transfecting DNA-Cationic Lipid Complexes. *FEBS Lett.* **1997**, *409*, 188–194.
- (275) MacDonald, R. C.; Rakhmanova, V. A.; Choi, K. L.; Rosenzweig, H. S.; Lahiri, M. K. O-Ethylphosphatidylcholine: A Metabolizable Cationic Phospholipid Which Is a Serum-Compatible DNA Transfection Agent. *J. Pharm. Sci.* **1999**, *88*, 896–904.
- (276) Behr, J. P.; Demeneix, B.; Loeffler, J. P.; Mutul, J. P. Efficient Gene-Transfer into Mammalian Primary Endocrine-Cells with Lipopolyamine-Coated DNA. *Proc. Natl. Acad. Sci. U. S. A.* **1989**, *86*, 6982–6986.
- (277) Ferrari, M. E.; Nguyen, C. M.; Zelphati, O.; Tsai, Y. L.; Felgner, P. L. Analytical Methods for the Characterization of Cationic Lipid Nucleic Acid Complexes. *Hum. Gene Ther.* **1998**, *9*, 341–351.
- (278) Mitchell, M. J.; Billingsley, M. M.; Haley, R. M.; Wechsler, M. E.; Peppas, N. A.; Langer, R. Engineering Precision Nanoparticles for Drug Delivery. *Nat. Rev. Drug Discovery* **2021**, *20*, 101–124.



US 2016/0178652 A1

United States

Patent Application Publication
VITALEANO et al.

Pub. No.: U.S. 2016/0178652 A1
Pub. Date: Jun. 23, 2016

INTELLIGENT POLYMER BEADPOOLS

Publication Classification

Applicant: PRYMIOPATENT LLC, 1975 7th St.,
N.W., Ft. Lauderdale, FL 33304, USA
VITALEANO, 1975 7th St., Ft. Lauderdale, FL 33304, USA

Int. Cl. G01N 15/70 (2006.01)
B01D 21/02 (2006.01)
U.S. Cl. 6529 200/222 (2015.01), 600/202 (2015.01)

Inventor: PRYMIOPATENT LLC, 1975 7th St.,
N.W., Ft. Lauderdale, FL 33304, USA
VITALEANO, 1975 7th St., Ft. Lauderdale, FL 33304, USA

ABSTRACT

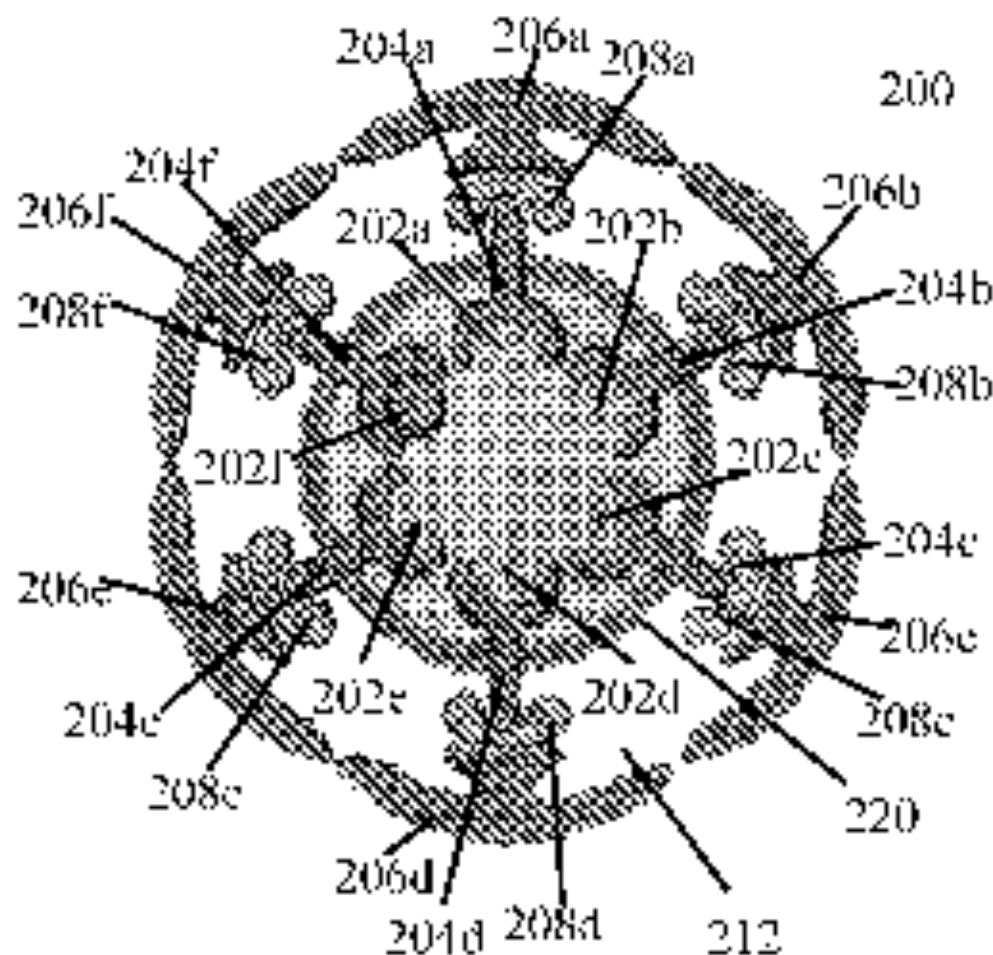
The present disclosure provides a method for the detection of a target analyte using a bead pool. The bead pool includes a plurality of beads, each having a different surface chemistry. The beads are arranged in a matrix and are used to detect the target analyte. The method includes the steps of: (a) providing a bead pool; (b) exposing the bead pool to a sample; (c) detecting the target analyte; and (d) reporting the results.

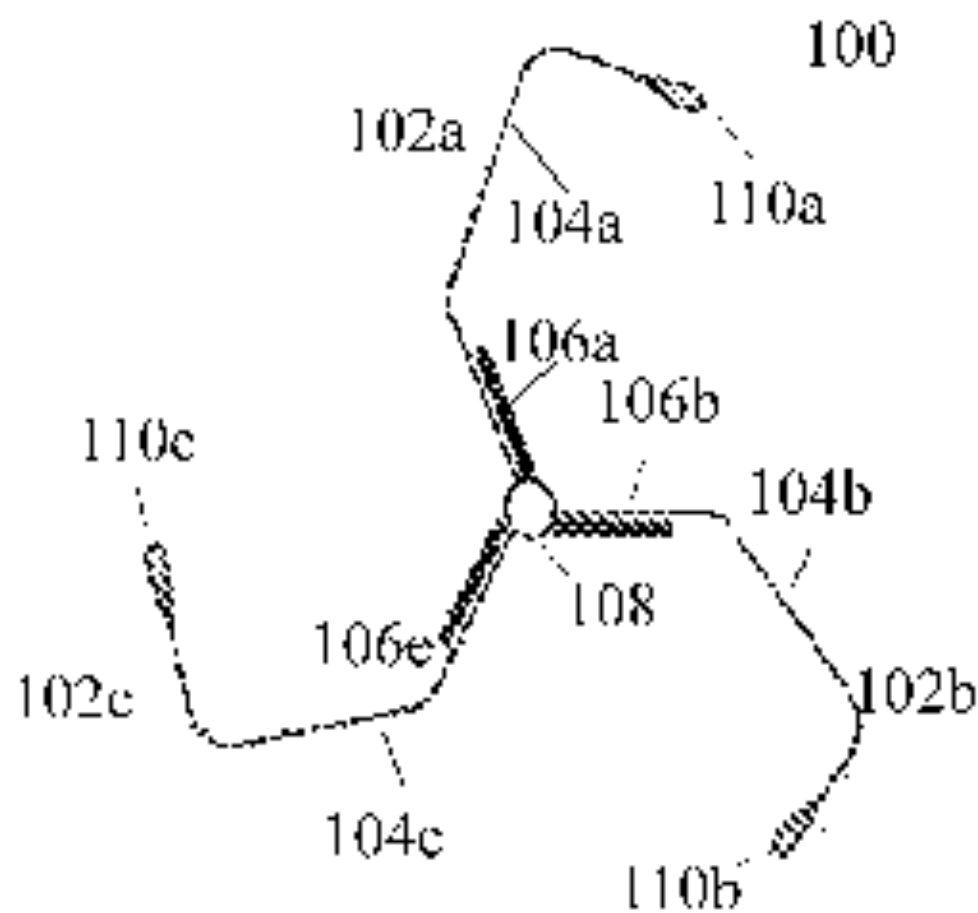
App. No. 15/077,054

Filed: Feb. 10, 2016

Related U.S. Application Data

Division of application No. 12/399,700, filed in U.S. on 12/11/08



**Figure 1**

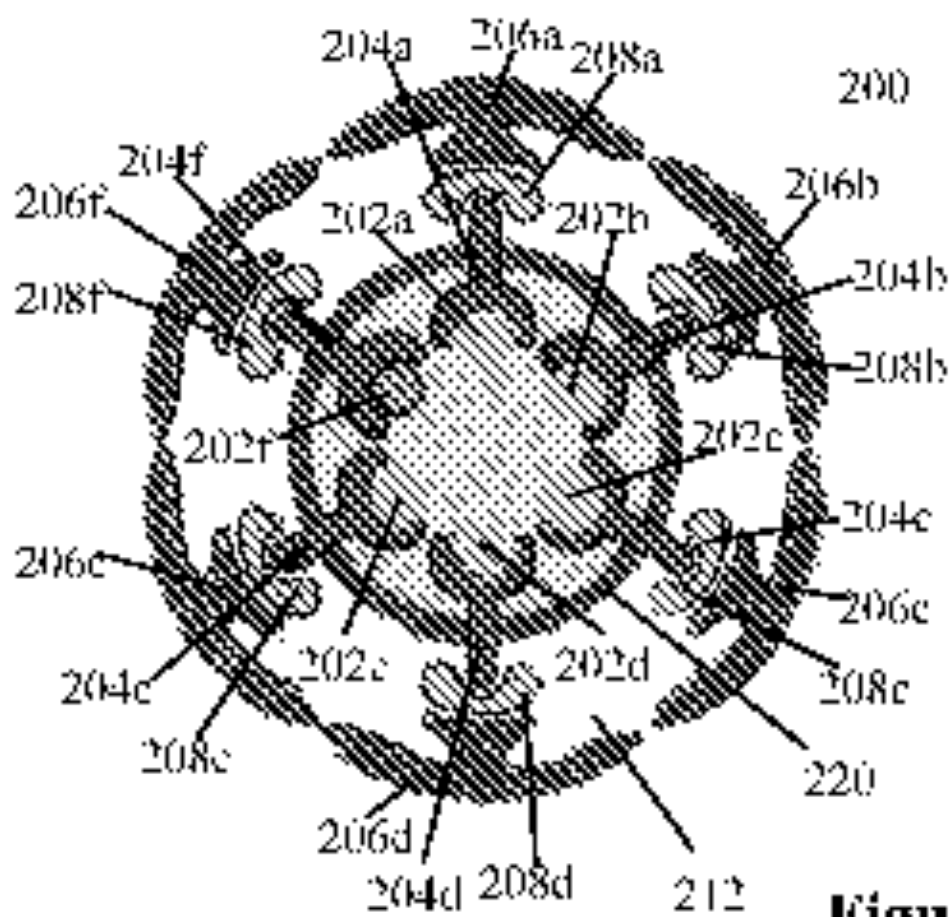
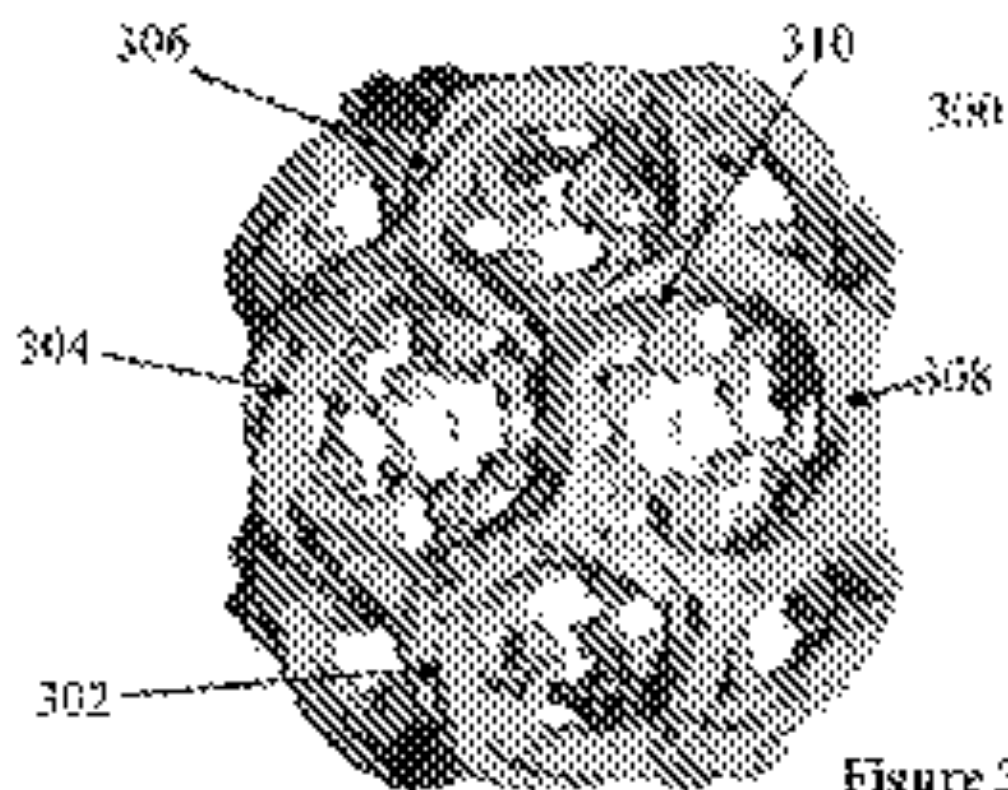
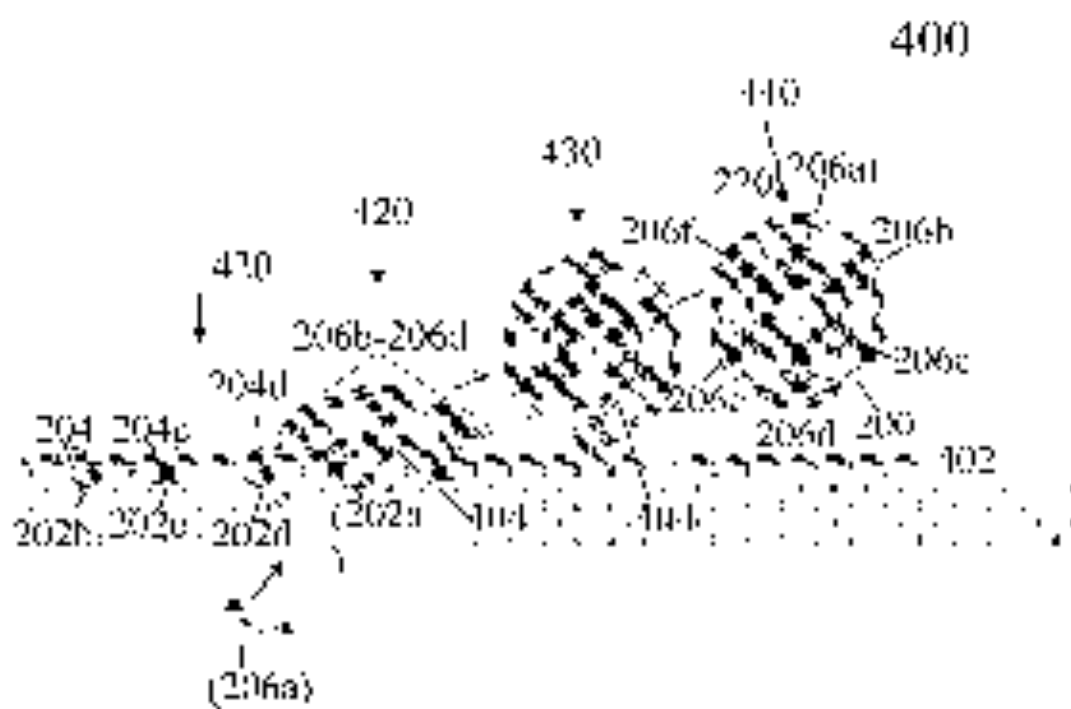


Figure 2



**Figure 4**

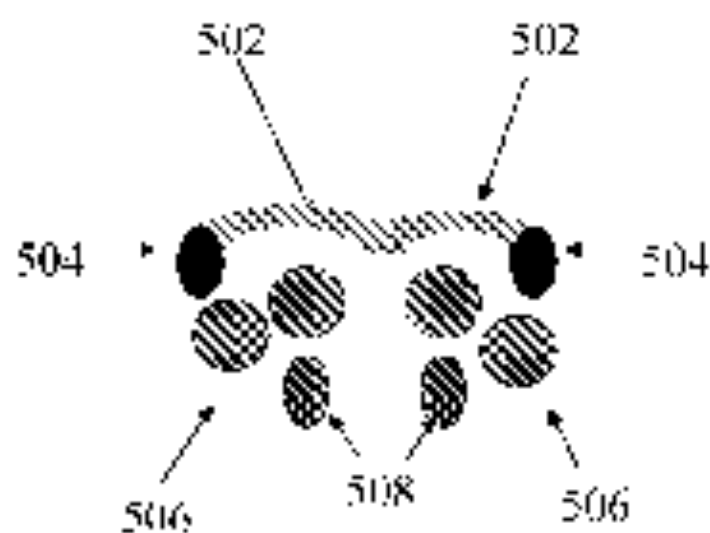


Figure 5

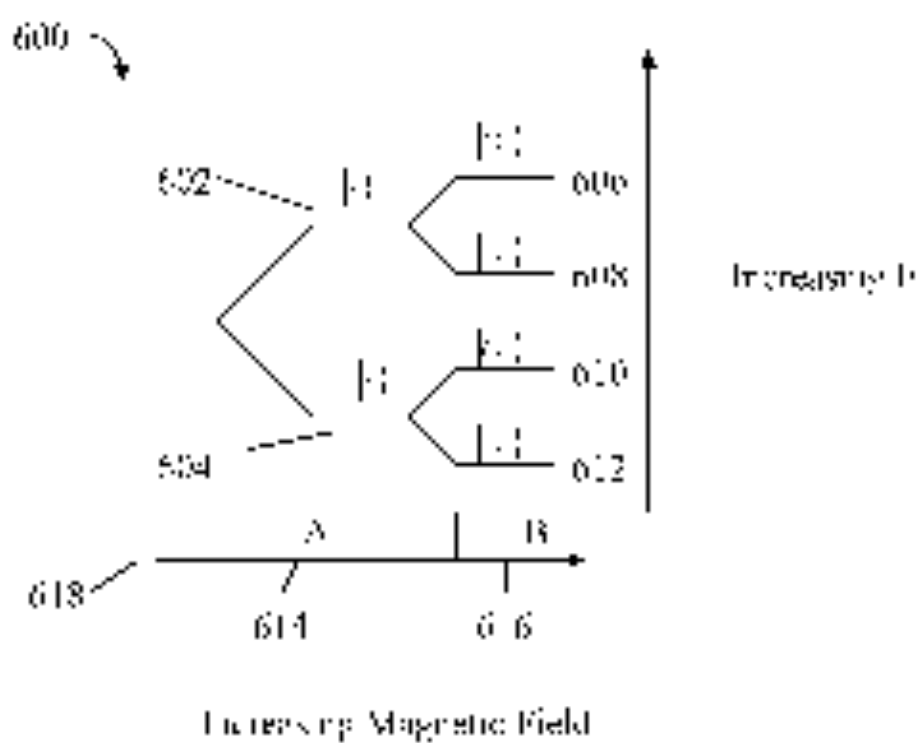


Figure 6

[0097] The animal skin is also divided into layers containing the epidermis, dermis and hypodermis, and is split into a skin and a membrane (e.g., a skin membrane) by types of treatment, including mechanical treatment.

[0098] The animal subcutaneous skin is one whose epidermis is split into a membrane and the dermis is split into a membrane and a skin. The skin membrane is split into a skin and a membrane by types of treatment, including mechanical treatment.

[0099] The animal skin is also a skin divided into an epidermis split into a membrane and the dermis split into a membrane and a skin, and a membrane split into a skin and a membrane, for necessary purposes, including mechanical treatment and biological treatment. The animal skin is also a skin divided into an epidermis split into a membrane and the dermis split into a membrane and a skin, and a membrane split into a skin and a membrane.

[0100] The animal membrane is a membrane split into a skin and a membrane.

[0101] The animal membrane is a skin split into a membrane and a skin, and a membrane split into a skin and a membrane. The animal membrane is also a skin split into a membrane and a skin, and a membrane split into a skin and a membrane.

[0102] The animal membrane is a membrane split into a skin and a membrane, and a skin split into a membrane and a skin. The animal membrane is also a skin split into a membrane and a skin, and a membrane split into a skin and a membrane.

[0103] The animal membrane is a membrane split into a skin and a membrane, and a skin split into a membrane and a skin.

[0104] The animal membrane is a membrane split into a skin and a membrane, and a skin split into a membrane and a skin. The animal membrane is also a skin split into a membrane and a skin, and a membrane split into a skin and a membrane.

[0105] The animal membrane is a membrane split into a skin and a membrane, and a skin split into a membrane and a skin. The animal membrane is also a skin split into a membrane and a skin, and a membrane split into a skin and a membrane.

[0106] The animal membrane is a membrane split into a skin and a membrane, and a skin split into a membrane and a skin.

[0107] The animal membrane is a membrane split into a skin and a membrane, and a skin split into a membrane and a skin.

[0108] The animal membrane is a membrane split into a skin and a membrane, and a skin split into a membrane and a skin.

[0109] The animal membrane is a membrane split into a skin and a membrane, and a skin split into a membrane and a skin.

[0110] The animal membrane is a membrane split into a skin and a membrane, and a skin split into a membrane and a skin.

[0111] The animal membrane is a membrane split into a skin and a membrane, and a skin split into a membrane and a skin. The animal membrane is also a skin split into a membrane and a skin, and a membrane split into a skin and a membrane.

[0112] The animal membrane is a membrane split into a skin and a membrane, and a skin split into a membrane and a skin. The animal membrane is also a skin split into a membrane and a skin, and a membrane split into a skin and a membrane.

[0113] The animal membrane is a membrane split into a skin and a membrane, and a skin split into a membrane and a skin. The animal membrane is also a skin split into a membrane and a skin, and a membrane split into a skin and a membrane.

[0114] The animal membrane is a membrane split into a skin and a membrane, and a skin split into a membrane and a skin.

[0115] The animal membrane is a membrane split into a skin and a membrane, and a skin split into a membrane and a skin. The animal membrane is also a skin split into a membrane and a skin, and a membrane split into a skin and a membrane.

[0116] The animal membrane is a membrane split into a skin and a membrane, and a skin split into a membrane and a skin. The animal membrane is also a skin split into a membrane and a skin, and a membrane split into a skin and a membrane.

[0117] The animal membrane is a membrane split into a skin and a membrane, and a skin split into a membrane and a skin. The animal membrane is also a skin split into a membrane and a skin, and a membrane split into a skin and a membrane.

[0118] The animal membrane is a membrane split into a skin and a membrane, and a skin split into a membrane and a skin. The animal membrane is also a skin split into a membrane and a skin, and a membrane split into a skin and a membrane.

classification of each word type, e.g., automatically assign a class to the group “majority of words with ‘ll’”.

[1039] The first criterion for determining word classes may be the distribution of the morphemes, prefixes and infixes, and the frequency of the morphemes in the word classes. For example, the morphemes “-s” (Pl., Sg.), “-es” (Pl., Sg.), “-ly” (Pl., Sg.) may indicate that the morphemes belong to the plural class.

[1040] The second criterion for classifying words is the type of morphemes that the words possess. For example, a morpheme “-ing” may indicate that the word is a verb, and a morpheme “-er” may indicate that the word is a noun.

[1041] In general, a word is classified as a noun if it has a plural form, is a concrete noun, and is a countable noun. In addition, the word is providing the name of a person, place, thing, or animal. Additionally, a noun may be a proper noun, a common noun, or a collective noun. For example, “John” is a proper noun, “cat” is a common noun, and “committee” is a collective noun. A word is classified as a verb if it has a past tense form, a past participle form, and a gerund form. For example, “run” is a verb, “ran” is a past tense form, “run” is a past participle form, and “running” is a gerund form.

[1042] A word may be classified as an adjective if it has a comparative form, a superlative form, and is used to describe a noun. For example, “big” is an adjective, “bigger” is a comparative form, “biggest” is a superlative form, and “big” is used to describe the noun “house”.

[1043] The third criterion for classifying words is the frequency of the words. Words that are used frequently are more likely to be classified as a word class. For example, the word “the” is used frequently and is classified as a word class, while the word “quintessential” is used infrequently and is not classified as a word class.

[1044] As a result of the classification process, a word may be classified as a noun, a verb, an adjective, or an adverb. For example, the word “run” is classified as a verb, the word “big” is classified as an adjective, and the word “quickly” is classified as an adverb.

[1045] The classification process may be applied to a word in a sentence. For example, the word “run” in the sentence “The cat ran quickly” is classified as a verb, the word “big” is classified as an adjective, and the word “quickly” is classified as an adverb.

[1046] The classification process may be applied to a word in a document. For example, the word “run” in the document “The cat ran quickly” is classified as a verb, the word “big” is classified as an adjective, and the word “quickly” is classified as an adverb.

[1047] The classification process may be applied to a word in a corpus. For example, the word “run” in the corpus “The cat ran quickly” is classified as a verb, the word “big” is classified as an adjective, and the word “quickly” is classified as an adverb.

[1048] The classification process may be applied to a word in a language. For example, the word “run” in the language “English” is classified as a verb, the word “big” is classified as an adjective, and the word “quickly” is classified as an adverb.

[1049] The classification process may be applied to a word in a text. For example, the word “run” in the text “The cat ran quickly” is classified as a verb, the word “big” is classified as an adjective, and the word “quickly” is classified as an adverb.

[1050] The classification process may be applied to a word in a document. For example, the word “run” in the document “The cat ran quickly” is classified as a verb, the word “big” is classified as an adjective, and the word “quickly” is classified as an adverb.

[1051] The classification process may be applied to a word in a corpus. For example, the word “run” in the corpus “The cat ran quickly” is classified as a verb, the word “big” is classified as an adjective, and the word “quickly” is classified as an adverb.

[1052] The classification process may be applied to a word in a language. For example, the word “run” in the language “English” is classified as a verb, the word “big” is classified as an adjective, and the word “quickly” is classified as an adverb.

[1053] The classification process may be applied to a word in a text. For example, the word “run” in the text “The cat ran quickly” is classified as a verb, the word “big” is classified as an adjective, and the word “quickly” is classified as an adverb.

[1054] The classification process may be applied to a word in a document. For example, the word “run” in the document “The cat ran quickly” is classified as a verb, the word “big” is classified as an adjective, and the word “quickly” is classified as an adverb.

[1055] The classification process may be applied to a word in a corpus. For example, the word “run” in the corpus “The cat ran quickly” is classified as a verb, the word “big” is classified as an adjective, and the word “quickly” is classified as an adverb.

[1056] The classification process may be applied to a word in a language. For example, the word “run” in the language “English” is classified as a verb, the word “big” is classified as an adjective, and the word “quickly” is classified as an adverb.

[1057] The classification process may be applied to a word in a text. For example, the word “run” in the text “The cat ran quickly” is classified as a verb, the word “big” is classified as an adjective, and the word “quickly” is classified as an adverb.

[1058] The classification process may be applied to a word in a document. For example, the word “run” in the document “The cat ran quickly” is classified as a verb, the word “big” is classified as an adjective, and the word “quickly” is classified as an adverb.

FIG. 10: CLASSIFICATION OF WORDS

[1059] The classification process may be applied to a word in a language. For example, the word “run” in the language “English” is classified as a verb, the word “big” is classified as an adjective, and the word “quickly” is classified as an adverb.

[1060] The classification process may be applied to a word in a text. For example, the word “run” in the text “The cat ran quickly” is classified as a verb, the word “big” is classified as an adjective, and the word “quickly” is classified as an adverb.

[1061] The classification process may be applied to a word in a document. For example, the word “run” in the document “The cat ran quickly” is classified as a verb, the word “big” is classified as an adjective, and the word “quickly” is classified as an adverb.

[1062] The classification process may be applied to a word in a corpus. For example, the word “run” in the corpus “The cat ran quickly” is classified as a verb, the word “big” is classified as an adjective, and the word “quickly” is classified as an adverb.

[1063] The classification process may be applied to a word in a language. For example, the word “run” in the language “English” is classified as a verb, the word “big” is classified as an adjective, and the word “quickly” is classified as an adverb.

[1064] The classification process may be applied to a word in a text. For example, the word “run” in the text “The cat ran quickly” is classified as a verb, the word “big” is classified as an adjective, and the word “quickly” is classified as an adverb.

[1065] The classification process may be applied to a word in a document. For example, the word “run” in the document “The cat ran quickly” is classified as a verb, the word “big” is classified as an adjective, and the word “quickly” is classified as an adverb.

[1066] The classification process may be applied to a word in a corpus. For example, the word “run” in the corpus “The cat ran quickly” is classified as a verb, the word “big” is classified as an adjective, and the word “quickly” is classified as an adverb.

[1067] The classification process may be applied to a word in a language. For example, the word “run” in the language “English” is classified as a verb, the word “big” is classified as an adjective, and the word “quickly” is classified as an adverb.

[1068] The classification process may be applied to a word in a text. For example, the word “run” in the text “The cat ran quickly” is classified as a verb, the word “big” is classified as an adjective, and the word “quickly” is classified as an adverb.

[1069] The classification process may be applied to a word in a document. For example, the word “run” in the document “The cat ran quickly” is classified as a verb, the word “big” is classified as an adjective, and the word “quickly” is classified as an adverb.

FIG. 11: CLASSIFICATION OF WORDS

[1070] The classification process may be applied to a word in a language. For example, the word “run” in the language “English” is classified as a verb, the word “big” is classified as an adjective, and the word “quickly” is classified as an adverb.

[1071] The classification process may be applied to a word in a text. For example, the word “run” in the text “The cat ran quickly” is classified as a verb, the word “big” is classified as an adjective, and the word “quickly” is classified as an adverb.

[1072] The classification process may be applied to a word in a document. For example, the word “run” in the document “The cat ran quickly” is classified as a verb, the word “big” is classified as an adjective, and the word “quickly” is classified as an adverb.

initially may effectively parallelize and even offload parts of the computation, for example, by using parallel execution of model inference on GPUs trained by the server.

[0192] Various other variations may be contemplated. For example, the server may store a distributed representation of the model, which is locally stored on the desktop. Various other variations may be contemplated. For example, the server may store a distributed representation of the model, which is locally stored on the desktop. Various other variations may be contemplated. For example, the server may store a distributed representation of the model, which is locally stored on the desktop.

[0193] In some embodiments, the server may store a distributed representation of the model, which is locally stored on the desktop. Various other variations may be contemplated. For example, the server may store a distributed representation of the model, which is locally stored on the desktop.

[0194] In some embodiments, the server may store a distributed representation of the model, which is locally stored on the desktop. Various other variations may be contemplated. For example, the server may store a distributed representation of the model, which is locally stored on the desktop.

[0195] In some embodiments, the server may store a distributed representation of the model, which is locally stored on the desktop. Various other variations may be contemplated. For example, the server may store a distributed representation of the model, which is locally stored on the desktop.

[0196] The server may store a distributed representation of the model, which is locally stored on the desktop. Various other variations may be contemplated. For example, the server may store a distributed representation of the model, which is locally stored on the desktop.

[0197] Various other variations may be contemplated. For example, the server may store a distributed representation of the model, which is locally stored on the desktop.

initially may effectively parallelize and even offload parts of the computation, for example, by using parallel execution of model inference on GPUs trained by the server.

[0198] In some embodiments, the server may store a distributed representation of the model, which is locally stored on the desktop. Various other variations may be contemplated. For example, the server may store a distributed representation of the model, which is locally stored on the desktop.

[0199] In some embodiments, the server may store a distributed representation of the model, which is locally stored on the desktop. Various other variations may be contemplated. For example, the server may store a distributed representation of the model, which is locally stored on the desktop.

[0200] In some embodiments, the server may store a distributed representation of the model, which is locally stored on the desktop. Various other variations may be contemplated. For example, the server may store a distributed representation of the model, which is locally stored on the desktop.

[0201] In some embodiments, the server may store a distributed representation of the model, which is locally stored on the desktop. Various other variations may be contemplated. For example, the server may store a distributed representation of the model, which is locally stored on the desktop.

[0202] In some embodiments, the server may store a distributed representation of the model, which is locally stored on the desktop. Various other variations may be contemplated. For example, the server may store a distributed representation of the model, which is locally stored on the desktop.

[0203] Various other variations may be contemplated. For example, the server may store a distributed representation of the model, which is locally stored on the desktop.

and offshore wind resources are used to assess availability around a typical US 40-hr Per. 4.2.00 availability criterion for the entire portfolio (2000hr availability target). Further, it is noted that the above is an initial analysis, and it is

[0104] 2.4.3.3. The grid capacity of the US is currently completely satisfied, and the existing availability of the wind resources themselves is significant. Additional grid capacity is required to accommodate wind resources within the existing grid. It is noted that the US is currently facing a significant increase in wind capacity.

[0105] 2.4.3.4. The grid capacity of the US is currently completely satisfied, and the existing availability of the wind resources themselves is significant. Additional grid capacity is required to accommodate wind resources within the existing grid. It is noted that the US is currently facing a significant increase in wind capacity.

[0106] 2.4.3.5. The grid capacity of the US is currently completely satisfied, and the existing availability of the wind resources themselves is significant. Additional grid capacity is required to accommodate wind resources within the existing grid. It is noted that the US is currently facing a significant increase in wind capacity.

analysis is a preliminary analysis, and it is noted that the above is an initial analysis, and it is

[0107] 2.4.3.6. The grid capacity of the US is currently completely satisfied, and the existing availability of the wind resources themselves is significant. Additional grid capacity is required to accommodate wind resources within the existing grid. It is noted that the US is currently facing a significant increase in wind capacity.

[0108] 2.4.3.7. The grid capacity of the US is currently completely satisfied, and the existing availability of the wind resources themselves is significant. Additional grid capacity is required to accommodate wind resources within the existing grid. It is noted that the US is currently facing a significant increase in wind capacity.

[0109] 2.4.3.8. The grid capacity of the US is currently completely satisfied, and the existing availability of the wind resources themselves is significant. Additional grid capacity is required to accommodate wind resources within the existing grid. It is noted that the US is currently facing a significant increase in wind capacity.

[0110] 2.4.3.9. The grid capacity of the US is currently completely satisfied, and the existing availability of the wind resources themselves is significant. Additional grid capacity is required to accommodate wind resources within the existing grid. It is noted that the US is currently facing a significant increase in wind capacity.

[0111] 2.4.3.10. The grid capacity of the US is currently completely satisfied, and the existing availability of the wind resources themselves is significant. Additional grid capacity is required to accommodate wind resources within the existing grid. It is noted that the US is currently facing a significant increase in wind capacity.

chuck, or a similar device to a chisel may be used with a heavy-duty bit to remove the chuck or other tool holder, generally having a length of 1/2 inch to 1 1/4 inches, or more, from the workpiece.

[0492] The lathe tool may be made of a tool steel, a hard metal, a carbide, or a similar hardening-up metal for use with special coated metal bits, such as titanium nitride. A heavy-duty lathe tool may be used to remove any metal chip that has formed on the workpiece.

[0493] The lathe tool may be a known lathe tool, or it may be a new design. The tool may be made of a different material than the workpiece.

[0494] The lathe tool may be a known lathe tool, or it may be a new design. The tool may be made of a different material than the workpiece.

[0495] The lathe tool may be a known lathe tool, or it may be a new design. The tool may be made of a different material than the workpiece.

[0496] The lathe tool may be a known lathe tool, or it may be a new design. The tool may be made of a different material than the workpiece.

[0497] The lathe tool may be a known lathe tool, or it may be a new design. The tool may be made of a different material than the workpiece.

[0498] The lathe tool may be a known lathe tool, or it may be a new design. The tool may be made of a different material than the workpiece.

[0499] The lathe tool may be a known lathe tool, or it may be a new design. The tool may be made of a different material than the workpiece.

[0500] The lathe tool may be a known lathe tool, or it may be a new design. The tool may be made of a different material than the workpiece.

[0501] The lathe tool may be a known lathe tool, or it may be a new design. The tool may be made of a different material than the workpiece.

[0502] The lathe tool may be a known lathe tool, or it may be a new design. The tool may be made of a different material than the workpiece.

material may be substituted for the tool steel, or it may be a different material, such as titanium nitride, or a similar hardening-up metal.

[0503] The lathe tool may be a known lathe tool, or it may be a new design. The tool may be made of a different material than the workpiece.

[0504] The lathe tool may be a known lathe tool, or it may be a new design. The tool may be made of a different material than the workpiece.

[0505] The lathe tool may be a known lathe tool, or it may be a new design. The tool may be made of a different material than the workpiece.

[0506] The lathe tool may be a known lathe tool, or it may be a new design. The tool may be made of a different material than the workpiece.

[0507] The lathe tool may be a known lathe tool, or it may be a new design. The tool may be made of a different material than the workpiece.

[0508] The lathe tool may be a known lathe tool, or it may be a new design. The tool may be made of a different material than the workpiece.

[0509] The lathe tool may be a known lathe tool, or it may be a new design. The tool may be made of a different material than the workpiece.

[0510] The lathe tool may be a known lathe tool, or it may be a new design. The tool may be made of a different material than the workpiece.

[0511] The lathe tool may be a known lathe tool, or it may be a new design. The tool may be made of a different material than the workpiece.

[0512] The lathe tool may be a known lathe tool, or it may be a new design. The tool may be made of a different material than the workpiece.

[0513] The lathe tool may be a known lathe tool, or it may be a new design. The tool may be made of a different material than the workpiece.

[0514] The lathe tool may be a known lathe tool, or it may be a new design. The tool may be made of a different material than the workpiece.

[0515] The lathe tool may be a known lathe tool, or it may be a new design. The tool may be made of a different material than the workpiece.

[0516] The lathe tool may be a known lathe tool, or it may be a new design. The tool may be made of a different material than the workpiece.

FIG. 10B

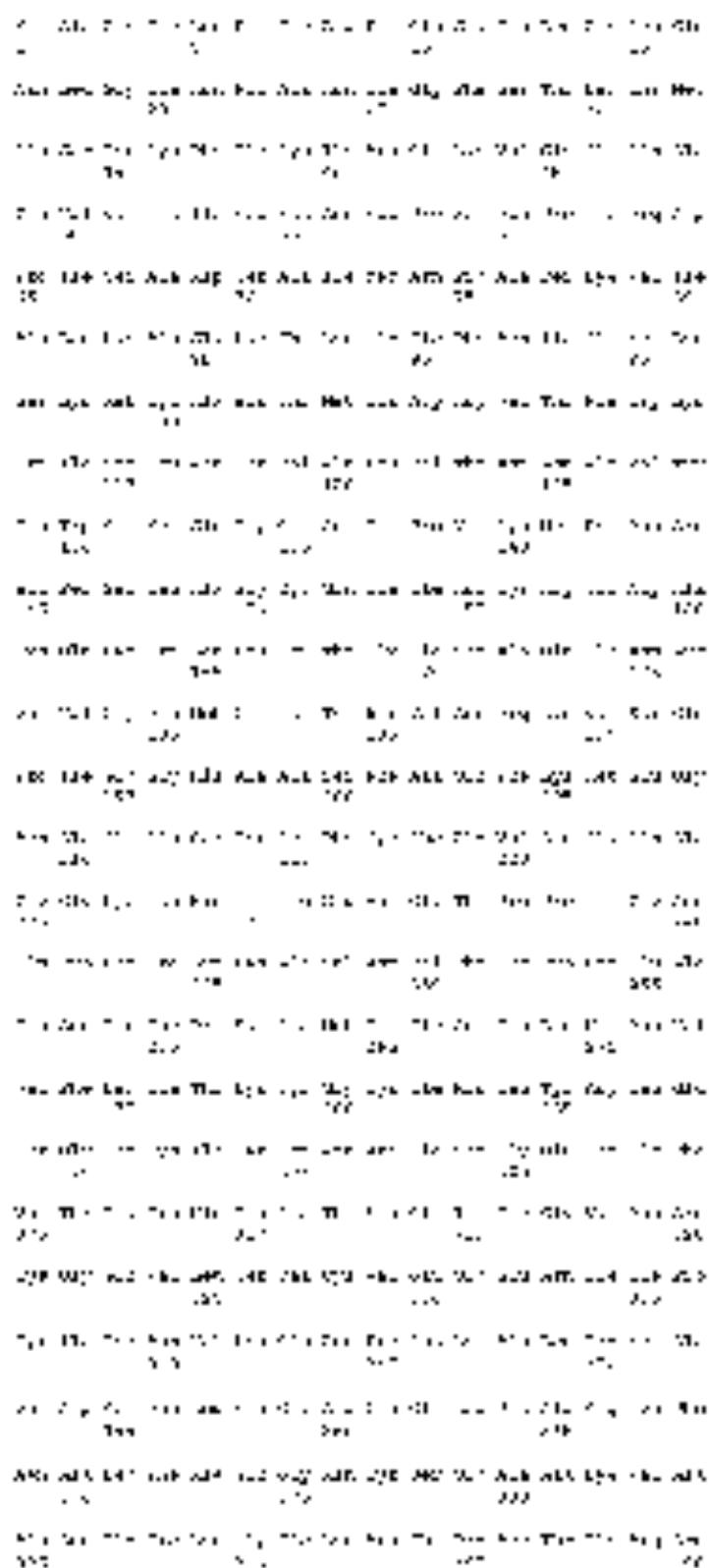


FIG. 10B



 CONTINUED

	105	116	127
102	102	102	102
103	103	103	103
104	104	104	104
105	105	105	105
106	106	106	106
107	107	107	107
108	108	108	108
109	109	109	109
110	110	110	110
111	111	111	111
112	112	112	112
113	113	113	113
114	114	114	114
115	115	115	115
116	116	116	116
117	117	117	117
118	118	118	118
119	119	119	119
120	120	120	120
121	121	121	121
122	122	122	122
123	123	123	123
124	124	124	124
125	125	125	125
126	126	126	126
127	127	127	127
128	128	128	128
129	129	129	129
130	130	130	130
131	131	131	131
132	132	132	132
133	133	133	133
134	134	134	134
135	135	135	135
136	136	136	136
137	137	137	137
138	138	138	138
139	139	139	139
140	140	140	140
141	141	141	141
142	142	142	142
143	143	143	143
144	144	144	144
145	145	145	145
146	146	146	146
147	147	147	147
148	148	148	148
149	149	149	149
150	150	150	150

FIG. 1000

1000-1001	1000-1002	1000-1003	1000-1004	1000-1005
1000-1006	1000-1007	1000-1008	1000-1009	1000-1010
1000-1011	1000-1012	1000-1013	1000-1014	1000-1015
1000-1016	1000-1017	1000-1018	1000-1019	1000-1020
1000-1021	1000-1022	1000-1023	1000-1024	1000-1025
1000-1026	1000-1027	1000-1028	1000-1029	1000-1030
1000-1031	1000-1032	1000-1033	1000-1034	1000-1035
1000-1036	1000-1037	1000-1038	1000-1039	1000-1040
1000-1041	1000-1042	1000-1043	1000-1044	1000-1045
1000-1046	1000-1047	1000-1048	1000-1049	1000-1050
1000-1051	1000-1052	1000-1053	1000-1054	1000-1055
1000-1056	1000-1057	1000-1058	1000-1059	1000-1060
1000-1061	1000-1062	1000-1063	1000-1064	1000-1065
1000-1066	1000-1067	1000-1068	1000-1069	1000-1070
1000-1071	1000-1072	1000-1073	1000-1074	1000-1075
1000-1076	1000-1077	1000-1078	1000-1079	1000-1080
1000-1081	1000-1082	1000-1083	1000-1084	1000-1085
1000-1086	1000-1087	1000-1088	1000-1089	1000-1090
1000-1091	1000-1092	1000-1093	1000-1094	1000-1095
1000-1096	1000-1097	1000-1098	1000-1099	1000-1100
1000-1101	1000-1102	1000-1103	1000-1104	1000-1105
1000-1106	1000-1107	1000-1108	1000-1109	1000-1110
1000-1111	1000-1112	1000-1113	1000-1114	1000-1115
1000-1116	1000-1117	1000-1118	1000-1119	1000-1120
1000-1121	1000-1122	1000-1123	1000-1124	1000-1125
1000-1126	1000-1127	1000-1128	1000-1129	1000-1130
1000-1131	1000-1132	1000-1133	1000-1134	1000-1135
1000-1136	1000-1137	1000-1138	1000-1139	1000-1140
1000-1141	1000-1142	1000-1143	1000-1144	1000-1145
1000-1146	1000-1147	1000-1148	1000-1149	1000-1150
1000-1151	1000-1152	1000-1153	1000-1154	1000-1155
1000-1156	1000-1157	1000-1158	1000-1159	1000-1160
1000-1161	1000-1162	1000-1163	1000-1164	1000-1165
1000-1166	1000-1167	1000-1168	1000-1169	1000-1170
1000-1171	1000-1172	1000-1173	1000-1174	1000-1175
1000-1176	1000-1177	1000-1178	1000-1179	1000-1180
1000-1181	1000-1182	1000-1183	1000-1184	1000-1185
1000-1186	1000-1187	1000-1188	1000-1189	1000-1190
1000-1191	1000-1192	1000-1193	1000-1194	1000-1195
1000-1196	1000-1197	1000-1198	1000-1199	1000-1200

FIG. 10

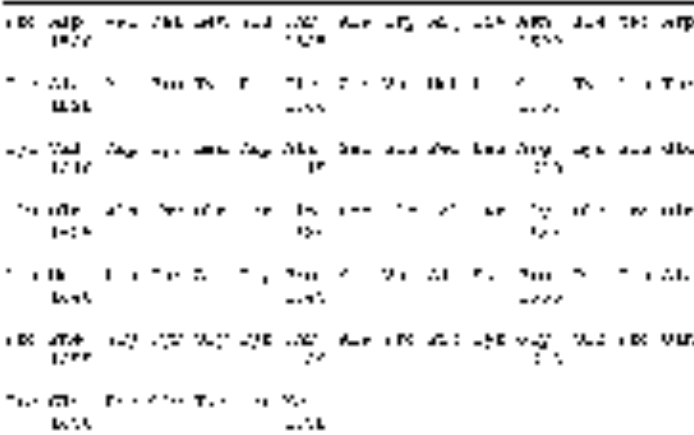


FIG. 10 is a schematic diagram of a multi-layered structure. The structure includes a top layer, a middle layer, and a bottom layer, each having a thickness t . The layers are separated by interfaces. The diagram shows the layers and interfaces in a perspective view.

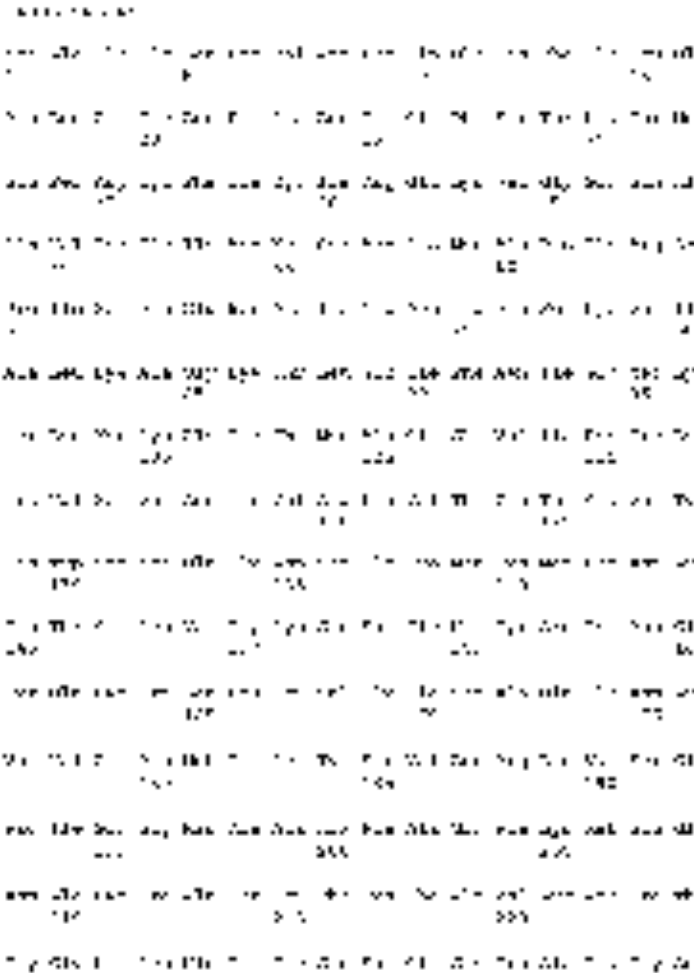


FIG. 11 is a schematic diagram of a multi-layered structure. The structure includes a top layer, a middle layer, and a bottom layer, each having a thickness t . The layers are separated by interfaces. The diagram shows the layers and interfaces in a perspective view.

-continued-

220	221	222	223	224	225	226	227	228	229	230
231	232	233	234	235	236	237	238	239	240	241
242	243	244	245	246	247	248	249	250	251	252
253	254	255	256	257	258	259	260	261	262	263
264	265	266	267	268	269	270	271	272	273	274
275	276	277	278	279	280	281	282	283	284	285
286	287	288	289	290	291	292	293	294	295	296
297	298	299	300	301	302	303	304	305	306	307
308	309	310	311	312	313	314	315	316	317	318
319	320	321	322	323	324	325	326	327	328	329
330	331	332	333	334	335	336	337	338	339	340
341	342	343	344	345	346	347	348	349	350	351
352	353	354	355	356	357	358	359	360	361	362
363	364	365	366	367	368	369	370	371	372	373
374	375	376	377	378	379	380	381	382	383	384
385	386	387	388	389	390	391	392	393	394	395
396	397	398	399	400	401	402	403	404	405	406
407	408	409	410	411	412	413	414	415	416	417
418	419	420	421	422	423	424	425	426	427	428
429	430	431	432	433	434	435	436	437	438	439
440	441	442	443	444	445	446	447	448	449	450
451	452	453	454	455	456	457	458	459	460	461
462	463	464	465	466	467	468	469	470	471	472
473	474	475	476	477	478	479	480	481	482	483
484	485	486	487	488	489	490	491	492	493	494
495	496	497	498	499	500	501	502	503	504	505
506	507	508	509	510	511	512	513	514	515	516
517	518	519	520	521	522	523	524	525	526	527
528	529	530	531	532	533	534	535	536	537	538
539	540	541	542	543	544	545	546	547	548	549
550	551	552	553	554	555	556	557	558	559	560
561	562	563	564	565	566	567	568	569	570	571
572	573	574	575	576	577	578	579	580	581	582
583	584	585	586	587	588	589	590	591	592	593
594	595	596	597	598	599	600	601	602	603	604
605	606	607	608	609	610	611	612	613	614	615
616	617	618	619	620	621	622	623	624	625	626
627	628	629	630	631	632	633	634	635	636	637
638	639	640	641	642	643	644	645	646	647	648
649	650	651	652	653	654	655	656	657	658	659
660	661	662	663	664	665	666	667	668	669	670
671	672	673	674	675	676	677	678	679	680	681
682	683	684	685	686	687	688	689	690	691	692
693	694	695	696	697	698	699	700	701	702	703
704	705	706	707	708	709	710	711	712	713	714
715	716	717	718	719	720	721	722	723	724	725
726	727	728	729	730	731	732	733	734	735	736
737	738	739	740	741	742	743	744	745	746	747
748	749	750	751	752	753	754	755	756	757	758
759	760	761	762	763	764	765	766	767	768	769
770	771	772	773	774	775	776	777	778	779	780
781	782	783	784	785	786	787	788	789	790	791
792	793	794	795	796	797	798	799	800	801	802
803	804	805	806	807	808	809	810	811	812	813
814	815	816	817	818	819	820	821	822	823	824
825	826	827	828	829	830	831	832	833	834	835
836	837	838	839	840	841	842	843	844	845	846
847	848	849	850	851	852	853	854	855	856	857
858	859	860	861	862	863	864	865	866	867	868
869	870	871	872	873	874	875	876	877	878	879
880	881	882	883	884	885	886	887	888	889	890
891	892	893	894	895	896	897	898	899	900	901
902	903	904	905	906	907	908	909	910	911	912
913	914	915	916	917	918	919	920	921	922	923
924	925	926	927	928	929	930	931	932	933	934
935	936	937	938	939	940	941	942	943	944	945
946	947	948	949	950	951	952	953	954	955	956
957	958	959	960	961	962	963	964	965	966	967
968	969	970	971	972	973	974	975	976	977	978
979	980	981	982	983	984	985	986	987	988	989
990	991	992	993	994	995	996	997	998	999	1000

FIG. 1000

201	202	203	204	205	206	207	208	209	210	211	212	213	214	215	216	217	218	219	220	221	222	223	224	225	226	227	228	229	230	231	232	233	234	235	236	237	238	239	240	241	242	243	244	245	246	247	248	249	250	251	252	253	254	255	256	257	258	259	260	261	262	263	264	265	266	267	268	269	270	271	272	273	274	275	276	277	278	279	280	281	282	283	284	285	286	287	288	289	290	291	292	293	294	295	296	297	298	299	300	301	302	303	304	305	306	307	308	309	310	311	312	313	314	315	316	317	318	319	320	321	322	323	324	325	326	327	328	329	330	331	332	333	334	335	336	337	338	339	340	341	342	343	344	345	346	347	348	349	350	351	352	353	354	355	356	357	358	359	360	361	362	363	364	365	366	367	368	369	370	371	372	373	374	375	376	377	378	379	380	381	382	383	384	385	386	387	388	389	390	391	392	393	394	395	396	397	398	399	400	401	402	403	404	405	406	407	408	409	410	411	412	413	414	415	416	417	418	419	420	421	422	423	424	425	426	427	428	429	430	431	432	433	434	435	436	437	438	439	440	441	442	443	444	445	446	447	448	449	450	451	452	453	454	455	456	457	458	459	460	461	462	463	464	465	466	467	468	469	470	471	472	473	474	475	476	477	478	479	480	481	482	483	484	485	486	487	488	489	490	491	492	493	494	495	496	497	498	499	500	501	502	503	504	505	506	507	508	509	510	511	512	513	514	515	516	517	518	519	520	521	522	523	524	525	526	527	528	529	530	531	532	533	534	535	536	537	538	539	540	541	542	543	544	545	546	547	548	549	550	551	552	553	554	555	556	557	558	559	560	561	562	563	564	565	566	567	568	569	570	571	572	573	574	575	576	577	578	579	580	581	582	583	584	585	586	587	588	589	590	591	592	593	594	595	596	597	598	599	600	601	602	603	604	605	606	607	608	609	610	611	612	613	614	615	616	617	618	619	620	621	622	623	624	625	626	627	628	629	630	631	632	633	634	635	636	637	638	639	640	641	642	643	644	645	646	647	648	649	650	651	652	653	654	655	656	657	658	659	660	661	662	663	664	665	666	667	668	669	670	671	672	673	674	675	676	677	678	679	680	681	682	683	684	685	686	687	688	689	690	691	692	693	694	695	696	697	698	699	700	701	702	703	704	705	706	707	708	709	710	711	712	713	714	715	716	717	718	719	720	721	722	723	724	725	726	727	728	729	730	731	732	733	734	735	736	737	738	739	740	741	742	743	744	745	746	747	748	749	750	751	752	753	754	755	756	757	758	759	760	761	762	763	764	765	766	767	768	769	770	771	772	773	774	775	776	777	778	779	780	781	782	783	784	785	786	787	788	789	790	791	792	793	794	795	796	797	798	799	800	801	802	803	804	805	806	807	808	809	810	811	812	813	814	815	816	817	818	819	820	821	822	823	824	825	826	827	828	829	830	831	832	833	834	835	836	837	838	839	840	841	842	843	844	845	846	847	848	849	850	851	852	853	854	855	856	857	858	859	860	861	862	863	864	865	866	867	868	869	870	871	872	873	874	875	876	877	878	879	880	881	882	883	884	885	886	887	888	889	890	891	892	893	894	895	896	897	898	899	900	901	902	903	904	905	906	907	908	909	910	911	912	913	914	915	916	917	918	919	920	921	922	923	924	925	926	927	928	929	930	931	932	933	934	935	936	937	938	939	940	941	942	943	944	945	946	947	948	949	950	951	952	953	954	955	956	957	958	959	960	961	962	963	964	965	966	967	968	969	970	971	972	973	974	975	976	977	978	979	980	981	982	983	984	985	986	987	988	989	990	991	992	993	994	995	996	997	998	999	1000
-----	-----	-----	-----	-----	-----	-----	-----	-----	-----	-----	-----	-----	-----	-----	-----	-----	-----	-----	-----	-----	-----	-----	-----	-----	-----	-----	-----	-----	-----	-----	-----	-----	-----	-----	-----	-----	-----	-----	-----	-----	-----	-----	-----	-----	-----	-----	-----	-----	-----	-----	-----	-----	-----	-----	-----	-----	-----	-----	-----	-----	-----	-----	-----	-----	-----	-----	-----	-----	-----	-----	-----	-----	-----	-----	-----	-----	-----	-----	-----	-----	-----	-----	-----	-----	-----	-----	-----	-----	-----	-----	-----	-----	-----	-----	-----	-----	-----	-----	-----	-----	-----	-----	-----	-----	-----	-----	-----	-----	-----	-----	-----	-----	-----	-----	-----	-----	-----	-----	-----	-----	-----	-----	-----	-----	-----	-----	-----	-----	-----	-----	-----	-----	-----	-----	-----	-----	-----	-----	-----	-----	-----	-----	-----	-----	-----	-----	-----	-----	-----	-----	-----	-----	-----	-----	-----	-----	-----	-----	-----	-----	-----	-----	-----	-----	-----	-----	-----	-----	-----	-----	-----	-----	-----	-----	-----	-----	-----	-----	-----	-----	-----	-----	-----	-----	-----	-----	-----	-----	-----	-----	-----	-----	-----	-----	-----	-----	-----	-----	-----	-----	-----	-----	-----	-----	-----	-----	-----	-----	-----	-----	-----	-----	-----	-----	-----	-----	-----	-----	-----	-----	-----	-----	-----	-----	-----	-----	-----	-----	-----	-----	-----	-----	-----	-----	-----	-----	-----	-----	-----	-----	-----	-----	-----	-----	-----	-----	-----	-----	-----	-----	-----	-----	-----	-----	-----	-----	-----	-----	-----	-----	-----	-----	-----	-----	-----	-----	-----	-----	-----	-----	-----	-----	-----	-----	-----	-----	-----	-----	-----	-----	-----	-----	-----	-----	-----	-----	-----	-----	-----	-----	-----	-----	-----	-----	-----	-----	-----	-----	-----	-----	-----	-----	-----	-----	-----	-----	-----	-----	-----	-----	-----	-----	-----	-----	-----	-----	-----	-----	-----	-----	-----	-----	-----	-----	-----	-----	-----	-----	-----	-----	-----	-----	-----	-----	-----	-----	-----	-----	-----	-----	-----	-----	-----	-----	-----	-----	-----	-----	-----	-----	-----	-----	-----	-----	-----	-----	-----	-----	-----	-----	-----	-----	-----	-----	-----	-----	-----	-----	-----	-----	-----	-----	-----	-----	-----	-----	-----	-----	-----	-----	-----	-----	-----	-----	-----	-----	-----	-----	-----	-----	-----	-----	-----	-----	-----	-----	-----	-----	-----	-----	-----	-----	-----	-----	-----	-----	-----	-----	-----	-----	-----	-----	-----	-----	-----	-----	-----	-----	-----	-----	-----	-----	-----	-----	-----	-----	-----	-----	-----	-----	-----	-----	-----	-----	-----	-----	-----	-----	-----	-----	-----	-----	-----	-----	-----	-----	-----	-----	-----	-----	-----	-----	-----	-----	-----	-----	-----	-----	-----	-----	-----	-----	-----	-----	-----	-----	-----	-----	-----	-----	-----	-----	-----	-----	-----	-----	-----	-----	-----	-----	-----	-----	-----	-----	-----	-----	-----	-----	-----	-----	-----	-----	-----	-----	-----	-----	-----	-----	-----	-----	-----	-----	-----	-----	-----	-----	-----	-----	-----	-----	-----	-----	-----	-----	-----	-----	-----	-----	-----	-----	-----	-----	-----	-----	-----	-----	-----	-----	-----	-----	-----	-----	-----	-----	-----	-----	-----	-----	-----	-----	-----	-----	-----	-----	-----	-----	-----	-----	-----	-----	-----	-----	-----	-----	-----	-----	-----	-----	-----	-----	-----	-----	-----	-----	-----	-----	-----	-----	-----	-----	-----	-----	-----	-----	-----	-----	-----	-----	-----	-----	-----	-----	-----	-----	-----	-----	-----	-----	-----	-----	-----	-----	-----	-----	-----	-----	-----	-----	-----	-----	-----	-----	-----	-----	-----	-----	-----	-----	-----	-----	-----	-----	-----	-----	-----	-----	-----	-----	-----	-----	-----	-----	-----	-----	-----	-----	-----	-----	-----	-----	-----	-----	-----	-----	-----	-----	-----	-----	-----	-----	-----	-----	-----	-----	-----	-----	-----	-----	-----	-----	-----	-----	-----	-----	-----	-----	-----	-----	-----	-----	-----	-----	-----	-----	-----	-----	-----	-----	-----	-----	-----	-----	-----	-----	-----	-----	-----	-----	-----	-----	-----	-----	-----	-----	-----	-----	-----	-----	-----	-----	-----	-----	-----	-----	-----	-----	-----	-----	-----	-----	-----	-----	-----	-----	-----	-----	-----	-----	-----	-----	-----	-----	-----	-----	-----	-----	-----	-----	-----	-----	-----	-----	-----	-----	-----	-----	-----	-----	-----	-----	-----	-----	-----	-----	-----	-----	-----	-----	-----	-----	-----	-----	-----	-----	-----	-----	-----	-----	-----	-----	-----	-----	-----	-----	-----	-----	-----	-----	-----	-----	-----	-----	-----	-----	-----	-----	-----	-----	-----	-----	-----	-----	-----	-----	-----	-----	-----	-----	-----	-----	-----	-----	-----	-----	-----	-----	-----	-----	-----	-----	-----	-----	-----	-----	-----	-----	-----	-----	------

FIG. 100

APR 10	147	148	149	150	151	152	153	154	155	156	157	158	159	160	161	162	163	164	165	166	167	168	169	170	171	172	173	174	175	176	177	178	179	180	181	182	183	184	185	186	187	188	189	190	191	192	193	194	195	196	197	198	199	200	201	202	203	204	205	206	207	208	209	210	211	212	213	214	215	216	217	218	219	220	221	222	223	224	225	226	227	228	229	230	231	232	233	234	235	236	237	238	239	240	241	242	243	244	245	246	247	248	249	250	251	252	253	254	255	256	257	258	259	260	261	262	263	264	265	266	267	268	269	270	271	272	273	274	275	276	277	278	279	280	281	282	283	284	285	286	287	288	289	290	291	292	293	294	295	296	297	298	299	300	301	302	303	304	305	306	307	308	309	310	311	312	313	314	315	316	317	318	319	320	321	322	323	324	325	326	327	328	329	330	331	332	333	334	335	336	337	338	339	340	341	342	343	344	345	346	347	348	349	350	351	352	353	354	355	356	357	358	359	360	361	362	363	364	365	366	367	368	369	370	371	372	373	374	375	376	377	378	379	380	381	382	383	384	385	386	387	388	389	390	391	392	393	394	395	396	397	398	399	400	401	402	403	404	405	406	407	408	409	410	411	412	413	414	415	416	417	418	419	420	421	422	423	424	425	426	427	428	429	430	431	432	433	434	435	436	437	438	439	440	441	442	443	444	445	446	447	448	449	450	451	452	453	454	455	456	457	458	459	460	461	462	463	464	465	466	467	468	469	470	471	472	473	474	475	476	477	478	479	480	481	482	483	484	485	486	487	488	489	490	491	492	493	494	495	496	497	498	499	500	501	502	503	504	505	506	507	508	509	510	511	512	513	514	515	516	517	518	519	520	521	522	523	524	525	526	527	528	529	530	531	532	533	534	535	536	537	538	539	540	541	542	543	544	545	546	547	548	549	550	551	552	553	554	555	556	557	558	559	560	561	562	563	564	565	566	567	568	569	570	571	572	573	574	575	576	577	578	579	580	581	582	583	584	585	586	587	588	589	590	591	592	593	594	595	596	597	598	599	600	601	602	603	604	605	606	607	608	609	610	611	612	613	614	615	616	617	618	619	620	621	622	623	624	625	626	627	628	629	630	631	632	633	634	635	636	637	638	639	640	641	642	643	644	645	646	647	648	649	650	651	652	653	654	655	656	657	658	659	660	661	662	663	664	665	666	667	668	669	670	671	672	673	674	675	676	677	678	679	680	681	682	683	684	685	686	687	688	689	690	691	692	693	694	695	696	697	698	699	700	701	702	703	704	705	706	707	708	709	710	711	712	713	714	715	716	717	718	719	720	721	722	723	724	725	726	727	728	729	730	731	732	733	734	735	736	737	738	739	740	741	742	743	744	745	746	747	748	749	750	751	752	753	754	755	756	757	758	759	760	761	762	763	764	765	766	767	768	769	770	771	772	773	774	775	776	777	778	779	780	781	782	783	784	785	786	787	788	789	790	791	792	793	794	795	796	797	798	799	800	801	802	803	804	805	806	807	808	809	810	811	812	813	814	815	816	817	818	819	820	821	822	823	824	825	826	827	828	829	830	831	832	833	834	835	836	837	838	839	840	841	842	843	844	845	846	847	848	849	850	851	852	853	854	855	856	857	858	859	860	861	862	863	864	865	866	867	868	869	870	871	872	873	874	875	876	877	878	879	880	881	882	883	884	885	886	887	888	889	890	891	892	893	894	895	896	897	898	899	900	901	902	903	904	905	906	907	908	909	910	911	912	913	914	915	916	917	918	919	920	921	922	923	924	925	926	927	928	929	930	931	932	933	934	935	936	937	938	939	940	941	942	943	944	945	946	947	948	949	950	951	952	953	954	955	956	957	958	959	960	961	962	963	964	965	966	967	968	969	970	971	972	973	974	975	976	977	978	979	980	981	982	983	984	985	986	987	988	989	990	991	992	993	994	995	996	997	998	999	1000
--------	-----	-----	-----	-----	-----	-----	-----	-----	-----	-----	-----	-----	-----	-----	-----	-----	-----	-----	-----	-----	-----	-----	-----	-----	-----	-----	-----	-----	-----	-----	-----	-----	-----	-----	-----	-----	-----	-----	-----	-----	-----	-----	-----	-----	-----	-----	-----	-----	-----	-----	-----	-----	-----	-----	-----	-----	-----	-----	-----	-----	-----	-----	-----	-----	-----	-----	-----	-----	-----	-----	-----	-----	-----	-----	-----	-----	-----	-----	-----	-----	-----	-----	-----	-----	-----	-----	-----	-----	-----	-----	-----	-----	-----	-----	-----	-----	-----	-----	-----	-----	-----	-----	-----	-----	-----	-----	-----	-----	-----	-----	-----	-----	-----	-----	-----	-----	-----	-----	-----	-----	-----	-----	-----	-----	-----	-----	-----	-----	-----	-----	-----	-----	-----	-----	-----	-----	-----	-----	-----	-----	-----	-----	-----	-----	-----	-----	-----	-----	-----	-----	-----	-----	-----	-----	-----	-----	-----	-----	-----	-----	-----	-----	-----	-----	-----	-----	-----	-----	-----	-----	-----	-----	-----	-----	-----	-----	-----	-----	-----	-----	-----	-----	-----	-----	-----	-----	-----	-----	-----	-----	-----	-----	-----	-----	-----	-----	-----	-----	-----	-----	-----	-----	-----	-----	-----	-----	-----	-----	-----	-----	-----	-----	-----	-----	-----	-----	-----	-----	-----	-----	-----	-----	-----	-----	-----	-----	-----	-----	-----	-----	-----	-----	-----	-----	-----	-----	-----	-----	-----	-----	-----	-----	-----	-----	-----	-----	-----	-----	-----	-----	-----	-----	-----	-----	-----	-----	-----	-----	-----	-----	-----	-----	-----	-----	-----	-----	-----	-----	-----	-----	-----	-----	-----	-----	-----	-----	-----	-----	-----	-----	-----	-----	-----	-----	-----	-----	-----	-----	-----	-----	-----	-----	-----	-----	-----	-----	-----	-----	-----	-----	-----	-----	-----	-----	-----	-----	-----	-----	-----	-----	-----	-----	-----	-----	-----	-----	-----	-----	-----	-----	-----	-----	-----	-----	-----	-----	-----	-----	-----	-----	-----	-----	-----	-----	-----	-----	-----	-----	-----	-----	-----	-----	-----	-----	-----	-----	-----	-----	-----	-----	-----	-----	-----	-----	-----	-----	-----	-----	-----	-----	-----	-----	-----	-----	-----	-----	-----	-----	-----	-----	-----	-----	-----	-----	-----	-----	-----	-----	-----	-----	-----	-----	-----	-----	-----	-----	-----	-----	-----	-----	-----	-----	-----	-----	-----	-----	-----	-----	-----	-----	-----	-----	-----	-----	-----	-----	-----	-----	-----	-----	-----	-----	-----	-----	-----	-----	-----	-----	-----	-----	-----	-----	-----	-----	-----	-----	-----	-----	-----	-----	-----	-----	-----	-----	-----	-----	-----	-----	-----	-----	-----	-----	-----	-----	-----	-----	-----	-----	-----	-----	-----	-----	-----	-----	-----	-----	-----	-----	-----	-----	-----	-----	-----	-----	-----	-----	-----	-----	-----	-----	-----	-----	-----	-----	-----	-----	-----	-----	-----	-----	-----	-----	-----	-----	-----	-----	-----	-----	-----	-----	-----	-----	-----	-----	-----	-----	-----	-----	-----	-----	-----	-----	-----	-----	-----	-----	-----	-----	-----	-----	-----	-----	-----	-----	-----	-----	-----	-----	-----	-----	-----	-----	-----	-----	-----	-----	-----	-----	-----	-----	-----	-----	-----	-----	-----	-----	-----	-----	-----	-----	-----	-----	-----	-----	-----	-----	-----	-----	-----	-----	-----	-----	-----	-----	-----	-----	-----	-----	-----	-----	-----	-----	-----	-----	-----	-----	-----	-----	-----	-----	-----	-----	-----	-----	-----	-----	-----	-----	-----	-----	-----	-----	-----	-----	-----	-----	-----	-----	-----	-----	-----	-----	-----	-----	-----	-----	-----	-----	-----	-----	-----	-----	-----	-----	-----	-----	-----	-----	-----	-----	-----	-----	-----	-----	-----	-----	-----	-----	-----	-----	-----	-----	-----	-----	-----	-----	-----	-----	-----	-----	-----	-----	-----	-----	-----	-----	-----	-----	-----	-----	-----	-----	-----	-----	-----	-----	-----	-----	-----	-----	-----	-----	-----	-----	-----	-----	-----	-----	-----	-----	-----	-----	-----	-----	-----	-----	-----	-----	-----	-----	-----	-----	-----	-----	-----	-----	-----	-----	-----	-----	-----	-----	-----	-----	-----	-----	-----	-----	-----	-----	-----	-----	-----	-----	-----	-----	-----	-----	-----	-----	-----	-----	-----	-----	-----	-----	-----	-----	-----	-----	-----	-----	-----	-----	-----	-----	-----	-----	-----	-----	-----	-----	-----	-----	-----	-----	-----	-----	-----	-----	-----	-----	-----	-----	-----	-----	-----	-----	-----	-----	-----	-----	-----	-----	-----	-----	-----	-----	-----	-----	-----	-----	-----	-----	-----	-----	-----	-----	-----	-----	-----	-----	-----	-----	-----	-----	-----	-----	-----	-----	-----	-----	-----	-----	-----	-----	-----	-----	-----	-----	-----	-----	-----	-----	-----	-----	-----	-----	-----	-----	-----	-----	-----	-----	-----	-----	-----	-----	-----	-----	-----	-----	-----	-----	-----	-----	-----	-----	-----	-----	-----	-----	-----	-----	-----	-----	-----	-----	-----	-----	-----	-----	-----	-----	-----	-----	-----	-----	-----	-----	-----	-----	-----	-----	-----	-----	-----	-----	-----	-----	-----	-----	-----	-----	-----	-----	-----	-----	-----	-----	-----	-----	-----	------

FIG. 100

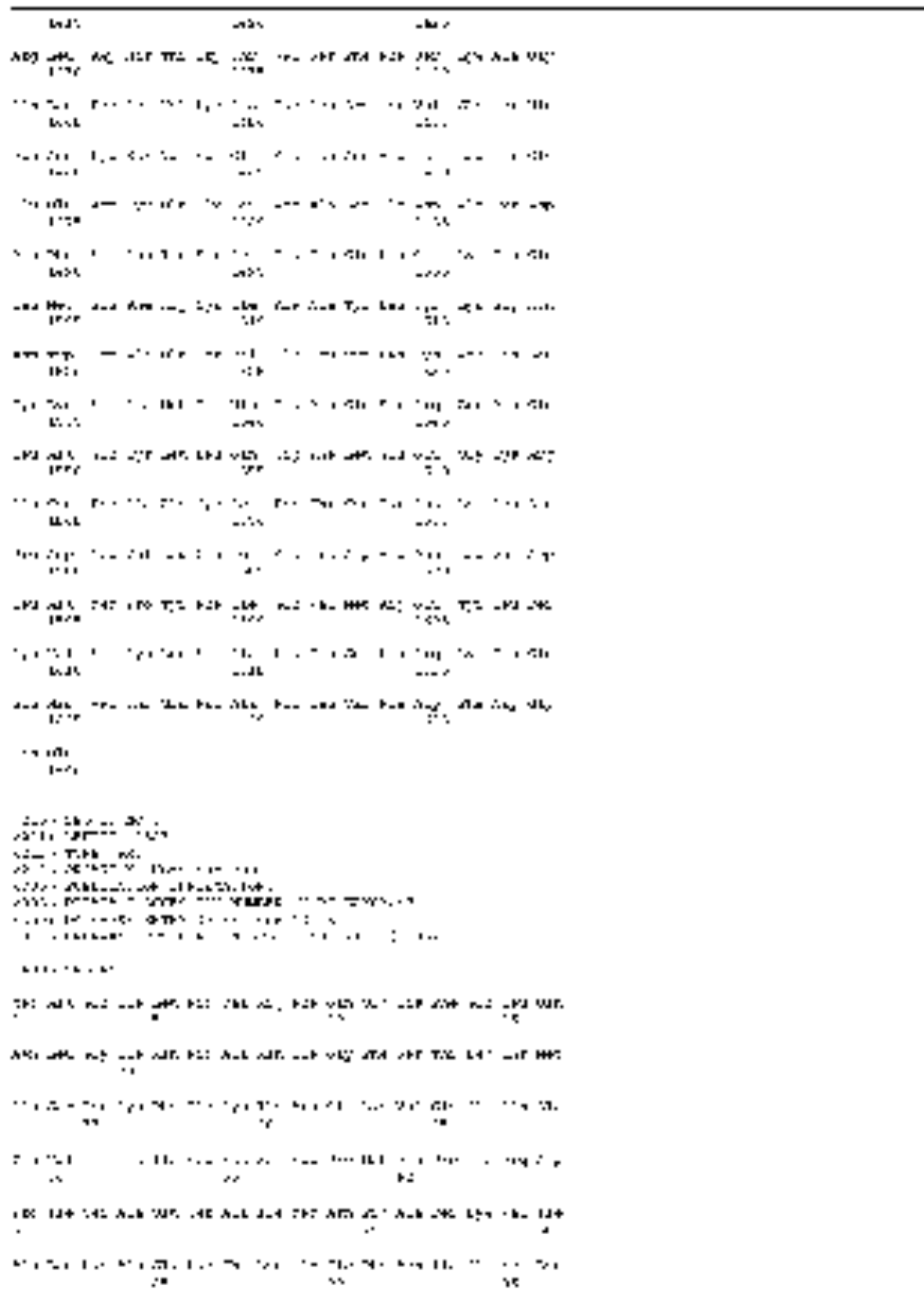


FIG. 10

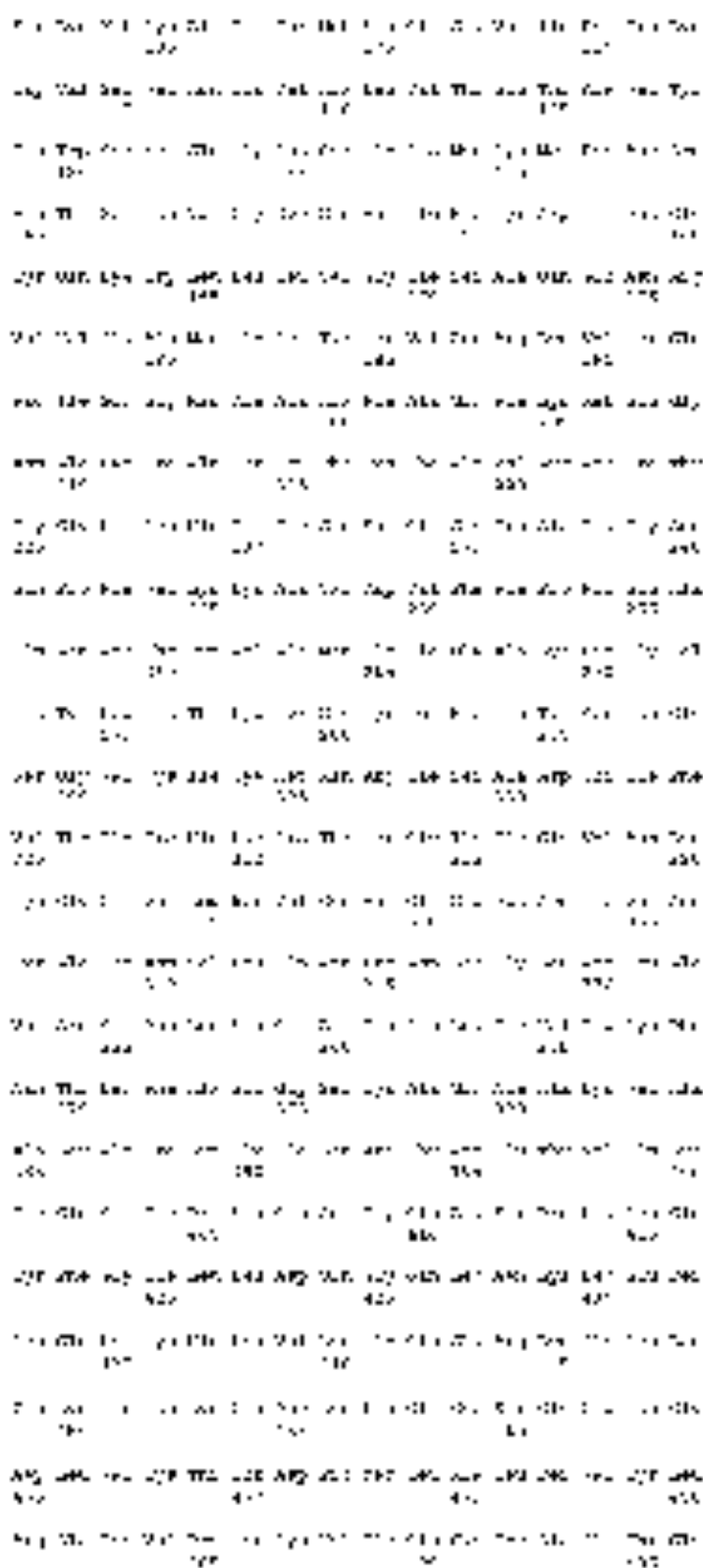


FIG. 10

201	202	203	204	205	206	207	208	209	210	211	212	213	214	215	216	217	218	219	220	221	222	223	224	225	226	227	228	229	230	231	232	233	234	235	236	237	238	239	240	241	242	243	244	245	246	247	248	249	250	251	252	253	254	255	256	257	258	259	260	261	262	263	264	265	266	267	268	269	270	271	272	273	274	275	276	277	278	279	280	281	282	283	284	285	286	287	288	289	290	291	292	293	294	295	296	297	298	299	300	301	302	303	304	305	306	307	308	309	310	311	312	313	314	315	316	317	318	319	320	321	322	323	324	325	326	327	328	329	330	331	332	333	334	335	336	337	338	339	340	341	342	343	344	345	346	347	348	349	350	351	352	353	354	355	356	357	358	359	360	361	362	363	364	365	366	367	368	369	370	371	372	373	374	375	376	377	378	379	380	381	382	383	384	385	386	387	388	389	390	391	392	393	394	395	396	397	398	399	400	401	402	403	404	405	406	407	408	409	410	411	412	413	414	415	416	417	418	419	420	421	422	423	424	425	426	427	428	429	430	431	432	433	434	435	436	437	438	439	440	441	442	443	444	445	446	447	448	449	450	451	452	453	454	455	456	457	458	459	460	461	462	463	464	465	466	467	468	469	470	471	472	473	474	475	476	477	478	479	480	481	482	483	484	485	486	487	488	489	490	491	492	493	494	495	496	497	498	499	500	501	502	503	504	505	506	507	508	509	510	511	512	513	514	515	516	517	518	519	520	521	522	523	524	525	526	527	528	529	530	531	532	533	534	535	536	537	538	539	540	541	542	543	544	545	546	547	548	549	550	551	552	553	554	555	556	557	558	559	560	561	562	563	564	565	566	567	568	569	570	571	572	573	574	575	576	577	578	579	580	581	582	583	584	585	586	587	588	589	590	591	592	593	594	595	596	597	598	599	600	601	602	603	604	605	606	607	608	609	610	611	612	613	614	615	616	617	618	619	620	621	622	623	624	625	626	627	628	629	630	631	632	633	634	635	636	637	638	639	640	641	642	643	644	645	646	647	648	649	650	651	652	653	654	655	656	657	658	659	660	661	662	663	664	665	666	667	668	669	670	671	672	673	674	675	676	677	678	679	680	681	682	683	684	685	686	687	688	689	690	691	692	693	694	695	696	697	698	699	700	701	702	703	704	705	706	707	708	709	710	711	712	713	714	715	716	717	718	719	720	721	722	723	724	725	726	727	728	729	730	731	732	733	734	735	736	737	738	739	740	741	742	743	744	745	746	747	748	749	750	751	752	753	754	755	756	757	758	759	760	761	762	763	764	765	766	767	768	769	770	771	772	773	774	775	776	777	778	779	780	781	782	783	784	785	786	787	788	789	790	791	792	793	794	795	796	797	798	799	800	801	802	803	804	805	806	807	808	809	810	811	812	813	814	815	816	817	818	819	820	821	822	823	824	825	826	827	828	829	830	831	832	833	834	835	836	837	838	839	840	841	842	843	844	845	846	847	848	849	850	851	852	853	854	855	856	857	858	859	860	861	862	863	864	865	866	867	868	869	870	871	872	873	874	875	876	877	878	879	880	881	882	883	884	885	886	887	888	889	890	891	892	893	894	895	896	897	898	899	900	901	902	903	904	905	906	907	908	909	910	911	912	913	914	915	916	917	918	919	920	921	922	923	924	925	926	927	928	929	930	931	932	933	934	935	936	937	938	939	940	941	942	943	944	945	946	947	948	949	950	951	952	953	954	955	956	957	958	959	960	961	962	963	964	965	966	967	968	969	970	971	972	973	974	975	976	977	978	979	980	981	982	983	984	985	986	987	988	989	990	991	992	993	994	995	996	997	998	999	1000
-----	-----	-----	-----	-----	-----	-----	-----	-----	-----	-----	-----	-----	-----	-----	-----	-----	-----	-----	-----	-----	-----	-----	-----	-----	-----	-----	-----	-----	-----	-----	-----	-----	-----	-----	-----	-----	-----	-----	-----	-----	-----	-----	-----	-----	-----	-----	-----	-----	-----	-----	-----	-----	-----	-----	-----	-----	-----	-----	-----	-----	-----	-----	-----	-----	-----	-----	-----	-----	-----	-----	-----	-----	-----	-----	-----	-----	-----	-----	-----	-----	-----	-----	-----	-----	-----	-----	-----	-----	-----	-----	-----	-----	-----	-----	-----	-----	-----	-----	-----	-----	-----	-----	-----	-----	-----	-----	-----	-----	-----	-----	-----	-----	-----	-----	-----	-----	-----	-----	-----	-----	-----	-----	-----	-----	-----	-----	-----	-----	-----	-----	-----	-----	-----	-----	-----	-----	-----	-----	-----	-----	-----	-----	-----	-----	-----	-----	-----	-----	-----	-----	-----	-----	-----	-----	-----	-----	-----	-----	-----	-----	-----	-----	-----	-----	-----	-----	-----	-----	-----	-----	-----	-----	-----	-----	-----	-----	-----	-----	-----	-----	-----	-----	-----	-----	-----	-----	-----	-----	-----	-----	-----	-----	-----	-----	-----	-----	-----	-----	-----	-----	-----	-----	-----	-----	-----	-----	-----	-----	-----	-----	-----	-----	-----	-----	-----	-----	-----	-----	-----	-----	-----	-----	-----	-----	-----	-----	-----	-----	-----	-----	-----	-----	-----	-----	-----	-----	-----	-----	-----	-----	-----	-----	-----	-----	-----	-----	-----	-----	-----	-----	-----	-----	-----	-----	-----	-----	-----	-----	-----	-----	-----	-----	-----	-----	-----	-----	-----	-----	-----	-----	-----	-----	-----	-----	-----	-----	-----	-----	-----	-----	-----	-----	-----	-----	-----	-----	-----	-----	-----	-----	-----	-----	-----	-----	-----	-----	-----	-----	-----	-----	-----	-----	-----	-----	-----	-----	-----	-----	-----	-----	-----	-----	-----	-----	-----	-----	-----	-----	-----	-----	-----	-----	-----	-----	-----	-----	-----	-----	-----	-----	-----	-----	-----	-----	-----	-----	-----	-----	-----	-----	-----	-----	-----	-----	-----	-----	-----	-----	-----	-----	-----	-----	-----	-----	-----	-----	-----	-----	-----	-----	-----	-----	-----	-----	-----	-----	-----	-----	-----	-----	-----	-----	-----	-----	-----	-----	-----	-----	-----	-----	-----	-----	-----	-----	-----	-----	-----	-----	-----	-----	-----	-----	-----	-----	-----	-----	-----	-----	-----	-----	-----	-----	-----	-----	-----	-----	-----	-----	-----	-----	-----	-----	-----	-----	-----	-----	-----	-----	-----	-----	-----	-----	-----	-----	-----	-----	-----	-----	-----	-----	-----	-----	-----	-----	-----	-----	-----	-----	-----	-----	-----	-----	-----	-----	-----	-----	-----	-----	-----	-----	-----	-----	-----	-----	-----	-----	-----	-----	-----	-----	-----	-----	-----	-----	-----	-----	-----	-----	-----	-----	-----	-----	-----	-----	-----	-----	-----	-----	-----	-----	-----	-----	-----	-----	-----	-----	-----	-----	-----	-----	-----	-----	-----	-----	-----	-----	-----	-----	-----	-----	-----	-----	-----	-----	-----	-----	-----	-----	-----	-----	-----	-----	-----	-----	-----	-----	-----	-----	-----	-----	-----	-----	-----	-----	-----	-----	-----	-----	-----	-----	-----	-----	-----	-----	-----	-----	-----	-----	-----	-----	-----	-----	-----	-----	-----	-----	-----	-----	-----	-----	-----	-----	-----	-----	-----	-----	-----	-----	-----	-----	-----	-----	-----	-----	-----	-----	-----	-----	-----	-----	-----	-----	-----	-----	-----	-----	-----	-----	-----	-----	-----	-----	-----	-----	-----	-----	-----	-----	-----	-----	-----	-----	-----	-----	-----	-----	-----	-----	-----	-----	-----	-----	-----	-----	-----	-----	-----	-----	-----	-----	-----	-----	-----	-----	-----	-----	-----	-----	-----	-----	-----	-----	-----	-----	-----	-----	-----	-----	-----	-----	-----	-----	-----	-----	-----	-----	-----	-----	-----	-----	-----	-----	-----	-----	-----	-----	-----	-----	-----	-----	-----	-----	-----	-----	-----	-----	-----	-----	-----	-----	-----	-----	-----	-----	-----	-----	-----	-----	-----	-----	-----	-----	-----	-----	-----	-----	-----	-----	-----	-----	-----	-----	-----	-----	-----	-----	-----	-----	-----	-----	-----	-----	-----	-----	-----	-----	-----	-----	-----	-----	-----	-----	-----	-----	-----	-----	-----	-----	-----	-----	-----	-----	-----	-----	-----	-----	-----	-----	-----	-----	-----	-----	-----	-----	-----	-----	-----	-----	-----	-----	-----	-----	-----	-----	-----	-----	-----	-----	-----	-----	-----	-----	-----	-----	-----	-----	-----	-----	-----	-----	-----	-----	-----	-----	-----	-----	-----	-----	-----	-----	-----	-----	-----	-----	-----	-----	-----	-----	-----	-----	-----	-----	-----	-----	-----	-----	-----	-----	-----	-----	-----	-----	-----	-----	-----	-----	-----	-----	-----	-----	-----	-----	-----	-----	-----	-----	-----	-----	------

FIG. 11B

	2013		2014		2015	
APR 2013	124	103	134	128	132	135
MAY 2013	103	101	107	103	108	104
JUN 2013	103	101	107	103	108	104
JUL 2013	103	101	107	103	108	104
AUG 2013	103	101	107	103	108	104
SEP 2013	103	101	107	103	108	104
OCT 2013	103	101	107	103	108	104
NOV 2013	103	101	107	103	108	104
DEC 2013	103	101	107	103	108	104
JAN 2014	103	101	107	103	108	104
FEB 2014	103	101	107	103	108	104
MAR 2014	103	101	107	103	108	104
APR 2014	103	101	107	103	108	104
MAY 2014	103	101	107	103	108	104
JUN 2014	103	101	107	103	108	104
JUL 2014	103	101	107	103	108	104
AUG 2014	103	101	107	103	108	104
SEP 2014	103	101	107	103	108	104
OCT 2014	103	101	107	103	108	104
NOV 2014	103	101	107	103	108	104
DEC 2014	103	101	107	103	108	104
JAN 2015	103	101	107	103	108	104
FEB 2015	103	101	107	103	108	104
MAR 2015	103	101	107	103	108	104
APR 2015	103	101	107	103	108	104
MAY 2015	103	101	107	103	108	104
JUN 2015	103	101	107	103	108	104
JUL 2015	103	101	107	103	108	104
AUG 2015	103	101	107	103	108	104
SEP 2015	103	101	107	103	108	104
OCT 2015	103	101	107	103	108	104
NOV 2015	103	101	107	103	108	104
DEC 2015	103	101	107	103	108	104

FIG. 10B

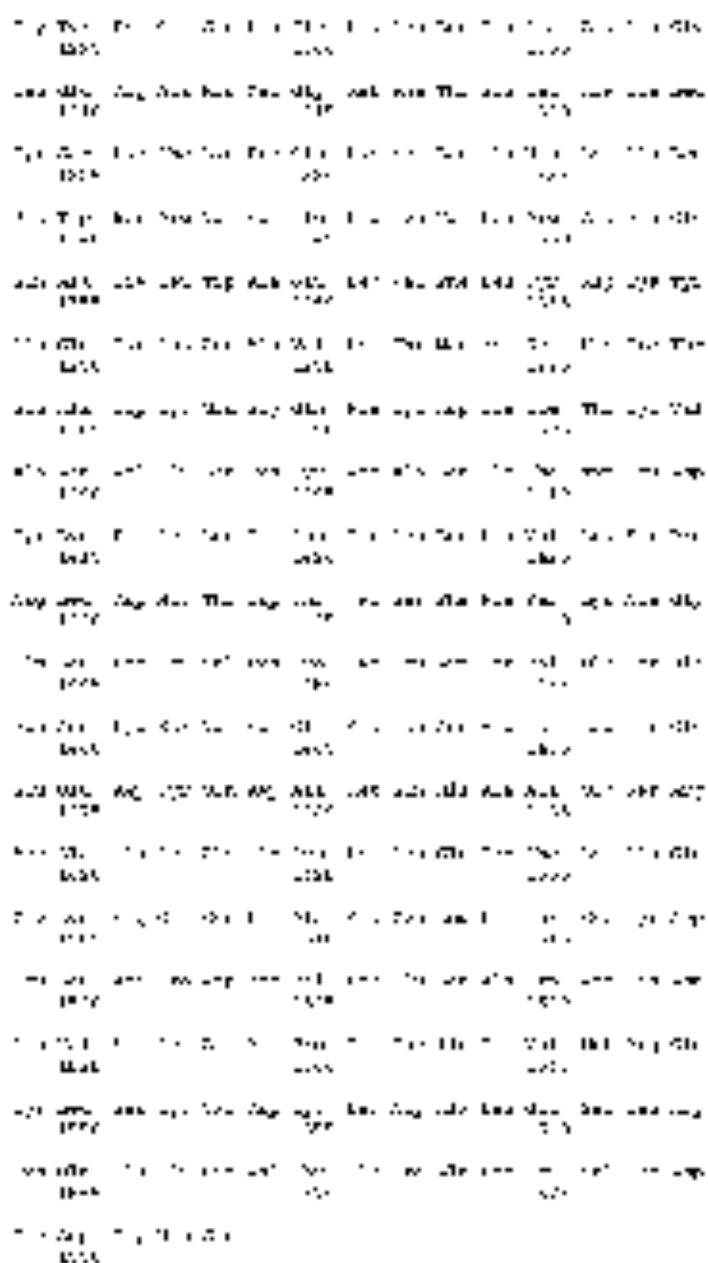


FIG. 10B-1
 FIG. 10B-2
 FIG. 10B-3
 FIG. 10B-4
 FIG. 10B-5
 FIG. 10B-6
 FIG. 10B-7
 FIG. 10B-8
 FIG. 10B-9
 FIG. 10B-10
 FIG. 10B-11
 FIG. 10B-12
 FIG. 10B-13
 FIG. 10B-14
 FIG. 10B-15
 FIG. 10B-16

FIG. 10C-1
 FIG. 10C-2
 FIG. 10C-3
 FIG. 10C-4
 FIG. 10C-5
 FIG. 10C-6
 FIG. 10C-7
 FIG. 10C-8
 FIG. 10C-9
 FIG. 10C-10
 FIG. 10C-11
 FIG. 10C-12
 FIG. 10C-13
 FIG. 10C-14
 FIG. 10C-15
 FIG. 10C-16
 FIG. 10C-17
 FIG. 10C-18
 FIG. 10C-19
 FIG. 10C-20
 FIG. 10C-21
 FIG. 10C-22
 FIG. 10C-23
 FIG. 10C-24
 FIG. 10C-25
 FIG. 10C-26
 FIG. 10C-27
 FIG. 10C-28
 FIG. 10C-29
 FIG. 10C-30
 FIG. 10C-31
 FIG. 10C-32
 FIG. 10C-33
 FIG. 10C-34
 FIG. 10C-35
 FIG. 10C-36
 FIG. 10C-37
 FIG. 10C-38
 FIG. 10C-39
 FIG. 10C-40
 FIG. 10C-41
 FIG. 10C-42
 FIG. 10C-43
 FIG. 10C-44
 FIG. 10C-45
 FIG. 10C-46
 FIG. 10C-47
 FIG. 10C-48
 FIG. 10C-49
 FIG. 10C-50
 FIG. 10C-51
 FIG. 10C-52
 FIG. 10C-53
 FIG. 10C-54
 FIG. 10C-55
 FIG. 10C-56
 FIG. 10C-57
 FIG. 10C-58
 FIG. 10C-59
 FIG. 10C-60
 FIG. 10C-61
 FIG. 10C-62
 FIG. 10C-63
 FIG. 10C-64
 FIG. 10C-65
 FIG. 10C-66
 FIG. 10C-67
 FIG. 10C-68
 FIG. 10C-69
 FIG. 10C-70
 FIG. 10C-71
 FIG. 10C-72
 FIG. 10C-73
 FIG. 10C-74
 FIG. 10C-75
 FIG. 10C-76
 FIG. 10C-77
 FIG. 10C-78
 FIG. 10C-79
 FIG. 10C-80
 FIG. 10C-81
 FIG. 10C-82
 FIG. 10C-83
 FIG. 10C-84
 FIG. 10C-85
 FIG. 10C-86
 FIG. 10C-87
 FIG. 10C-88
 FIG. 10C-89
 FIG. 10C-90
 FIG. 10C-91
 FIG. 10C-92
 FIG. 10C-93
 FIG. 10C-94
 FIG. 10C-95
 FIG. 10C-96
 FIG. 10C-97
 FIG. 10C-98
 FIG. 10C-99
 FIG. 10C-100

 CONTINUOUS

201 202 203 204 205 206 207 208 209 210 211 212 213 214 215 216 217 218 219 220 221 222 223 224 225 226 227 228 229 230 231 232 233 234 235 236 237 238 239 240 241 242 243 244 245 246 247 248 249 250
 251 252 253 254 255 256 257 258 259 260 261 262 263 264 265 266 267 268 269 270 271 272 273 274 275 276 277 278 279 280 281 282 283 284 285 286 287 288 289 290 291 292 293 294 295 296 297 298 299 300
 301 302 303 304 305 306 307 308 309 310 311 312 313 314 315 316 317 318 319 320 321 322 323 324 325 326 327 328 329 330 331 332 333 334 335 336 337 338 339 340 341 342 343 344 345 346 347 348 349 350
 351 352 353 354 355 356 357 358 359 360 361 362 363 364 365 366 367 368 369 370 371 372 373 374 375 376 377 378 379 380 381 382 383 384 385 386 387 388 389 390 391 392 393 394 395 396 397 398 399 400
 401 402 403 404 405 406 407 408 409 410 411 412 413 414 415 416 417 418 419 420 421 422 423 424 425 426 427 428 429 430 431 432 433 434 435 436 437 438 439 440 441 442 443 444 445 446 447 448 449 450
 451 452 453 454 455 456 457 458 459 460 461 462 463 464 465 466 467 468 469 470 471 472 473 474 475 476 477 478 479 480 481 482 483 484 485 486 487 488 489 490 491 492 493 494 495 496 497 498 499 500
 501 502 503 504 505 506 507 508 509 510 511 512 513 514 515 516 517 518 519 520 521 522 523 524 525 526 527 528 529 530 531 532 533 534 535 536 537 538 539 540 541 542 543 544 545 546 547 548 549 550
 551 552 553 554 555 556 557 558 559 560 561 562 563 564 565 566 567 568 569 570 571 572 573 574 575 576 577 578 579 580 581 582 583 584 585 586 587 588 589 590 591 592 593 594 595 596 597 598 599 600
 601 602 603 604 605 606 607 608 609 610 611 612 613 614 615 616 617 618 619 620 621 622 623 624 625 626 627 628 629 630 631 632 633 634 635 636 637 638 639 640 641 642 643 644 645 646 647 648 649 650
 651 652 653 654 655 656 657 658 659 660 661 662 663 664 665 666 667 668 669 670 671 672 673 674 675 676 677 678 679 680 681 682 683 684 685 686 687 688 689 690 691 692 693 694 695 696 697 698 699 700
 701 702 703 704 705 706 707 708 709 710 711 712 713 714 715 716 717 718 719 720 721 722 723 724 725 726 727 728 729 730 731 732 733 734 735 736 737 738 739 740 741 742 743 744 745 746 747 748 749 750
 751 752 753 754 755 756 757 758 759 760 761 762 763 764 765 766 767 768 769 770 771 772 773 774 775 776 777 778 779 780 781 782 783 784 785 786 787 788 789 790 791 792 793 794 795 796 797 798 799 800
 801 802 803 804 805 806 807 808 809 810 811 812 813 814 815 816 817 818 819 820 821 822 823 824 825 826 827 828 829 830 831 832 833 834 835 836 837 838 839 840 841 842 843 844 845 846 847 848 849 850
 851 852 853 854 855 856 857 858 859 860 861 862 863 864 865 866 867 868 869 870 871 872 873 874 875 876 877 878 879 880 881 882 883 884 885 886 887 888 889 890 891 892 893 894 895 896 897 898 899 900
 901 902 903 904 905 906 907 908 909 910 911 912 913 914 915 916 917 918 919 920 921 922 923 924 925 926 927 928 929 930 931 932 933 934 935 936 937 938 939 940 941 942 943 944 945 946 947 948 949 950
 951 952 953 954 955 956 957 958 959 960 961 962 963 964 965 966 967 968 969 970 971 972 973 974 975 976 977 978 979 980 981 982 983 984 985 986 987 988 989 990 991 992 993 994 995 996 997 998 999 1000

FIG. 111

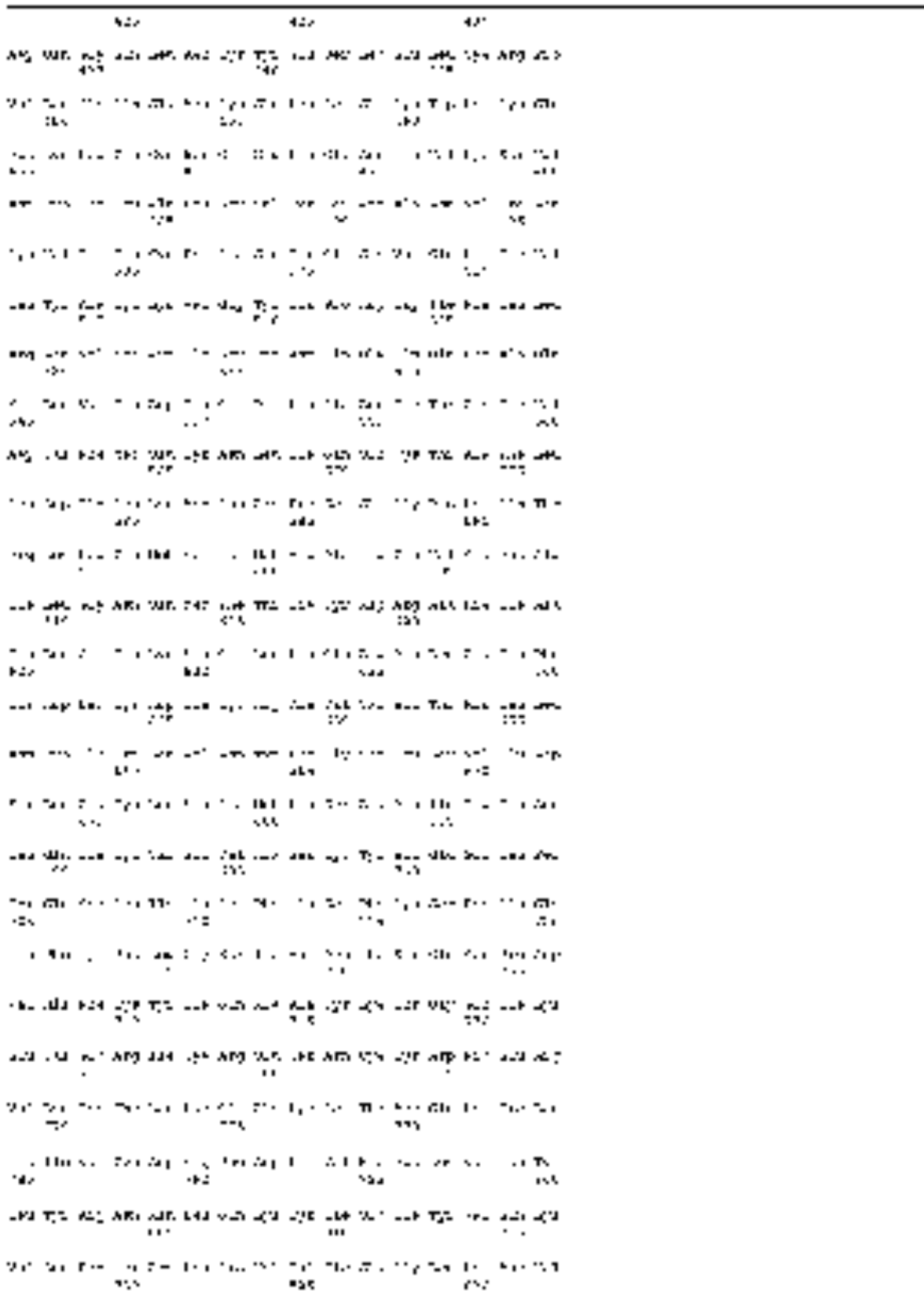


FIG. 10B

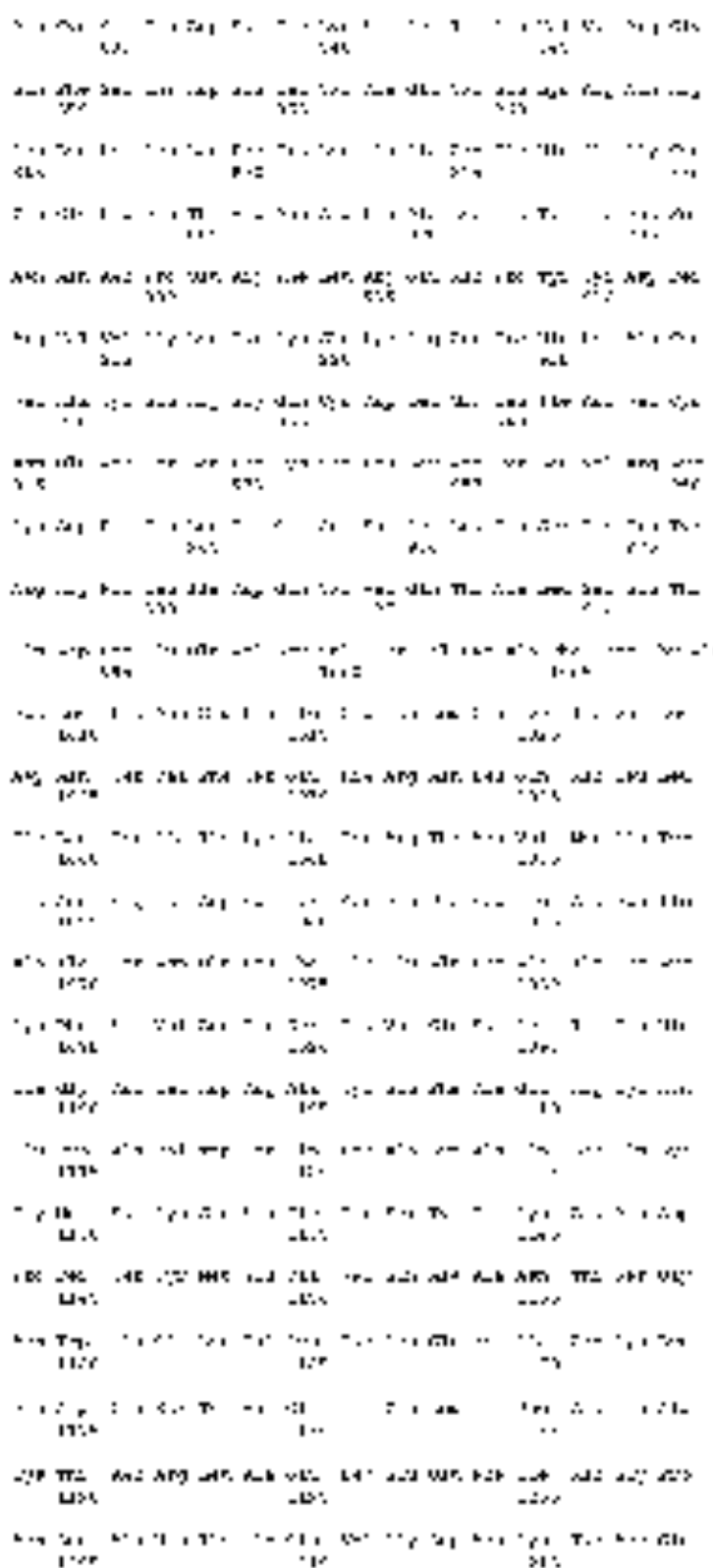


FIG. 10

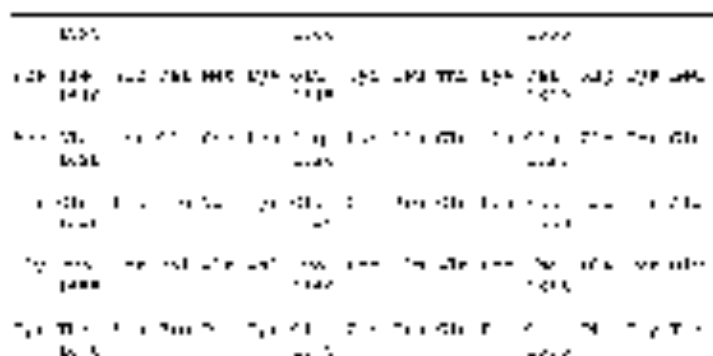


FIG. 10

FIG. 10 is a schematic diagram of a multi-layered structure.

FIG. 10 is a schematic diagram of a multi-layered structure.

FIG. 10 is a schematic diagram of a multi-layered structure.

FIG. 10 is a schematic diagram of a multi-layered structure.

FIG. 10 is a schematic diagram of a multi-layered structure.

FIG. 10 is a schematic diagram of a multi-layered structure.

FIG. 10 is a schematic diagram of a multi-layered structure.

FIG. 10 is a schematic diagram of a multi-layered structure.

FIG. 10 is a schematic diagram of a multi-layered structure.

FIG. 10 is a schematic diagram of a multi-layered structure.

FIG. 10 is a schematic diagram of a multi-layered structure.

FIG. 10 is a schematic diagram of a multi-layered structure.

FIG. 10 is a schematic diagram of a multi-layered structure.

FIG. 10 is a schematic diagram of a multi-layered structure.

FIG. 10 is a schematic diagram of a multi-layered structure.

FIG. 10 is a schematic diagram of a multi-layered structure.

FIG. 10 is a schematic diagram of a multi-layered structure.

FIG. 10 is a schematic diagram of a multi-layered structure.

FIG. 10 is a schematic diagram of a multi-layered structure.

FIG. 10 is a schematic diagram of a multi-layered structure.

FIG. 10 is a schematic diagram of a multi-layered structure.

FIG. 10 is a schematic diagram of a multi-layered structure.

FIG. 10 is a schematic diagram of a multi-layered structure.

FIG. 10 is a schematic diagram of a multi-layered structure.

FIG. 10B

101	102	103	104	105	106	107	108	109	110	111	112	113	114	115	116	117	118	119	120	121	122	123	124	125	126	127	128	129	130	131	132	133	134	135	136	137	138	139	140	141	142	143	144	145	146	147	148	149	150	151	152	153	154	155	156	157	158	159	160	161	162	163	164	165	166	167	168	169	170	171	172	173	174	175	176	177	178	179	180	181	182	183	184	185	186	187	188	189	190	191	192	193	194	195	196	197	198	199	200	201	202	203	204	205	206	207	208	209	210	211	212	213	214	215	216	217	218	219	220	221	222	223	224	225	226	227	228	229	230	231	232	233	234	235	236	237	238	239	240	241	242	243	244	245	246	247	248	249	250	251	252	253	254	255	256	257	258	259	260	261	262	263	264	265	266	267	268	269	270	271	272	273	274	275	276	277	278	279	280	281	282	283	284	285	286	287	288	289	290	291	292	293	294	295	296	297	298	299	300	301	302	303	304	305	306	307	308	309	310	311	312	313	314	315	316	317	318	319	320	321	322	323	324	325	326	327	328	329	330	331	332	333	334	335	336	337	338	339	340	341	342	343	344	345	346	347	348	349	350	351	352	353	354	355	356	357	358	359	360	361	362	363	364	365	366	367	368	369	370	371	372	373	374	375	376	377	378	379	380	381	382	383	384	385	386	387	388	389	390	391	392	393	394	395	396	397	398	399	400	401	402	403	404	405	406	407	408	409	410	411	412	413	414	415	416	417	418	419	420	421	422	423	424	425	426	427	428	429	430	431	432	433	434	435	436	437	438	439	440	441	442	443	444	445	446	447	448	449	450	451	452	453	454	455	456	457	458	459	460	461	462	463	464	465	466	467	468	469	470	471	472	473	474	475	476	477	478	479	480	481	482	483	484	485	486	487	488	489	490	491	492	493	494	495	496	497	498	499	500	501	502	503	504	505	506	507	508	509	510	511	512	513	514	515	516	517	518	519	520	521	522	523	524	525	526	527	528	529	530	531	532	533	534	535	536	537	538	539	540	541	542	543	544	545	546	547	548	549	550	551	552	553	554	555	556	557	558	559	560	561	562	563	564	565	566	567	568	569	570	571	572	573	574	575	576	577	578	579	580	581	582	583	584	585	586	587	588	589	590	591	592	593	594	595	596	597	598	599	600	601	602	603	604	605	606	607	608	609	610	611	612	613	614	615	616	617	618	619	620	621	622	623	624	625	626	627	628	629	630	631	632	633	634	635	636	637	638	639	640	641	642	643	644	645	646	647	648	649	650	651	652	653	654	655	656	657	658	659	660	661	662	663	664	665	666	667	668	669	670	671	672	673	674	675	676	677	678	679	680	681	682	683	684	685	686	687	688	689	690	691	692	693	694	695	696	697	698	699	700	701	702	703	704	705	706	707	708	709	710	711	712	713	714	715	716	717	718	719	720	721	722	723	724	725	726	727	728	729	730	731	732	733	734	735	736	737	738	739	740	741	742	743	744	745	746	747	748	749	750	751	752	753	754	755	756	757	758	759	760	761	762	763	764	765	766	767	768	769	770	771	772	773	774	775	776	777	778	779	780	781	782	783	784	785	786	787	788	789	790	791	792	793	794	795	796	797	798	799	800	801	802	803	804	805	806	807	808	809	810	811	812	813	814	815	816	817	818	819	820	821	822	823	824	825	826	827	828	829	830	831	832	833	834	835	836	837	838	839	840	841	842	843	844	845	846	847	848	849	850	851	852	853	854	855	856	857	858	859	860	861	862	863	864	865	866	867	868	869	870	871	872	873	874	875	876	877	878	879	880	881	882	883	884	885	886	887	888	889	890	891	892	893	894	895	896	897	898	899	900	901	902	903	904	905	906	907	908	909	910	911	912	913	914	915	916	917	918	919	920	921	922	923	924	925	926	927	928	929	930	931	932	933	934	935	936	937	938	939	940	941	942	943	944	945	946	947	948	949	950	951	952	953	954	955	956	957	958	959	960	961	962	963	964	965	966	967	968	969	970	971	972	973	974	975	976	977	978	979	980	981	982	983	984	985	986	987	988	989	990	991	992	993	994	995	996	997	998	999	1000
-----	-----	-----	-----	-----	-----	-----	-----	-----	-----	-----	-----	-----	-----	-----	-----	-----	-----	-----	-----	-----	-----	-----	-----	-----	-----	-----	-----	-----	-----	-----	-----	-----	-----	-----	-----	-----	-----	-----	-----	-----	-----	-----	-----	-----	-----	-----	-----	-----	-----	-----	-----	-----	-----	-----	-----	-----	-----	-----	-----	-----	-----	-----	-----	-----	-----	-----	-----	-----	-----	-----	-----	-----	-----	-----	-----	-----	-----	-----	-----	-----	-----	-----	-----	-----	-----	-----	-----	-----	-----	-----	-----	-----	-----	-----	-----	-----	-----	-----	-----	-----	-----	-----	-----	-----	-----	-----	-----	-----	-----	-----	-----	-----	-----	-----	-----	-----	-----	-----	-----	-----	-----	-----	-----	-----	-----	-----	-----	-----	-----	-----	-----	-----	-----	-----	-----	-----	-----	-----	-----	-----	-----	-----	-----	-----	-----	-----	-----	-----	-----	-----	-----	-----	-----	-----	-----	-----	-----	-----	-----	-----	-----	-----	-----	-----	-----	-----	-----	-----	-----	-----	-----	-----	-----	-----	-----	-----	-----	-----	-----	-----	-----	-----	-----	-----	-----	-----	-----	-----	-----	-----	-----	-----	-----	-----	-----	-----	-----	-----	-----	-----	-----	-----	-----	-----	-----	-----	-----	-----	-----	-----	-----	-----	-----	-----	-----	-----	-----	-----	-----	-----	-----	-----	-----	-----	-----	-----	-----	-----	-----	-----	-----	-----	-----	-----	-----	-----	-----	-----	-----	-----	-----	-----	-----	-----	-----	-----	-----	-----	-----	-----	-----	-----	-----	-----	-----	-----	-----	-----	-----	-----	-----	-----	-----	-----	-----	-----	-----	-----	-----	-----	-----	-----	-----	-----	-----	-----	-----	-----	-----	-----	-----	-----	-----	-----	-----	-----	-----	-----	-----	-----	-----	-----	-----	-----	-----	-----	-----	-----	-----	-----	-----	-----	-----	-----	-----	-----	-----	-----	-----	-----	-----	-----	-----	-----	-----	-----	-----	-----	-----	-----	-----	-----	-----	-----	-----	-----	-----	-----	-----	-----	-----	-----	-----	-----	-----	-----	-----	-----	-----	-----	-----	-----	-----	-----	-----	-----	-----	-----	-----	-----	-----	-----	-----	-----	-----	-----	-----	-----	-----	-----	-----	-----	-----	-----	-----	-----	-----	-----	-----	-----	-----	-----	-----	-----	-----	-----	-----	-----	-----	-----	-----	-----	-----	-----	-----	-----	-----	-----	-----	-----	-----	-----	-----	-----	-----	-----	-----	-----	-----	-----	-----	-----	-----	-----	-----	-----	-----	-----	-----	-----	-----	-----	-----	-----	-----	-----	-----	-----	-----	-----	-----	-----	-----	-----	-----	-----	-----	-----	-----	-----	-----	-----	-----	-----	-----	-----	-----	-----	-----	-----	-----	-----	-----	-----	-----	-----	-----	-----	-----	-----	-----	-----	-----	-----	-----	-----	-----	-----	-----	-----	-----	-----	-----	-----	-----	-----	-----	-----	-----	-----	-----	-----	-----	-----	-----	-----	-----	-----	-----	-----	-----	-----	-----	-----	-----	-----	-----	-----	-----	-----	-----	-----	-----	-----	-----	-----	-----	-----	-----	-----	-----	-----	-----	-----	-----	-----	-----	-----	-----	-----	-----	-----	-----	-----	-----	-----	-----	-----	-----	-----	-----	-----	-----	-----	-----	-----	-----	-----	-----	-----	-----	-----	-----	-----	-----	-----	-----	-----	-----	-----	-----	-----	-----	-----	-----	-----	-----	-----	-----	-----	-----	-----	-----	-----	-----	-----	-----	-----	-----	-----	-----	-----	-----	-----	-----	-----	-----	-----	-----	-----	-----	-----	-----	-----	-----	-----	-----	-----	-----	-----	-----	-----	-----	-----	-----	-----	-----	-----	-----	-----	-----	-----	-----	-----	-----	-----	-----	-----	-----	-----	-----	-----	-----	-----	-----	-----	-----	-----	-----	-----	-----	-----	-----	-----	-----	-----	-----	-----	-----	-----	-----	-----	-----	-----	-----	-----	-----	-----	-----	-----	-----	-----	-----	-----	-----	-----	-----	-----	-----	-----	-----	-----	-----	-----	-----	-----	-----	-----	-----	-----	-----	-----	-----	-----	-----	-----	-----	-----	-----	-----	-----	-----	-----	-----	-----	-----	-----	-----	-----	-----	-----	-----	-----	-----	-----	-----	-----	-----	-----	-----	-----	-----	-----	-----	-----	-----	-----	-----	-----	-----	-----	-----	-----	-----	-----	-----	-----	-----	-----	-----	-----	-----	-----	-----	-----	-----	-----	-----	-----	-----	-----	-----	-----	-----	-----	-----	-----	-----	-----	-----	-----	-----	-----	-----	-----	-----	-----	-----	-----	-----	-----	-----	-----	-----	-----	-----	-----	-----	-----	-----	-----	-----	-----	-----	-----	-----	-----	-----	-----	-----	-----	-----	-----	-----	-----	-----	-----	-----	-----	-----	-----	-----	-----	-----	-----	-----	-----	-----	-----	-----	-----	-----	-----	-----	-----	-----	-----	-----	-----	-----	-----	-----	-----	-----	-----	-----	-----	-----	-----	-----	-----	-----	-----	-----	-----	-----	-----	-----	-----	-----	-----	-----	-----	-----	-----	-----	-----	-----	-----	-----	-----	-----	-----	-----	-----	-----	-----	-----	-----	-----	-----	-----	-----	-----	-----	-----	-----	-----	-----	-----	-----	-----	-----	-----	-----	-----	-----	-----	-----	-----	-----	-----	-----	-----	-----	-----	-----	-----	-----	-----	-----	-----	-----	-----	-----	-----	-----	-----	-----	-----	-----	-----	-----	-----	-----	-----	-----	-----	-----	-----	-----	-----	-----	-----	-----	-----	-----	-----	-----	-----	-----	-----	-----	-----	-----	-----	-----	-----	-----	-----	-----	-----	-----	-----	-----	-----	-----	-----	------

FIG. 10B



FIG. 10B

100	104	106	108	110	112	114	116	118	120	122	124	126	128	130	132	134	136	138	140	142	144	146	148	150	152	154	156	158	160	162	164	166	168	170	172	174	176	178	180	182	184	186	188	190	192	194	196	198	200	202	204	206	208	210	212	214	216	218	220	222	224	226	228	230	232	234	236	238	240	242	244	246	248	250	252	254	256	258	260	262	264	266	268	270	272	274	276	278	280	282	284	286	288	290	292	294	296	298	300	302	304	306	308	310	312	314	316	318	320	322	324	326	328	330	332	334	336	338	340	342	344	346	348	350	352	354	356	358	360	362	364	366	368	370	372	374	376	378	380	382	384	386	388	390	392	394	396	398	400	402	404	406	408	410	412	414	416	418	420	422	424	426	428	430	432	434	436	438	440	442	444	446	448	450	452	454	456	458	460	462	464	466	468	470	472	474	476	478	480	482	484	486	488	490	492	494	496	498	500	502	504	506	508	510	512	514	516	518	520	522	524	526	528	530	532	534	536	538	540	542	544	546	548	550	552	554	556	558	560	562	564	566	568	570	572	574	576	578	580	582	584	586	588	590	592	594	596	598	600	602	604	606	608	610	612	614	616	618	620	622	624	626	628	630	632	634	636	638	640	642	644	646	648	650	652	654	656	658	660	662	664	666	668	670	672	674	676	678	680	682	684	686	688	690	692	694	696	698	700	702	704	706	708	710	712	714	716	718	720	722	724	726	728	730	732	734	736	738	740	742	744	746	748	750	752	754	756	758	760	762	764	766	768	770	772	774	776	778	780	782	784	786	788	790	792	794	796	798	800	802	804	806	808	810	812	814	816	818	820	822	824	826	828	830	832	834	836	838	840	842	844	846	848	850	852	854	856	858	860	862	864	866	868	870	872	874	876	878	880	882	884	886	888	890	892	894	896	898	900	902	904	906	908	910	912	914	916	918	920	922	924	926	928	930	932	934	936	938	940	942	944	946	948	950	952	954	956	958	960	962	964	966	968	970	972	974	976	978	980	982	984	986	988	990	992	994	996	998	1000
100	104	106	108	110	112	114	116	118	120	122	124	126	128	130	132	134	136	138	140	142	144	146	148	150	152	154	156	158	160	162	164	166	168	170	172	174	176	178	180	182	184	186	188	190	192	194	196	198	200	202	204	206	208	210	212	214	216	218	220	222	224	226	228	230	232	234	236	238	240	242	244	246	248	250	252	254	256	258	260	262	264	266	268	270	272	274	276	278	280	282	284	286	288	290	292	294	296	298	300	302	304	306	308	310	312	314	316	318	320	322	324	326	328	330	332	334	336	338	340	342	344	346	348	350	352	354	356	358	360	362	364	366	368	370	372	374	376	378	380	382	384	386	388	390	392	394	396	398	400	402	404	406	408	410	412	414	416	418	420	422	424	426	428	430	432	434	436	438	440	442	444	446	448	450	452	454	456	458	460	462	464	466	468	470	472	474	476	478	480	482	484	486	488	490	492	494	496	498	500	502	504	506	508	510	512	514	516	518	520	522	524	526	528	530	532	534	536	538	540	542	544	546	548	550	552	554	556	558	560	562	564	566	568	570	572	574	576	578	580	582	584	586	588	590	592	594	596	598	600	602	604	606	608	610	612	614	616	618	620	622	624	626	628	630	632	634	636	638	640	642	644	646	648	650	652	654	656	658	660	662	664	666	668	670	672	674	676	678	680	682	684	686	688	690	692	694	696	698	700	702	704	706	708	710	712	714	716	718	720	722	724	726	728	730	732	734	736	738	740	742	744	746	748	750	752	754	756	758	760	762	764	766	768	770	772	774	776	778	780	782	784	786	788	790	792	794	796	798	800	802	804	806	808	810	812	814	816	818	820	822	824	826	828	830	832	834	836	838	840	842	844	846	848	850	852	854	856	858	860	862	864	866	868	870	872	874	876	878	880	882	884	886	888	890	892	894	896	898	900	902	904	906	908	910	912	914	916	918	920	922	924	926	928	930	932	934	936	938	940	942	944	946	948	950	952	954	956	958	960	962	964	966	968	970	972	974	976	978	980	982	984	986	988	990	992	994	996	998	1000

FIG. 10C

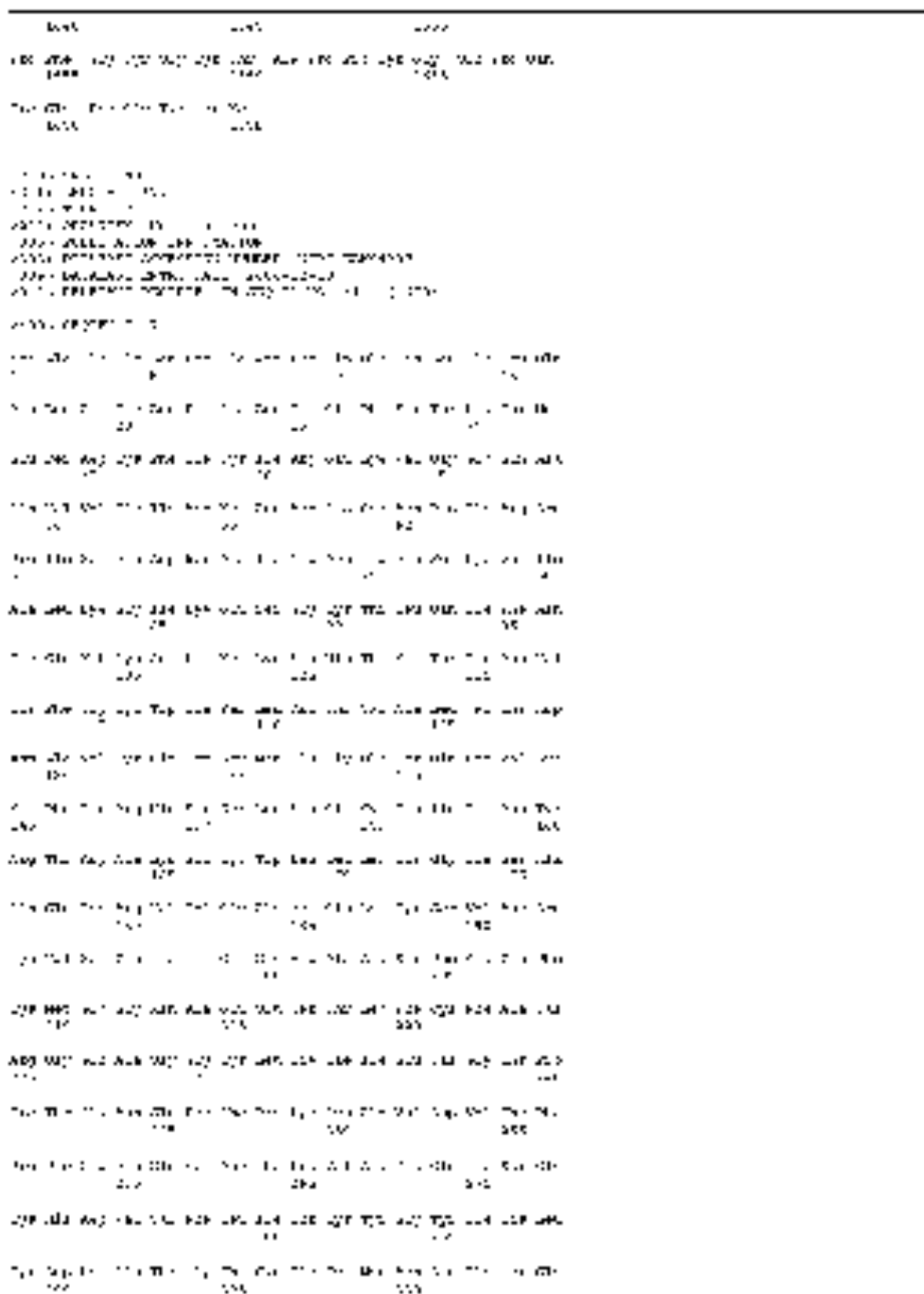


FIG. 10B

The figure displays a grid of 24 small diagrams, arranged in 8 rows and 3 columns. Each diagram represents a different configuration of components, likely related to a system architecture or a specific implementation. The diagrams use various symbols and patterns to denote different parts of the system.

Diagram 1 (Row 1, Col 1)	Diagram 2 (Row 1, Col 2)	Diagram 3 (Row 1, Col 3)
Diagram 4 (Row 2, Col 1)	Diagram 5 (Row 2, Col 2)	Diagram 6 (Row 2, Col 3)
Diagram 7 (Row 3, Col 1)	Diagram 8 (Row 3, Col 2)	Diagram 9 (Row 3, Col 3)
Diagram 10 (Row 4, Col 1)	Diagram 11 (Row 4, Col 2)	Diagram 12 (Row 4, Col 3)
Diagram 13 (Row 5, Col 1)	Diagram 14 (Row 5, Col 2)	Diagram 15 (Row 5, Col 3)
Diagram 16 (Row 6, Col 1)	Diagram 17 (Row 6, Col 2)	Diagram 18 (Row 6, Col 3)
Diagram 19 (Row 7, Col 1)	Diagram 20 (Row 7, Col 2)	Diagram 21 (Row 7, Col 3)
Diagram 22 (Row 8, Col 1)	Diagram 23 (Row 8, Col 2)	Diagram 24 (Row 8, Col 3)

FIG. 11



FIG. 10C



FIG. 10C1 1 2 3 4 5
 FIG. 10C2 2 3 4 5 1
 FIG. 10C3 3 4 5 1 2
 FIG. 10C4 4 5 1 2 3
 FIG. 10C5 5 1 2 3 4
 FIG. 10C6 1 2 3 4 5
 FIG. 10C7 2 3 4 5 1
 FIG. 10C8 3 4 5 1 2
 FIG. 10C9 4 5 1 2 3
 FIG. 10C10 5 1 2 3 4



FIG. 10D1 1 2 3 4 5
 FIG. 10D2 2 3 4 5 1
 FIG. 10D3 3 4 5 1 2
 FIG. 10D4 4 5 1 2 3
 FIG. 10D5 5 1 2 3 4
 FIG. 10D6 1 2 3 4 5
 FIG. 10D7 2 3 4 5 1
 FIG. 10D8 3 4 5 1 2
 FIG. 10D9 4 5 1 2 3
 FIG. 10D10 5 1 2 3 4

FIG. 10



FIG. 10C

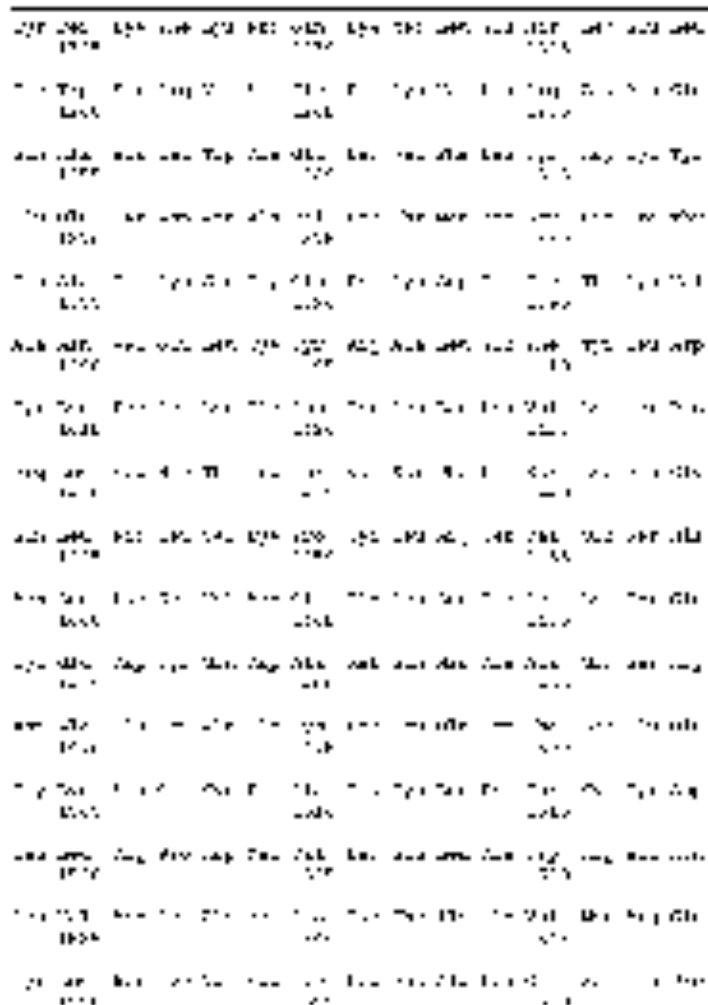


FIG. 10C

FIG. 10C-1
 FIG. 10C-2
 FIG. 10C-3
 FIG. 10C-4
 FIG. 10C-5
 FIG. 10C-6
 FIG. 10C-7
 FIG. 10C-8
 FIG. 10C-9
 FIG. 10C-10
 FIG. 10C-11
 FIG. 10C-12
 FIG. 10C-13
 FIG. 10C-14
 FIG. 10C-15
 FIG. 10C-16

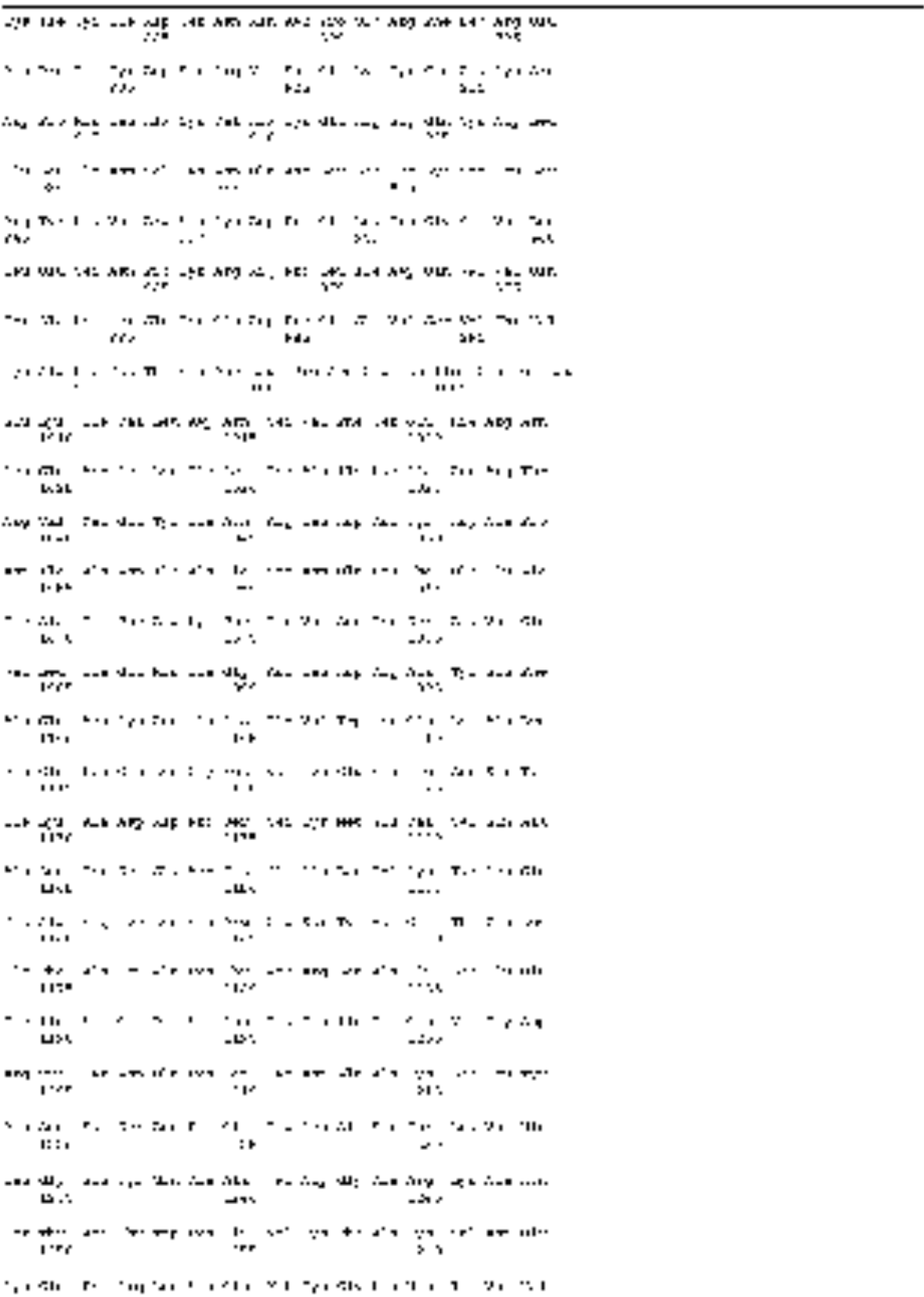
FIG. 10

10	20	30	40	50	60	70	80	90	100
Asp 496, 498, 499, 500, 501, 502, 503, 504, 505, 506, 507, 508, 509, 510, 511, 512, 513, 514, 515, 516, 517, 518, 519, 520, 521, 522, 523, 524, 525, 526, 527, 528, 529, 530, 531, 532, 533, 534, 535, 536, 537, 538, 539, 540, 541, 542, 543, 544, 545, 546, 547, 548, 549, 550, 551, 552, 553, 554, 555, 556, 557, 558, 559, 560, 561, 562, 563, 564, 565, 566, 567, 568, 569, 570, 571, 572, 573, 574, 575, 576, 577, 578, 579, 580, 581, 582, 583, 584, 585, 586, 587, 588, 589, 590, 591, 592, 593, 594, 595, 596, 597, 598, 599, 600, 601, 602, 603, 604, 605, 606, 607, 608, 609, 610, 611, 612, 613, 614, 615, 616, 617, 618, 619, 620, 621, 622, 623, 624, 625, 626, 627, 628, 629, 630, 631, 632, 633, 634, 635, 636, 637, 638, 639, 640, 641, 642, 643, 644, 645, 646, 647, 648, 649, 650, 651, 652, 653, 654, 655, 656, 657, 658, 659, 660, 661, 662, 663, 664, 665, 666, 667, 668, 669, 670, 671, 672, 673, 674, 675, 676, 677, 678, 679, 680, 681, 682, 683, 684, 685, 686, 687, 688, 689, 690, 691, 692, 693, 694, 695, 696, 697, 698, 699, 700, 701, 702, 703, 704, 705, 706, 707, 708, 709, 710, 711, 712, 713, 714, 715, 716, 717, 718, 719, 720, 721, 722, 723, 724, 725, 726, 727, 728, 729, 730, 731, 732, 733, 734, 735, 736, 737, 738, 739, 740, 741, 742, 743, 744, 745, 746, 747, 748, 749, 750, 751, 752, 753, 754, 755, 756, 757, 758, 759, 760, 761, 762, 763, 764, 765, 766, 767, 768, 769, 770, 771, 772, 773, 774, 775, 776, 777, 778, 779, 780, 781, 782, 783, 784, 785, 786, 787, 788, 789, 790, 791, 792, 793, 794, 795, 796, 797, 798, 799, 800, 801, 802, 803, 804, 805, 806, 807, 808, 809, 810, 811, 812, 813, 814, 815, 816, 817, 818, 819, 820, 821, 822, 823, 824, 825, 826, 827, 828, 829, 830, 831, 832, 833, 834, 835, 836, 837, 838, 839, 840, 841, 842, 843, 844, 845, 846, 847, 848, 849, 850, 851, 852, 853, 854, 855, 856, 857, 858, 859, 860, 861, 862, 863, 864, 865, 866, 867, 868, 869, 870, 871, 872, 873, 874, 875, 876, 877, 878, 879, 880, 881, 882, 883, 884, 885, 886, 887, 888, 889, 890, 891, 892, 893, 894, 895, 896, 897, 898, 899, 900, 901, 902, 903, 904, 905, 906, 907, 908, 909, 910, 911, 912, 913, 914, 915, 916, 917, 918, 919, 920, 921, 922, 923, 924, 925, 926, 927, 928, 929, 930, 931, 932, 933, 934, 935, 936, 937, 938, 939, 940, 941, 942, 943, 944, 945, 946, 947, 948, 949, 950, 951, 952, 953, 954, 955, 956, 957, 958, 959, 960, 961, 962, 963, 964, 965, 966, 967, 968, 969, 970, 971, 972, 973, 974, 975, 976, 977, 978, 979, 980, 981, 982, 983, 984, 985, 986, 987, 988, 989, 990, 991, 992, 993, 994, 995, 996, 997, 998, 999, 1000									

FIG. 13



FIG. 10C



 CONT. NUMS

NUM	NUM	NUM
133 405 225 345 465 585	147 525 645 765 885	161 605 725 845 965
134 405 225 345 465	148 525 645 765 885	162 605 725 845 965
135 405 225 345 465	149 525 645 765 885	163 605 725 845 965
136 405 225 345 465	150 525 645 765 885	164 605 725 845 965
137 405 225 345 465	151 525 645 765 885	165 605 725 845 965
138 405 225 345 465	152 525 645 765 885	166 605 725 845 965
139 405 225 345 465	153 525 645 765 885	167 605 725 845 965
140 405 225 345 465	154 525 645 765 885	168 605 725 845 965
141 405 225 345 465	155 525 645 765 885	169 605 725 845 965
142 405 225 345 465	156 525 645 765 885	170 605 725 845 965
143 405 225 345 465	157 525 645 765 885	171 605 725 845 965
144 405 225 345 465	158 525 645 765 885	172 605 725 845 965
145 405 225 345 465	159 525 645 765 885	173 605 725 845 965
146 405 225 345 465	160 525 645 765 885	174 605 725 845 965
147 405 225 345 465	161 525 645 765 885	175 605 725 845 965
148 405 225 345 465	162 525 645 765 885	176 605 725 845 965
149 405 225 345 465	163 525 645 765 885	177 605 725 845 965
150 405 225 345 465	164 525 645 765 885	178 605 725 845 965
151 405 225 345 465	165 525 645 765 885	179 605 725 845 965
152 405 225 345 465	166 525 645 765 885	180 605 725 845 965
153 405 225 345 465	167 525 645 765 885	181 605 725 845 965
154 405 225 345 465	168 525 645 765 885	182 605 725 845 965
155 405 225 345 465	169 525 645 765 885	183 605 725 845 965
156 405 225 345 465	170 525 645 765 885	184 605 725 845 965
157 405 225 345 465	171 525 645 765 885	185 605 725 845 965
158 405 225 345 465	172 525 645 765 885	186 605 725 845 965
159 405 225 345 465	173 525 645 765 885	187 605 725 845 965
160 405 225 345 465	174 525 645 765 885	188 605 725 845 965
161 405 225 345 465	175 525 645 765 885	189 605 725 845 965
162 405 225 345 465	176 525 645 765 885	190 605 725 845 965
163 405 225 345 465	177 525 645 765 885	191 605 725 845 965
164 405 225 345 465	178 525 645 765 885	192 605 725 845 965
165 405 225 345 465	179 525 645 765 885	193 605 725 845 965
166 405 225 345 465	180 525 645 765 885	194 605 725 845 965
167 405 225 345 465	181 525 645 765 885	195 605 725 845 965
168 405 225 345 465	182 525 645 765 885	196 605 725 845 965
169 405 225 345 465	183 525 645 765 885	197 605 725 845 965
170 405 225 345 465	184 525 645 765 885	198 605 725 845 965
171 405 225 345 465	185 525 645 765 885	199 605 725 845 965
172 405 225 345 465	186 525 645 765 885	200 605 725 845 965

FIG. 10B

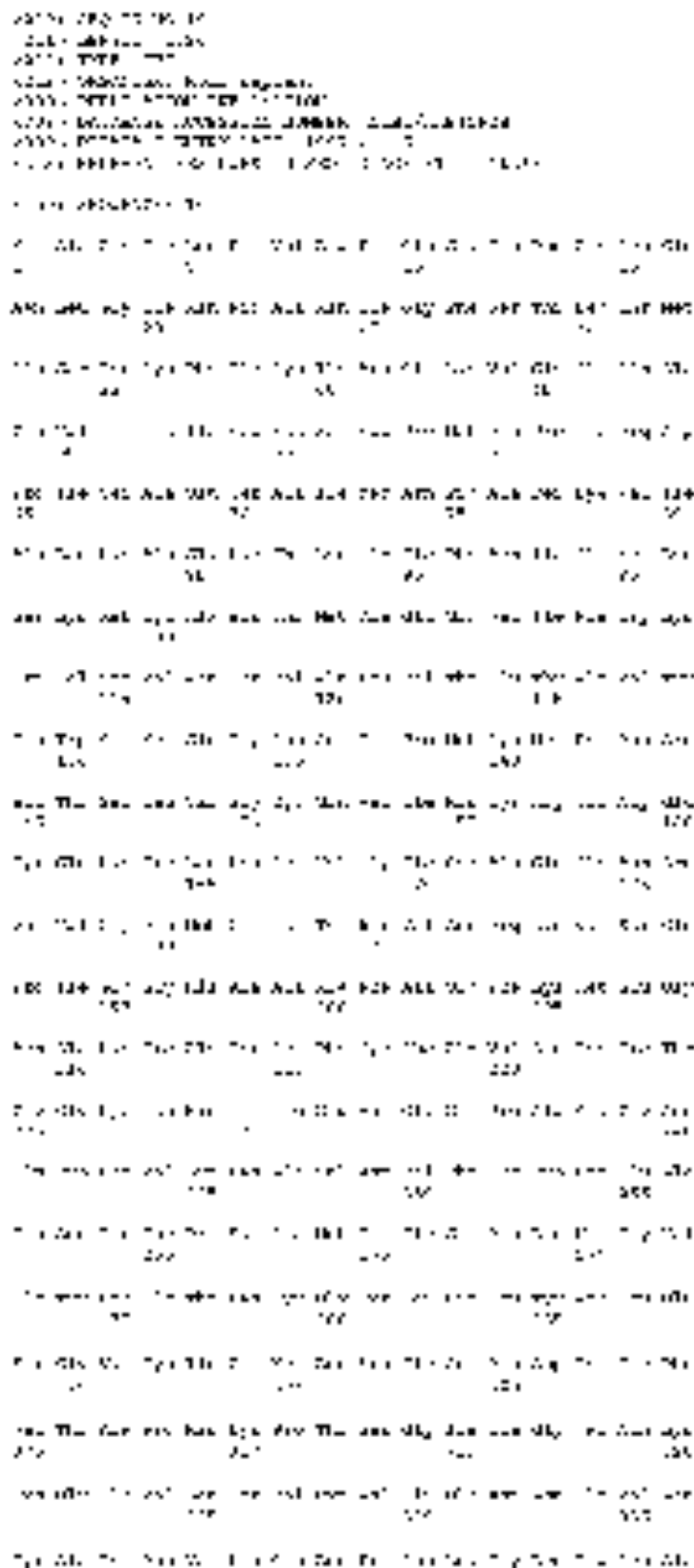


FIG. 10



FIG. 110C

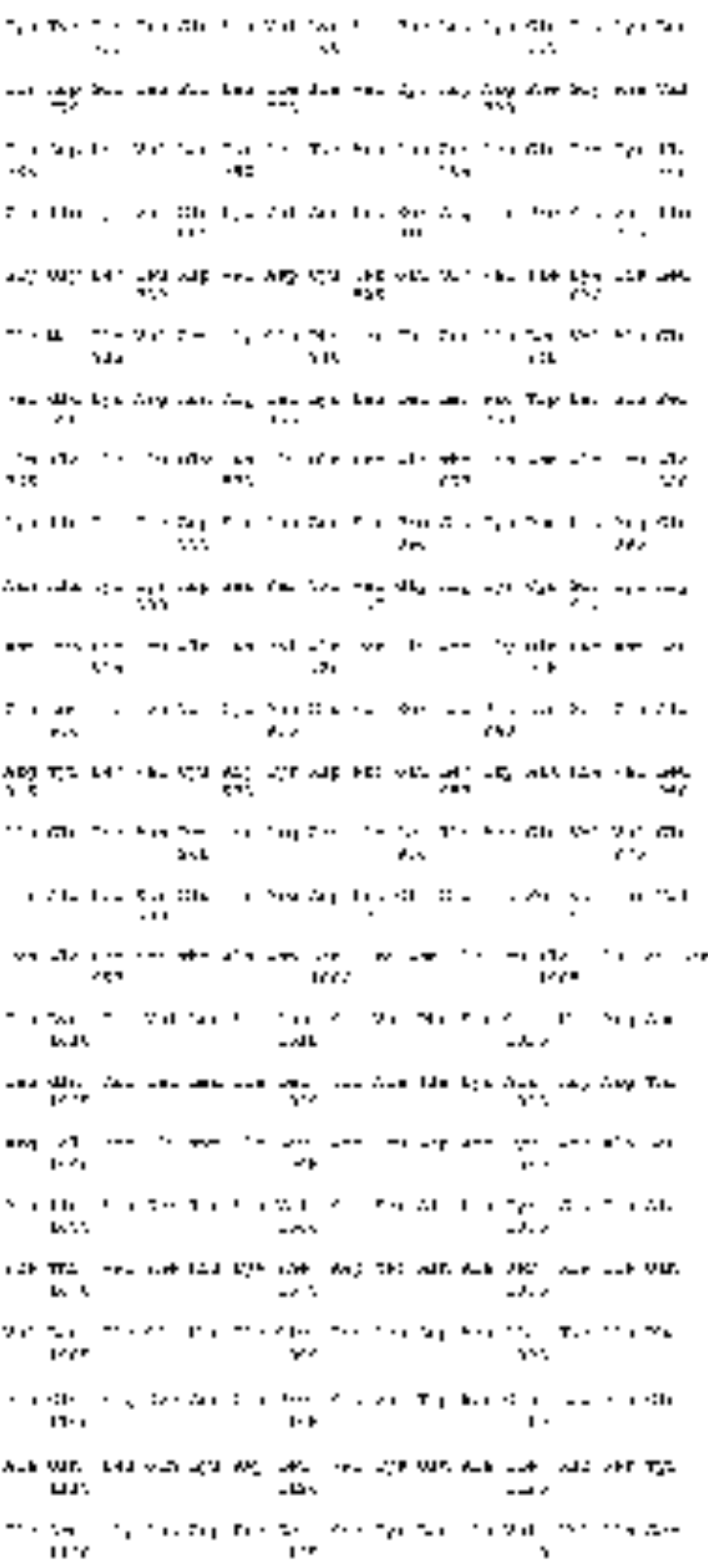


FIG. 10B



FIG. 10B

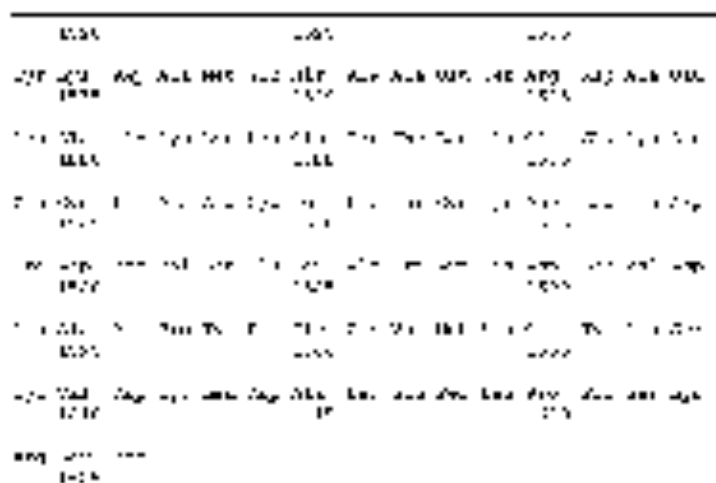


FIG. 10B is a schematic diagram of a network topology. The network includes nodes 1000, 1001, and 1002. Node 1000 is connected to nodes 1001 and 1002. Node 1001 is connected to node 1002. There are also connections between nodes 1000 and 1001, and 1001 and 1002, representing a mesh or ring topology.

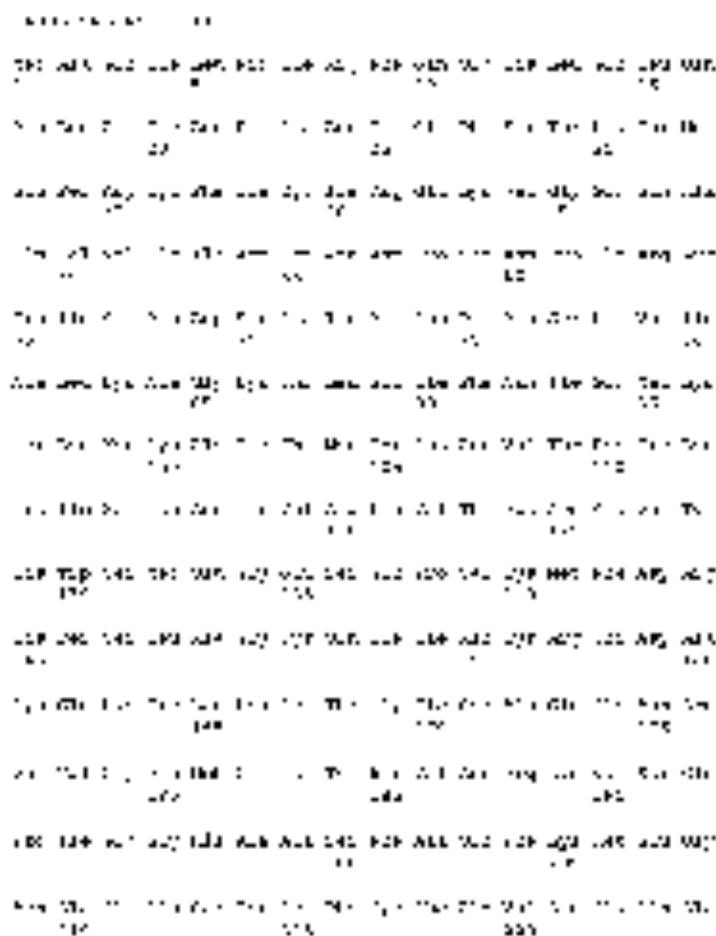


FIG. 10C is a schematic diagram of a network topology. The network includes nodes 1000, 1001, and 1002. Node 1000 is connected to nodes 1001 and 1002. Node 1001 is connected to node 1002. There are also connections between nodes 1000 and 1001, and 1001 and 1002, representing a mesh or ring topology.

FIG. 10

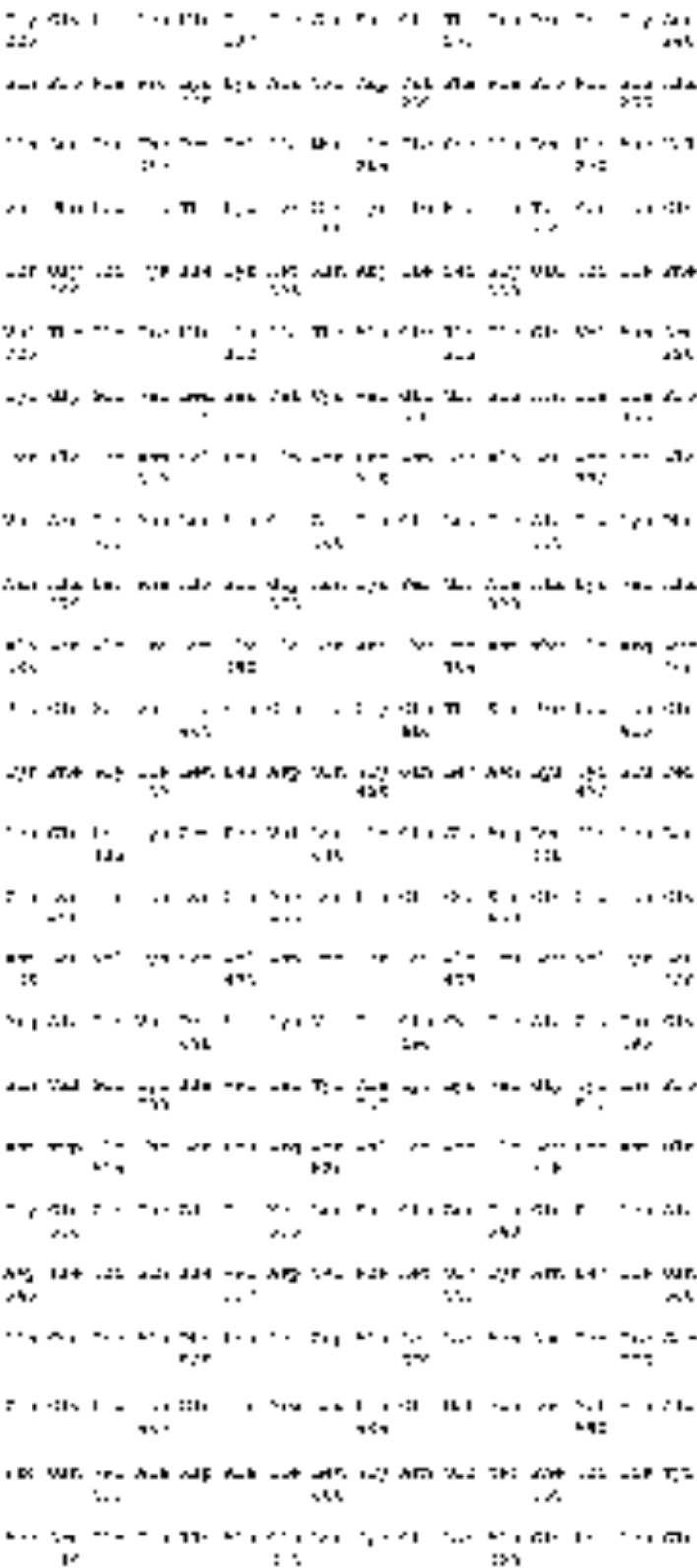


FIG. 10B



 FIG. 10

1001	1002	1003	1004	1005	1006	1007	1008	1009	1010
1011	1012	1013	1014	1015	1016	1017	1018	1019	1020
1021	1022	1023	1024	1025	1026	1027	1028	1029	1030
1031	1032	1033	1034	1035	1036	1037	1038	1039	1040
1041	1042	1043	1044	1045	1046	1047	1048	1049	1050
1051	1052	1053	1054	1055	1056	1057	1058	1059	1060
1061	1062	1063	1064	1065	1066	1067	1068	1069	1070
1071	1072	1073	1074	1075	1076	1077	1078	1079	1080
1081	1082	1083	1084	1085	1086	1087	1088	1089	1090
1091	1092	1093	1094	1095	1096	1097	1098	1099	1100
1101	1102	1103	1104	1105	1106	1107	1108	1109	1110
1111	1112	1113	1114	1115	1116	1117	1118	1119	1120
1121	1122	1123	1124	1125	1126	1127	1128	1129	1130
1131	1132	1133	1134	1135	1136	1137	1138	1139	1140
1141	1142	1143	1144	1145	1146	1147	1148	1149	1150
1151	1152	1153	1154	1155	1156	1157	1158	1159	1160
1161	1162	1163	1164	1165	1166	1167	1168	1169	1170
1171	1172	1173	1174	1175	1176	1177	1178	1179	1180
1181	1182	1183	1184	1185	1186	1187	1188	1189	1190
1191	1192	1193	1194	1195	1196	1197	1198	1199	1200
1201	1202	1203	1204	1205	1206	1207	1208	1209	1210
1211	1212	1213	1214	1215	1216	1217	1218	1219	1220
1221	1222	1223	1224	1225	1226	1227	1228	1229	1230
1231	1232	1233	1234	1235	1236	1237	1238	1239	1240
1241	1242	1243	1244	1245	1246	1247	1248	1249	1250
1251	1252	1253	1254	1255	1256	1257	1258	1259	1260
1261	1262	1263	1264	1265	1266	1267	1268	1269	1270
1271	1272	1273	1274	1275	1276	1277	1278	1279	1280
1281	1282	1283	1284	1285	1286	1287	1288	1289	1290
1291	1292	1293	1294	1295	1296	1297	1298	1299	1300

FIG. 10



FIG. 10C

1010 1011 1012 1013 1014 1015 1016 1017 1018 1019 1020 1021 1022 1023 1024 1025 1026 1027 1028 1029 1030
 1031 1032 1033 1034 1035 1036 1037 1038 1039 1040 1041 1042 1043 1044 1045 1046 1047 1048 1049 1050 1051
 1052 1053 1054 1055 1056 1057 1058 1059 1060 1061 1062 1063 1064 1065 1066 1067 1068 1069 1070 1071 1072
 1073 1074 1075 1076 1077 1078 1079 1080 1081 1082 1083 1084 1085 1086 1087 1088 1089 1090 1091 1092 1093

FIG. 10C (continued)

```

1094 1095 1096 1097 1098 1099 1100 1101 1102 1103 1104 1105 1106 1107 1108 1109 1110 1111 1112 1113 1114
1115 1116 1117 1118 1119 1120 1121 1122 1123 1124 1125 1126 1127 1128 1129 1130 1131 1132 1133 1134 1135
1136 1137 1138 1139 1140 1141 1142 1143 1144 1145 1146 1147 1148 1149 1150 1151 1152 1153 1154 1155 1156
1157 1158 1159 1160 1161 1162 1163 1164 1165 1166 1167 1168 1169 1170 1171 1172 1173 1174 1175 1176 1177
1178 1179 1180 1181 1182 1183 1184 1185 1186 1187 1188 1189 1190 1191 1192 1193 1194 1195 1196 1197 1198
1199 1200 1201 1202 1203 1204 1205 1206 1207 1208 1209 1210 1211 1212 1213 1214 1215 1216 1217 1218 1219
1220 1221 1222 1223 1224 1225 1226 1227 1228 1229 1230 1231 1232 1233 1234 1235 1236 1237 1238 1239 1240
  
```

FIG. 10C (continued)

1241 1242 1243 1244 1245 1246 1247 1248 1249 1250 1251 1252 1253 1254 1255 1256 1257 1258 1259 1260 1261
 1262 1263 1264 1265 1266 1267 1268 1269 1270 1271 1272 1273 1274 1275 1276 1277 1278 1279 1280 1281 1282
 1283 1284 1285 1286 1287 1288 1289 1290 1291 1292 1293 1294 1295 1296 1297 1298 1299 1300 1301 1302 1303
 1304 1305 1306 1307 1308 1309 1310 1311 1312 1313 1314 1315 1316 1317 1318 1319 1320 1321 1322 1323 1324
 1325 1326 1327 1328 1329 1330 1331 1332 1333 1334 1335 1336 1337 1338 1339 1340 1341 1342 1343 1344 1345

FIG. 10C (continued)

1346 1347 1348 1349 1350 1351 1352 1353 1354 1355 1356 1357 1358 1359 1360 1361 1362 1363 1364 1365 1366
 1367 1368 1369 1370 1371 1372 1373 1374 1375 1376 1377 1378 1379 1380 1381 1382 1383 1384 1385 1386 1387
 1388 1389 1390 1391 1392 1393 1394 1395 1396 1397 1398 1399 1400 1401 1402 1403 1404 1405 1406 1407 1408
 1409 1410 1411 1412 1413 1414 1415 1416 1417 1418 1419 1420 1421 1422 1423 1424 1425 1426 1427 1428 1429
 1430 1431 1432 1433 1434 1435 1436 1437 1438 1439 1440 1441 1442 1443 1444 1445 1446 1447 1448 1449 1450

FIG. 10C (continued)

1451 1452 1453 1454 1455 1456 1457 1458 1459 1460 1461 1462 1463 1464 1465 1466 1467 1468 1469 1470 1471
 1472 1473 1474 1475 1476 1477 1478 1479 1480 1481 1482 1483 1484 1485 1486 1487 1488 1489 1490 1491 1492
 1493 1494 1495 1496 1497 1498 1499 1500 1501 1502 1503 1504 1505 1506 1507 1508 1509 1510 1511 1512 1513
 1514 1515 1516 1517 1518 1519 1520 1521 1522 1523 1524 1525 1526 1527 1528 1529 1530 1531 1532 1533 1534
 1535 1536 1537 1538 1539 1540 1541 1542 1543 1544 1545 1546 1547 1548 1549 1550 1551 1552 1553 1554 1555

FIG. 10C (continued)

1556 1557 1558 1559 1560 1561 1562 1563 1564 1565 1566 1567 1568 1569 1570 1571 1572 1573 1574 1575 1576
 1577 1578 1579 1580 1581 1582 1583 1584 1585 1586 1587 1588 1589 1590 1591 1592 1593 1594 1595 1596 1597
 1598 1599 1600 1601 1602 1603 1604 1605 1606 1607 1608 1609 1610 1611 1612 1613 1614 1615 1616 1617 1618
 1619 1620 1621 1622 1623 1624 1625 1626 1627 1628 1629 1630 1631 1632 1633 1634 1635 1636 1637 1638 1639
 1640 1641 1642 1643 1644 1645 1646 1647 1648 1649 1650 1651 1652 1653 1654 1655 1656 1657 1658 1659 1660

FIG. 10C (continued)

```

1661 1662 1663 1664 1665 1666 1667 1668 1669 1670 1671 1672 1673 1674 1675 1676 1677 1678 1679 1680 1681
1682 1683 1684 1685 1686 1687 1688 1689 1690 1691 1692 1693 1694 1695 1696 1697 1698 1699 1700 1701 1702
1703 1704 1705 1706 1707 1708 1709 1710 1711 1712 1713 1714 1715 1716 1717 1718 1719 1720 1721 1722 1723
1724 1725 1726 1727 1728 1729 1730 1731 1732 1733 1734 1735 1736 1737 1738 1739 1740 1741 1742 1743 1744
1745 1746 1747 1748 1749 1750 1751 1752 1753 1754 1755 1756 1757 1758 1759 1760 1761 1762 1763 1764 1765
  
```

FIG. 10A

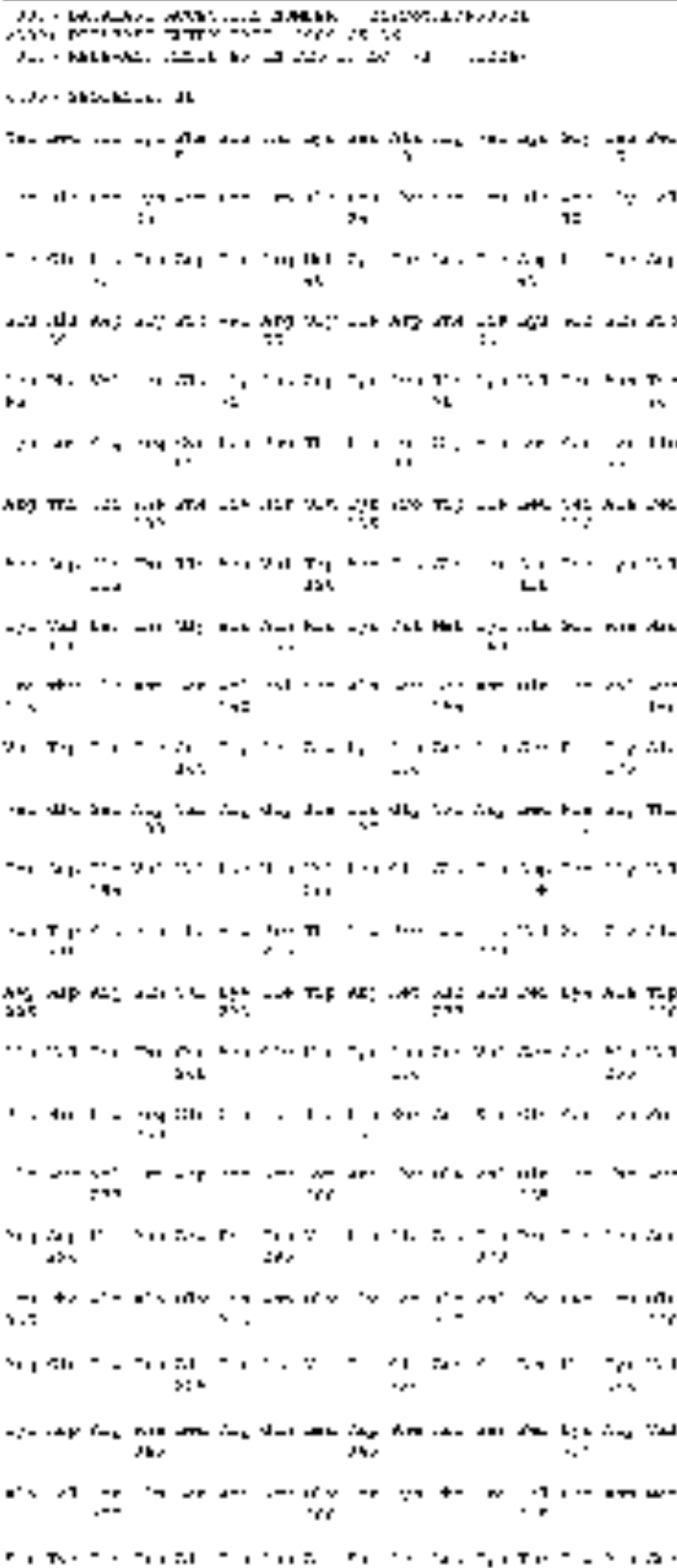


FIG. 1000



FIG. 11

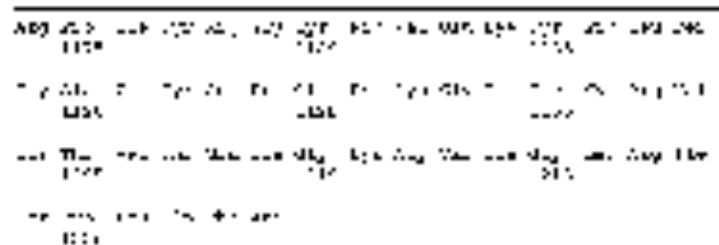


FIG. 11 is a diagram illustrating a sequence of operations for a first device. The sequence starts with 'Device 1' and 'Device 2' at the top. Below, a series of operations are shown in boxes: 'Device 1 sends data to Device 2', 'Device 2 receives data from Device 1', 'Device 1 sends data to Device 2', 'Device 2 receives data from Device 1', 'Device 1 sends data to Device 2', 'Device 2 receives data from Device 1', 'Device 1 sends data to Device 2', 'Device 2 receives data from Device 1'. The operations are connected by arrows indicating the flow of data.

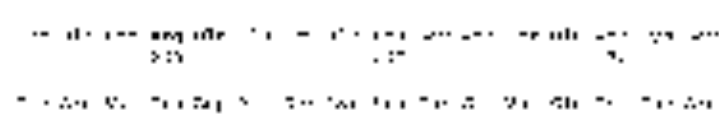
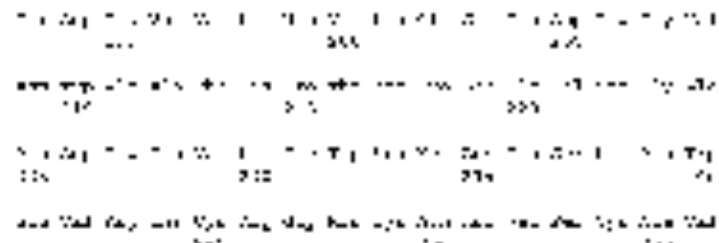
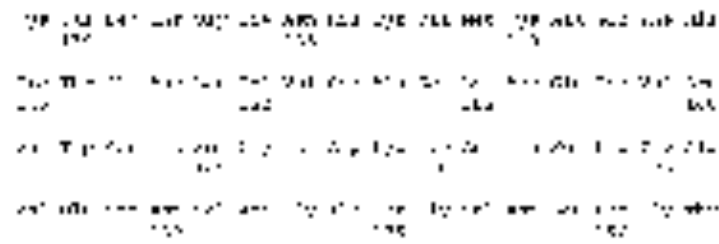
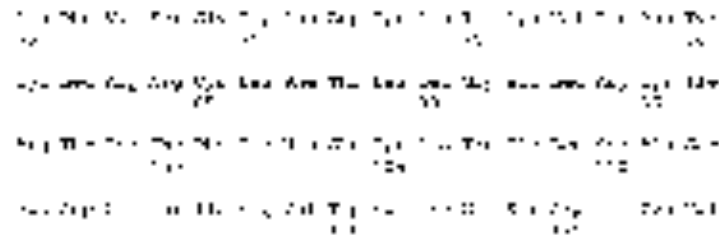
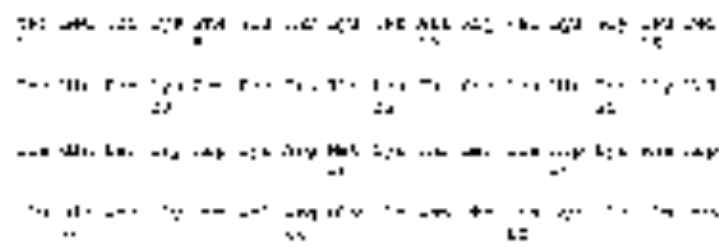


FIG. 10

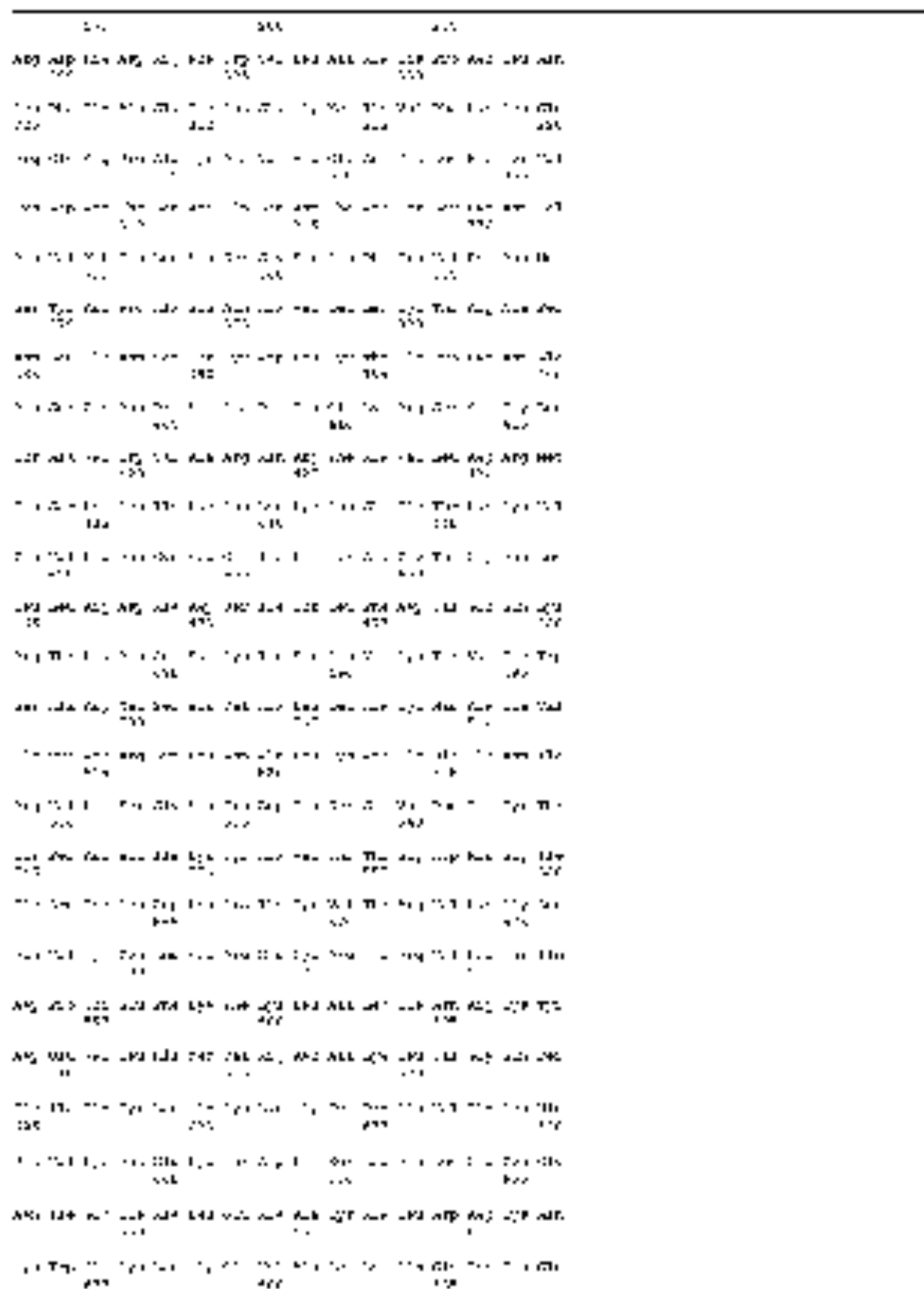


FIG. 10C

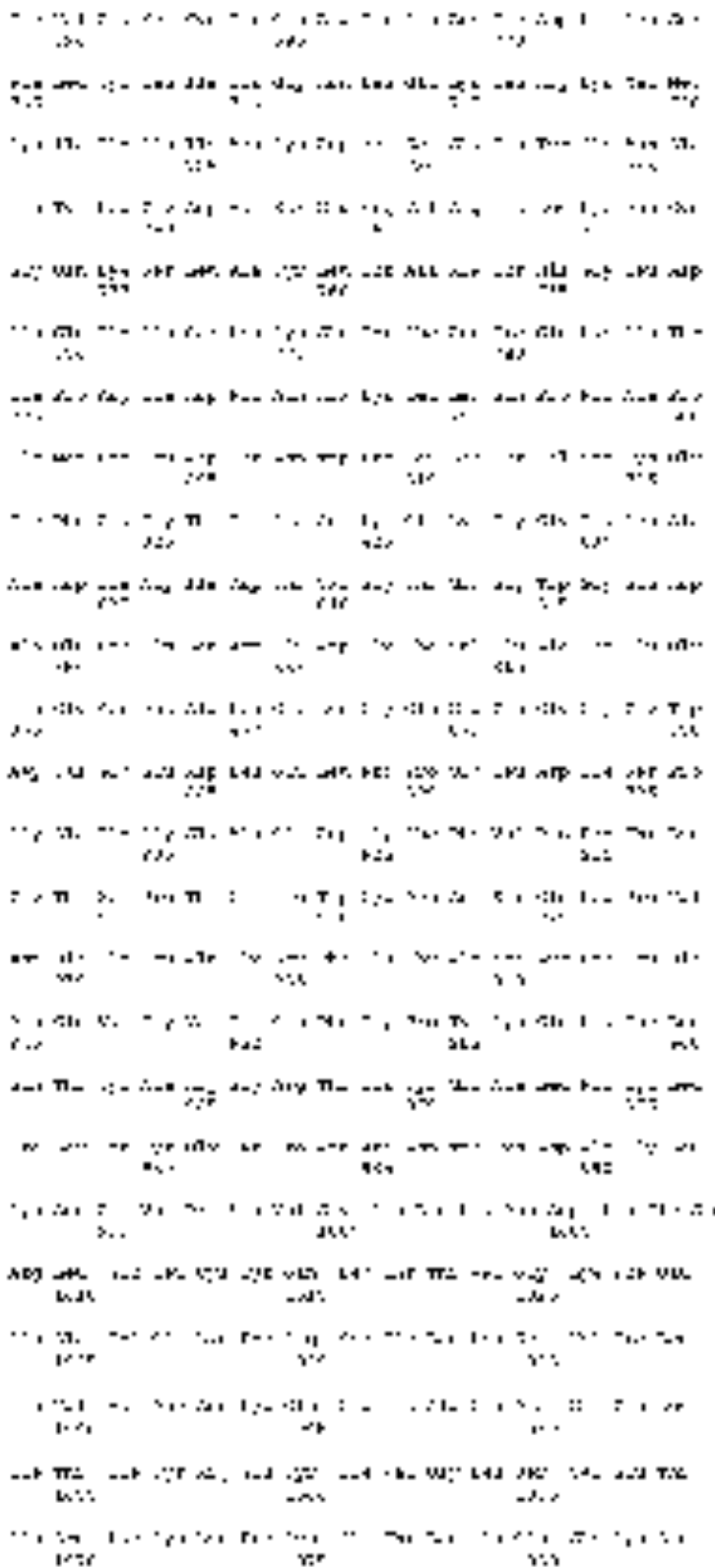


FIG. 1000



FIG. 10C

	100	200	300	400	500	600	700	800	900	1000	1100	1200	1300
2015 Jun	195	194	195	197	199	201	203	205	207	209	211	213	215
2015 Jul	193	194	195	197	199	201	203	205	207	209	211	213	215
2015 Aug	191	192	193	195	197	199	201	203	205	207	209	211	213
2015 Sep	189	190	191	193	195	197	199	201	203	205	207	209	211
2015 Oct	187	188	189	191	193	195	197	199	201	203	205	207	209
2015 Nov	185	186	187	189	191	193	195	197	199	201	203	205	207
2015 Dec	183	184	185	187	189	191	193	195	197	199	201	203	205
2016 Jan	181	182	183	185	187	189	191	193	195	197	199	201	203
2016 Feb	179	180	181	183	185	187	189	191	193	195	197	199	201
2016 Mar	177	178	179	181	183	185	187	189	191	193	195	197	199
2016 Apr	175	176	177	179	181	183	185	187	189	191	193	195	197
2016 May	173	174	175	177	179	181	183	185	187	189	191	193	195
2016 Jun	171	172	173	175	177	179	181	183	185	187	189	191	193
2016 Jul	169	170	171	173	175	177	179	181	183	185	187	189	191
2016 Aug	167	168	169	171	173	175	177	179	181	183	185	187	189
2016 Sep	165	166	167	169	171	173	175	177	179	181	183	185	187
2016 Oct	163	164	165	167	169	171	173	175	177	179	181	183	185
2016 Nov	161	162	163	165	167	169	171	173	175	177	179	181	183
2016 Dec	159	160	161	163	165	167	169	171	173	175	177	179	181
2017 Jan	157	158	159	161	163	165	167	169	171	173	175	177	179
2017 Feb	155	156	157	159	161	163	165	167	169	171	173	175	177
2017 Mar	153	154	155	157	159	161	163	165	167	169	171	173	175
2017 Apr	151	152	153	155	157	159	161	163	165	167	169	171	173
2017 May	149	150	151	153	155	157	159	161	163	165	167	169	171
2017 Jun	147	148	149	151	153	155	157	159	161	163	165	167	169
2017 Jul	145	146	147	149	151	153	155	157	159	161	163	165	167
2017 Aug	143	144	145	147	149	151	153	155	157	159	161	163	165
2017 Sep	141	142	143	145	147	149	151	153	155	157	159	161	163
2017 Oct	139	140	141	143	145	147	149	151	153	155	157	159	161
2017 Nov	137	138	139	141	143	145	147	149	151	153	155	157	159
2017 Dec	135	136	137	139	141	143	145	147	149	151	153	155	157
2018 Jan	133	134	135	137	139	141	143	145	147	149	151	153	155
2018 Feb	131	132	133	135	137	139	141	143	145	147	149	151	153
2018 Mar	129	130	131	133	135	137	139	141	143	145	147	149	151
2018 Apr	127	128	129	131	133	135	137	139	141	143	145	147	149
2018 May	125	126	127	129	131	133	135	137	139	141	143	145	147
2018 Jun	123	124	125	127	129	131	133	135	137	139	141	143	145
2018 Jul	121	122	123	125	127	129	131	133	135	137	139	141	143
2018 Aug	119	120	121	123	125	127	129	131	133	135	137	139	141
2018 Sep	117	118	119	121	123	125	127	129	131	133	135	137	139
2018 Oct	115	116	117	119	121	123	125	127	129	131	133	135	137
2018 Nov	113	114	115	117	119	121	123	125	127	129	131	133	135
2018 Dec	111	112	113	115	117	119	121	123	125	127	129	131	133
2019 Jan	109	110	111	113	115	117	119	121	123	125	127	129	131
2019 Feb	107	108	109	111	113	115	117	119	121	123	125	127	129
2019 Mar	105	106	107	109	111	113	115	117	119	121	123	125	127
2019 Apr	103	104	105	107	109	111	113	115	117	119	121	123	125
2019 May	101	102	103	105	107	109	111	113	115	117	119	121	123
2019 Jun	99	100	101	103	105	107	109	111	113	115	117	119	121
2019 Jul	97	98	99	101	103	105	107	109	111	113	115	117	119
2019 Aug	95	96	97	99	101	103	105	107	109	111	113	115	117
2019 Sep	93	94	95	97	99	101	103	105	107	109	111	113	115
2019 Oct	91	92	93	95	97	99	101	103	105	107	109	111	113
2019 Nov	89	90	91	93	95	97	99	101	103	105	107	109	111
2019 Dec	87	88	89	91	93	95	97	99	101	103	105	107	109
2020 Jan	85	86	87	89	91	93	95	97	99	101	103	105	107
2020 Feb	83	84	85	87	89	91	93	95	97	99	101	103	105
2020 Mar	81	82	83	85	87	89	91	93	95	97	99	101	103
2020 Apr	79	80	81	83	85	87	89	91	93	95	97	99	101
2020 May	77	78	79	81	83	85	87	89	91	93	95	97	99
2020 Jun	75	76	77	79	81	83	85	87	89	91	93	95	97
2020 Jul	73	74	75	77	79	81	83	85	87	89	91	93	95
2020 Aug	71	72	73	75	77	79	81	83	85	87	89	91	93
2020 Sep	69	70	71	73	75	77	79	81	83	85	87	89	91
2020 Oct	67	68	69	71	73	75	77	79	81	83	85	87	89
2020 Nov	65	66	67	69	71	73	75	77	79	81	83	85	87
2020 Dec	63	64	65	67	69	71	73	75	77	79	81	83	85
2021 Jan	61	62	63	65	67	69	71	73	75	77	79	81	83
2021 Feb	59	60	61	63	65	67	69	71	73	75	77	79	81
2021 Mar	57	58	59	61	63	65	67	69	71	73	75	77	79
2021 Apr	55	56	57	59	61	63	65	67	69	71	73	75	77
2021 May	53	54	55	57	59	61	63	65	67	69	71	73	75
2021 Jun	51	52	53	55	57	59	61	63	65	67	69	71	73
2021 Jul	49	50	51	53	55	57	59	61	63	65	67	69	71
2021 Aug	47	48	49	51	53	55	57	59	61	63	65	67	69
2021 Sep	45	46	47	49	51	53	55	57	59	61	63	65	67
2021 Oct	43	44	45	47	49	51	53	55	57	59	61	63	65
2021 Nov	41	42	43	45	47	49	51	53	55	57	59	61	63
2021 Dec	39	40	41	43	45	47	49	51	53	55	57	59	61
2022 Jan	37	38	39	41	43	45	47	49	51	53	55	57	59
2022 Feb	35	36	37	39	41	43	45	47	49	51	53	55	57
2022 Mar	33	34	35	37	39	41	43	45	47	49	51	53	55
2022 Apr	31	32	33	35	37	39	41	43	45	47	49	51	53
2022 May	29	30	31	33	35	37	39	41	43	45	47	49	51
2022 Jun	27	28	29	31	33	35	37	39	41	43	45	47	49
2022 Jul	25	26	27	29	31	33	35	37	39	41	43	45	47
2022 Aug	23	24	25	27	29	31	33	35	37	39	41	43	45
2022 Sep	21	22	23	25	27	29	31	33	35	37	39	41	43
2022 Oct	19	20	21	23	25	27	29	31	33	35	37	39	41
2022 Nov	17	18	19	21	23	25	27	29	31	33	35	37	39
2022 Dec	15	16	17	19	21	23	25	27	29	31	33	35	37
2023 Jan	13	14	15	17	19	21	23	25	27	29	31	33	35
2023 Feb	11	12	13	15	17	19	21	23	25	27	29	3	

FIG. 10B

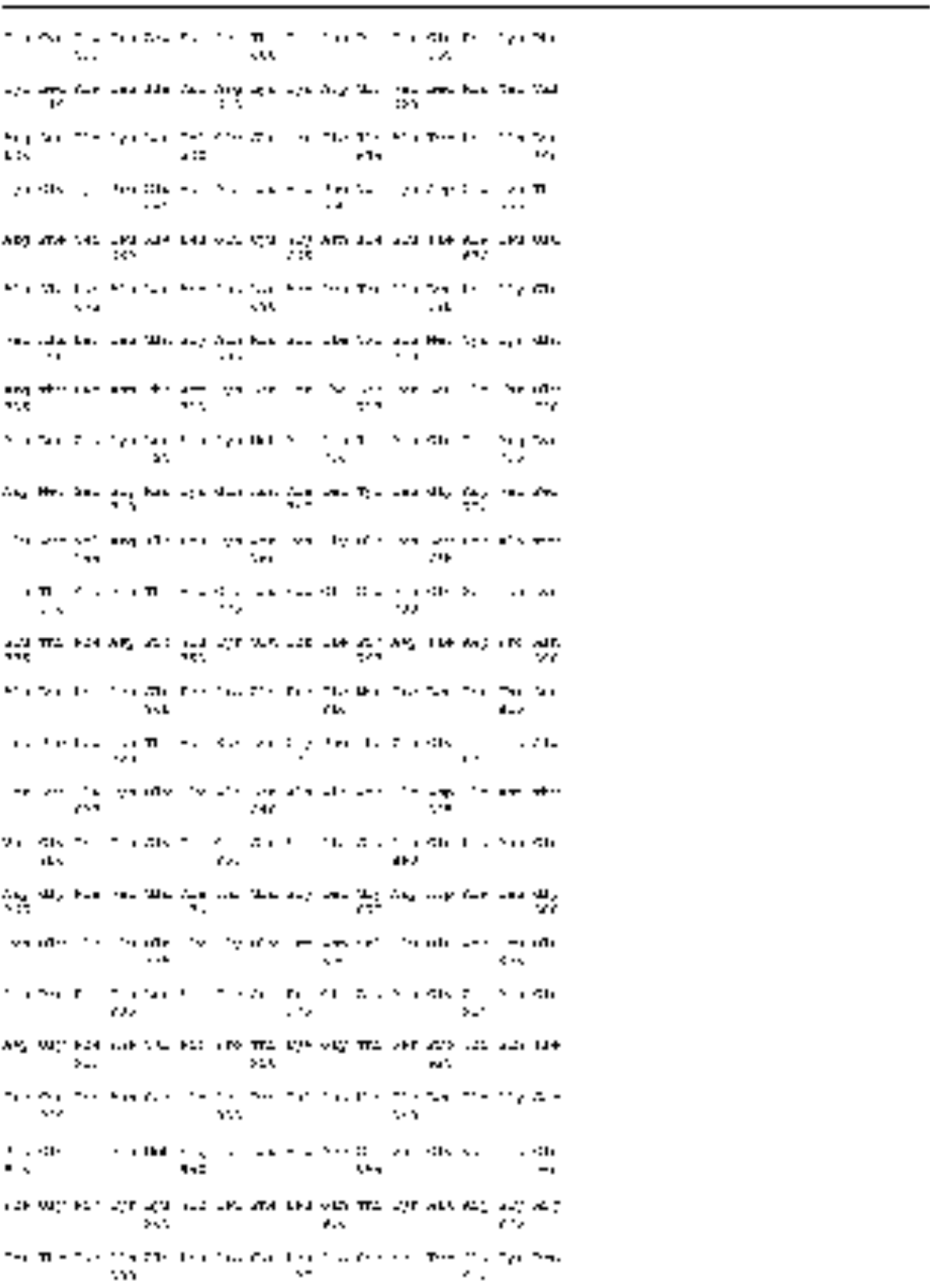
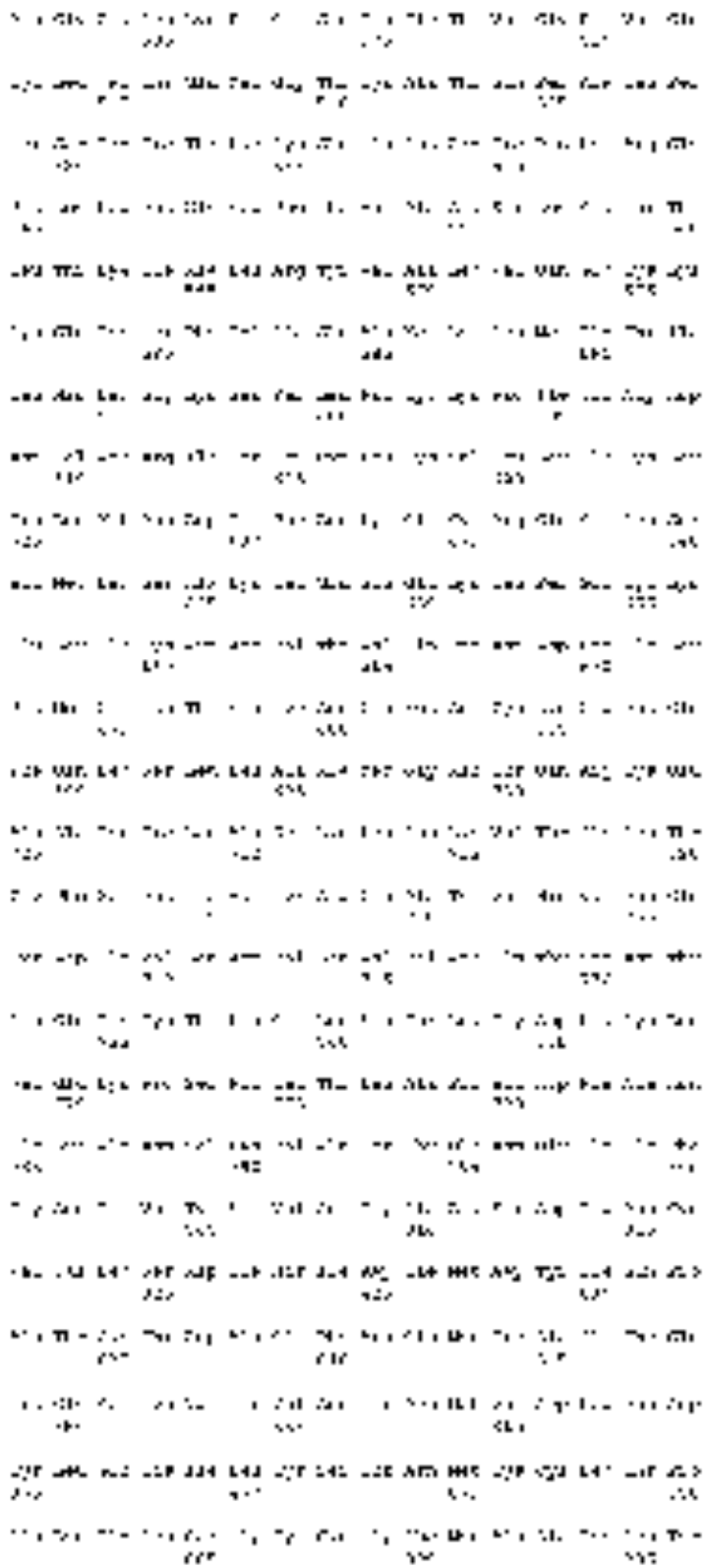


FIG. 10



FIG. 10 is a flowchart illustrating a process for collecting user information. The process starts at block 101 (START) and proceeds to block 102 (GET USER ID). From block 102, the process moves to block 103 (GET USER NAME), then to block 104 (GET USER ADDRESS), block 105 (GET USER PHONE NUMBER), block 106 (GET USER EMAIL ADDRESS), block 107 (GET USER SOCIAL MEDIA ACCOUNTS), block 108 (GET USER INTERESTS), block 109 (GET USER PREFERENCES), block 110 (GET USER LOCATION), block 111 (GET USER DEVICE INFORMATION), and block 112 (GET USER BROWSER INFORMATION). The process concludes at block 113 (END).

FIG. 11C



- CONTINUED -

410	415	420	425	430	435	440	445	450	455	460	465	470	475	480	485	490	495	500	505	510			
and 102	and 103	and 104	and 105	and 106	and 107	and 108	and 109	and 110	and 111	and 112	and 113	and 114	and 115	and 116	and 117	and 118	and 119	and 120	and 121	and 122	and 123		
and 124	and 125	and 126	and 127	and 128	and 129	and 130	and 131	and 132	and 133	and 134	and 135	and 136	and 137	and 138	and 139	and 140	and 141	and 142	and 143	and 144	and 145	and 146	
and 147	and 148	and 149	and 150	and 151	and 152	and 153	and 154	and 155	and 156	and 157	and 158	and 159	and 160	and 161	and 162	and 163	and 164	and 165	and 166	and 167	and 168	and 169	and 170
and 171	and 172	and 173	and 174	and 175	and 176	and 177	and 178	and 179	and 180	and 181	and 182	and 183	and 184	and 185	and 186	and 187	and 188	and 189	and 190	and 191	and 192	and 193	and 194
and 195	and 196	and 197	and 198	and 199	and 200	and 201	and 202	and 203	and 204	and 205	and 206	and 207	and 208	and 209	and 210	and 211	and 212	and 213	and 214	and 215	and 216	and 217	and 218
and 219	and 220	and 221	and 222	and 223	and 224	and 225	and 226	and 227	and 228	and 229	and 230	and 231	and 232	and 233	and 234	and 235	and 236	and 237	and 238	and 239	and 240	and 241	and 242
and 243	and 244	and 245	and 246	and 247	and 248	and 249	and 250	and 251	and 252	and 253	and 254	and 255	and 256	and 257	and 258	and 259	and 260	and 261	and 262	and 263	and 264	and 265	and 266
and 267	and 268	and 269	and 270	and 271	and 272	and 273	and 274	and 275	and 276	and 277	and 278	and 279	and 280	and 281	and 282	and 283	and 284	and 285	and 286	and 287	and 288	and 289	and 290
and 291	and 292	and 293	and 294	and 295	and 296	and 297	and 298	and 299	and 300	and 301	and 302	and 303	and 304	and 305	and 306	and 307	and 308	and 309	and 310	and 311	and 312	and 313	and 314
and 315	and 316	and 317	and 318	and 319	and 320	and 321	and 322	and 323	and 324	and 325	and 326	and 327	and 328	and 329	and 330	and 331	and 332	and 333	and 334	and 335	and 336	and 337	and 338
and 339	and 340	and 341	and 342	and 343	and 344	and 345	and 346	and 347	and 348	and 349	and 350	and 351	and 352	and 353	and 354	and 355	and 356	and 357	and 358	and 359	and 360	and 361	and 362
and 363	and 364	and 365	and 366	and 367	and 368	and 369	and 370	and 371	and 372	and 373	and 374	and 375	and 376	and 377	and 378	and 379	and 380	and 381	and 382	and 383	and 384	and 385	and 386
and 387	and 388	and 389	and 390	and 391	and 392	and 393	and 394	and 395	and 396	and 397	and 398	and 399	and 400	and 401	and 402	and 403	and 404	and 405	and 406	and 407	and 408	and 409	and 410
and 411	and 412	and 413	and 414	and 415	and 416	and 417	and 418	and 419	and 420	and 421	and 422	and 423	and 424	and 425	and 426	and 427	and 428	and 429	and 430	and 431	and 432	and 433	and 434
and 435	and 436	and 437	and 438	and 439	and 440	and 441	and 442	and 443	and 444	and 445	and 446	and 447	and 448	and 449	and 450	and 451	and 452	and 453	and 454	and 455	and 456	and 457	and 458
and 459	and 460	and 461	and 462	and 463	and 464	and 465	and 466	and 467	and 468	and 469	and 470	and 471	and 472	and 473	and 474	and 475	and 476	and 477	and 478	and 479	and 480	and 481	and 482
and 483	and 484	and 485	and 486	and 487	and 488	and 489	and 490	and 491	and 492	and 493	and 494	and 495	and 496	and 497	and 498	and 499	and 500	and 501	and 502	and 503	and 504	and 505	and 506

FIG. 10B



1010 1011 1100 1101
 1010 1011 1100 1101
 1010 1011 1100 1101
 1010 1011 1100 1101
 1010 1011 1100 1101
 1010 1011 1100 1101
 1010 1011 1100 1101
 1010 1011 1100 1101
 1010 1011 1100 1101
 1010 1011 1100 1101

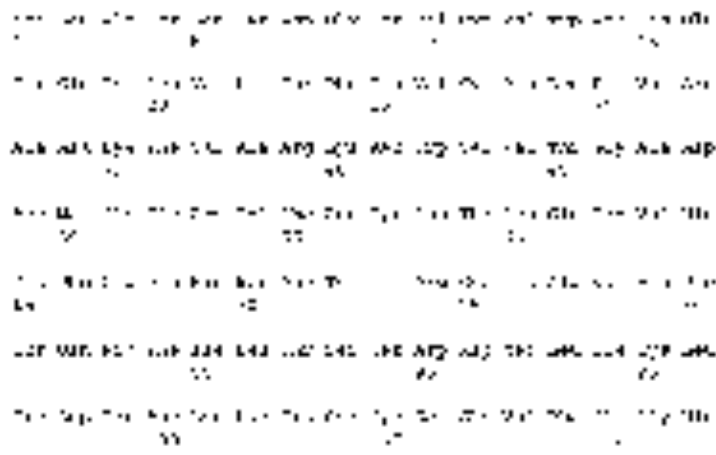


FIG. 10

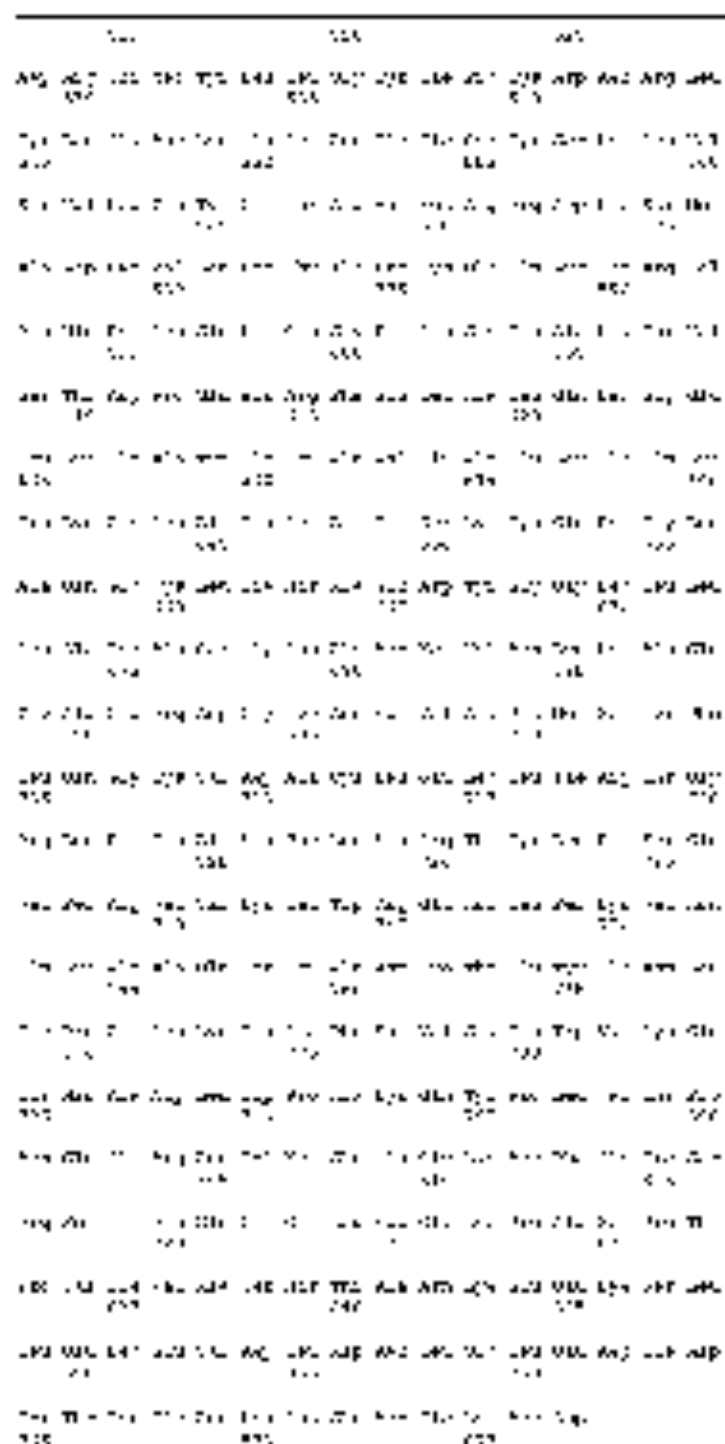


FIG. 10 is a sequence of diagrams illustrating a data processing flow. The diagrams show a sequence of data elements (A through Z) and their relationships. The flow starts at (a) with 'A' and 'B' and proceeds through various combinations and operations, ending at (t) with 'Z'. The diagrams are arranged in a grid-like fashion, with some elements appearing in multiple diagrams.

FIG. 10



-continued-

225	226	227
225 226 227 228 229 230 231 232 233 234 235 236 237 238 239 240 241 242 243 244 245 246 247 248 249 250 251 252 253 254 255 256 257 258 259 260 261 262 263 264 265 266 267 268 269 270 271 272 273 274 275 276 277 278 279 280 281 282 283 284 285 286 287 288 289 290 291 292 293 294 295 296 297 298 299 300 301 302 303 304 305 306 307 308 309 310 311 312 313 314 315 316 317 318 319 320 321 322 323 324 325 326 327 328 329 330 331 332 333 334 335 336 337 338 339 340 341 342 343 344 345 346 347 348 349 350 351 352 353 354 355 356 357 358 359 360 361 362 363 364 365 366 367 368 369 370 371 372 373 374 375 376 377 378 379 380 381 382 383 384 385 386 387 388 389 390 391 392 393 394 395 396 397 398 399 400 401 402 403 404 405 406 407 408 409 410 411 412 413 414 415 416 417 418 419 420 421 422 423 424 425 426 427 428 429 430 431 432 433 434 435 436 437 438 439 440 441 442 443 444 445 446 447 448 449 450 451 452 453 454 455 456 457 458 459 460 461 462 463 464 465 466 467 468 469 470 471 472 473 474 475 476 477 478 479 480 481 482 483 484 485 486 487 488 489 490 491 492 493 494 495 496 497 498 499 500 501 502 503 504 505 506 507 508 509 510 511 512 513 514 515 516 517 518 519 520 521 522 523 524 525 526 527 528 529 530 531 532 533 534 535 536 537 538 539 540 541 542 543 544 545 546 547 548 549 550 551 552 553 554 555 556 557 558 559 560 561 562 563 564 565 566 567 568 569 570 571 572 573 574 575 576 577 578 579 580 581 582 583 584 585 586 587 588 589 590 591 592 593 594 595 596 597 598 599 600 601 602 603 604 605 606 607 608 609 610 611 612 613 614 615 616 617 618 619 620 621 622 623 624 625 626 627 628 629 630 631 632 633 634 635 636 637 638 639 640 641 642 643 644 645 646 647 648 649 650 651 652 653 654 655 656 657 658 659 660 661 662 663 664 665 666 667 668 669 670 671 672 673 674 675 676 677 678 679 680 681 682 683 684 685 686 687 688 689 690 691 692 693 694 695 696 697 698 699 700 701 702 703 704 705 706 707 708 709 710 711 712 713 714 715 716 717 718 719 720 721 722 723 724 725 726 727 728 729 730 731 732 733 734 735 736 737 738 739 740 741 742 743 744 745 746 747 748 749 750 751 752 753 754 755 756 757 758 759 760 761 762 763 764 765 766 767 768 769 770 771 772 773 774 775 776 777 778 779 780 781 782 783 784 785 786 787 788 789 790 791 792 793 794 795 796 797 798 799 800 801 802 803 804 805 806 807 808 809 810 811 812 813 814 815 816 817 818 819 820 821 822 823 824 825 826 827 828 829 830 831 832 833 834 835 836 837 838 839 840 841 842 843 844 845 846 847 848 849 850 851 852 853 854 855 856 857 858 859 860 861 862 863 864 865 866 867 868 869 870 871 872 873 874 875 876 877 878 879 880 881 882 883 884 885 886 887 888 889 890 891 892 893 894 895 896 897 898 899 900 901 902 903 904 905 906 907 908 909 910 911 912 913 914 915 916 917 918 919 920 921 922 923 924 925 926 927 928 929 930 931 932 933 934 935 936 937 938 939 940 941 942 943 944 945 946 947 948 949 950 951 952 953 954 955 956 957 958 959 960 961 962 963 964 965 966 967 968 969 970 971 972 973 974 975 976 977 978 979 980 981 982 983 984 985 986 987 988 989 990 991 992 993 994 995 996 997 998 999 1000		

FIG. 10B

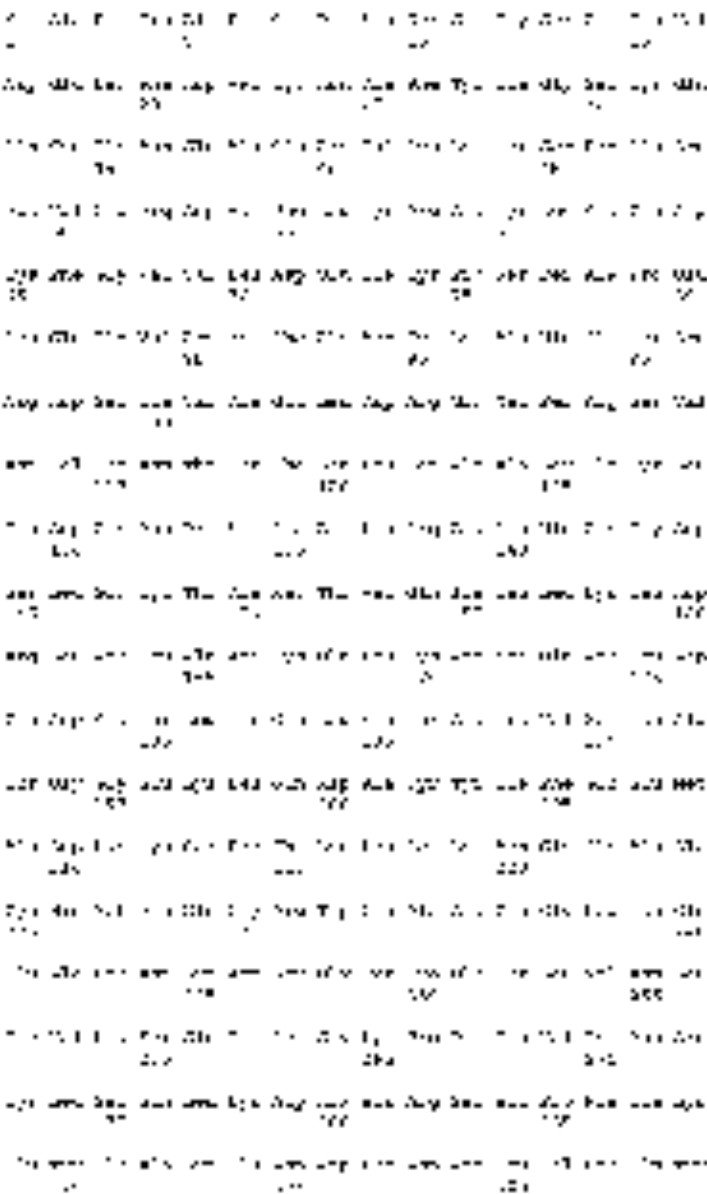


FIG. 10B

FIG. 10B is a sequence diagram illustrating a process flow between a device and a server. The process flow includes the following steps:

- The device sends a request to the server.
- The server responds to the device with data.
- The device sends a request to the server.
- The server responds to the device with data.
- The device sends a request to the server.
- The server responds to the device with data.
- The device sends a request to the server.
- The server responds to the device with data.
- The device sends a request to the server.
- The server responds to the device with data.

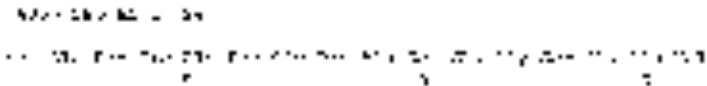


FIG. 10C

FIG. 10B

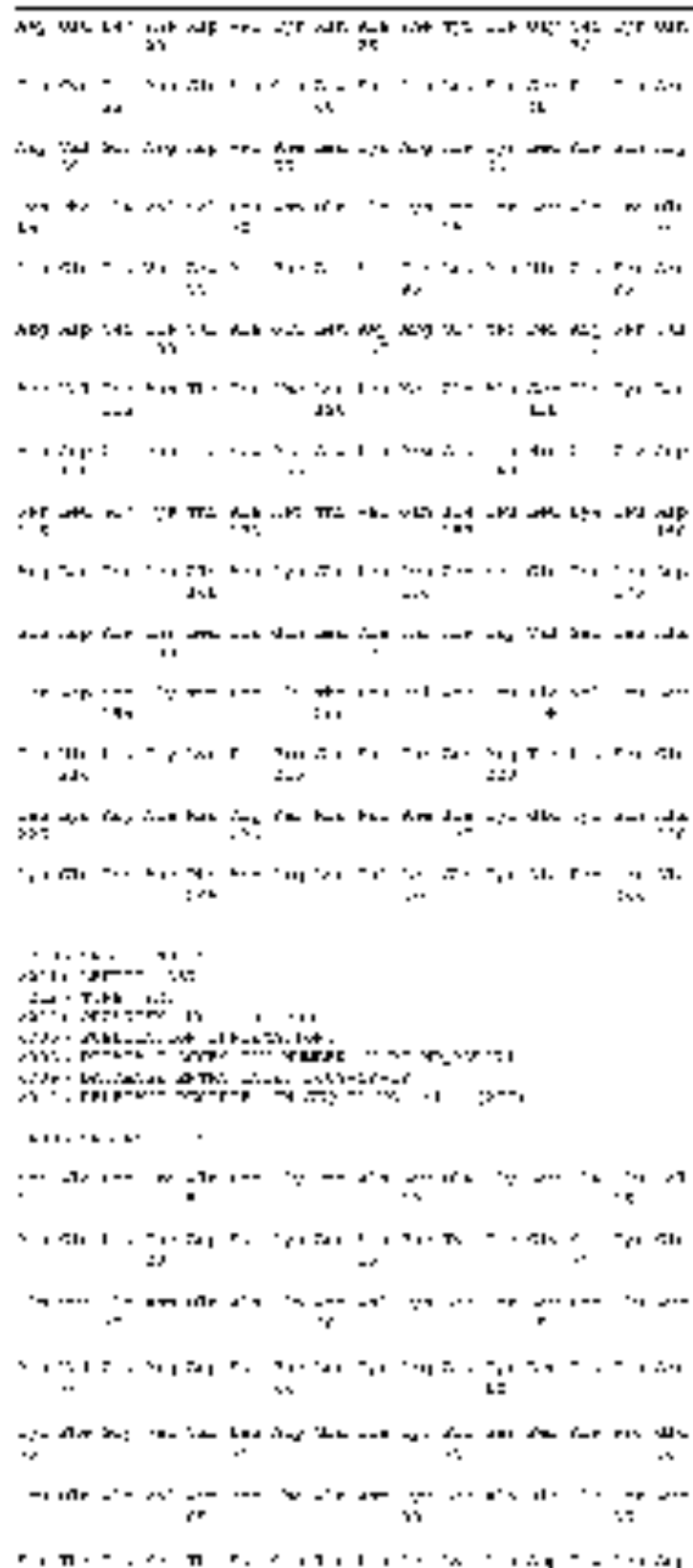


FIG. 10



FIG. 10



FIG. 10B

201	202	203	204	205	206	207	208	209	210	211	212	213	214	215	216	217	218	219	220	221	222	223	224	225	226	227	228	229	230	231	232	233	234	235	236	237	238	239	240	241	242	243	244	245	246	247	248	249	250	251	252	253	254	255	256	257	258	259	260	261	262	263	264	265	266	267	268	269	270	271	272	273	274	275	276	277	278	279	280	281	282	283	284	285	286	287	288	289	290	291	292	293	294	295	296	297	298	299	300	301	302	303	304	305	306	307	308	309	310	311	312	313	314	315	316	317	318	319	320	321	322	323	324	325	326	327	328	329	330	331	332	333	334	335	336	337	338	339	340	341	342	343	344	345	346	347	348	349	350	351	352	353	354	355	356	357	358	359	360	361	362	363	364	365	366	367	368	369	370	371	372	373	374	375	376	377	378	379	380	381	382	383	384	385	386	387	388	389	390	391	392	393	394	395	396	397	398	399	400	401	402	403	404	405	406	407	408	409	410	411	412	413	414	415	416	417	418	419	420	421	422	423	424	425	426	427	428	429	430	431	432	433	434	435	436	437	438	439	440	441	442	443	444	445	446	447	448	449	450	451	452	453	454	455	456	457	458	459	460	461	462	463	464	465	466	467	468	469	470	471	472	473	474	475	476	477	478	479	480	481	482	483	484	485	486	487	488	489	490	491	492	493	494	495	496	497	498	499	500	501	502	503	504	505	506	507	508	509	510	511	512	513	514	515	516	517	518	519	520	521	522	523	524	525	526	527	528	529	530	531	532	533	534	535	536	537	538	539	540	541	542	543	544	545	546	547	548	549	550	551	552	553	554	555	556	557	558	559	560	561	562	563	564	565	566	567	568	569	570	571	572	573	574	575	576	577	578	579	580	581	582	583	584	585	586	587	588	589	590	591	592	593	594	595	596	597	598	599	600	601	602	603	604	605	606	607	608	609	610	611	612	613	614	615	616	617	618	619	620	621	622	623	624	625	626	627	628	629	630	631	632	633	634	635	636	637	638	639	640	641	642	643	644	645	646	647	648	649	650	651	652	653	654	655	656	657	658	659	660	661	662	663	664	665	666	667	668	669	670	671	672	673	674	675	676	677	678	679	680	681	682	683	684	685	686	687	688	689	690	691	692	693	694	695	696	697	698	699	700	701	702	703	704	705	706	707	708	709	710	711	712	713	714	715	716	717	718	719	720	721	722	723	724	725	726	727	728	729	730	731	732	733	734	735	736	737	738	739	740	741	742	743	744	745	746	747	748	749	750	751	752	753	754	755	756	757	758	759	760	761	762	763	764	765	766	767	768	769	770	771	772	773	774	775	776	777	778	779	780	781	782	783	784	785	786	787	788	789	790	791	792	793	794	795	796	797	798	799	800	801	802	803	804	805	806	807	808	809	810	811	812	813	814	815	816	817	818	819	820	821	822	823	824	825	826	827	828	829	830	831	832	833	834	835	836	837	838	839	840	841	842	843	844	845	846	847	848	849	850	851	852	853	854	855	856	857	858	859	860	861	862	863	864	865	866	867	868	869	870	871	872	873	874	875	876	877	878	879	880	881	882	883	884	885	886	887	888	889	890	891	892	893	894	895	896	897	898	899	900	901	902	903	904	905	906	907	908	909	910	911	912	913	914	915	916	917	918	919	920	921	922	923	924	925	926	927	928	929	930	931	932	933	934	935	936	937	938	939	940	941	942	943	944	945	946	947	948	949	950	951	952	953	954	955	956	957	958	959	960	961	962	963	964	965	966	967	968	969	970	971	972	973	974	975	976	977	978	979	980	981	982	983	984	985	986	987	988	989	990	991	992	993	994	995	996	997	998	999	1000
-----	-----	-----	-----	-----	-----	-----	-----	-----	-----	-----	-----	-----	-----	-----	-----	-----	-----	-----	-----	-----	-----	-----	-----	-----	-----	-----	-----	-----	-----	-----	-----	-----	-----	-----	-----	-----	-----	-----	-----	-----	-----	-----	-----	-----	-----	-----	-----	-----	-----	-----	-----	-----	-----	-----	-----	-----	-----	-----	-----	-----	-----	-----	-----	-----	-----	-----	-----	-----	-----	-----	-----	-----	-----	-----	-----	-----	-----	-----	-----	-----	-----	-----	-----	-----	-----	-----	-----	-----	-----	-----	-----	-----	-----	-----	-----	-----	-----	-----	-----	-----	-----	-----	-----	-----	-----	-----	-----	-----	-----	-----	-----	-----	-----	-----	-----	-----	-----	-----	-----	-----	-----	-----	-----	-----	-----	-----	-----	-----	-----	-----	-----	-----	-----	-----	-----	-----	-----	-----	-----	-----	-----	-----	-----	-----	-----	-----	-----	-----	-----	-----	-----	-----	-----	-----	-----	-----	-----	-----	-----	-----	-----	-----	-----	-----	-----	-----	-----	-----	-----	-----	-----	-----	-----	-----	-----	-----	-----	-----	-----	-----	-----	-----	-----	-----	-----	-----	-----	-----	-----	-----	-----	-----	-----	-----	-----	-----	-----	-----	-----	-----	-----	-----	-----	-----	-----	-----	-----	-----	-----	-----	-----	-----	-----	-----	-----	-----	-----	-----	-----	-----	-----	-----	-----	-----	-----	-----	-----	-----	-----	-----	-----	-----	-----	-----	-----	-----	-----	-----	-----	-----	-----	-----	-----	-----	-----	-----	-----	-----	-----	-----	-----	-----	-----	-----	-----	-----	-----	-----	-----	-----	-----	-----	-----	-----	-----	-----	-----	-----	-----	-----	-----	-----	-----	-----	-----	-----	-----	-----	-----	-----	-----	-----	-----	-----	-----	-----	-----	-----	-----	-----	-----	-----	-----	-----	-----	-----	-----	-----	-----	-----	-----	-----	-----	-----	-----	-----	-----	-----	-----	-----	-----	-----	-----	-----	-----	-----	-----	-----	-----	-----	-----	-----	-----	-----	-----	-----	-----	-----	-----	-----	-----	-----	-----	-----	-----	-----	-----	-----	-----	-----	-----	-----	-----	-----	-----	-----	-----	-----	-----	-----	-----	-----	-----	-----	-----	-----	-----	-----	-----	-----	-----	-----	-----	-----	-----	-----	-----	-----	-----	-----	-----	-----	-----	-----	-----	-----	-----	-----	-----	-----	-----	-----	-----	-----	-----	-----	-----	-----	-----	-----	-----	-----	-----	-----	-----	-----	-----	-----	-----	-----	-----	-----	-----	-----	-----	-----	-----	-----	-----	-----	-----	-----	-----	-----	-----	-----	-----	-----	-----	-----	-----	-----	-----	-----	-----	-----	-----	-----	-----	-----	-----	-----	-----	-----	-----	-----	-----	-----	-----	-----	-----	-----	-----	-----	-----	-----	-----	-----	-----	-----	-----	-----	-----	-----	-----	-----	-----	-----	-----	-----	-----	-----	-----	-----	-----	-----	-----	-----	-----	-----	-----	-----	-----	-----	-----	-----	-----	-----	-----	-----	-----	-----	-----	-----	-----	-----	-----	-----	-----	-----	-----	-----	-----	-----	-----	-----	-----	-----	-----	-----	-----	-----	-----	-----	-----	-----	-----	-----	-----	-----	-----	-----	-----	-----	-----	-----	-----	-----	-----	-----	-----	-----	-----	-----	-----	-----	-----	-----	-----	-----	-----	-----	-----	-----	-----	-----	-----	-----	-----	-----	-----	-----	-----	-----	-----	-----	-----	-----	-----	-----	-----	-----	-----	-----	-----	-----	-----	-----	-----	-----	-----	-----	-----	-----	-----	-----	-----	-----	-----	-----	-----	-----	-----	-----	-----	-----	-----	-----	-----	-----	-----	-----	-----	-----	-----	-----	-----	-----	-----	-----	-----	-----	-----	-----	-----	-----	-----	-----	-----	-----	-----	-----	-----	-----	-----	-----	-----	-----	-----	-----	-----	-----	-----	-----	-----	-----	-----	-----	-----	-----	-----	-----	-----	-----	-----	-----	-----	-----	-----	-----	-----	-----	-----	-----	-----	-----	-----	-----	-----	-----	-----	-----	-----	-----	-----	-----	-----	-----	-----	-----	-----	-----	-----	-----	-----	-----	-----	-----	-----	-----	-----	-----	-----	-----	-----	-----	-----	-----	-----	-----	-----	-----	-----	-----	-----	-----	-----	-----	-----	-----	-----	-----	-----	-----	-----	-----	-----	-----	-----	-----	-----	-----	-----	-----	-----	-----	-----	-----	-----	-----	-----	-----	-----	-----	-----	-----	-----	-----	-----	-----	-----	-----	-----	-----	-----	-----	-----	-----	-----	-----	-----	-----	-----	-----	-----	-----	-----	-----	-----	-----	-----	-----	-----	-----	-----	-----	-----	-----	-----	-----	-----	-----	-----	-----	-----	-----	-----	-----	-----	-----	-----	-----	-----	-----	-----	-----	-----	-----	-----	-----	-----	-----	-----	-----	-----	-----	-----	-----	-----	-----	-----	-----	-----	-----	-----	-----	-----	-----	-----	-----	-----	-----	-----	-----	-----	-----	-----	-----	-----	-----	-----	-----	-----	-----	-----	-----	-----	-----	------

FIG. 10



FIG. 10B

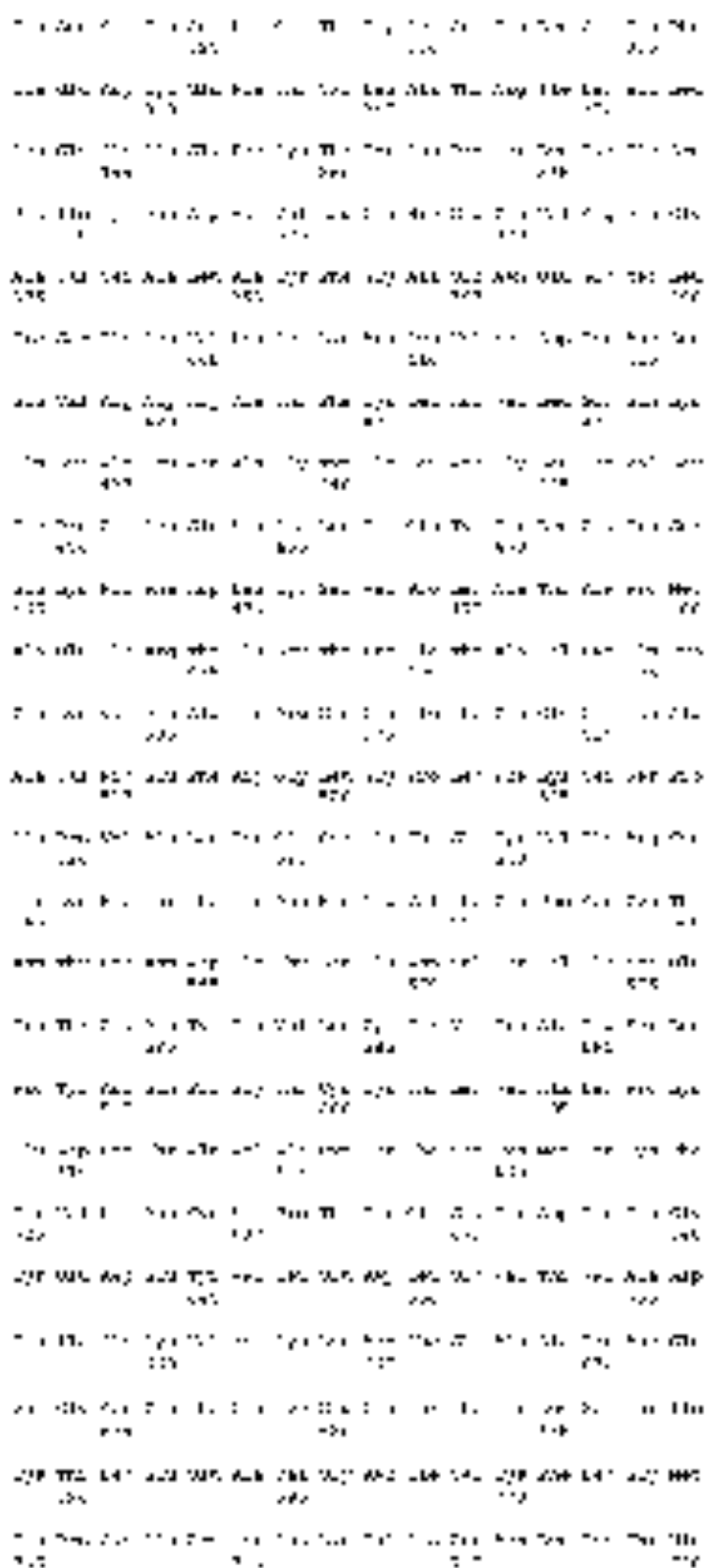


FIG. 1000

1000 1001 1002 1003 1004 1005 1006 1007 1008 1009 1010 1011
 1012 1013 1014 1015 1016 1017 1018 1019 1020 1021 1022 1023
 1024 1025 1026 1027 1028 1029 1030 1031 1032 1033 1034 1035

1036 1037 1038
 1039 1040
 1041 1042 1043 1044 1045 1046 1047 1048 1049 1050 1051 1052
 1053 1054 1055 1056 1057 1058 1059 1060 1061 1062 1063 1064
 1065 1066 1067 1068 1069 1070 1071 1072 1073 1074 1075 1076

1077 1078 1079 1080 1081 1082 1083 1084 1085 1086 1087 1088

1089 1090 1091 1092 1093 1094 1095 1096 1097 1098 1099 1100 1101 1102 1103 1104
 1105 1106 1107 1108 1109 1110 1111 1112 1113 1114 1115 1116 1117 1118 1119 1120
 1121 1122 1123 1124 1125 1126 1127 1128 1129 1130 1131 1132 1133 1134 1135 1136

1137 1138 1139 1140 1141 1142 1143 1144 1145 1146 1147 1148 1149 1150 1151 1152

1153 1154 1155 1156 1157 1158 1159 1160 1161 1162 1163 1164 1165 1166 1167 1168

1169 1170 1171 1172 1173 1174 1175 1176 1177 1178 1179 1180 1181 1182 1183 1184

1185 1186 1187 1188 1189 1190 1191 1192 1193 1194 1195 1196 1197 1198 1199 1200

1201 1202 1203 1204 1205 1206 1207 1208 1209 1210 1211 1212 1213 1214 1215 1216

1217 1218 1219 1220 1221 1222 1223 1224 1225 1226 1227 1228 1229 1230 1231 1232

1233 1234 1235 1236 1237 1238 1239 1240 1241 1242 1243 1244 1245 1246 1247 1248

1249

1250 1251 1252
 1253 1254
 1255 1256 1257 1258 1259 1260 1261 1262 1263 1264 1265 1266 1267 1268 1269 1270
 1271 1272 1273 1274 1275 1276 1277 1278 1279 1280 1281 1282 1283 1284 1285 1286
 1287 1288 1289 1290 1291 1292 1293 1294 1295 1296 1297 1298 1299 1300 1301 1302

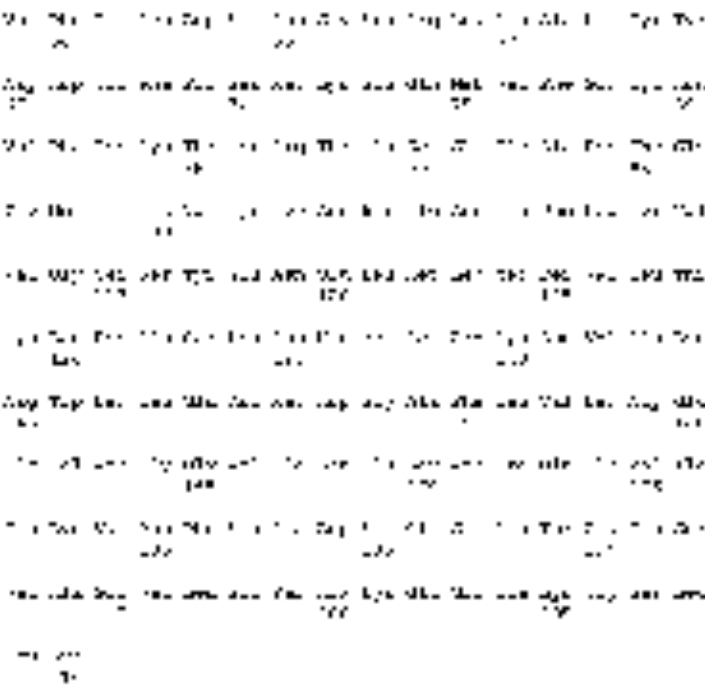
1303 1304 1305 1306 1307 1308 1309 1310 1311 1312 1313 1314 1315 1316 1317 1318

1319 1320 1321 1322 1323 1324 1325 1326 1327 1328 1329 1330 1331 1332 1333 1334

1335 1336 1337 1338 1339 1340 1341 1342 1343 1344 1345 1346 1347 1348 1349 1350

1351 1352 1353 1354 1355 1356 1357 1358 1359 1360 1361 1362 1363 1364 1365 1366

FIG. 100



1. The intelligent user platform (101) is used to
 1.1. Analyze the user's past behavior (e.g., past purchases, past search history, etc.) to determine the user's preferences and interests.
 1.2. Identify the user's current behavior (e.g., current purchases, current search history, etc.) to determine the user's current preferences and interests.
 1.3. Compare the user's current behavior with the user's past behavior to determine the user's current preferences and interests.
 1.4. Identify the user's current preferences and interests based on the comparison.
 1.5. Provide the user with recommendations based on the user's current preferences and interests.
 1.6. Provide the user with recommendations based on the user's past preferences and interests.
 1.7. Provide the user with recommendations based on the user's current and past preferences and interests.
 1.8. Provide the user with recommendations based on the user's current and past preferences and interests, and the user's current and past behavior.

2. The intelligent user platform (102) is used to
 2.1. Analyze the user's past behavior (e.g., past purchases, past search history, etc.) to determine the user's preferences and interests.
 2.2. Identify the user's current behavior (e.g., current purchases, current search history, etc.) to determine the user's current preferences and interests.
 2.3. Compare the user's current behavior with the user's past behavior to determine the user's current preferences and interests.
 2.4. Identify the user's current preferences and interests based on the comparison.
 2.5. Provide the user with recommendations based on the user's current preferences and interests.
 2.6. Provide the user with recommendations based on the user's past preferences and interests.
 2.7. Provide the user with recommendations based on the user's current and past preferences and interests.
 2.8. Provide the user with recommendations based on the user's current and past preferences and interests, and the user's current and past behavior.

